Relationship between mix design, concrete performance and carbon footprint

Ahmad Al-Naqkeeb

Submitted in accordance with the requirements for the degree of
Doctor of Philosophy

The University of Leeds
School of Civil Engineering

June, 2020

The candidate confirms that the work submitted is his own, except where work which has formed part of jointly-authored publications has been included. The contribution of the candidate and the other authors to this work has been explicitly indicated below. The candidate confirms that appropriate credit has been given within the thesis where reference has been made to the work of others.

Acknowledgements

Beside hard work and dedication, it is not possible to accomplish a mammoth task of writing a PhD thesis without constant inspiration, advice and moral supports from a group of people who are closely associated with me. This is the time to appreciate those invaluable supports.

I would like to thank my supervisors, Professor Leon Black and Dr Emilio Garcia Taengua, for their guidance and support and helpful discussions which have been of great value.

My great parents who inspired me in every success of my life and encouraged in any difficulties I might have faced, must be honoured and appreciated during this great moment of my life. They are my beloved and cherished mother and father. Both of them at their own capacity have greatly influenced, encouraged and contributed to successfully complete this thesis by means of moral support, compassions and perseverance.

I would like to express appreciation to my beloved wife Shahd, who spent her days and nights to be on my side and was always supportive in the moments when there was no one standing next to me.

My thanks and appreciation to all the civil engineering technical staff at the University of Leeds and to the rest of my research group, Julia, Joe, , Sam, Suma, Sola, Mubarak and Suraj who have always offered their help and support. Thanks to the staff in LEMAS for their valuable help and training.

Abstract

Reducing the carbon footprint of concrete is an imperative. Judicious concrete mix design is one means of achieving this, including the use of supplementary cementitious materials, water reducing admixtures and reduced concrete workability. However, a truly sustainable concrete should also, in addition to having a low embodied carbon, provide long-term durability.

In the present work, many factors have been adopted to reduce the embodied carbon dioxide in concrete. Eighteen concrete mixes were designed to provide low-carbon concrete while maintaining durability. To achieve these requirements, it was necessary to cast a series of concrete samples with compositions designed to vary key components known to control embodied carbon dioxide. Based on the statistical approach, 18 concrete mixtures were produced and designed in L18 orthogonal array with six design variables. The work is divided into three complementary parts as follows:

Part one characterizes of the constituent concrete materials, including Portland cement and three different supplementary cementitious materials (pulverized fuel ash, plus course and fine ground granulated blast furnace slag) at different replacement levels (0%, 15%, 30% of the total binder content by mass). A superplasticizer, Sika Viscocrete 25 MP, was used at either 0.2%, 0.6% or 1.0% binder weight. Crushed aggregate of maximum size of 10 and 20mm while the crushed fine aggregate were of 5mm maximum size were used.

Part two of the works highlights the performance of hardened state concrete (mechanical properties) including the time-dependent deformations and durability. These properties have been investigated by testing 100mm cubes for compressive strength, 75 x 75 x 200 mm prisms for shrinkage, and transport properties (sorptivity and permeability on 100mm cubes and 40mm thick x 50 mm Ø cylinders. Durability was assessed through measuring the depth of carbonation following accelerated carbonation of 100 mm cube samples.

Finally, in the third part, microstructural investigations were undertaken using pastes that were prepared with the same composition as the concrete, but without any aggregates. The pastes were investigated using thermogravimetric analysis

(TGA) and scanning electron microscopy (SEM). Moreover, hydration was investigated using isothermal conduction calorimetry.

Test results proved that some mix design variables have a significant positive impact on the performance; for example strength enhancement, improving carbonation resistance meanwhile, satisfying the requirement of reducing carbon dioxide emissions.

Numerically speaking a concrete containing fine slag at 15 or 30% replacement, low w/b ratio (0.35) above and high dosage of superplasticizer (1.0%) was found to meet the engineering performance, carbonation resistance, and environmental sustainability. It was also found that coarse slag might be another choice of cement replacement but with slightly decreased carbonation resistance. Slag showed better performance than PFA. This can be attributed to the role of slag in refining the microstructure by: (i) leading to finer porosity, increased degree of hydration, (iii) by inference, changing the C-S-H from fibrillary to foil-like (iiii) improving carbonation resistance.

The above significant conclusions are the result of the high fineness of slag which in turn reduced the pore structure, high reactivity of slag which in turn accelerated the hydration at early age and the pozzolanic reaction which improved the microstructure at long age.

This study has considered a range of concrete mix designs known to yield concrete with a reduced carbon footprint. It has looked at the effects of mix design on mechanical performance, transport properties and resistance to carbonation. Using the Taguchi method, 18 concrete mixtures are produced and designed in L18 orthogonal array with six design variables (binder content, superplasticizer, supplementary cementitious materials, percentage of SCMs, aggregate Size (10-20) mm and water-to-binder ratio) set at one of three levels have been prepared.

Table of Contents

List of Figures

List of Tables

List of Abbreviations

Cement oxide compositions

A	Al_2O_3
C	CaO
F	Fe_2O_3
H	H_2O
K	K_2O
M	MgO
N	Na_2O
S	SiO_2

Cement compounds

Alite (C_3S)	$3CaO.SiO_2$
Belite (C_2S)	$2CaO.SiO_2$
Calcium Silicate Hydrate (C-S-H)	$CaO\text{-}SiO_2\text{-}H_2O$
Ettringite / AFt	$3CaO.Al_2O_3.3CaSO_4.32H_2O$
Gypsum	$CaSO_4.2H_2O$
Portlandite (CH)	$Ca(OH)_2$
Tricalcium Aluminate / (C_3A)	$3CaO.Al_2O_3$
Tetracalcium aluminoferrite (C_4AF)	$4CaO.Al_2O_3.Fe_2O_3$

Techniques

BSE	Back scattered electron
DTA	Differential thermal analysis
EDX	Energy dispersive x-ray
ICC	Isothermal conduction calorimetry

SEM	Scanning electron microscopy
SEM-IA	Scanning electron microscopy – Image analysis
STA	Simultaneous thermal analysis
TGA	Thermogravimetric analysis

Symbols

CO_2	Carbon dioxide
DoH	Degree of hydration
eCO_2	Embodied carbon dioxide
GGBS	Ground granulated blast-furnace slag
FS	Fine slag
PC	Portland cement
PFA	Pulverised fuel ash
RH	Relative humidity
SCM	Supplementary cementitious material
W/C	Water/cement ratio
W/b	Water/binder ratio

Chapter 1 : Introduction

1.1 General introduction

The industrial sector is responsible for approximately 25% of global carbon dioxide (CO_2) emissions among which CO_2 emissions from cement plants represent no less than 5% of total anthropogenic emissions (Brand et al., 2004). Carbon dioxide emissions arise from the clinkering process where, limestone (80%) and clay (20%) are burnt at 1450 °C to produce clinker and are then blended with additives. The finished product is finely ground to manufacture different types of cement. Through the cement production process, around 0.706 ton of CO_2 is released per ton of clinker produced. This emission is mainly due to the de-carbonation of limestone (0.521 ton), and the use of coal and fossil fuels for heating (0.185 ton), (Gartner, 2004).

As a result of the emissions per tonne of cement produced, plus the huge quantities of concrete consumed globally, cement producers and the construction industry as a whole are under pressure to reduce their carbon footprint. There have been many developments to reduce the carbon footprint, and the term low-carbon concrete is somewhat of a catchall term and rather a qualitative definition more than a quantitative one. Using the definition of carbon footprint as being "a measure of the exclusive total amount of carbon dioxide emissions that is directly and indirectly caused by an activity or is accumulated over the life stages of a product" (Wiedmann and Minx, 2008), then low-carbon concrete can be considered as any concrete designed with an eye on lowering the carbon footprint. It is known that cement makes the biggest contribution in CO_2 emissions, with 75% of the total. This is followed by aggregate contributing less than 20%. CO_2 emitted by aggregate is mainly due to electricity and to a lesser extent due to excavation, hauling, blasting, and transportation.

Researchers have made numerous attempts to produce concrete with lowest possible CO_2 emissions. The use of superplasticizers and highly reactive cements as well as an optimization of particle-size distribution and reduction in water content allow a significant reduction in Portland cement clinker in the cement and concrete. Essential is the addition of mineral fillers (e.g., limestone

powder) to provide an optimal paste volume. In addition, the already practicable substitution of secondary raw materials like fly ash or furnace slag for cement clinker is an appropriate option that is, however, limited by the availability of these resources (Proske, et al., 2013).

However, a key, important aspect in this present study is reducing the embodied carbon dioxide of fresh concrete so as to result in a hardened concrete where the long-term deterioration is minimised or even eliminated. Carbonation itself is influenced by the paste content, the presence of SCM, the period of curing and water content. All these factors affect the quantity of carbonatable matter, which correlates inversely with the carbonation progress (Lagerblad, 2005b)

There are two aspects to the carbon footprint of a built environment component, be it a brick, a bungalow, or a bridge. First, there is the CO_2 produced as a consequence of its ongoing operation, associated with the energy used by heating, lighting, air conditioning, maintenance, and its eventual disposal. This operational CO_2 emission (OC) increases with the lifetime of the component, analogous to a recurring running cost. OC is the current exclusive focus of U.K. zero-carbon construction legislation. Second, there is the CO_2 emitted as a consequence of the manufacture of the component, generated during mining, processing, and transport of raw materials, site operations, etc. This embodied CO_2 (EC) is product specific and does not vary over the lifetime of the component, analogous to a fixed capital cost. For most building and infrastructure projects, it is dominated by emissions associated with the extraction and processing of materials (steel, timber, concrete, aluminum, plastics, etc.). (Harrison et al., 2010).

It’s of a common knowledge that concrete is a product subject to carbon emission which cause deterioration with time bot at early stages and long term scale. There exist different ways to reduce the greenhouse gas emissions from cement production, one of them is replacing the clinker partially by other equivalent material and considered as additives such as; fly ashes from coal-fired thermal power plants, slag from blast furnaces in the iron and steel industry, natural pozzolans, limestone fillers, and various other wastes. These additives contain large quantities of reactive SiO_2 and Al_2O_3, which produce cementitious materials in the presence of lime. (Habert and Roussel, 2009).

It is observed that the current work on eCO_2 underestimates the complicated relationship with concrete mix design (Purnell and Black, 2012). The production

of concrete, a major construction material, emits a large amount of CO_2 from the material production stage, such as in the production of cement, aggregates, and admixtures, to the manufacturing stage. As a result of the presence of different variables, concrete mix design can affect eCO_2. These effects are due to the physical and chemical constituent of various materials used (Kim et al., 2013). Many commentators have published eCO_2 values for concrete, either as individual values or a small range depending on certain properties (mainly compressive strength grade and the use of supplementary cementitious materials) (Purnell and Black, 2012). Previous work has analysed either the embodied carbon dioxide (ECO_2) of plain concrete as a function of strength grade and mix design. (Hammond and Jones, 2008) give a general value of 0.107 $kgCO_2/kg$ and a monotonic relationship between eCO_2 (0.061 – 0.188 $kgCO_2/kg$) and characteristic cube strength (8 – 50 MPa) for CEM I and CEM II concretes. However, they do advise against the indiscriminate use of these values. Meanwhile, (Hacker et al., 2008) uses a value of 0.200 $kgCO_2/kg$ with no strength discrimination, whilst Harrison uses 0.13 $kgCO_2/kg$ for plain concrete and 0.24 $kgCO_2/kg$ for “2% reinforced”; the additional CO_2 attributable to the steel. Among those reporting on a volumetric basis, (Flower and Sanjayan, 2007a) use values of 0.225 - 0.322 $kgCO_2/m^3$ for normal and blended cement concretes, corresponding to eCO_2 ~ 0.09 – 0.12 $kgCO_2/kg$. (Purnell, 2013) analysed the variation of EC per unit of structural performance for reinforced concrete components as a function of concrete compressive strength grade, reinforcement steel strength and concrete mix design for beams, short columns and slender columns. In a theoretical study (Purnell and Black, 2012) calculated the eCO_2 for 512 concrete mixes as a function of the most important mix design variables concluding that considerable eCO_2 savings can be made by careful attention to basic mix design. On the other hand, (Berndt, 2015) reported that the selection of concrete ingredients and appropriate design could be used to reduce carbon dioxide emissions for specific concrete members (turbine foundations) without changing strength and performance requirements. (Kim et al., 2013) evaluated the appropriateness and the reduction performance of the low-carbon-emission concrete mix design system and the deduced mix design results using an evolutionary algorithm (EA), the optimal mix design method, which minimizes the CO_2 emission of the concrete mix design.

On other hand,(Hong et al., 2012) proposed an integrated model for assessing the cost and CO_2 emission (IMACC) at the same time. IMACC is a model that assesses the cost and CO_2 emissions of the various structural-design alternatives proposed in the structural-design process. To develop the IMACC, a standard to assess cost and CO_2 emission generated during construction was proposed, along with the CO_2 emission factors in the structural materials, based on such materials' strengths.

However; all of the above studies were concerned with the immediate (short-term) characteristics of concrete and none of them consider the long-term performance and the interplay with eCO_2. When considering different ways to reduce the embodied carbon dioxide, there is a need to consider both the short and long term concrete performance.

1.2 **Scope of the Study**

It is possible to reduce the carbon footprint of construction through several ways including using supplementary cementitious materials (SCM), lower workability mixes or using a superplasticizer. Since different variables may affect eCO_2, it is necessary to examine how these variables also affect physical and durability properties at the same time. This study presents an attempt to minimize the embodied carbon of concrete while maintaining carbonation resistance. The effect of each individual mix design variables such as cement content, maximum size of aggregate, slump value, type of addition of cement replacement, all play an important role in changing the performance of concrete and the carbon dioxide emissions. Whilst there is a basic understanding of the effects of these variables, this understanding has not been combined to consider engineering performance, microstructural development, durability, and carbon footprint in the available previous studies.

To fulfil such a requirement, a number of mix design variables known to give low carbon concrete were varied to examine these effects and their influence on the resulting concrete properties such as strength and durability. This was coupled with microstructural characterization, hence enabling to use low carbon concrete over longer period of time without deterioration caused because of environmental conditions such as carbonation. The concrete and cement paste samples were cast and cured under the same conditions at 20 °C and removed

after specific ages to test the mechanical properties, durability parameters and permeation properties.

All tests that were used in this work are based on specifications outlined by methods of British standards (BS), American Society for Testing and Materials (ASTM). Other tests (permeability and sorptivity) have also been used in the design of tests based on reviewed literature. Concrete samples were tested in order to examine the influence of the mix design variables on the strength, permeation and durability properties. The durability of the concrete samples was examined by an accelerated carbonation test, where the conditions of carbonation included 4% CO_2 concentration, 60% RH and 22 °C temperature. Binder pastes were tested under the same conditions as the concrete samples to investigate their microstructures to relate the performance of low carbon concrete to binder compositions. As part of this project, evaluation of the environmental impact of concrete was also made by making comparisons of calculated embodied carbon dioxide (ECO_2) for each of the concrete mixes, per tonne of production.

1.3 **Significance of Study**

Reports show an annual increase in cement production of 4% due to rapidly increasing construction in developing countries (Damtoft et al., 2008). Due to the excessive cement content in concrete construction and increases in demand, the cement industry aims to identify and use the most appropriate cement content for different applications (pavements, dams, high building, bridges, etc.). Since concrete is the second most consumed entity after water it accounts for around 7% of the world‘s total CO_2 emission (Worrell et al., 2001).

Global warming because of carbon dioxide emissions is a real threat (Limbachiya et al., 2014). Approximately 80% of the greenhouse gas emissions associated with concrete are released during Portland cement manufacture (Flower and Sanjayan, 2007). Therefore, there is pressure from environmental organisations on the cement industry to reduce its carbon footprint.

Considering the direct relationship between the amounts of cement clinker produced and the CO_2 generated, the construction industry aims to reduce its carbon footprint by using several techniques, including reducing the amount of cement in a mixture. The easiest sustainable solution for the concrete

construction industry is using cement more efficiently (Hendriks et al., 1998). In addition to using cement more efficiently, listed hereafter the advantages related to low carbon concrete:

- Little change is required for the preparation of green concrete compared to conventional concrete.
- Reduces environmental pollution.
- Has good thermal and acid resistance.
- Reduces the consumption of cement overall.
- Green concrete is economical compared to conventional concrete.
- Application of lower clinker/binder ratio.

The detailed study presented in this report, on factors affecting the carbon footprint and its relationship to short and long term performance of concrete, will indicate as to how changing mix design variables will have an important role for reducing carbon dioxide emissions while maintaining long-term performance. The significance of this study is systematically looking at mix design variables that affect the carbon footprint and examine how can they affect the performance over the short and long term, considering the system as an integrated whole. Hence, trying to link carbon footprint and concrete performance. However, this is complemented because of an underpinning microstructural study to explain performance. These findings will have an impact on the concrete industry because minimising the cement content in concrete will not only reduce costs but may also lead to more sustainable methods of concrete construction.

1.4 **The Aim and Objectives of Study**

The aim of the present study is to investigate whether the concrete mix design variables which theoretically reduce carbon dioxide emissions have an important role in optimizing the low-carbon in practice, while maintaining the long-term performance (carbonation resistance) of the resulting concrete. The concrete mixes will be tested to understand their eCO_2 and its relationship with concrete mix design variables. Additionally, the short and long-term engineering performance for each mix will be complemented by investigating their microstructures to relate the performance to composition. These steps will give a deeper insight and demonstrate how eCO_2 of concrete is not a simple function

related with changing of mix design variables hence, providing an engineering key (slump value, compressive strength, and drying shrinkage), durability (permeability, sorpitivity and carbonation resistance) and microstructural investigations to compare the performance to compositions. Based on that, a programme and a set of objectives were designed to assess if the proposed concrete mix proportions would achieve the required performance. The major objectives are as follows:

1. To investigate the factors which should result in low-carbon concrete, such as, using chemical admixtures, partial clinker replacement and aggregate size, and use these to design a range of concrete mixes spanning a range of strengths.
2. Examine these mix design variables and their influence on the resulting concrete properties such as strength, permeability and durability specifically (carbonation resistance).
3. To study the relationship between hydration products and the porosity, with regards to control of the carbonation progress.
4. To determine the effects of mix design variables, such as clinker content, addition of pulverized fly ash (PFA), ground granulated blast furnace (GGBS) and fine slag, in addition to the different water-binder ratio (w/b) , on hydration products.
5. Assess the eCO_2 of the concrete mixes in relation to the strength, permeation and durability properties in order to consider the whole-life environmental impact.

1.5 **Methodology of Study**

The programme and methodology of the work are explained in the following chapter (Chapter 3) where the work method of different type of tests on concrete and paste to analyse their mechanical, durability and microstructure will be explained. In subsequent chapters the results of these tests in terms of their mechanical properties (compressive strength, modulus of elasticity and drying shrinkage) durability parameters (resistance of carbonation) and permeation properties (gas permeability and water sorpitivety) are presented and discussed. Among the mechanical properties, performance of low carbon concrete mixes

have been determined to give a key engineering and indication for using it in construction field.

Through the durability parameters, resistance of carbonation to low carbon concrete mixes and the effect of the accelerated carbonation on permeation properties have been investigated. The analytical properties of the microstructure of cement paste to evaluate their hydration products and pore structures are presented and discussed using techniques like thermogravimetry analysis (TGA), scanning electron microscopy (SEM and isothermal conduction calorimetry (ICC).

1.6 **Limitations of the study**

Concerning the factors and variables that were considered in the present work, the findings and limitations of this study are:

- Mix design variables: using supplementary cementitious materials (SCM), lower workability mixes and using a superplasticizer.
- Variables ranges:
    - Binder content (kg/m3): 350, 400 and 450
    - Supplementary cementitious materials (%): 0, 15 and 30
    - Superplasticizer (%): 0.2, 0.6 and 1.0
    - Aggregate Size (mm): 10 to 20
    - w/b ratio: 0.35, 0.45 and 0.55
- Concrete samples were tested in order to examine the influence of the mix design variables on the strength, permeation, shrinkage and durability properties (carbonation resistance).
- Binder pastes were tested under the same conditions as the concrete samples to investigate their microstructures to relate the performance of low carbon concrete to binder compositions.
- ANOVA was used to analyze the effects of mix design variables on compressive strength, carbonation depth and embodied carbon dioxide. Where, ANOVA of test results in this present study was done with the software named MINITAB.
- A set of a durable low-carbon concretes were achieved with reduced Portland cement by incorporating fine slag and coarse slag with 15% and

30%, reduced w/b ratio with 0.35 and reduce the water content by using SP with1.0% (wt%).

This could be adopted by industry for looking to reduce the carbon footprint. If want a low carbon construction, it needs to look for these mixes what coming factors includes slag and w/b.

On other hand, the limitations of this study that the design of mixes didn't based on the specific strength, but rather the strength was an outcome of the mix design. This is the reverse of what would be done in practice. The same applies to workability, where not all of the mixes were really suitable for use on site. The methodology assumed that all of the variables were independent. This is not necessarily the case. Which means that the methodology by Taguchi method does not able to optimize practical levels and rock with rigid matrix and that one of limitations of Taguchi method. Using 15 and 30% replacement are not typical for both SCMs, with 15% being a little low for GGBS and 30% is too high for PFA. That means the percentage of replacements not really realistic, 15% for slag and 30% for PFA.

In concern with the factors and variables that were considered in the present work, the study and its findings are applied to the following practical cases:

a) Cases where the concrete members are constructed with composite cements, if other type of cement is used, it is recommended to fulfil an extension of the work to evaluate the effect of different type of cement.
b) Cases of concrete members having normal crushing strength, for high strength concrete which is manufactured using special additives, an extension of the work is recommended.
c) Cases where normal size of concrete members is used, massive concrete is to be treated according to its own merit.
d) The study is applicable for cases where high carbonation is expected.

1.7 **Layout of Study**

This investigation is presented in eight chapters, as follows:

Chapter One: Introduction, which presents an overview of the report and shows the research aim and objectives.

Chapter Two: Literature review, which presents a brief review of the recent studies that related to the research and the knowledge gap, showing the understanding the cement hydration and SCM. The effect of mix design variables on mechanical and permeation properties.

Chapter Three: Experimental programme, this chapter introduces the details of experimental plan, parameters of the study, material properties, concrete mix, tests specimens and tests procedure.

Chapter Four: The effect of mix design variables on concrete performance which included the compressive strength, drying shrinkage, transport properties, carbonation resistance and the environmental sustainability.

Chapter Five: The effect of paste mix variables on microstructures for blended cement paste and their hydration progress.

Chapter Six: Presents the results and discussion of the relationships between the concrete performance and blended cement composites**.**

Chapter seven: Presents the results and discussion of the relationships between the concrete performance and embodied carbon dioxide.

Chapter Eight: Presents the conclusions and further works.

Chapter 2 : Literature review

2.1 Mix design and components

Concrete is a composite material comprising aggregates of different types and sizes and cementitious paste. The paste binds the aggregates together and when it hardens, concrete becomes a rock-like material. The paste itself is made of cementitious materials, such as Portland cement, pulverised fuel ash, ground granulated blast furnace slag, microsilica and metakaolin, water, and chemical and mineral admixtures. The properties of the hardened mass are governed to a large extent by the properties of the materials used to manufacture the paste. The aggregate is divided into two types, coarse and fine, and the main difference between them is in their size fractions. Normally fine aggregate size ranges from 150 microns (10^{-6} m) to 4.75 mm and the coarse aggregate ranges from size fractions above 4.75 mm, and the nominal maximum sizes of the coarse aggregate are 10 mm, 20 mm and 40 mm. Some small percentages of size fractions other than those specified are normally allowed. As shown in Figure 2.1, in a unit volume of concrete the volume of paste varies from 7% to 15%, water between 16% to 21%, air content in air-entrained concrete between 4% and 8% and the rest is aggregate (i.e. 60 to 75% of the total volume of concrete is occupied by aggregates) (Kosmatka et al., 2011).

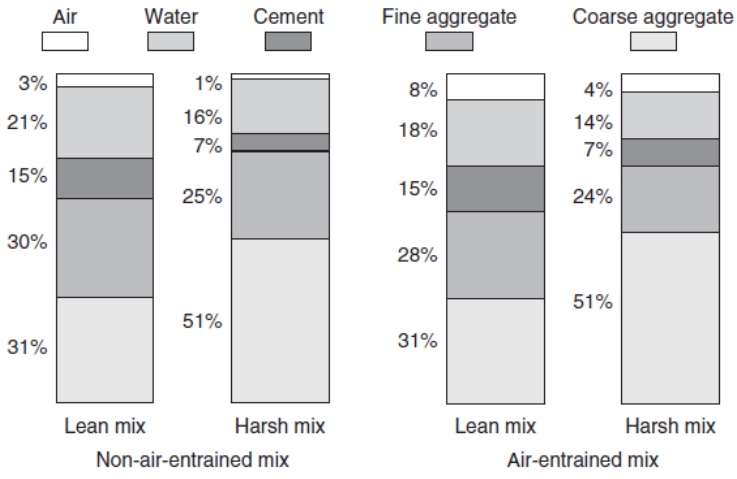

Figure 2-1 Range of relative volumetric proportions of coarse aggregate, fine aggregate, cement, water and air in a cubic metre of concrete (Kosmatka et al., 2011)

The process of selecting suitable ingredients in concrete and determining their relative amounts with the objective of producing a concrete of the required strength, durability and workability, as economically as possible, is termed the concrete mix design. The proportioning of concrete ingredients is governed by the required performance of concrete in 2 states, namely the plastic and the hardened states. If the plastic concrete is not workable, it cannot be properly placed and compacted. The property of workability, therefore, becomes of vital importance.

The purpose of the mix design is to obtain proportions of concrete ingredients which will satisfy certain predetermined requirements, as following:

- the workability of the fresh concrete
- strength of the hardened concrete
- durability of the concrete in the service environment (resistance to cracking, interactions with the service environment that led to chemical and/or physical processes of deterioration, etc.), and
- Short-term and medium-term dimensional stability (shrinkage and creep).

2.1.1 **The contributions of concrete mix design procedures**

In 1881 Preadeau reported the importance of discontinuous granulometry in terms of the volume of voids in the aggregate (Monteiro and Helene, 1994). From his investigations he suggested that in an ‘ideal’ concrete the volume of cement paste should be 5% higher than the volume of voids in the fine aggregate and the volume of mortar should be 10% higher than the volume of voids in the coarse aggregate. This approach was later expanded upon by Lecleroc du Sablon in 1927 (Monteiro and Helene, 1994). Fuller in 1901 made a very significant contribution when he established the effect of granulometry on compressive strength (Monteiro and Helene, 1994). The main findings from his work were the establishment of ‘ideal’ aggregate grading curves that ensured the concrete produced had maximum density (maximum compressive strength). At the time, the main criticism of the Fuller curves was that the concrete produced was harsh and unworkable. To try to correct this, Bolomey in 1925 (Monteiro and Helene, 1994) studied the effect of Fuller’s curves on workability and, after doing this, modified the curves to include the cement content. Although discontinuous

granulometry had been used quite extensively, the two most significant contributions during this period were undoubtedly the correlation between concrete compressive strength and water/cement ratio w/c reported by Abrams (1919, 1922) and the relationship between water content and the consistency of fresh concrete reported by Lyse in 1931 (Monteiro and Helene, 1994). The significance of these two relationships will become clearer as some of the significant individual contributions are discussed.

2.1.1.1 British approach of standard mixes

At one time it was common practice to specify concrete as one part cement, two parts fine aggregate and four parts coarse aggregate (1:2:4) or 1:1:2 when stronger concrete was required (Day, 2006). The main drawback with this approach was that these particular mixes could have very different fresh and hardened properties depending on the grading of the fine aggregate used. To control this, a grading specification was published in 1944 (BS 882: 1944) and two grading envelopes were available: class A and class B. The specification suggested that if class A fine aggregate was proportioned in the ratio 1:2:4 then ‘good’ concrete was produced and if class B fine aggregate was used in the same proportions then ‘reasonable’ but not ‘good’ concrete was produced. Newman and Teychenne (1954) then demonstrated that equally good concrete could be produced from class B fine aggregate provided the relative proportion of fine to coarse aggregate was adjusted accordingly. They proposed the division of fine aggregate into four grading zones instead of two classes (BS 882: 1955). Fine aggregate as a percentage of total aggregate was to range from 40% with the coarsest (Zone 1) to 22% with the finest (Zone 4). Zone 2 at 33% was the old 1:2 ratio (i.e. 1:2:4 and 1:1:2 mixes) and Zone 3 was to contain 25% fine aggregate. This general approach continued into the Road Note 4 (HMSO, 1958) and DoE/BRE methods (Teychenné et al., 1975).

2.1.1.2 BRE method

The first edition of this method was published in 1975 (Teychenne et al., 1975), revised in 1988 (Teychenne et al., 1988) and the current second edition published in 1997 (Marsh, 1997). It is restricted to designing concrete mixes to meet workability, compressive strength and durability requirements. The method was developed primarily for designing concrete mixes containing Portland cements and natural aggregates, but guidance is also given on the application of the

method to mixes incorporating pfa, ggbs and air entrainment. The starting point for the procedure is to specify the characteristic strength (please refer to Marsh, 1997 for a detailed description of statistical concepts used to determine the characteristic strength of concrete) and the workability (in terms of slump) required and the type of cement and aggregates used. From the characteristic strength, the target mean strength is calculated. This calculation is based essentially on the level of quality control likely to be achieved. The next step is to determine the w/c ratio required. The factor that has the greatest influence on the w/c ratio is the specified compressive strength. The graph relationship that is used to determine the required w/c ratio is essentially Abrams' law, modified slightly to take account of aggregate/cement ratio, aggregate and cement type and concrete age. The next step in the procedure is to determine the required water content. This depends primarily on the specified workability, but the maximum size of aggregate and the type of aggregate can also influence the workability. The required water content is simply read from a table that takes account of these factors. After determining the water content, the cement content is calculated by dividing the water content by the w/c ratio. The fresh concrete density is the next parameter to be determined. The graph relationship used for this is essentially the yield equation presented in a slightly different format. The information required to determine the concrete density is the water content and the specific gravity of the aggregates. From the concrete density, the total aggregate content is obtained by subtracting the cement and water contents. The final step in the procedure is to proportion the fine and coarse aggregates. The main influencing factor here is the percentage of the fine aggregate passing a 600 mm sieve determined from the fine aggregate grading curve. The specified workability, the maximum aggregate size and the w/c ratio also influence the required proportion of the fine and coarse aggregates. Combining all this information, the percentage of fine aggregate required is determined. After determining the fine aggregate content, the coarse aggregate content is calculated by simply subtracting the fine aggregate content from the total aggregate content. Another very important feature of this method is that throughout the method provision is made to allow a durable concrete mix to be achieved. As has been reported in many publications, a major factor in providing durable concrete is the production of a dense impermeable concrete which is fully compacted and properly cured. To achieve this, many codes and standards

specify limits on the cement content or w/c ratio to be used. Provision is made in this mix design procedure to override the cement content and w/c ratio values obtained from the specified strength and workability should these calculated values be less stringent than those obtained from durability requirements. The final step in this procedure is to produce a trial mix to confirm that the calculated mix proportions produce a concrete with the required fresh and hardened properties.

2.1.1.3 American Concrete Institute (ACI)

This procedure is probably the most widely used throughout the world. The first version was published in 1944 and the most recent version in 2002 (ACI 211, 2002). It allows mix design for air- and non-air-entrained concrete and concrete containing supplementary cementitious materials. Similar to the previous mix design procedures discussed, the starting point is to specify the required compressive strength and workability and the type of aggregates used. Using a simple table of relationships, from the workability specified and the maximum size of aggregate to be used, the water content is determined. This approach is essentially the same as that used in the DoE/BRE method. The w/c ratio required is determined from the specified compressive strength (Abrams' law). The cement content is calculated by dividing the water content by the w/c ratio. The next step in the process is to determine the coarse aggregate content. The technique used to do this is to proportion the fine and coarse aggregates independently of the specified strength or workability in such a way that 'particle interference' and 'volume of voids' are kept to a minimum. To do this, the dry-rodded volume of the coarse aggregate per unit volume of concrete is used. This is influenced by the maximum size of aggregate and the grading of the fine aggregate (fineness modulus). The actual coarse aggregate content is determined by multi plying the dry-rodded volume of coarse aggregate with the bulk density of the coarse aggregate. The use of the bulk density is quite clever because, in one number, this allows for the combined effect of grading, specific gravity, void volume and particle shape of the coarse aggregate on the desirable fine aggregate content. An estimate of the fresh concrete density for different coarse aggregate sizes is the next parameter to be determined. This is then used to calculate the fine aggregate content by subtracting the water, cement and coarse aggregate contents. Similar to most of the other concrete mix design

procedures, the facility is also available throughout the procedure to override the w/c ratio and cement content determined from the specified compressive strength and workability, should these be less stringent than those determined from durability considerations.

2.2 Factors affecting the choice of mix proportions

The basic factors that affect the choice of mix proportions are as follows (Gambhir and Jamwal, 2014) :

• Compressive strength

• Workability

• Binder content and the use of supplementary cementitious materials

• Grading and type of aggregate

2.2.1 Compressive strength

Probably the most important concrete property is the compressive strength which dominates and also influences the other properties of hardened concrete. (Kong and Evans, 1987) defines the strength of concrete as “the value of compressive strength below which not more than a prescribed percentage of the test result should fall”.

In spite of the importance for other properties such as the durability and shrinkage, which can give assessment for concrete quality, the strength of concrete gives a big indication for this purpose, especially in the structural fields (Taylor et al., 2006). (Salihu, 2011) presented a classification of the concrete classes and their recommended usage in line with BS812 (1975, 1989, 1995) as shown in the Table 2.1. However, these ratios must be treated with caution since variations in the source of raw materials and differences in properties may affect performance.

Based on that, strength is a function which be affected by several variables such as water to cement ratio, aggregate to cement ratio and maximum size of aggregate, etc. (Wassermann et al., 2009, Dhir et al., 2006).

Table 2.1 Concrete grades, mix proportions, and usage.

Concrete grade (N/mm^2)	**Mix proportion** (Cement : Sand : Gravel)	**Recommended usage**
10	1:4:8	Blinding concrete
15	1:3:6	Mass concrete
20	1:2.5:5	Light reinforced concrete
25	1:2:4	Reinforced concrete
30	1:1.5:3	Heavy reinforced concrete/precast
35	1:1.5:2	Pre-stress concrete/precast
40	1:1:1	Very heavy reinforced concrete

2.2.2 **Workability**

It can be assumed that w/c has the greatest influence on strength, whereas the other factors affect the strength indirectly by influencing the water/ cement ratio (Shetty, 2005). Compressive strength is derived from the hydration products formed as a result of the reaction between the cementitious materials and water. These reactions will produce bonding agents between the concrete ingredients and reduce the porosity (Kosmatka et al., 2011). The water content has a major responsibility for the strength of concrete because of the porosity and transition zone will be affected by the amount of water in a negative way or positive away (Mindess et al. 2003; Kosmatka et al. 2002; Mehta and Monteiro 1993). Strength decreases with increasing w/c as a result of capillary porosity increasing as shown in Figure 2.2.

On the other hand, the requirement for workability is considered an important factor to achieve decent performance of structural members. The conventional method for improving workability was by adding more water. However, this affects the strength and durability. Plasticizers help to improve workability, by enhancing the homogeneity and cohesiveness, without increasing the water content, which in turn improve the strength (Shetty, 2005, Alsadey, 2015).

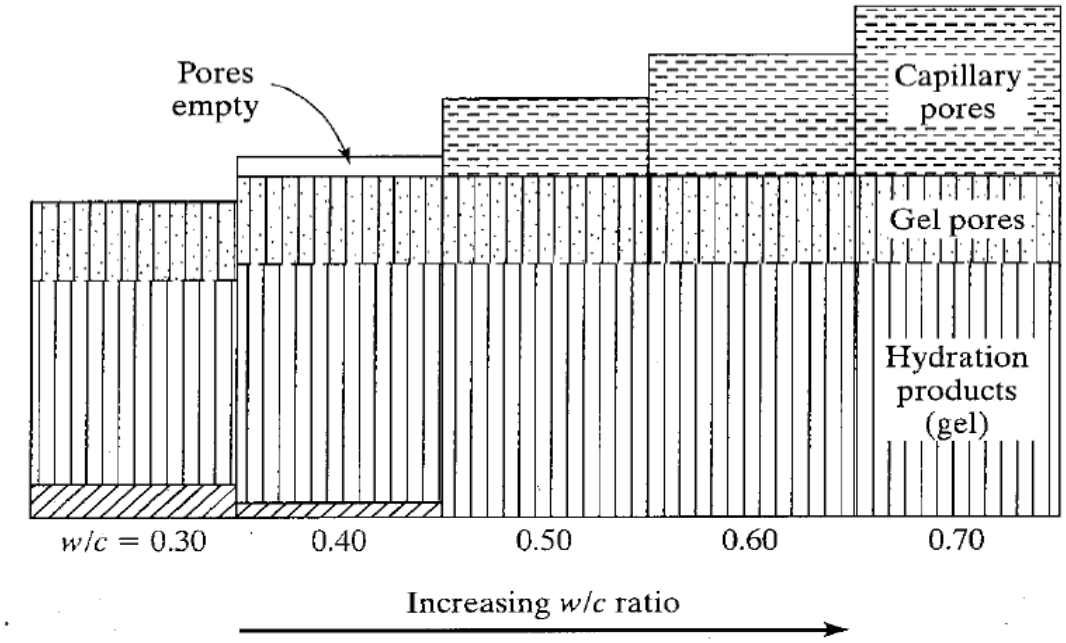

Figure 2-2 The relationship between Porosity and w/c ratio (Mindess et al., 2003)

Water-reducing admixtures work as indirect factors to increase strength due to a reduced w/c (Mindess et al., 2003). Table 2.2 summarizes the types of water reducing admixtures available. The slump value is affected with using the mid and high range of water-reducing positively, with no any side effect on setting time and air entrainment (Mindess et al., 2003).

Table 2-2 Different types of superplasticizer and its affect in workability (Mindess et al., 2003)

Classification	*Common Name*	*Typical Dose* (%)*	*Slump Increase (mm)*	*Water Reduction*		*ASTM Spec.*
				percent	*w/c*	
Low-range	Regular	0.1%	50–85	5–10	−0.05	C 494
Mid-range	Mid-range	0.5%	50–100	10–15	−0.10	
High-range	Superplasticizer	1.0%	>100	15–30	−0.15	C 494, C 1017

*Active ingredient by weight of cement.

2.2.3 **Binder content and use of SCMs**

2.2.3.1 **Cement content**

According to Abrams' rule, strength is a function of w/c and is not affected by the paste content as it is affected by paste quality (Schulze, 1999). The weakness in this rule is the strength requirements cannot be met when the cement content is insufficient. Furthermore, when the cement content is below 350 kg/m^3, it is difficult to obtain high strength concrete (Mailvaganam and Rixom, 2002). These

findings prove that the cement content plays a significant role in determining the strength of concrete. Cement hydration begins when water touches the cement. As hydration continues the strength of concrete increases. Hydration is influenced by the cement composition and fineness, and the cement content. The major compounds are consisted of cement as shown in Figure 2.3. Whereas, the silicate alite (C_3S) hydrates more rapidly than belite (C_2S) and contributes to early strength (Dhir et al., 2006) .

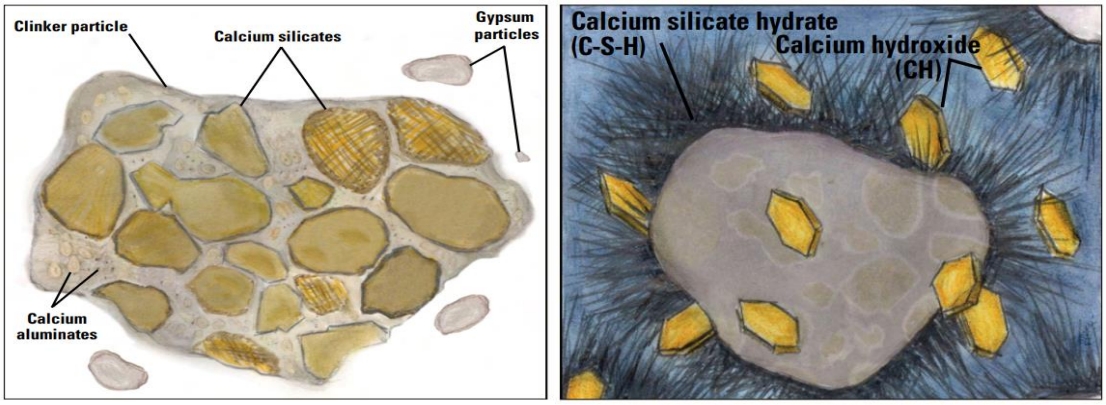

Figure 2-3 Cement components (Taylor et al., 2006)

In contrast, belite (C_2S) hydrates more slowly but continues hydrating longer, thus increasing later strengths by contributing the fill of concrete voids and achieving low permeability. Figure 2.4 shows the cement compositions and hydration products (Taylor et al., 2006).

	Name	Phase (compound)	Shorthand notation	Effect	Amount (%)	
Aluminates		Tricalcium aluminate	C_3A	• Liberates a large amount of heat • Can cause early stiffening and flash set • Prone to sulfate attack	5–10%	Clinker
	Ferrite	Tetracalcium aluminoferrite	C_4AF	• Contributes little to strength • Contributes to gray color	5–15%	
Silicates	Alite	Tricalcium silicate	C_3S	• Hydrates and hardens rapidly • Largely responsible for initial set and early strength	50–70%	
	Belite	Dicalcium silicate	C_2S	• Hydrates and hardens slowly • Contributes to strength increase after one week • Contributes to low concrete permeability	15–30%	
Sulfates	Gypsum*	Calcium sulfate	$C\bar{S}$	• Controls the hydration of C_3A	3–5%	Gypsum

Figure 2-4 Cement microstructure (i) compounds in cement (Ohga and NagatakiI) hydration products (Taylor et al., 2006)

There are a number of stages to cement hydration, as illustrated in Figure 2.5. At first stage (pre-induction period) occurs, producing an alkaline sulphate solution, as a result of gypsum and clinker dissolution after adding the water directly. This results in the formation of small crystals of ettringite, formed through the reaction between aluminate gel and sulphate (Hewlett, 2003).

At the second stage, the heat flow drops and this is known as the induction period, which can take a few hours. The third stage of hydration is where the concrete gets its strength, based on the reactions of alite and belite producing calcium silicate hydrate and calcium hydroxide.

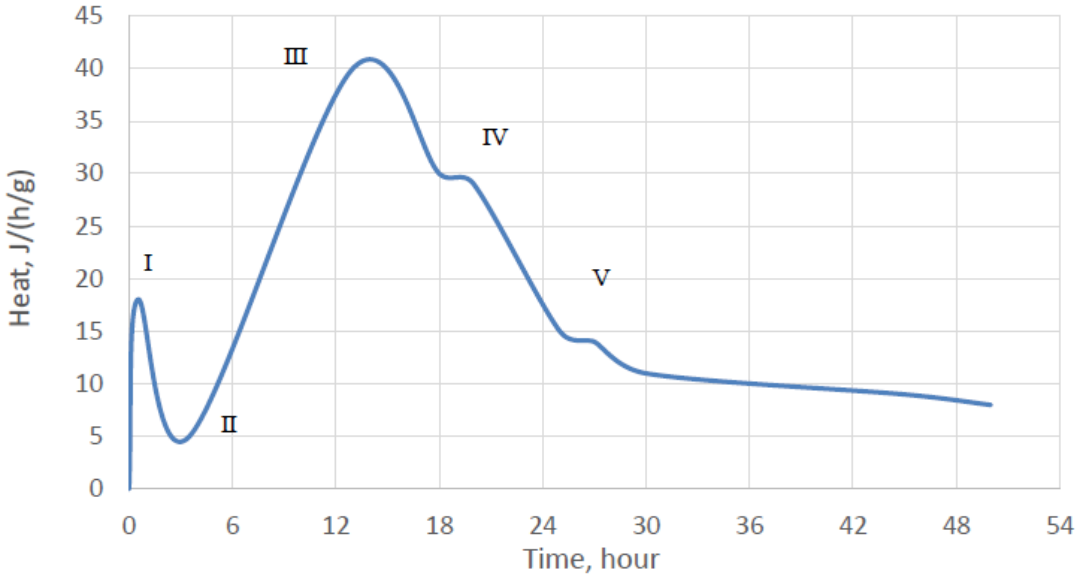

Figure 2-5 Heat flow curve for hydrating Portland cement (Hewlett, 2003)

Ettringite formation still continuous due to interaction between sulphates in solution and C_3A. However, once the sulphate is consumed, there is conversion of ettringite to monosulfate. Monosulfate begins to appear as hydration products at stage five. During the 7 days, ettringite will disappear while $Ca(OH)_2$ and C-S-H is created. By 28 days, most of the hydration has occurred and the C-S-H fills many of the pores (Sivakumar and Ravibaskar, 2009).

2.2.3.2 **Supplementary Cementitious Materials**

There are many types of SCMs that used as a replacement to reduce producing and using the CEMI. The main benefit of replacing the PC with SCMs is reducing the emission of CO_2 (Lothenbach et al., 2011). There is a different type of SCMs that used as a replacement, the most commonly used are GGBS and PFA. SCMs

types may be classified into two categories; pozzolanic materials and latently hydraulic materials (Hill and Sharp, 2002).

What characterizes a pozzolanic material is a low CaO and high SiO_2 which means the material won't hydrate without presence of an activator. In other words, when the clinker reacts with water the produced CH will react with these materials (pozzolanic) and form C-S-H. As for latently hydraulic materials, their chemical composition lays between pozzolanic material and PC. Therefore, they will hydrate like PC to from C-S-H, additionally, the can react with CH to form C-S-H (Hill and Sharp, 2002). Figure 2.6 illustrates the basic chemical composition of various SCMs compared to Portland cement.

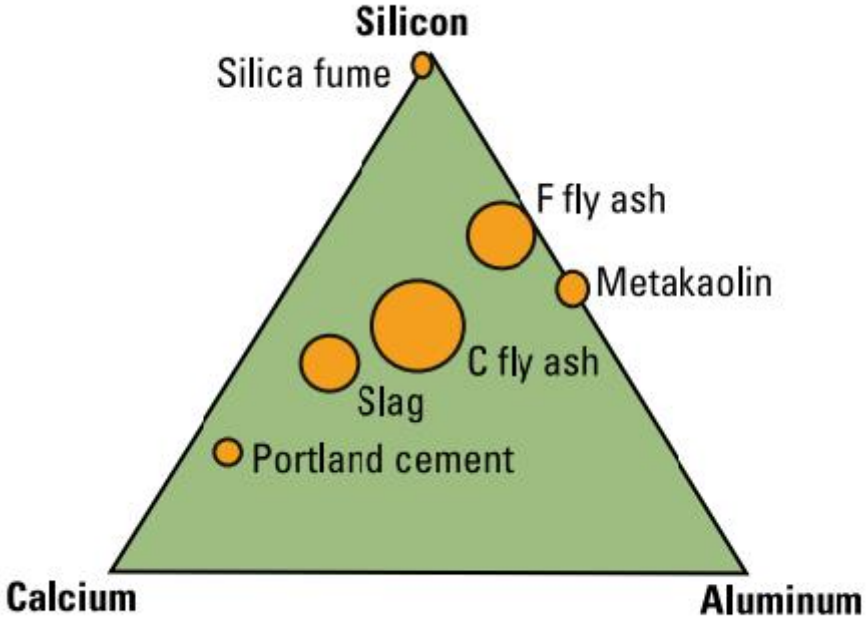

Figure 2-6 Ternary diagram various SCMs compared to Portland cement (Taylor et al., 2006)

Using supplementary cementitious materials as Portland cement replacement reduces the pore sizes and the porosity which in turn increases the strength (Barbhuiya et al., 2009) . However, the effectiveness of an SCM depends on the chemistry, fineness and the content of SCM.

2.2.3.2.1 Ground Blast Furnace Slag Blended Cement

Concrete which contains granulated blast-furnace slag and fly ash gets lower strength at an early age compared with neat Portland cement concrete. However, these materials increase the ultimate strength in the long term (Mehta and

Monteiro, 1993). Figure 2.7 illustrates the role of pozzolanic materials on the hydration of paste

Blast furnace slag is a by-product of the iron manufacturing process. The process includes removing the impurities from the iron. Where the slagging agent removes the impurities from the iron as a result of float the slag on top of the molten iron. The slag essentially consists of silicates and aluminosilicates of calcium and other compounds (Liu et al., 2010). The chemical composition of slag basically consists of four Components i. lime ii. silica (SiO_2) iii. alumina (Al_2O_3) and iv. magnesia (MgO) and some minor components of sulphur in the form of sulphide and ferrous and manganese oxides. This proportion of the components may vary depending on the nature of the iron ore, the composition of the limestone flux, the coke consumption and the kind of iron being made (Moranville-Regourd, 2003).

It has been observed that the glass content influences slag activity (Liu et al., 2010). Where the relationship between the strength and glass content is linear, which means the increasing of crystalline content reduce the engineering properties of concrete (Moranville-Regourd, 2003).

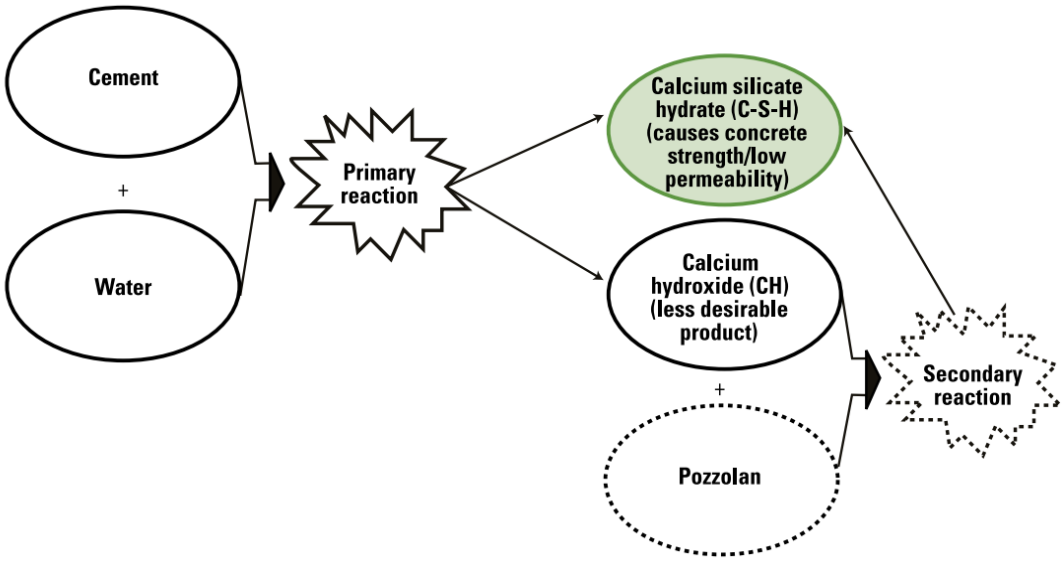

Figure 2-7 Effect of pozzolans on cement hydration (Taylor et al., 2006)

GGBS is a latently hydraulic material which means that it may react with water, but the reaction rate is greatly increased by the addition of an activator such as lime. Thus, hydration of slag is influenced by calcium hydroxide (CH) resulting from Portland cement hydration. Both calcium hydroxide and calcium silicate

hydrate (C-S-H) are Portland cement hydration products, but when GGBS is used, the C-S-H content will increase due to the slag's reaction with CH (Taylor et al., 2006). Thus, strength and permeability are enhanced by using SCMs.

The hydration of slag is affected by Portland cement and a different kind of activator such as alkaline activators and sulfate activators which in turn specify the hydration products of GGBS. Table 2.3 describes the slag hydration under impact different kind of activators.

Table 2-3 Slag hydration products in the presence of various activators

Nature of activator	Crystalline phases
Portland cement	C-S-H, AFt, AFm, Hydrogarnet C_3AH_6, hydrotalcite $Mg_6Al_2(CO_3)(OH)_{16}{\cdot}4(H_2O)$ like phase, and vicatite ($C_3S_2H_3$)
NaOH, Na_2CO_3, Na silicate	C-S-H, C_4AH_{13}, C_2AH_8, $Mg(OH)_2$
$Ca(OH)_2$	C-S-H, C_4AH_{13}
Sulfate eg. gypsum, hemihydrates, phosphogypsum	C-S-H, AFt, $Al(OH)_3$

The GGBS hydration reactions are slower than those during cement hydration, which causes low heat flow compared with CEMI. (Kolani et al., 2012) have shown that pastes containing 30% CEMI and 70% GGBS give lower heat lower than paste containing 100% CEM I as shown in Figure 2.8

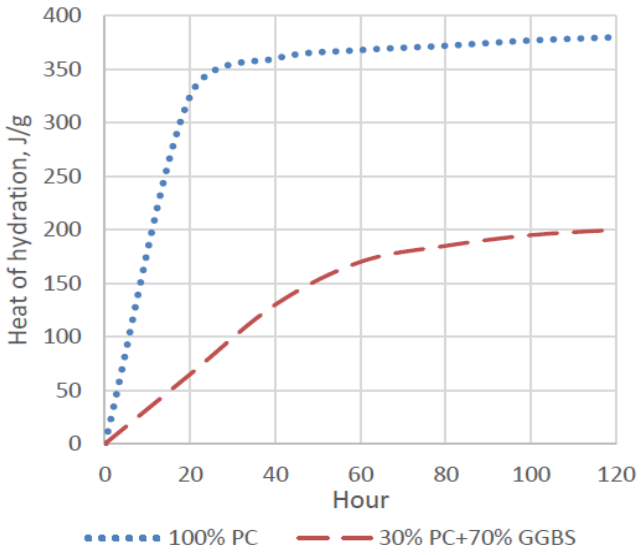

Figure 2-8 heat of for 100% PC and 30% slag plus 70% PC (Kolani et al., 2012)

The hydration of GGBS can be induced rapidly by increasing the w/c and curing temperature, where the excess amount of water provides more space for hydration (Escalante et al., 2001).

When GGBS and cement hydrate, the process may similarly be divided into stages. The first stage of hydration is dominated by dissolution of alkalis and sulphates. At the second stage, the hydration of Alite and Belite is formed by OH- which produced by CH (Siddique and Bennacer, 2012, Pal et al., 2003). Additionally, using GGBS as a replacement produces more C-S-H at a later age of hydration process in which turn that can get more chance to fill the capillary porous and gaps with this product. On another hand, the C-S-H which produced from GGBS will be more stable which has lower CaO/SiO_2 and higher Al_2O_3/SiO_2 (Taylor, 1997).

On the other hand, Adding GGBS to the binder has an effect on the heat of hydration release. This impact appears aa the second peak due to the GGBS hydration, this means that the dissolution of alite is quicker, resulting in its early hydration (Gruyaert et al., 2010). However, the magnitude of this peak reduces because of the total volume of alite being replaced with the GGBS. That means the adding GGBS causes an acceleration in hydration at the initiation but at the same time reducing the amount of C-S-H which cause lower heat flow because of the specific area for GGBS is high which means low C-S-H production (Stark et al., 2007).

2.2.3.2.2 Pulverised Fly Ash Blended Cement

Fly ash is a pozzolanic material comprising SiO_2, Al_2O_3, and Fe_2O_3 in a reactive system (Neville, 2011). Fly ash is produced by burning pulverized coal in power stations. It contains spherical glass particles which are formed as a result of rapid cooling of melted minerals from combustion of pulverized coal. Fly ash is classified into two types based on the lime percentage; Class F with CaO contents below 10% and class C ashes with CaO contents higher than 20%. The difference between the two classes is that fly ash C doesn't require an activator compared with class F.

Fly ash hydration starts when the high pH induced by cement hydration causes partial dissolution of the aluminosilicate within the ash. The aluminosilicate ions then combine with portlandite to produce calcium aluminosilicate hydrates (C-A-

S-H). The resultant hydrates are: C-S-H, $Ca(OH)_2$, Ettringite, Tetracalcium aluminate hydrate (often carbonated), Monosulfoaluminate, C_2ASH_8 (gehlenite hydrate), and $CaCO_3$. (Thomas, 2013).

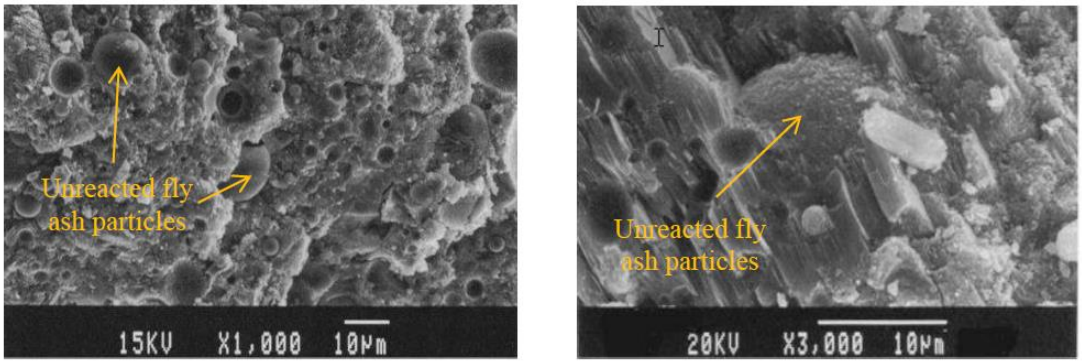

Figure 2-9 Hydrated cement paste with 30% fly ash (class F) (Aimin, 1997)

Because of the slow reaction of pozzolanic materials, since CH is only present after the initial hydration of alite and belite (Luke, 2002), only a small proportion of fly ash will be reacted at early age and the remainder needs longer to complete hydration. Thus, $Ca(OH)_2$ is gradually consumed when water is available. Figure 2.9 shows the hydration of 30% fly ash at 90 and 180 days. which illustrates that the fly ash particles are not completely hydrated (Aimin, 1997).

As cement hydration progresses during the early stages of the reaction, the CH content increases until the pozzolanic reaction is activated. Once triggered the OH^- provides the conditions needed to break down the structure of PFA leading to the formation of C-S-H gel. This C-S-H can fill the pores, resulting in the blocking up of the larger capillary pores or air voids with hydration product.

As for PFA, the value of CaO/SiO_2 is low and the ratio of Al_2O_3/SiO_2 is higher than in Portland cement. This change in composition leads to a change in C-S-H morphology, where the fibrillar structure changes to a fine foil-like structure which in turn refines the pore structure. Additionally, Luke et al. and Lothenbach et al. also highlighted that the hydration of PFA produces AFt and AFm and other hydration products like calcium aluminate hydrate and strätlingite. However, because of the differences in CaO/SiO2 ratios, this makes the C-S-H gel produced more chemically stable. Also, the CH content is significantly reduced. Finally, because there is less free CaO ion available, the amount of AFt produced in PFA blended cement will be far less, which results in a concrete that's less reactive with sulphates.

Regarding the heat flow of hydration when adding PFA to blended cement, the peak of heat evolution reduces as results of replacing alite with PFA (Klemczak and Batog, 2016). This also means more water is able to hydrate the PC when the PFA content increased (Escalante-Garcia and Sharp, 1998). (Bai et al., 2000, Baert et al., 2008) concluded as the replacing PFA with PC leads to retarding on initiation of alite hydration which in turn reduce the amount of C-S-H and causes lower heat flow.

2.2.4 **Aggregate**

The effect of aggregate size on strength differs based on the concrete type, with the strength decreasing when using larger aggregates, due to a lower surface area which in turn reduces the gel bonds (Shetty, 2005). Another reason is the development of microcracks which results in a weakness of the transition zone (Mehta and Monteiro, 1993). Figure 2.10 describes the influence of aggregate size on compressive strength for different w/c ratios.

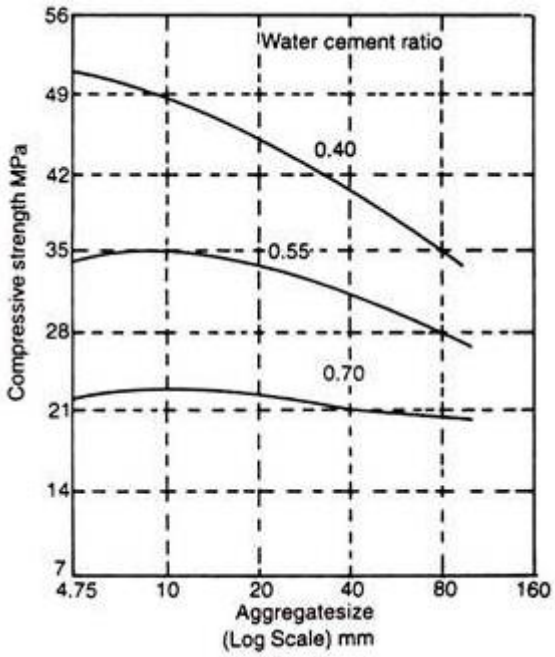

Figure 2-10 Effect of aggregate size on concrete strength with different w/c ratio

However, it is observed that the strength of concrete is positively affected by increasing the size of aggregate, specifically in lean concrete due to lower surface area and it makes the w/c ratio low which gives higher strength (Cordon and Gillespie, 1963). Figure 2.11 depicts the effect of aggregate size on strength.

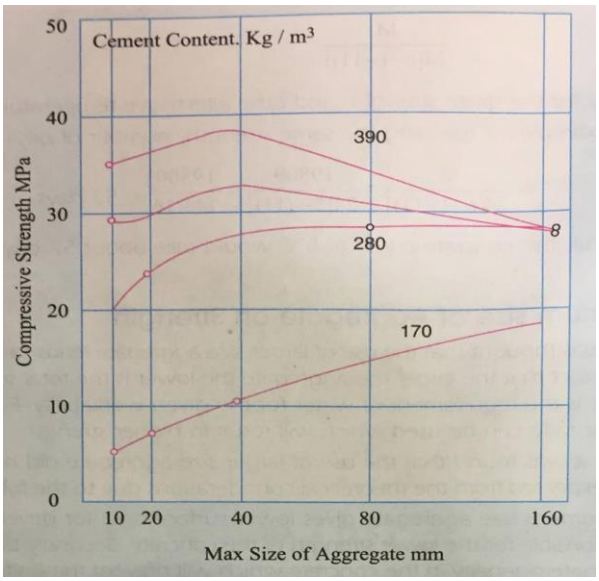

Figure 2-11 Effect of aggregate size on concrete strength with different cement content (Shetty, 2005)

2.3 Concrete Durability Assessment (carbonation resistance)

The essential principle for concrete design is to perform the required functions such as the strength and serviceability up to the expected service life. Thus, the concrete must resist deterioration throughout its service life. Many factors can be responsible for the deterioration, be they internal or external, and these aspects can be classified further, such as physical, chemical and mechanical.

In the following sections, the external chemical deterioration by carbon dioxide is discussed to understand all aspects and the relationships between the mix design parameters and the carbonation progress.

2.3.1 Carbonation

Carbonation is the process by which CO_2 reacts with hydrated cement. The process occurs as CO_2 diffuses through the concrete, dissolving in the pore fluid and reacting with the alkaline hardened cement paste. Based on the reaction, the pore fluid properties change as the result of $Ca(OH)_2$ conversion to $CaCO_3$ which in turn lowers the pH and destroys the alkaline passivating layer on reinforcement steel, potentially leading to corrosion (Neville, 2011).

2.3.2 Mechanism and chemistry of carbonation

The air contains carbon dioxide. The gas cannot react directly with cement hydrates, except when dissolved in water. When carbon dioxide dissolves in the

water which leads to form bicarbonate and because of the high pH of concrete the bicarbonate dissociates and forms carbonate ions that in turn react with hydrates of cement Ca ions in pore solution and precipitate calcium carbonate crystals (Lagerblad, 2005a). The carbonation process is described by the following chemical reactions (Lagerblad, 2005a):

1. CO_2 (g) + H_2O = HCO_3 - (bicarbonate ion) +H^+

2. HCO_3- = CO_3^{2-} (carbonate ion) + H^+

The carbonate ion will react with Ca ions in the pore solution.

3. $Ca^{2+} + CO_3^{2-} = CaCO_3$

Calcium carbonate ($CaCO_3$) may assume one of three crystallographic forms aragonite, vaterite and calcite. A schematic diagram of carbonation process is shown in Figure 2.12

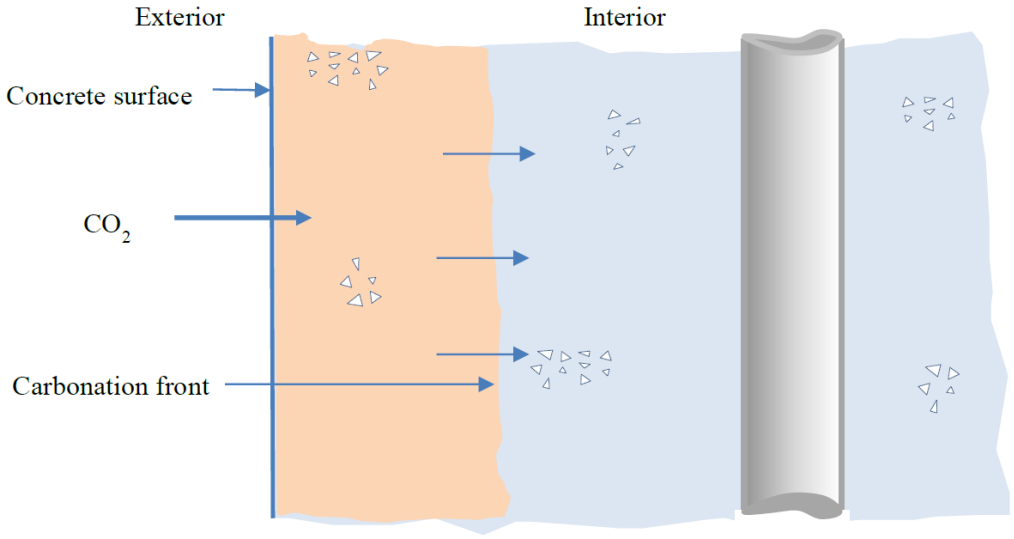

Figure 2-12 Carbonation progress (Abu Saleh, 2014)

The precipitation of $CaCO_3$ comes from consuming $Ca(OH)_2$. Furthermore, the other components of the cement paste (calcium silicate hydrate and ettringite/monosulphate) will be affected when (CH) is consumed and the pH falls, unsettling the equilibrium of these components. However, some amount of Ca will exist inside the silica gel (Lagerblad, 2005a).

The mechanism of carbonation reaction has an important effect because it's responsible for the changes that happen for the carbonated layer. The mechanism of carbonation reaction has an important effect because it’s responsible for the changes that happen in the carbonated layer. Carbonation

itself is influenced by the cement paste composition, which in turn, is affected by the paste content, the presence of SCMs, the period of curing and the water content. All of these factors have effects on the quantity of carbonatable matter, which correlate inversely with the carbonation progress (Lagerblad, 2005a).

The two major things controlling the carbonation mechanism are solubility and speed of diffusion. Diffusion relies on the concentration of carbon dioxide and the humidity inside the concrete which means when the concrete is dry the speed of penetration of carbon dioxide will be fast but there will not be enough water to dissolve the carbon dioxide and get carbonate ions for carbonation reaction. On another hand, when the concrete fully saturated just the carbonate ions can move inside the concrete but the carbonation process will be slow. Based on that, the carbonation speed depends on the optimum value of water content which dissolves the CO_2 and which not prevent gas diffusion. Figure 2.14 shows the effect of humidity which represents the water content inside the pores which affects the progression of carbonation.

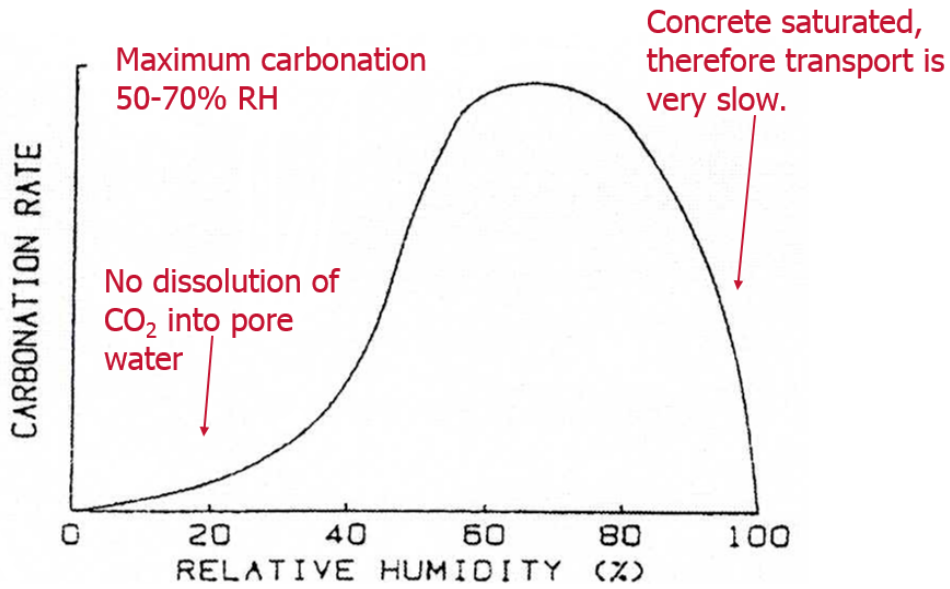

Figure 2-13 Schematic representation of the rate of carbonation of concrete effects by relative humidity

Factors affecting carbonation

Carbonation is a chemical process and is affected by physical and chemical properties of concrete (Abu Saleh, 2014). Among the environmental factors are, water-cement ratio, cement content and using SCMs.

2.3.2.1 **Grade of concrete**

The rate of carbonation is influenced by the type of cement and the degree of hydration, factors which also affect the strength of concrete. Thus the carbonation rate is a function of concrete strength (Neville, 2011). (Neville, 2011), with the rate of carbonation decreasing when the strength of concrete high because of the stronger concrete is denser and less permeable. For this reason, the diffusion of CO_2 will be slower, as shown in Figure 2.14, (Shetty, 2005). The cement content should meet the requirement of durability, which the ACI recommended that the minimum cement content should be not more than the values in Table 2.4 to meet the workability and durability requirements (Kosmatka et al., 2011)

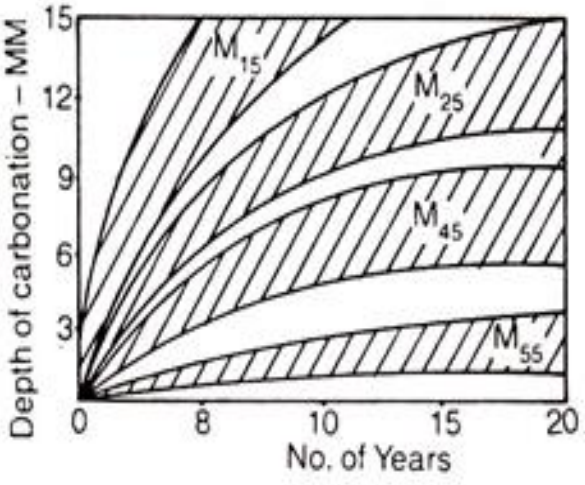

Figure 2-14 Carbonation depth as a function of concrete strength (Shetty, 2005)

Table 2-4 Minimum contents of cementitious materials for concrete structure members

Nominal maximum size of aggregate, mm (in.)	Cementitious content, kg/m^3 (lb/yd^3)*
37.5 (1½)	280 (470)
25 (1)	310 (520)
19 (¾)	320 (540)
12.5 (½)	350 (590)
9.5 (3/8)	360 (610)

* Cementing materials quantities may need to be greater for severe exposure. For example, for deicer exposures, concrete should contain at least 335 kg/m^3 (564 lb/yd^3) of cementitious materials.

Source: ACI 302

2.3.2.2 **Water cement ratio**

Water to cement ratio is the most important factor defining concrete porosity. When the cement content is constant, a lower water-cement ratio leads to denser concrete. For concrete with 0.6 w/c, the carbonation depth would be 15mm after 15 years, while concrete with 0.45 w/c, the carbonation depth will reach 15mm just after 100 years (Gao et al., 2013).

(Valcuende and Parra, 2010) studied the carbonation resistance of SCC with limestone filler and found that lower w/b reduced the carbonation depth. Based on that, the dense concrete depends on the water/ cement ratio which in turn reduce the porosity and the porosity connection when the w/c low and that helps to low the carbonation progress (Lagerblad, 2005a). In other words, lower w/c or w/b with high degree of hydration give much dense concrete with less connective porosity. It will also result in denser carbonate products and in same time slow down carbonation in all environments. Also, denser microstructure and increased tortuosity due to the reduction of water/cement ratio reduce the ingress of carbon dioxide, thus reduce the carbonation. Improvement of permeation properties would improve the resistance to the carbonation process.

On the other hand, superplasticizers help to maintain workability with reduced w/c ratio. This, in turn decreases the capillary porosity. Thus, the diffusion of CO_2 will be reduced and the carbonation rate decreased.

2.3.2.3 **Supplementary cementitious materials**

The carbonation rate is simply a function of concrete strength. For this reason, the reactions for SCMs are slow but a higher strength can get in late ages comparing with Portland cement (Lagerblad, 2005a). The action of supplementary cementitious materials has conflicting consequences. Firstly, the pozzolanic reaction consumes $Ca(OH)_2$ and reduces the pH. However, conversely, the reaction also forms C-S-H which fills the capillary pores and slows carbonation (SCHUBERT, 1987). Due to this twofold action should know the positive and negative effects of using SCMs on the durability of concrete.

The SCMs can be classified into three categories, inert mineral fillers, latent hydraulic binders and pozzolanas.

Granulated blast furnace slag (GGBS) is latently hydraulic and does not require an activator, this means that it can be used at higher replacement levels.

Portland-slag cement (CEM II/A-S) contains up to 20 % granulated blastfurnace slag (GBFS). CEM II/BS contains up to 35 % and CEM III contains between 35 and 95 % GBFS. The hydration of GGBS consumes CH to produce more C-S-H. Moreover, the C-S-H will have a lower Ca/Si ratio (Taylor et al., 2007). According to (Trill and Kawamura, 1992) the carbonation rate when using a mineral additive will; be higher than Portland cement. (Bouikni et al., 2009) noted that the concrete containing 65% GGBS had a higher carbonation depth than 50% slag

Fly ash is a pozzolanic material and may be mixed with Portland cement in different percentages such as CEM III and CEM IV. The role of pozzolanas depends on the degree of reaction and the rate. The pozzolanic reaction is accompanied by CH consumption with increasing C-S-H production. The structure and the mode of carbonation will be affected depending on the type and the amount of pozzolana (Lagerblad, 2005a).

When adding PFA, concrete carbonation increases (Ho and Lewis, 1987). (Thomas and Matthews, 2004) reported an increase in concrete carbonation in the case of using fly ash in comparing with concrete without FA. However, (Ohga and NagatakiI, 1989) reported that the carbonation depth decreased despite using PFA in concrete when keeping the concrete strength high. In addition, (Siddique, 2011) found that a PFA content of between 25% and 35% in concrete slowed the carbonation depth. For this reason, it can be said that addition of fly ash to concrete depends on two-fold. Knowing the effective amount which used and the impact on the strength development.

(Shi et al., 2009) investigated the different percentage of FA and GGBS and found that the FA increases the carbonation depth at level (0-60%) with 0.3 w/b ratio. Also, they observed that concrete which contained 30% FA and 0.25 w/b ratio showed greater carbonation than that of concrete with GGBS.

2.3.2.4 **Binder content**

The diffusion will occur in the paste and not through aggregate, assuming that the aggregate is dense. The amount of cement does not affect the rate of carbonation as long as the w/c ratio is kept constant (Concrete Society 1999). This is due to fact that the flux (J) is measured as material passing through a unit area and that the unit area becomes larger with an increasing amount of cement paste. Thus a larger amount of paste with the same porosity will give the

same carbonation depth but a larger volume of carbonated paste. Thus, in order to estimate the carbonated paste volume, the amount of cement in the concrete mix must be known (Lagerblad, 2005a).

2.4 Effect of concrete variables on drying shrinkage

Concrete may be subjected to changes in volume and this volume change is an important property for long-term performance. Shrinkage is defined as the loss of free water from the hardened concrete (gel pores water) which leads to a change in the volume (Zhang et al., 2013a). One of the most important negative side effects in concrete is the presence of cracks which occur for several reasons including shrinkage.

One of the most important factors affecting concrete shrinkage is w/c ratio. Decreasing the water content of concrete leads to decreased shrinkage, as shown in Figure 2.20 (Kosmatka et al., 2011).

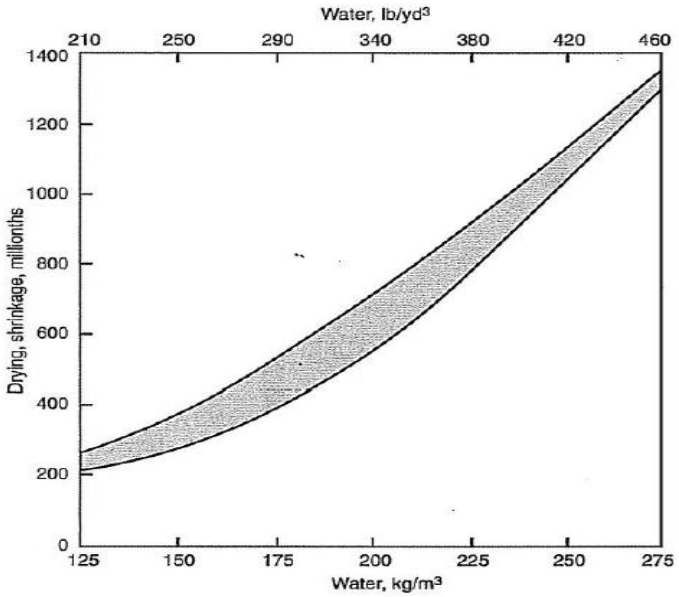

Figure 2-15 Effect of water content on shrinkage (Kosmatka et al., 2011)

Another important factor which affects shrinkage behaviour is aggregate size. Coarse aggregates reduce the shrinkage of concrete which occurs during cement hydration (Kosmatka et al., 2011). Meanwhile, increasing the maximum size of aggregates causes an increase in shrinkage due to the increasing the stress load between the blended cement and the aggregate at the interfacing zone (Mindess

et al., 2003). However, increasing the aggregate content could decrease the shrinkage of concrete as shown in Figure 2.21.

Cement content plays an important role in shrinkage properties. (Wassermann et al., 2009) state that shrinkage decreases when the cement content increases in order to decrease the w/c ratio and this shrinkage reduction because of water content reduction. But shrinkage increases when cement content increases at a given w/c ratio due to there being more cement to shrink (Dhir et al., 2006). (Schmitt and Darwin, 1999) found a relationship between cement content and cracking and stated that concrete with a high amount of cement cause more shrinkage.

On the other hand, shrinkage is affected by using supplementary cementitious materials as replacements, with the results using ground granulated blast-furnace slag depending on the proportions and conditions. For instance, (Lim and Wee, 2000) found that using GGBS in concrete at 0%, 30%, and 50% replacement gave increased shrinkage at 91 days. In addition, the autogenous shrinkage increased due to the high fineness and this led to more cracks.

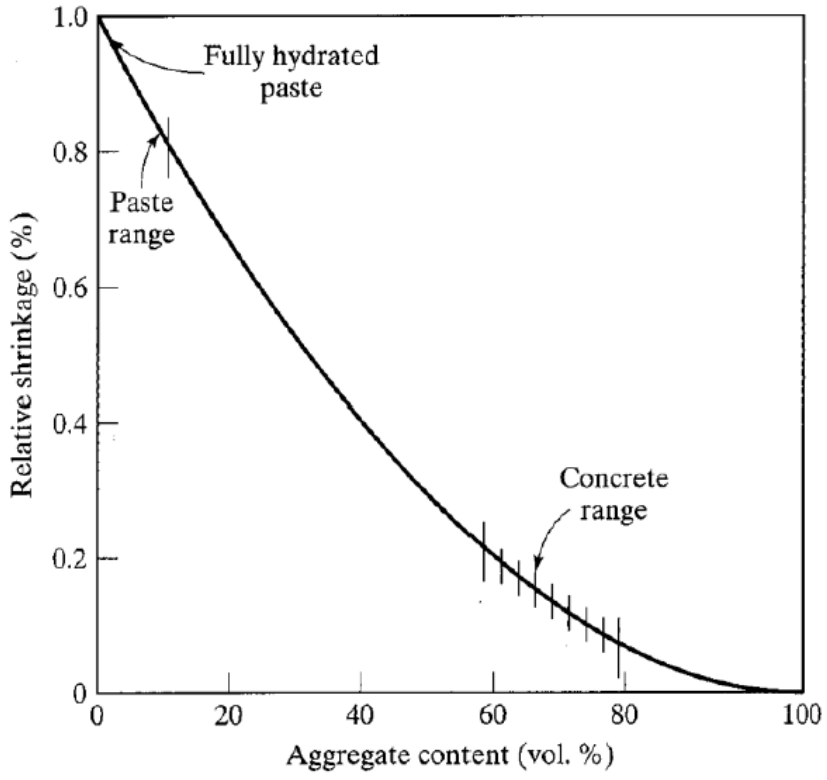

Figure 2-16 The relationship between aggregate content and the shrinkage of concrete and paste (Mindess et al., 2003)

Concrete containing fly ash shows different shrinkage behaviour due to the delayed hydration of fly ash which causes a decrease in shrinkage. (Khatib, 2008, Gesoğlu et al., 2009) reported that using FA and in SCC has reduced the shrinkage and the addition amount of FA results in a clear reduction in shrinkage as shown in Figure 2.22.

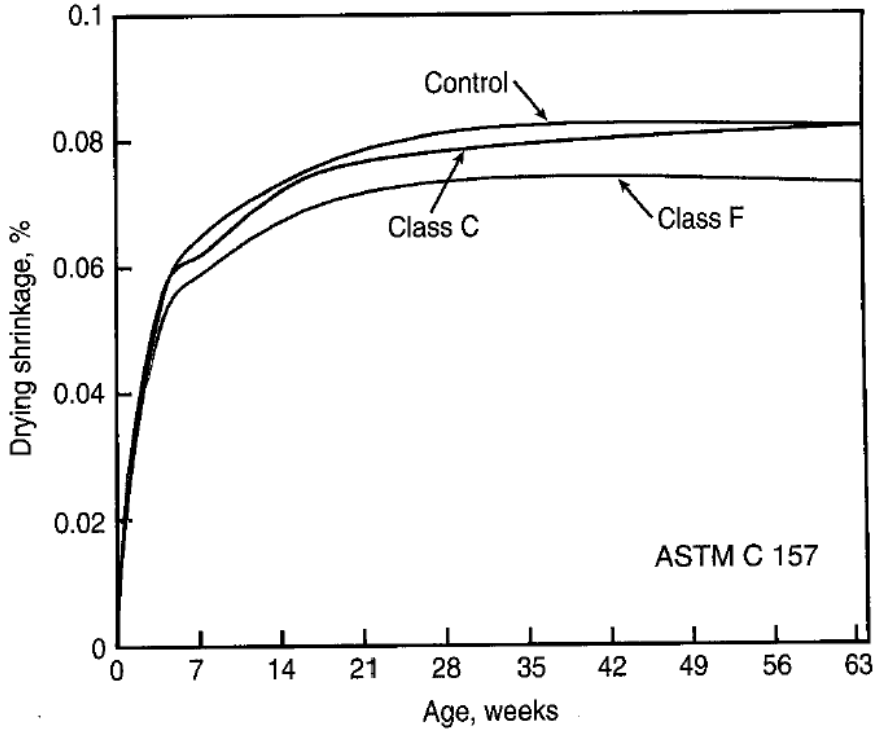

Figure 2-17 The role of PFA incorporation on shrinkage compared with Portland (Gesoğlu et al., 2009)

2.4.1 **Durability indices (transport properties)**

Concrete is a durable material, but because of aggressive environments, it can be subjected to degradation under different conditions. Deterioration depends on the movement of water and gases inside the concrete. Based on that, the transport properties are the most important factors affecting the mechanism deterioration. The ability of materials to transport fluids or gases can be defined as penetrability which covers the concepts of permeability, sorption, and diffusion (Mindess et al., 2003). Permeability of concrete is controlled by the microstructure of cement in which diffusion by the capillary porosity (Richardson, 2014).

(Kosmatka et al., 2011) defines concrete permeability as a function of the permeability of the paste, the permeability and gradation of the aggregate, the

quality of paste and aggregate related transition zone, and the relative proportion of paste to aggregate (Kosmatka et al., 2011). However, the concrete variables have an influence on permeability mechanism as well. The concrete consists of cement paste and aggregates that influences the type of porosity and its distribution. Figure 2.16 shows the diversity of pores inside the cement paste. (Aligizaki, 2014) classified the pores found in concrete into different types:

- Cement paste pores (gel-, capillary- and hollow-shell pores and air voids)
- Pores in aggregates
- Pores inside the ITZ
- Water voids which are created by water bleeding
- Pores in cement paste caused by humidity and temperature variations.

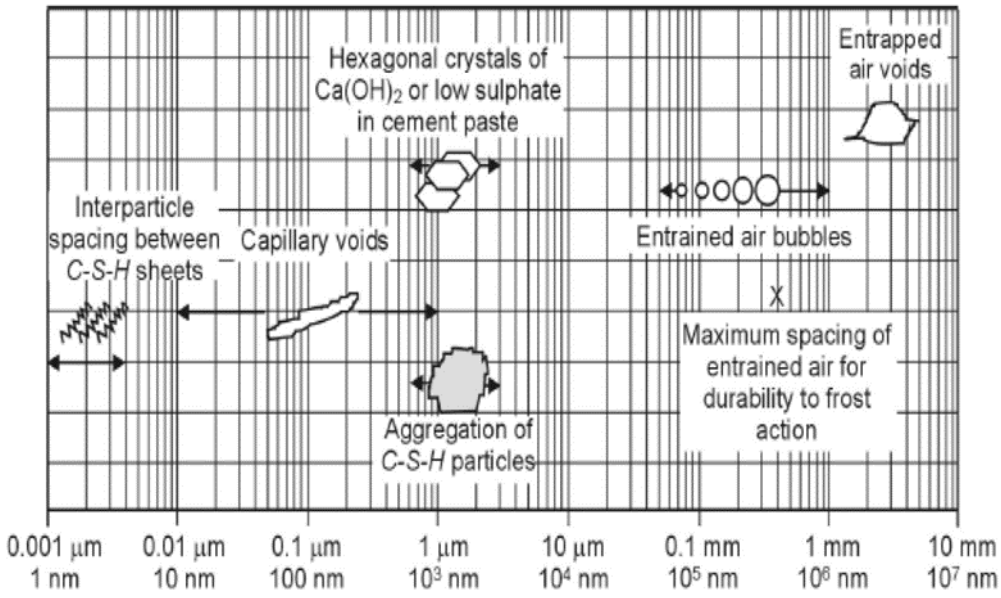

Figure 2-18 pores system in cementitious paste

W/C ratio affects the concrete permeability according to its effects on paste porosity, in that reducing the w/c ratio decreases the paste porosity and so decreases the concrete permeability as shown in Figure 2.12 (Mindess et al., 2003). Figure 2.17 shows the relation between the w/c and capillary volume, which in turn clarifies the reason of w/c ratio affects the permeability (Hansen, 1986).

The permeability can be affected by the cement properties, in that the coarse cement leads to form hardened cement paste with increased porosity compared with fine cement (Hanaor and Sullivan, 1983). Whereas, the presence capillary cavities inside the paste reduce the strength of the paste and low the dense.

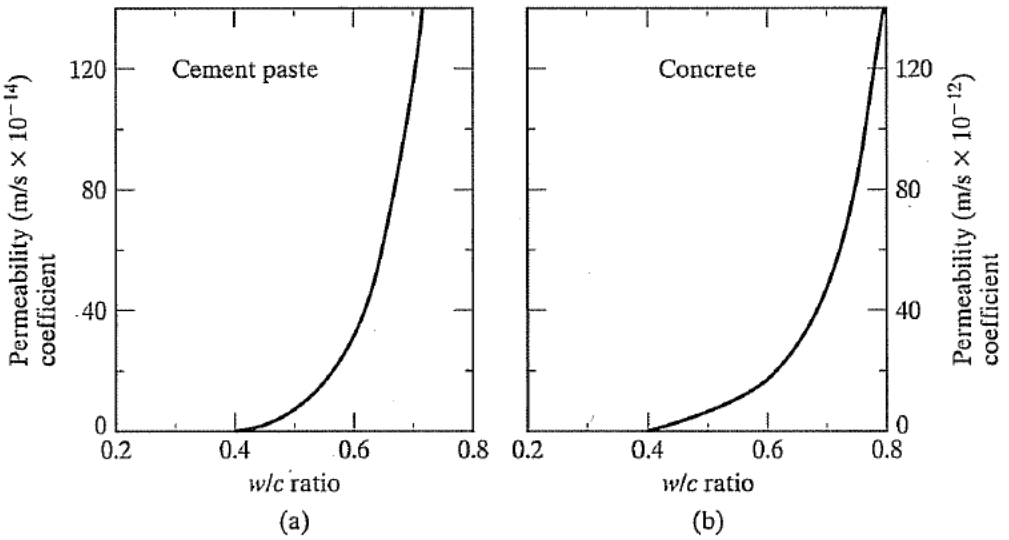

Figure 2-19 Effect of w/c ratio on permeability for cement and concrete samples (Mindess et al., 2003)

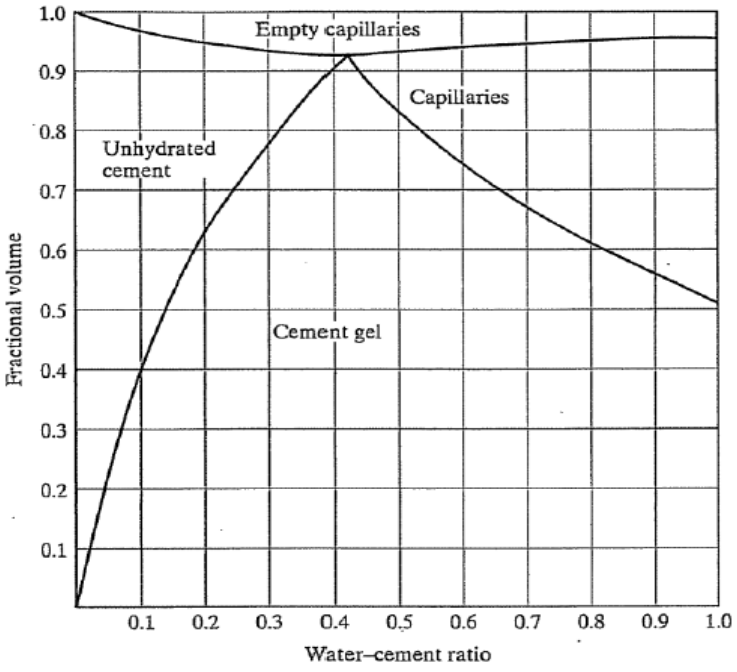

Figure 2-20 The effect of w/c on the capillary volume (Hansen, 1986)

The ITZ is developed as a result of the formation of a thin water film adjacent to aggregate particles in the fresh paste. Adhesion of the paste to aggregates takes place through this narrow (20–50 lm) layer of weaker paste around aggregate grains, with different microstructure and porosity. The role of aggregates is centred on formatting the ITZ which considers weakness point between the paste and the aggregate and any increasing of this layer lead to decrease the

permeability (Kang, 2010). However, the influence of aggregates on permeability is small and the significant effect of permeability revert to the capillaries existed in cement paste (Neville, 2011). (Basheer et al., 2005) reported that the aggregates size affected permeability. Figure 2.19 showed that the increase of aggregates size has increased the permeability index.

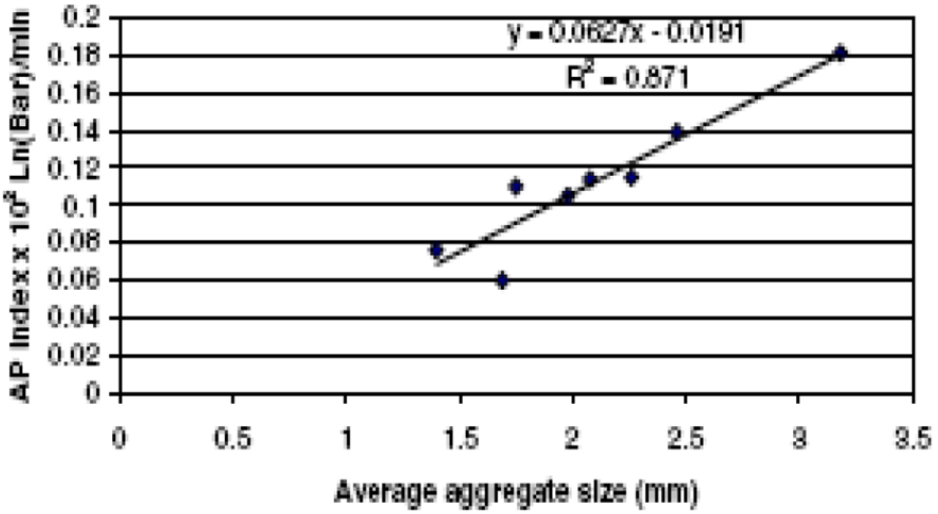

Figure 2-21 Influence of maximum aggregate size on air permeability (Basheer et al., 2005)

Supplementary cementitious materials have an important role significantly controlling the permeability and porosity of concrete. In general, using SCMs as a replacement for CEMI decreases the permeability, depending on the amount, the type of SCMs and concrete properties(Barbhuiya et al., 2009). The big effect of replacing CEMI with SCMs is on the ITZ by densification the bonding agent by reducing the portlandite content and enhancing the microstructure at the ITZ (Gao et al., 2005). On the one hand, some studies mentioned that fly ash and GGBS increase the permeability when using mineral admixture (Shi et al., 2009), while many researchers reported that using fly ash and GGBS has a significant effect on permeability. The reason for the reduction in permeability is the pozzolanic reaction reducing the fine capillary volume, reducing the pore continuity (Feldman, 1984, Hooton, 1986).

2.5 **Embodied carbon dioxide and sustainable concrete**

Each of the raw materials used in concrete construction consumes energy during its production, in turn emitting carbon dioxide. Embodied carbon is a methodology to assess the CO_2 emissions associated with the production of a given quantity

of material (functional unit). This methodology encompasses all stages of a material's production, from the extraction of the raw materials, through its production, conversion into a finished good, its lifetime and finishing with any treatment at the end of its life (Dixit et al., 2012). Most analyses of eCO_2 in construction have concluded that it is dominated by the emissions associated with the industrial production of materials (BIS, October 2011).

Concrete is the world's predominant construction material, with global production approaching 20×10^{12} kg per annum, significantly more than all other construction materials combined; and increasing (Krausmann et al., 2009). Clinker is the main material used in cement and releases just less than 1t of CO_2 per tonne of clinker produced (Habert and Roussel, 2009). However, concrete consists of many other major materials, being a complicated composite offering a wide palette of engineering properties such as compressive strength, workability, permeability, chemical resistance etc. Each of these properties can vary dramatically depending on mix design in most cases there are many mix recipes that will result in a concrete which fulfils the designer's requirements (Purnell and Black, 2012).

Based on that, many commentators have published the values of eCO_2 for concrete either as individual values or a small range depending on specific properties (mainly compressive strength grade and the use of supplementary cementitious materials).

(Purnell, 2013) classified the embodied carbon dioxide calculation according to whether the concrete was reinforced or not. Plain concrete is critically dependent on the mix design and the compressive strength grade, while the embodied carbon dioxide of reinforced concrete is related to structural design and loading. (Hammond and Jones, 2008) used 0.13 kg CO_2/kg for plain concrete and 0.24 kg CO_2/kg for 2% reinforced concrete, the additional carbon dioxide attributable to reinforcement, whilst (Flower and Sanjayan, 2007a) used different values for concrete depending on the using the SCMs. Where 0.23 $teCO_2/m^3$ (100% cement), 0.273 $teCO_2/m^3$ (25% FA) and 0.251 $teCO_2/m^3$ (40% GGBS). Other studies have focused on how to reduce the emission of carbon dioxide (CO_2) from cement production. (Habert and Roussel, 2009) evaluated two different environmental options for sustainable concrete mix-design. The first one is the substitution of clinker by mineral additions in cement in order to reduce the environmental cost of the material for a given volume of concrete produced. The

second one is the reduction of the concrete amount needed for a given construction process by enhancing the concrete properties. (Gartner, 2004) discussed the practicality of replacing Portland cement with alternative hydraulic cement that could result in lower total CO_2 emissions per unit volume of concrete of equivalent performance. An alternative solution is to use natural pozzolans, although they must still be activated either by Portland cement or lime or by alkali silicates or hydroxides, the production of all of which still involves significant CO_2 emissions, but the eCO_2 reduction can be as low as 10% lower in concrete volume than pure Portland concrete.

2.5.1 Embodied CO_2 in cement

The embodied carbon dioxide of concrete depends on the cement, where the cement percentage ranges between 12%- 15%. of total concrete by weight. In 2001 around 1.6 billion ton of cement was used around the world, which represents very nearly 7% of the world's aggregate CO_2 emission (Mehta, 2001). Cement production has increased to 2.5 billion ton in 2009 and the anticipation number of cement production would be 3.2 billion ton in 2020. The eCO_2 of 1 tonne of Portland cement is 930 kg. This is due to the process by which cement is manufactured (BCA, 2009). (Abu Saleh, 2014) mentioned that CO_2 emissions in cement production is due to two stages:

- Burning of fuel to create for the energy required to raise the kiln temperature to 1450°C, and the subsequent grinding of the clinker.
- The calcination of limestone ($CaCO_3$).

The normal amount of cement is in concrete varying depending on mix design requirements and concrete performances. Based on that, the embodied CO_2 of 1 cubic metre of concrete is about 100 to 300 kg of CO_2 is released for each cubic meter of cement, or approximately 5% to 13% ($kgCO_2/kg$) of concrete weight, depending on the mix design (Marceau et al., 2007).

2.5.1 Embodied CO_2 in blended cement

To diminish the eCO_2 of the concrete, Portland cement or clinker can be replaced by supplementary cementitious materials (SCMs), for example, ground granulated Blast blast furnace slag (GGBS), fly ash, microsilica, rice husk ash, or inert materials. As all these cementitious materials are industrial by-products results of different materials, the eCO_2 of these materials is to low (Abu Saleh,

2014). The embodied carbon dioxide of blended cements is classified in the Table 2.5. So can be seen that there is a direct relationship between the reducing eCO_2 values and using replacement materials, as listed in the British Standard for 'Concrete – Complementary British Standard to BS EN 206-1' BS 8500:2006. Figure 2.22, shows the CO_2 emissions depending on the amounts of SCMs besides clinker. It shows the raw materials related and energy-related CO_2 emissions in the production of composite cement as a function of the content of other main cement constituents (Hoenig and Schneider, 2002).

Table 2-5 Embodied carbon dioxide for different types of Portland cement (BCA, 2009)

Types of common cement	Proportions (%)	eCO_2 (Kg-CO_2/ ton)
CEMI	95-100 Clinker	930
CEM II/A-LL or L Portland limestone cement	6–20 Limestone	880 - 750
CEM II /A-V Portland fly-ash cement	6 - 20 Fly ash	870 - 750
CEM II/B-V Portland fly ash cement	21 - 35 Fly ash	730 - 610
CEM II/B-S Portland slag cement	21 - 35 GGBS	740 - 620
CEM III/A Blast furnace cement	36 - 65 GGBS	610 – 360
CEM III/B Blast furnace cement	66 - 80 GGBS	340 – 230
CEM IV/B-V Pozzolanic cement	36 - 55 Fly ash	590 - 420

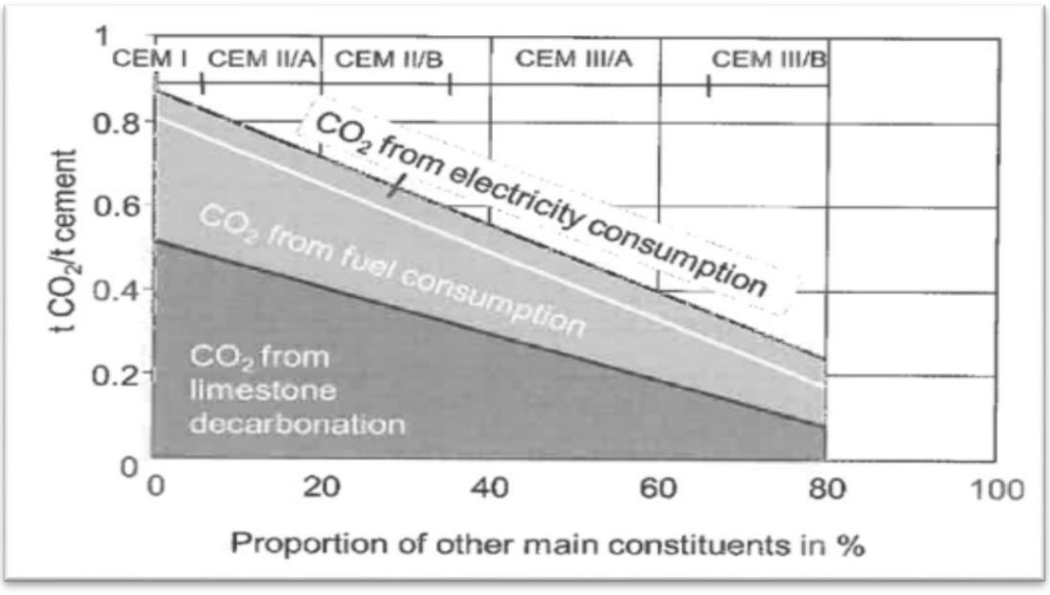

Figure 2-22 Carbon dioxide emissions according to the content different cement types (Hoenig and Schneider, 2002)

2.5.2 Embodied CO_2 in aggregate

All-inclusive the aggregate utilization of sand, rock and crushed rock is around 10-11 billion ton a year (Mehta, 2001). While aggregates comprise the largest volume fraction in cement, at about 70-80% by weight, the embodied carbon dioxide of aggregate is low compared to Portland cement. Subsequently, aggregates do not make a large contribution to the eCO_2 of concrete.

2.5.3 Embodied CO_2 in admixtures

Apart from the three main ingredients of concrete (cement, water and aggregate) mineral and chemical admixtures when added to concrete tend to raise the amount of eCO_2 according to energy that required for processing and transportation (Mehta, 2001).

(Flower and Sanjayan, 2007b) illustrated the effect of different types of superplasticizer which included four different admixture types, as shown in Table 2.6. However, the impact of superplasticizer is quite small as the amount of admixture added to the concrete tends to be very small.

Table 2-6 Effect of superplasticizer on CO_2 emissions

Admixture type	Primary raw mMaterial	Production energy (kWh/L)	CO_2 emissions (t CO_2-e/L)
Superplasticiser	Polycarboxylate	0.0037	5.2×10^{-6}
Set accelerating	Calcium nitrate	0.0380	53×10^{-6}
Mid range water reducing	Calcium nitrate	0.0290	40×10^{-6}
Water reducing	Lignin	0.0016	2.2×10^{-6}

2.6 The carbon footprint due to concrete

Materials used for concrete structure typically consists of a mixture of Portland cement, fine aggregate, coarse aggregate, water and admixtures to improve workability. Supplementary cementitious materials such as fly ash, ground granulated blast furnace slag, or silica fume are used as partial replacements for

Portland cement. The production of Portland cement involves considerable generation of CO_2 and accounts for approximately 5–7% of anthropogenic CO_2 emissions worldwide.

Cement typically comprises 12–16% by weight of structural grade concrete. Given the volume of concrete used in concrete constructions, that cement constitutes about 90% of the carbon footprint of concrete.

The carbon dioxide emissions of concrete constituents have been analysed by different authors. For example, (Purnell, 2013) presented the eCO_2 of reinforced concrete as a function of: concrete strength grade; steel strength; mix design; cement replacement; and structural form. Where the suggestion was that ECf is minimised by using C50 concrete. Savings in ECf achieved by adjusting mix design parameters (20–35%) generally exceed those achieved by replacing cement with pulverised fuel ash (10–25%). Also, C50 beams of all mix designs have lower ECf than comparable timber composite or steel beams.

There are a number of ways to reduce the greenhouse gas emissions from concrete production. A key approach is partially replacing the clinker with other equivalent materials considered as additives, such as; fly ashes from coal-fired thermal power plants, slag from blast furnaces in the iron and steel industry, natural pozzolans, limestone fillers, and various other wastes (Elchalakani and Elgaali, 2010). These additives contain large quantities of reactive SiO_2 and Al_2O_3, which produce cementitious materials in the presence of lime. (Habert and Roussel, 2009). Using additional cementitious materials such as fly ash or slag and silica fume in binary and ternary systems in concrete has adopted and promoted to achieve the sustainability (Yang et al., 2015).

Much work on eCO_2 underestimates the complicated relationship with concrete mix design (Purnell and Black, 2012). The production of concrete, a major construction material, emits a large amount of CO_2 from the material production stage, such as in the production of cement, aggregates, and admixtures, to the manufacturing stage. Various aspects of the concrete mix design process can affect eCO_2 (Kim et al., 2013).

Many commentators have published eCO_2 values for concrete, either as individual values or a small range, depending on certain properties (mainly compressive strength and the use of supplementary cementitious materials) (Purnell and Black, 2012). Previous work has analysed either the embodied

carbon dioxide (ECO_2) of plain concrete as a function of strength grade and mix design. (Hammond and Jones, 2008) give a general value of 0.107 $kgCO_2/kg$ and a monotonic relationship between eCO_2 (0.061 – 0.188 $kgCO_2/kg$) and characteristic cube strength (8 – 50 MPa) for CEM I and CEM II concretes. However, they do advise against the indiscriminate use of these values. Meanwhile, (Hacker et al., 2008) uses a value of 0.200 $kgCO_2/kg$ with no strength discrimination, whilst Harrison uses 0.13 $kgCO_2/kg$ for plain concrete and 0.24 $kgCO_2/kg$ for "2% reinforced"; the additional CO_2 attributable to the steel. Among those reporting on a volumetric basis, (Flower and Sanjayan, 2007a) use values of 0.225 - 0.322 $kgCO_2/m^3$ for normal and blended cement concretes, corresponding to eCO_2 ~ 0.09 – 0.12 $kgCO_2/kg$. (Purnell, 2013) analysed the variation of EC per unit of structural performance for reinforced concrete components as a function of concrete compressive strength grade, reinforcement steel strength and concrete mix design for beams, short columns and slender columns. In a theoretical study (Purnell and Black, 2012) calculated the eCO_2 for 512 concrete mixes as a function of the most important mix design variables concluding that considerable eCO_2 savings can be made by careful attention to basic mix design. On the other hand, (Berndt, 2015) reported that the selection of concrete ingredients and appropriate design could be used to reduce carbon dioxide emissions for specific concrete members (turbine foundations) without changing strength and performance requirements. (Kim et al., 2013) evaluated the appropriateness and assessed the reduction potential of a low-carbon concrete mix design system and deduced mix design results using an evolutionary algorithm (EA) to optimise the mix design to minimize the CO_2 emissions. Meanwhile, (Hong et al., 2012) proposed an integrated model for assessing the cost and CO_2 emissions (IMACC). IMACC is a model that assesses the cost and CO_2 emissions of various structural-design alternatives proposed in the structural-design process. To develop the IMACC, a standard to assess cost and CO_2 emissions generated during construction was proposed, along with the CO_2 emission factors in the structural materials, based on such materials' strengths.

Several studies with different types of replacements provide discriminate values for embodied carbon dioxide of concrete. Producing sustainable concrete with a low carbon foot print is among the aims of many researches. It is well known that

the production of OPC produces a carbon foot print of about 1000 kg/m^3 (Malhotra and Mehta, 2008).

(Elchalakani et al., 2014) presented the experimental test results of 13 types of concrete mixes made with high volume of ground granulated blast furnace slag (GGBFS) cement with 50%, 60%, 70% and 80% replacement of ordinary Portland cement (OPC) to reduce the carbon emissions. A fly ash-blended mix made with 30% fly ash was also tested. The results showed that the slag concrete mixes significantly reduce the carbon footprint and meet the requirements of strength and sustainability. Where the concrete mix with 80% GGBFS and 20% OPC was nominated for use in the future construction with 154 kg/m^3 carbon foot print.

On the other hand, some methods have been proposed for the material design of low-CO_2. Based on neural networks and the genetic algorithm, (Yeh et al., 2007) proposed software for designing concrete mixtures with the lowest possible cost. (Mosaberpanah and Eren, 2018) proposed a full factorial method to maximize the strength and minimize the carbon dioxide emissions. The effects of cement content, silica fume content, fiber content, water-to-binder ratio, and superplasticizer are considered for determining strength and CO_2 emissions. (Yang et al., 2016) proposed an approach for designing low-CO_2 concrete containing various supplementary cementitious materials such as fly ash, slag, and silica fume. (Tapali et al., 2013) proposed an iteration approach to design concrete with a low environmental cost, considering strength and service life. (Khan et al., 2016) designed low-cost high-strength self-compacting concrete using a response surface methodology. The optimal combinations of cement, water-to-binder ratio, fine aggregate, fly ash, and superplasticizer were determined using a desirability function.

Many studies have evaluated the CO_2 emissions of concrete by incorporating mineral admixtures.

(Robati et al., 2016) found that the application of supplementary cementitious materials can reduce CO_2 emissions by 16% compared with general practices. (Zhang et al., 2019) proposed that concrete containing silica fume and fly ash shows superior environmental performance over plain concrete. (Passuello et al., 2017) reported that the use of rice husk ash-derived sodium silicate can reduce the environment impact of geopolymer concrete by about 60%. (Teh et al., 2017) determined greenhouse emissions of blended concrete based on process-based

life cycle assessment and hybrid life cycle assessment. They found that hybrid life cycle assessment resulted in higher greenhouse emissions. (Oliveira et al., 2016) estimated CO_2 life cycle emissions of concrete block manufacturers and found that cement consumption is the dominant factor for CO_2 emissions. (Kim et al., 2017) determined greenhouse gas emissions for concrete with different strengths. They found that the raw material stage accounted for more than 90% of the greenhouse gas emissions.

Although many studies have been conducted to evaluate the CO_2 emissions of concrete, the number of studies on mixture designs of low-CO_2 concrete is relatively insufficient. (Kim et al., 2016) proposed an evolution algorithm to produce concrete with minimum CO_2 emissions or cost. Based on the optimization method, 34% of CO_2 emissions can be reduced compared to the standard concrete production process. (Park et al., 2013) used a genetic algorithm to design low-CO_2 concrete containing recycled concrete aggregate. The required properties of concrete, such as workability, strength, carbonation, and drying shrinkage, were considered (Park et al. 2013).

(Yang et al., 2015) examined the effectiveness of supplementary cementitious materials (SCMs) such as ground granulated blast-furnace slag (GGBS), fly ash (FA), and silica fume(Sulapha et al.), in reducing CO_2 emissions from ordinary Portland cement (OPC) concrete. The CO_2 intensity decreased sharply as the substitution level of the SCMs increased up to approximately 15–20%, beyond which the rate of decrease gradually slowed. In general, the binder content and CO_2 intensities could be formulated as a function of the individual substitution level of each SCM.

(Turner and Collins, 2013) showed the comprehensive carbon footprint estimates for both geopolymer and OPC concrete, including energy expending activities associated with mining and transport of raw materials, manufacturing and concrete construction. The eCO_2 of geopolymer concrete is 9% less than OPC.

(Paya-Zaforteza et al., 2009) described a methodology to design reinforced concrete (RC) building frames based on minimum embodied CO_2. The method indicated that the embodied CO_2 and cost are closely related and that more environmentally-friendly solutions than the lowest cost solution are available at a cost increment which is quite acceptable in practice. Further, the best solutions for the environment are only at most 2.77% more expensive than the best cost

solutions. Alternatively, the best cost solutions increase CO_2 emissions by 3.8%. Finally, the methodology suggested that structural engineers will be able to mitigate CO_2 emissions in their RC structural designs

Otherwise, (Berndt, 2015) showed that the CO_2 emissions associated with concrete foundations has been analysed to examine means of reducing the materials-related impact on the carbon footprint of wind power construction. The effects of strength class, cement content, partial replacement of cement and use of recycled concrete aggregate were investigated. It was determined that use of 32 MPa class concrete rather than 40 MPa can reduce the concrete generated emissions by at least 11%. The greatest decrease in emissions for the studied mixes was found for concrete with 65% replacement of cement with blast furnace slag and the reductions were 42.7–44.8%, depending on strength class. The use of recycled concrete aggregate resulted in moderate reductions in emissions and would have other environmental benefits. The study has shown that selection of concrete constituents and appropriate mix design can be used to minimise CO_2 emissions associated with large wind turbine foundations without compromising strength and performance requirements (Berndt, 2015).

While, (Long et al., 2015) reported it is possible to design green self-compacting concrete by understanding the relationship between the mixing proportion parameters of self-compacting concrete (SCC) and its environmental impact. Results indicated the ecological impact index of SCC closely depends on the mixing proportions. The addition of high volume mineral admixtures not only can effectively reduce the eCO_2 and e-resource indices but also decrease the e-energy index. Selecting a reasonable aggregate volume can help decrease the environmental impact of SCC. Employing recycled limestone sand to replace river sand will increase the eCO_2 index and energy index of SCC. Regardless of the mixing proportion parameters, the eCO_2, e-energy and resource index of SCC both decrease with the increasing compressive strength for SCCs with a compressive strength ranging from 30 to 60 MPa

On the other hand, the calculation of eCO_2 for concrete classifies for two types, one of them for reinforced concrete and another for concrete which considers more complex. It comprises contributions from cement, reinforcing steel, aggregate, water and admixtures, which are combined in an almost infinite variety of proportions according to the design requirements of the structural component

under study. While some investigators have used single values for carbon dioxide emissions (e.g. Hacker et al., 2008; Harrison et al., 2010), it has been shown that the EC of reinforced concrete is in fact a strong function of structural design and loading (Purnell and Black, 2012), whereas that of plain concrete is critically dependent on the mix design and the compressive strength grade (Purnell and Black, 2012).

Past studies have often focused on one or two life-cycle stages, most frequently product or construction embodied energy and carbon dioxide.

(Vukotic et al., 2010) analysed the life-cycle embodied energy and carbon dioxide emissions of a building's structural elements, and examined which stages within a building's life are the most significant and offer the most opportunities for a reduction of embodied energy and carbon dioxide. A simple single-storey structure was used as a case study to perform comparative analyses between two structural design alternatives: glue-laminated timber panels and steel frame with infill concrete blockwork.

(De Wolf et al., 2016) described a specific method by quantifying material weights and finally calculating embodied carbon dioxide. The survey contains data on 200 recently completed buildings obtained from industry. The results showed that structural material quantities vary between 200 kg/m^2 and 1800 kg/m^2 and embodied carbon dioxide various over the range 150–600 kgCO_2/m^2

A life cycle inventory (LCI) was determined for concrete with slag cement used as a partial replacement for Portland cement. The LCI was determined for three combinations of cement for each concrete performance criteria: 100 percent Portland cement, and 35 and 50 percent substitution of slag cement for the Portland. Energy, CO_2 emissions to air, and most other emissions to air are significantly reduced when slag cement is used as a partial replacement for Portland cement in concrete. The slag cement mixtures produced an energy savings ranging from 21.1 to 48.4 percent; a savings in carbon dioxide emissions of 29.2 to 46.1 percent; and a virgin material savings of 4.3 to 14.6 percent when compared with 100 percent Portland cement concrete mixtures (Prusinski et al., 2004).

2.7 **Taguchi method**

The quality engineering method proposed by Taguchi is commonly known as the Taguchi method or Taguchi approach. The Taguchi method is a systematic application of design and analysis of experiments to design purposes and quality improvement for products (Ross and Ross, 1988). Recently, the Taguchi method has become a promising tool which has the ability to enhance productivity by optimizing the quality of products in line with quick producing and low cost, where many applications have been used the Taguchi method in different industry and engineering fields (Yang and Tarng, 1998)

This approach provides an experimental strategy in which a modified and standardized form of design of experiment (DOE) is used. In other words, the Taguchi approach is a form of DOE with special application principles. This technique helps to study the effect of several factors (variables) on the desired quality characteristic most economically. By studying the effect of the different factors on the experimental results, the best combinations can be identified (Unal and Dean, 1990).

Ten steps need to be followed systematically during Taguchi design (Antony et al., 2006). Figure 2.23 clarifies the steps of Taguchi design.

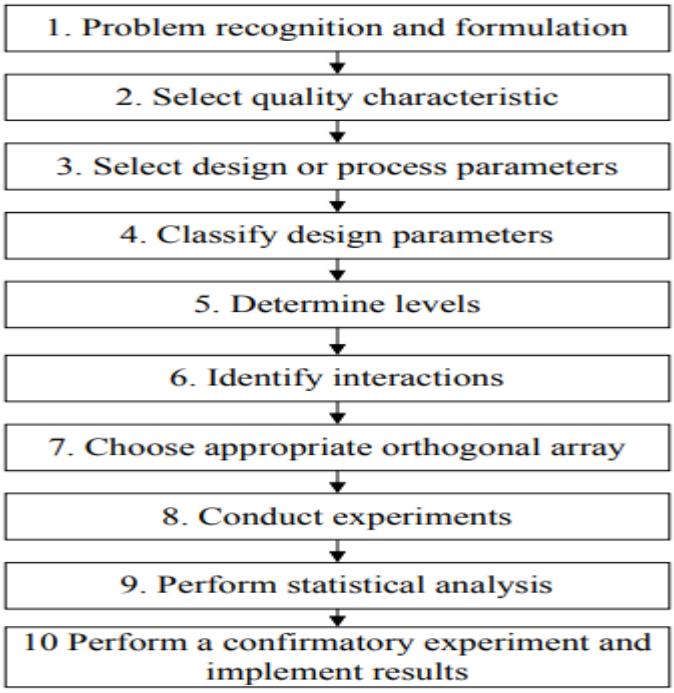

Figure 2-23 Taguchi method methodology

Taguchi methods have been discussed extensively in different platforms. Taguchi's two most important contributions to quality engineering are the use of Gauss's quadratic loss function to quantify quality and the development of robust designs (parameter and tolerance design. Nearly half of this article deals with Taguchi's parameter and tolerance designs. A number of reports evaluated Taguchi methods from a statistical standpoint. The primary ones are by Box and Fung (1986); Box, Bisgaard, and Fung (1988); Box and Jones (1992); Bisgaard (1990, 1991, 1992); Czitrom (1990); Bisgaard and Diamond (1990); Bisgaard and Ankenman (1993); and Steinberg and Burnsztyn (1993). In these reports, the parameter design received the most attention. These authors confirm that the Taguchi method has made important contributions to quality engineering; however, it may not be easy to apply the techniques to real-life problems without some statistical knowledge. Taguchi's parameter design is discussed extensively by a group of scientists in a discussion panel chaired by Nair (1992). They claimed that putting controllable and uncontrollable factors in two separate arrays, inner and outer, will result in more experimental runs. Montgomery (1997, pp. 622-641) highlighted the same difficulty in a Taguchi parameter design. Tsui (1996) reviewed and gave probable problems with Taguchi methods. He compared Taguchi methods with other alternative. Where it was expensive to arrive at a process having on-target mean and minimum variance with Taguchi methods. They suggested an alternative model based on an asymmetric quality loss to obtain the most economical process mean. Robinson, Borror, and Myers (2004) in a recent article gathered previous arguments and alternative approaches to Taguchi methods. Alternative performance measures are discussed and are compared with signal-to-noise ratios.

One of the advantages of Taguchi method over the conventional experimental design, in addition to keeping the experimental cost at the minimum level, is that it minimizes the variability around the investigated parameters when bringing the performance value to target value. Its other advantage is that the optimum working conditions determined from the laboratory work can also be reproduced in the real production environment (Bayuaji and Nuruddin, 2014).

Also, the main advantages of using Taguchi method over the other methods are that numerous factors can be simultaneously optimized and more quantitative information can be extracted from fewer experimental trials. Taguchi methods

have been used for op-timization in various fields of wastewater treatment (Pundir et al., 2018).

In addition, Taguchi method it emphasizes a mean performance characteristic value close to the target value rather than a value within certain specification limits, thus improving the product quality. Additionally, Taguchi's method for experimental design is straightforward and easy to apply to many engineering situations, making it a powerful yet simple tool. It can be used to quickly narrow down the scope of a research project or to identify problems in a manufacturing process from data already in existence. Also, the Taguchi method allows for the analysis of many different parameters without a prohibitively high amount of experimentation. For example, a process with 8 variables, each with 3 states, would require 6561 experiments to test all variables. However using Taguchi's orthogonal arrays, only 18 experiments are necessary, a 97% reduction in the number of experiments. In this way, it allows for the identification of key parameters that have the most effect on the performance characteristic value so that further experimentation on these parameters can be performed and the parameters that have little effect can be ignored. The main disadvantage of the Taguchi method is that the results obtained are only relative and do not exactly indicate what parameter has the highest effect on the performance characteristic value. Also, since orthogonal arrays do not test all variable combinations, this method should not be used with all relationships between all variables are needed. The Taguchi method has been criticized in the literature for difficulty in accounting for interactions between parameters. Another limitation is that the Taguchi methods are offline, and therefore inappropriate for a dynamically changing process such as a simulation study. Furthermore, since Taguchi methods deal with designing quality in rather than correcting for poor quality, they are applied most effectively at early stages of process development. After design variables are specified, use of experimental design may be less cost effective. Taguchi is very limited method compared to surface response, factorial design, and Genetic algorithm. It cannot be used to fit higher empirical models and is not effective (Fadda, 2016).

Many researchers have studied the mechanical properties of concrete using the Taguchi method, changing the number of variables and then determining the impact of those variables on performance (Sari et al., 1999, Türkmen et al., 2003).

Moreover, the experiments designed using the Taguchi method gives the optimum working conditions of the experimental parameters for the experimental results (Nian et al., 1999)

(Hınıslıoğlu and Bayrak, 2004) studied the effect of silica fume and fly ash on the flexural strength of concrete pavement by using Taguchi method. (Ozbay et al., 2009) determined the most important parameter affecting high strength self-compacting concrete properties by using Taguchi method. (Ribeiro et al., 2003) analysed the effect of curing regime and the composition on bending strength with epoxy and polyester concrete. (HINISLIOGLU et al., 2003) found the optimal level for each pavement concrete variables by using the Taguchi method which was shown that the concrete design by using Taguchi method was suitable to determine the optimum value for concrete variables which in turn enhanced the pavement concrete properties.

Taguchi designs are particular types of the so-called “orthogonal arrays” (OA). The use of these arrays makes the design of experiments very easy and consistent (Phadke, 1995) and it requires fewer experimental trials to study the entire parameter space. The experimental results are then analyzed by means of analysis of variance (ANOVA), which is the statistical technique most commonly applied to assess the relative contribution of each factor and any significant interactions between them. Study of the ANOVA table for a given analysis helps to determine which of the factors need control and which do not (Sari et al., 1999).

2.8 **Conclusion from literature review**

In order to establish the current knowledge of the low carbon concrete and assess the sustainability of concrete, considering the durability (carbonation resistance), since the comprehensive review of the literature has been undertaken. The main sections of the literature reviews are:

- Mix design and components
- The contributions of concrete mix design procedures
- Factors affecting the choice of mix proportions
- Taguchi method
- Durability assessment of the concrete (carbonation resistance)
- Embodied carbon dioxide and sustainable concrete

The main conclusions are:

Reduction of eCO_2 of cementitious materials is the most important factor to reduce the overall eCO_2 of concrete as Portland cement has the maximum contribution of eCO_2 per m^3 compared to any other constituent materials of concrete. The eCO_2 in Portland cement can either be reduced by optimizing its manufacturing process by adopting low energy, low CO_2 emitting process or by replacing the clinker by supplementary cementitious materials (SCM) such as GGBS and fly ash materials. The effects of SCMs are reducing CH content, densifying the ITZ and also on changing the pore structure (both via reduction in permeability based on the pozzolanic reaction) and on changing the C-S-H morphology.

This review has revealed that an experimental study of affecting embodied carbon dioxide by mix design variables is still limited. Hence, it is necessary to have a study to find a suitable low carbon concrete mix design while satisfying physical and durability properties (carbonation resistance). The aim of this thesis to study the effect of producing low carbon concrete on their carbonation resistance to optimize low-carbon concrete, while maintaining the carbonation resistance. The modifications effect of mix design variables in carbonation resistance of concrete will be investigated, examining their microstructures to relate the carbonation behaviour of concrete to binder compositions

Chapter 3 : Materials, Methods & Experimental Programme

3.1 Introduction

In this chapter, the experimental programme details are presented. It includes details of the materials used, mix proportions, preparations, curing, and testing of specimens. The experimental works have been carried out to study the effect of variation in concrete mix design variables on the short and long-term performance by assessing their relative importance, especially considering the durability (carbonation resistance) of the resulting low carbon concrete.

In order to achieve this aim, raw materials and the performance of the samples at specified periods have been characterised using a number of methods. First of all, the constituent materials have been characterised. Subsequently, mechanical properties of concrete specimens have been determined. These were complemented by studies related to transport properties (water sorptivity and gas permeability) having the most important role of carbon dioxide diffusion into the concrete. Finally, so as to relate concrete performance to composition, a series of equivalent paste samples have been prepared for characterisation of phase assemblage and microstructure.

The mechanical performance, transport properties of concrete and the microstructural investigations of paste were tested under constant environmental expose conditions (e.g. temperature, relative humidity and CO_2 concentration). Figure 3.1 illustrates the work flow programme for the entire work. Hence, the experimental programme of the whole work was divided into the following three sections:

1. Characterization of concrete constituent materials
2. Concrete test programme
3. Analysis of hydration products

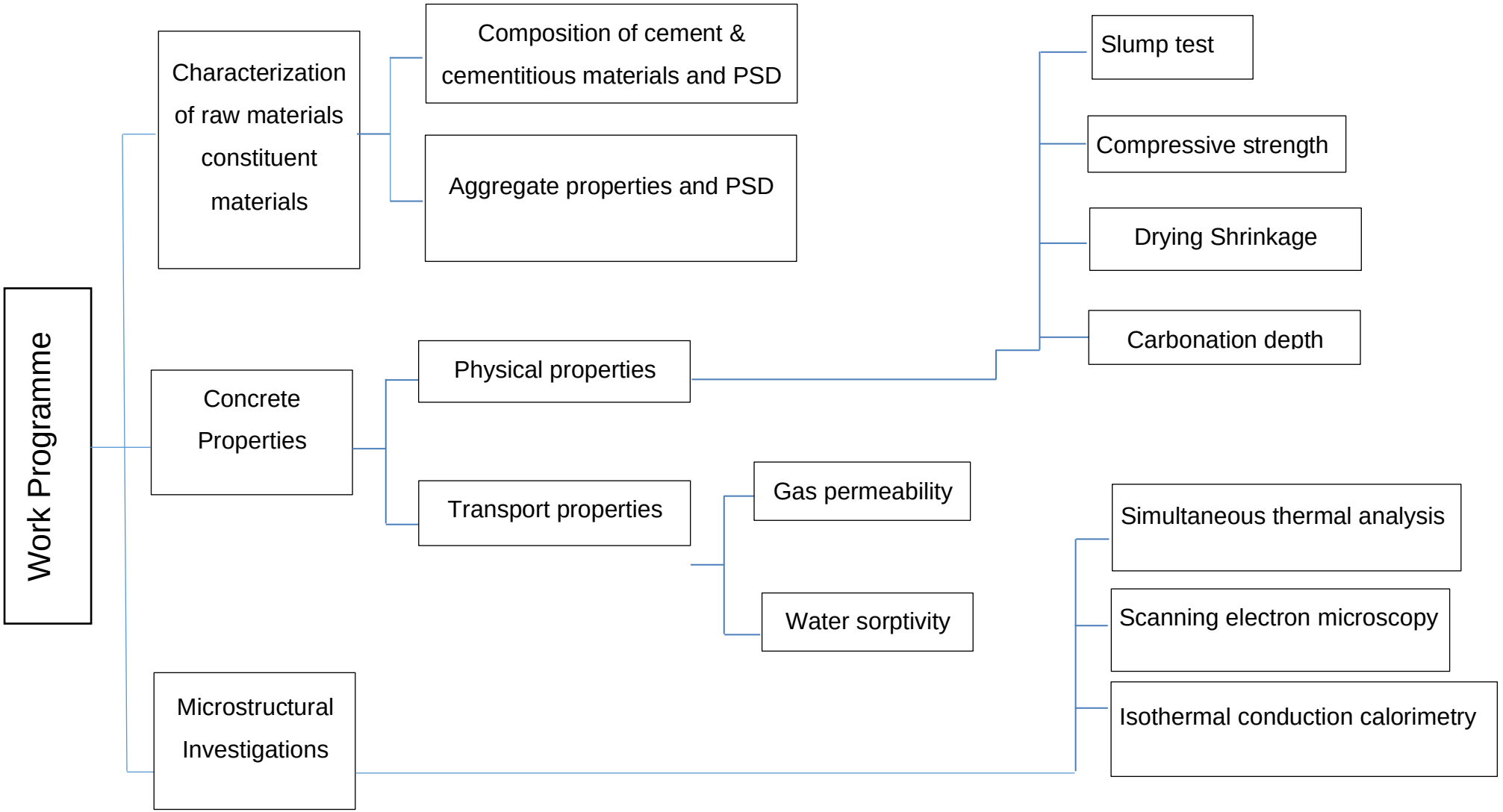

Figure 3-1 Flow chart of experimental work.

3.2 An overview of experimental work

This study looking of mix design variables and their impact on the various short-long term performance. Where these variables chose based on Leon and Full work, but that only considered a theoretical 28 days characteristic strength. A lot of study on carbon footprint concrete considered 28 days, but the difference in this study to look beyond 28 days and design of low carbon footprint. Designing a series of low carbon concrete mixes by using Taguchi method which theoretically reduce carbon dioxide emissions ensure mechanical performance while maintaining long-term performance. Testing their strength, permeation properties, and carbonation resistance to find out which factors are significant in terms of engineering performance, durability and carbon footprint. A series of concrete performance have been chosen (not just strength), other factors which knew have impact on concrete performance (permeability, porosity) were included as the result of changing mix design variables such as w/b and using SCM have a role to reduce the permeability and improve the permeability. This study looked at mix design variables and their impact on the various short-long term performance measures. These variables were chosen based on the work of Based on the work of (Purnell and Black, 2012), a number of factors have been identified which affect the carbon footprint of concrete, but that theoretical study only considered a 28 days characteristic strength. Similarly, many studies on carbon footprint concrete considered 28 days, but since SCMs are known to lead to long-term improvements in strength, this study looked beyond 28 days. Furthermore, since examining each level of each variable would prove time consuming, the Taguchi method was used to reduce the number of experiments to a manageable number. Similarly, this lab-based study moved beyond that of Purnell & Black by considering performance measures beyond compressive strength. In particular, it tried to examine factors known to be relevant to concrete durability, e.g. permeability and porosity.

As previously mentioned, the most effective means of reducing concrete' carbon footprint is to reduce the cement content. Therefore, many of these factors revolved around reducing the cement content. These includes using of supplementary cementitious materials (pulverized fly ash, ground granulated

blast furnace, and fine slag) which replaced with CEM I at 0%, 15%, and 30% of the total binder content by mass. Sika Viscocrete 25 MP was used as a superplasticizer at different dosages (0.2%, 0.6%, and 1.0%) over binder weight. Crushed aggregate with the maximum size of 10 or 20 mm as coarse aggregates and 5mm as fine aggregates. Therefore, this study has looked at the following mix design variables -that have the greatest effect on a concrete mix- when designing appropriate low-carbon mixes. In particular, table F (EN 206:2013) was used to select the variable ranges, where these limiting values were chosen depending on the exposure class (carbonation-induced corrosion). SCM replacement levels were set at 15% and 30%. While 15% slag replacement is not really realistic, and circa 30% replacement would be more typical, such levels at least offered the opportunity to compare slag and PFA with a degree of overlap (Pacheco-Torgal et al., 2013a). A similar approach was used to define other variables such as superplasticizer dose and w/b ratio, where the minimum and maximum value of superplasticizer was that described by the supplier, while the w/b ratios were chosen to provide a suitable range without exceeding the maximum water binder ratio of 0.55 (Darwin et al., 2016). As for aggregate size, the two different sizes were used according to the effect of aggregate size on permeation properties and to look at that effect on carbonation progress. Total binder contents were chosen typical of general purpose concrete where the minimum cement contents are in the range of 300–360 kg/m^3 (Levy, 2011).

Table 3-1Mix design variables and their variation levels

Mix design variables	Values
w/b ratio	0.35-0.45-0.55
Max. aggregate size	10 – 20 mm
Total binder content	350 – 400 – 450 (kg/m^3)
SCMs	PFA – FS – GGBS
% SCMs	0% - 15% - 30%
SP dosage	0.2% - 0.6% - 1.0%

Subsequently, 18 mixes were designed so that each variable could be set at one of three levels. This would give a range of mixes with a range of embodied carbon values. In order to achieve the requirements of this project, it is necessary to cast a series of concrete samples and these would be classified depending on the

principal needs that serve research objectives. This research has been comprised of three parts and each part complements the other part.

The first part deals with the characterization of the constituent concrete materials such as the density, fineness and particle size distribution.

The second part deals with hardened state performance (mechanical properties) and durability (carbonation resistance). These properties have been investigated by testing the concrete mixes for compressive strength with 100 mm cube samples, slump value for each mix and shrinkage with 75 x 75 x 200 mm prism samples. On other hand, the durability which involved measuring the depth of carbonated area with using accelerated carbonation with 100 mm cube samples. Permeation test includes two methods (Sorptivity and permeability) with 50mm cube samples and 40 height x 50 Ø mm. To understand how the different mix parameters will affect performance.

Finally, microstructural investigation such as thermogravimetric analysis (STA), isothermal conduction calorimetry (ICC) and scanning electron microscopy (Akçaözoğlu and Atiş) have investigated to relate the performance of these concrete mixes to composition.

3.3 Characterization of constituent materials

3.3.1 Cement

Portland cement (CEM I 52.5R) was used for all concrete and paste samples in this project within different contents were varied at 350, 400, and 450 kg/m^3. This cement complied with the British standard specifications (BS EN 197-1, 2011). The particle size distribution (Figure 3.2) was measured using Malvern Mastersizer 2000.The chemical composition and physical properties of the cement are given in Table 3.2 and Table 3.3. Also, the clinker composition was calculated according to the Bogue equations (Neville, 2011) as listed in Table 3.2

3.3.2 Supplementary Cementitious Materials

The supplementary cementitious materials (SCMs) were used such as ground granulated blast furnace slag, finely ground granulated blast furnace slag and pulverised fuel ash, at either 15 or 30 wt.% replacement for cement. A number of physical tests were carried out to determine the particle size distribution,

density, and fineness of each binder materials. The particle size distribution was measured using Malvern Mastersizer 2000, illustrated in Figure 3.2. The fineness was tested using Blaine air permeability apparatus in accordance with (BS EN 196-6:2010) and the density was determined by Helium Pycnomety. The chemical composition and physical properties for cement and cementitious materials were summarised in Table 3.2 and Table 3.3, respectively.

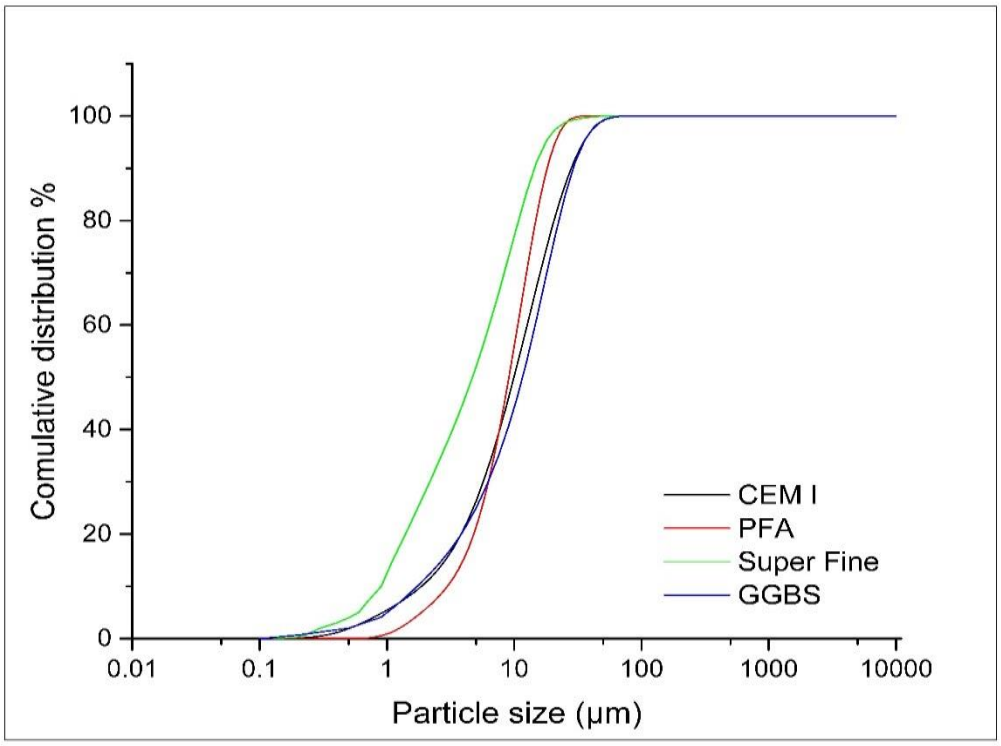

Figure 3-2 Particle size distribution of cement, GGBS and fly ash

Table 3-2 Chemical compositions of the cement and SCMs (%weight)

Oxide	**SiO_2**	**Al_2O_3**	**Fe_2O_3**	**CaO**	**MgO**	**TiO_2**	**SO_3**
PFA	50.7	25.5	10.0	2.28	1.63	1.0	0.4
GGBS/Fine slag	34.11	11.16	0.85	41.1	6.57	0.87	1.1
CEM I	20.58	4.93	2.59	63.25	1.17	-	3.93
Phase composition	**C_3S**	**C_2S**	**C_3A**	**C_4AF**			
	62.4	14.9	7.6	6.6			

***According to the manufacturer.**

Table 3-3 Physical properties of Binders

Binder	PFA	GGBS	Fine slag	CEM I
Density (gm/cm^3)	2.31	2.89	2.89	3.3
Fineness (m^2/kg)	3013	4093	7904	3125

3.3.3 **Properties of the aggregates**

The fine and coarse aggregates were tested to check their specific gravity, water absorption and moisture content, according to (BS EN 1097-6, 2013). The results are shown in Table 3.4. This allowed the total water content of the concrete to be controlled by calculating the water absorption capacity and aggregate moisture content, and hence the effective water content adjustments. Hence, for aggregates that have batched in a dry environment which leads to the high absorption of mix water, the amount of absorbed water was calculated to keep the mix water constant without any change. The gradation of coarse aggregate and sand was tested according to the (BS 882, 1992). This was done by passing the aggregates through a series or stack of sieves. For 20mm coarse aggregate, sieves size of 20 mm, 14 mm, 10 mm, 5 mm, 2.36 mm and 1.18 mm were used. Sieves of 10 mm, 5 mm, 2.36 mm, 1.18 mm, 600 µm, 300 µm and 150 gm were used for 10mm coarse aggregate. The gradation curves for coarse aggregates and sand are shown in Figure 3.3.

Table 3-4 Properties of coarse aggregate

Properties	**Aggregate type (Value)**		
	10mm	**20mm**	**Sand**
Moisture content (%)	0.25	0.3	0.13
Water absorption (%)	0.85	0.2	0.5

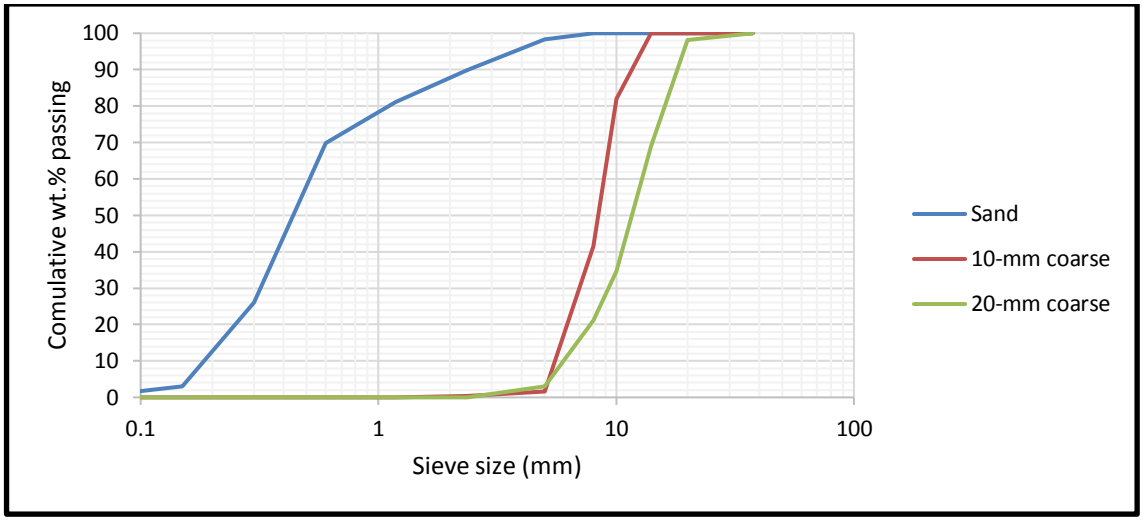

Figure 3-3 Particle size distribution of the aggregate

The proportions of coarse and fine aggregate were specified by combining the aggregate gradation to obtain continuous grading, thus reducing the gaps with different maximum size of aggregate. This was to keep the gradation of aggregate in line with the theoretical Bolomey's curve which provide good aggregate packing.

To determine the proportions of fine aggregate and coarse aggregate (10- 20 mm) and total amount of aggregates in each mix, the spreadsheet was created to draw up the curves of particle size distribution for both types of aggregate and draw up the theoretical curves by using Bolomey's method as follows:

$$P(d) = a + (100 - a)\sqrt{\frac{d}{d_{max}}} \quad \text{------ Equation 3-1}$$

Where:

a=8...14 and typically a = 12.

d= sieve opening (mm).

d_{max} = maximum aggregate size of the aggregate mix.

P (d) = passing through sieve with opening d.

The chart shows both the individual gradation trends of fine and coarse aggregates with 10mm and 20mm, and the combined aggregate as shown in Figure 3.4. The area coloured in Figure 3.4 is represented the minimum value for each case to obtain the proportions for sand and coarse aggregate.

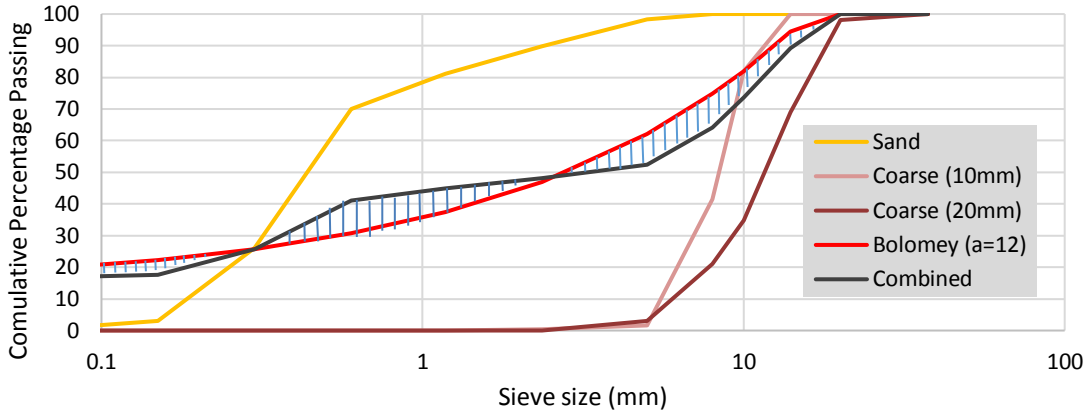

Figure 3-4 Gradation curves of coarse and fine aggregate

3.3.4 **Superplasticizer**

The study used Sika ViscoCrete 25MP as the superplasticiser which complies (BS EN 934-1, 2008), used in this investigation with 0.2%, 0.6%, and 1.0% of the binder content, to improve the workability for mixes. Where these doses were used according to the minimum and maximum values that the product recommended. Furthermore, the water content of the superplasticizer is 60%, and therefore this added water has been subtracted. The technical data of the superplasticiser is presented in Table 3.5.

Table 3-5 Technical description of the Sika Viscocrete 25 MP

Technical description	**Properties**
Appearance	Viscous liquid
Colour	yellow
Specific gravity	1.06 kg/l at +20˚C
PH- value	6.5 ± 0.5
Main component	Polycarboxylate ether (PCL)

3.4 **Mix Design and Proportions**

Eighteen different concrete mixes were chosen. The variables were selected according to those identified theoretically as having the greatest effect on a concrete mix (Purnell and Black, 2012) such as cement content, supplementary cementitious material type (Fly ash, GGBS and fine slag), maximum aggregate

size and the workability (by changing w/b ratio and superplasticizer dosage). These variables, with a full set of mixes encompassing all levels of each variable would give over 400 mixes. It was not feasible to test such a number of samples. Thus, it was reduced by using the Taguchi method to 18 mixes. This allowed a more detailed investigation using a range of techniques, resulting in more data for each mix and a more accurate analysis (Montgomery, 2013). The Taguchi method has been used in the design of the experiment by selection of the variables and their levels, then select the appropriate orthogonal array. Selection of the levels of the five key mix design factors, namely, binder content, water/binder ratio, supplementary cementitious materials and super-plasticizer, has been made to ensure that enough experimental data are generated for obtaining a regression model for the mechanical properties. Two levels of the aggregate size and three levels each of the other five variables were selected as shown in Table 3.6.

Table 3-6 Variables and their variation levels

Parameters	**Unit**	**Level**		
Binder Content	Kg/m^3	350	400	450
SCMs type	----	PFA	GGBS	FS
SCMs Content	%	0	15	30
W/b	%	0.35	0.45	0.55
Superplasticiser	%	0.2	0.6	1.0
Max. Aggregate size	mm	10		20

The Taguchi method was developed by Genichi Taguchi in Japan to improve the implementation of off-line total quality control. The method is related to finding the best values of the controllable factors to make the problem less sensitive to the variations in uncontrollable factors. This kind of problem was called by Taguchi a robust parameter design problem (Cavazzuti, 2012). To cover all these variables, as mentioned earlier, it was necessary to systematically follow 10 steps during Taguchi design. But the most important of these is to classify the design parameters, determine their levels and chose the appropriate orthogonal array. In this project, there were six variables and three levels for each variable,

apart from the aggregate size which included 2 levels. The Taguchi orthogonal arrays are tabulated in the literature with the letter L, or LP for the four-level ones, followed by their sample size. Suggestions on which array to use, depending on the number of parameters and on the numbers of levels, are provided in and are summarized in Table 3.7.

Table 3-7 Taguchi designs synoptic table

Number of variables	Number of levels			
	2	3	4	5
2, 3	L4	L9	LP16	L25
4	L8	L9	LP16	L25
5	L8	L18	LP16	L25
6	L8	L18	LP32	L25
7	L8	L18	LP32	L50
8	L12	L18	LP32	L50
9, 10	L12	L27	LP32	L50
11	L12	L27	N./A.	L50
12	L16	L27	N./A.	L50
13	L16	L27	N./A.	N./A.
14, 15	L16	L36	N./A.	N./A.
from 16 to 23	L32	L36	N./A.	N./A.
from 24 to 31	L32	N./A.	N./A.	N./A.

The selection of an appropriate orthogonal array (OA) depends on the total degrees of freedom of the parameters. Degrees of freedom are defined as the number of comparisons between process parameters that need to be made to determine which level is better and specifically how much better it is. In this study, since each parameter has three levels except maximum aggregate size, which has two levels the total degrees of freedom (DOF) for the parameters, are equal to 11. The degrees of freedom for the OA should be greater than or at least equal to those for the process parameters. Therefore, an L_{18} ($2^1 \times 3^5$) orthogonal array with six columns and eighteen rows was appropriate and used in this study. The experimental layout for the mix design parameters using the L_{18} OA is shown in Table 3.8.

On the other hand, SCM materials have used with 15% and 30% percentage because of 15% by slag not really realistic and normally starts with about 30%, but to make comparison between these materials (slag and PFA) to know somewhere and where is it the degree of overlap. This exactly with other variables such as using superplasticizer and changing w/b ratio. As for aggregate

size the two different size have used according to the effect of aggregate size on permeation properties and to look at that effect on carbonation progress. The minimum and maximum value of superplasticizer described by supplier. Total binder content are chosen typical of general purpose concrete.

The column which included in Table 3-8 represents the distribution of SCM levels, where the zero value represents the CEM I mixes. However, in order to maintain the orthogonal array, they are flagged is having on of these supplementary cementitious materials to maintenance the orthogonally.

Table 3-8 Proportions of concrete mixtures

No.	Cement	SCM (kg/m³)	SP (L/m³)	w/b	SCM type	Sand (kg/m³)	Coarse (10mm) (kg/m³)	Coarse (20mm) (kg/m³)
1	450	0%	0.2%	0.35	PFA	1135	900	0
2	382.5	(15%) 67.5	0.6%	0.45	GGBS	1051	858	0
3	315	(30%) 135	1.0%	0.55	SLAG	967	815	0
4	297.5	(15%) 52.5	0.2%	0.35	GGBS	1309	915	0
5	245	(30%) 105	0.6%	0.45	SLAG	1244	882	0
6	350	0%	1.0%	0.55	PFA	1178	849	0
7	280	(30%) 120	0.6%	0.35	PFA	1222	908	0
8	400	0%	1.0%	0.45	GGBS	1147	870	0
9	340	(15%) 60	0.2%	0.55	SLAG	1073	832	0
10	382.5	(15%) 67.5	1.0%	0.35	SLAG	849	813	383
11	325	(30%) 135	0.2%	0.45	PFA	780	778	361
12	450	0%	0.6%	0.55	GGBS	710	742	339
13	350	0%	0.6%	0.35	SLAG	1012	813	411
14	297.5	(15%) 52.5	1.0%	0.45	PFA	958	785	394
15	215	(30%) 105	0.2%	0.55	GGBS	904	757	376
16	280	(30%) 120	1.0%	0.35	GGBS	931	813	397
17	400	0%	0.2%	0.45	SLAG	869	781	377
18	340	(15%) 60	0.6%	0.55	PFA	807	750	358

The concrete design in this study it's not limited by slump and strength as would be typical when designing concrete mixes. This was a deliberate approach in adopting the Taguchi design method, selecting the mix design variables as independent variables and defining slump and strength as dependent variables. As stated earlier, the independent variables were set at levels typical for general purpose concrete but with some of these combinations not being realistic in terms of strength and workability delivered, but maintaining the orthogonal array required by the Taguchi method. A possible limitation of the approach and use of the Taguchi method is that it is not possible to define mixes based on their characteristic strengths or workability. Thus, some of the mixes may seem unrealistic, but are a constraint of the use of an orthogonal array.

The column which included in Table 3-8 represents the distribution of SCM levels, where the zero value represents the CEM I mixes. However, in order to maintain the orthogonal array, they are flagged is having on of these supplementary cementitious materials to maintenance the orthogonally.

3.5 **Casting procedure of concrete specimens**

Concrete was mixed in a drum rotating laboratory mixer with a capacity of 0.1 m^3. The interior surface of the mixer was always cleaned before placing the materials. The mixing method is important to obtain the required homogeneity of concrete mix. Dry components were mixed for specific period then water is added. When a superplasticizer was used, it was mixed with the mix water before adding it to the dry components. Moisture content and absorption tests were tested on the oven dried aggregates to find the amount of water that needed to be added to the total water for each mix.

After mixing, the molds were prepared by cleaning, and their internal surfaces were covered with oil to prevent adhesion with concrete after 24 hours. The concrete was poured into different PVC molds to construct specimens depending on the tests that to be performed. Compaction was achieved by placing the mold on a vibrating table and subjected to shots of vibration for each layer. Finally, the concrete specimens were leveled by hand troweling, after that the specimens were covered and placed in the laboratory for about 24 hours at laboratory temperature of 20 °C to maintain the moisture content in the concrete in accordance with (BS EN 12390-2, 2009). Then the concrete specimens were

drawn from the molds and placed in the curing room depending on the age of testing. Curing at 20 °C was carried out in the fog room at 99% relative humidity.

3.5.1 **Mixing regime**

Concrete was mixed in a drum rotating laboratory mixer with a capacity of 0.1 m3. The interior surface of the mixer should always be cleaned before placing the materials. The mixing method is important to obtain the required homogeneity of concrete mix. Dry components mixed for specific period then water added. Superplasticizer was added to the mix water before adding to the dry components.

Moisture content and absorption tests were tested on the aggregates to find the amount of water that will be added to the mix to replace it by adding these amounts to total water content that will be used for each mixes. The absorption and density of aggregates were determined according to (BS EN 1097-6, 2013). This process is necessary to maintain the workability and the slump required by correction of weighted amounts to keep effective water contents under control.

Oven dried coarse and fine aggregate were added to moisture content determination then put in the pan of the mixer and mixed together with a small amount part of mixing water, then the cement and the residual mixing water.

Compaction

After mixing, the molds were prepared by cleaning, and their internal surfaces were covered with oil to prevent adhesion with concrete after 24 hours. The concrete was poured into different steel molds to construct specimens depending on the tests that will be achieved. The casting was carried out with each layer being 50mm deep for cubes and 100mm for cylinders. Compaction was achieved by placing the mold on a vibrating table and subjected to shots of vibration for each layer.

3.5.2 **Curing**

After compaction, the concrete specimens were leveled by hand troweling, and then placed in the laboratory for about 24 hours at laboratory temperature of 20 °C to maintain the moisture content in the concrete in accordance with (BS EN 12390-2, 2009). The concrete specimens were then demolded and placed in the curing room at 20oC and 99% RH, until testing.

3.6 Mechanical properties testing

3.6.1 Unconfined compressive strength test

As one of the main objectives of this work was to study the effect of changing the mix design variables, observing the level of compressive strength was required to find the capability of using these mixes in the field. The compressive strength test has been tested to find the capability of the concrete samples to resist the compressive load. This performance is the most important one because it is the property that engineers use to design.

Compressive strength was determined in compliance with (BS EN 12390-3, 2002) using an automatic compression testing machine. The test was carried out on three 100mm cube specimens for each mixture and testing day. The specimens were tested at 7, 28, 56 and 90 days, these chosen ages covered a suitable period of short and long-term strength evolution. Before testing, the cubes were removed from the curing room, and surface dried with a towel. The compressive strength was then calculated as follows:

$$fc = \frac{P}{A} \quad \text{------ Equation 3-2}$$

Where;

fc: Compressive strength, MPa

P: Maximum applied load,(N)

A: Surface area, (mm²).

3.6.2 Shrinkage test

Shrinkage is a phenomenon that occurs when the concrete exposure to the environment which take place a reduction in the volume, result of the effecting of moisture loss which evaporated from the pores starting from the concrete surface. Due to the significant of concrete variables which have the ability to minimize or maximize the amount of shrinkage has been studied to indicate the effect of shrinkage that leads to change in the pore structure which is considered responsible about the transition of deterioration factors.

The shrinkage strain was measured using 75x75x200 mm concrete prisms, cured under standard conditions, as mentioned above, for 28 days. The samples were then placed in a dry environment (22 C° and 55% Relative humidity) in

accordance with (BS ISO 1920-8, 2009). Demec points were fixed on the concrete samples and used as the reference point to measure the change in length over time, as shown in Figure 3.5. The specific ages for the measuring length changes were 3, 7, 14, 28, 56 and 90-days.

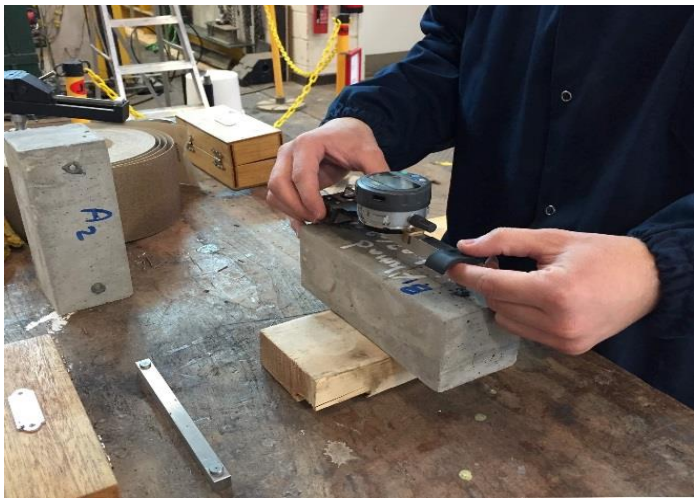

Figure 3-5 Shrinkage specimen and Demec strain gauge.

3.6.3 **Carbonation Depth Test**

Carbonation depth was measured on 100mm concrete cube samples. Samples were first cured in accordance with (BS 1881-210, 2013) for 28 days. After that, the cubes were transferred from the curing room to the laboratory air drying environment where these have been dried between 18 °C to 25 °C and relative humidity between 50% to 65% for 14 days.

After the drying period, the samples were sealed on all faces except two sides with paraffin wax to prevent ingress of CO_2 and allow the carbonation on two cast longitudinal surfaces. Accelerated carbonation conditions (4% CO_2, 20 °C and 60% relative humidity) were selected to provide an indication of long-term carbonation resistance (Pacheco-Torgal et al., 2013b). These conditions were also in line with (Dhir et al., 2007), who argued that the method can provide an indication of likely long term concrete carbonation resistance.

Figure 3-6 CO_2 curing set-up and carbonation depth measuring

Finally, the carbonation depth was measured after 28, 56, 90 and 180 days. The depth was measured by splitting the cube concrete into two halves, vertically on the surface of the exposure. Then, spraying an indicator solution (1g phenolphthalein, 70 ml ethanol and 30 ml of demineralized water) (DE LA RILEM, 1988) on the two concrete surfaces. Figure 3.6 shows the stages of CO_2 curing set-up and carbonation depth measurement. Measure the carbonation depth at five points on each exposed face. To locate these points, the edge length divided divide into six equal distances and use the five points.

3.6.4 **Water sorptivity test**

Water absorption is the ability that the concrete transporting the water through the concrete body by capillary action (Sabir et al., 1998). It is the function which is affected by the moisture content, capillary pore size, inter-connectivity of concrete pores and the microstructure of the hydrates. These factors would be influenced by the aggregate type, water/cement ratio and cement type of concrete (Concrete Society Working, 1988). Sorptivity has been calculated with the aid of equation (Tasdemir, 2003):

$$\frac{Q}{A} = k\sqrt{t}$$ ------ Equation 3-3

Where:

Q = volume of water adsorbed (cm^3)

A = cross-section of specimen in contact with the water (cm^2)

t = time (seconds)

k = the sorptivity coefficient of the specimen ($cm/s^{1/2}$)

The sorptivity coefficient is determined through plotting $\frac{Q}{A}$ against$\sqrt{t}$, where k is equivalent to the slope of the linear relationship. After water curing, the concrete cubes were dried in an oven at 40°C to constant weight. The samples were then placed onto mesh stands in a tray containing water. The water level was maintained at ~5mm above the base of the sample. The mass of each sample was then recorded at 1, 4, 9, 16, 25, 36, 49, and 64 minutes. The change in mass (Q) was then normalized and plotted against the square root of time √t to calculate the sorptivity coefficient (k). A schematic of the test set-up is shown in Figure 3.7.

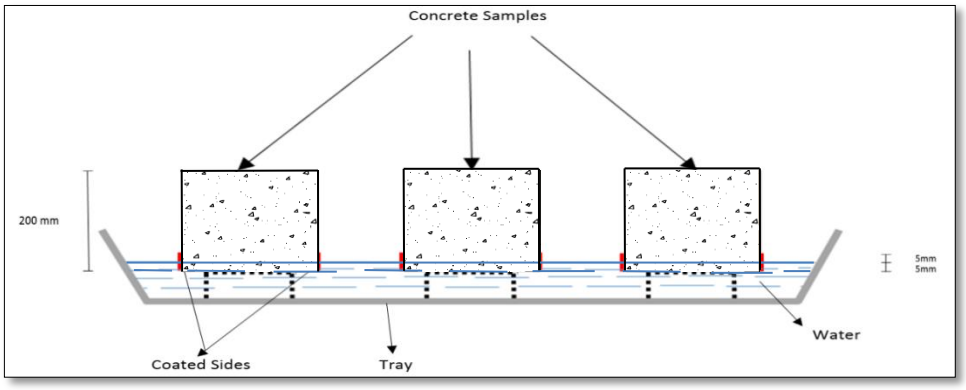

Figure 3-6 Schematic of the sorptivity test

3.6.5 **Gas permeability test**

This test was relied on to evaluate the permeability of the concrete samples that having a different of mix design variables with a various level. This approach gives an understanding about the limit of porous and extent of their connection. Which in turn clarify to know the transport mechanism of carbon dioxide through the body of concrete construction by measuring the ability of Nitrogen gas to

penetrate the sample. The testing has been carried out using the Leeds permeability cell developed by (Cabrera and Lynsdale, 1988) and its schematic diagram and components of the Leeds cell are given in Figure 3.8. When a compressible fluid, such as nitrogen or oxygen is used, a modified D'Arcy's equation should be applied. The intrinsic gas permeability was calculated by using Equation 3.4

$$k = \frac{2P_2 V l \times 2.02 \times 10^{-6}}{A(P_1^{\,2} - P_2^{\,2})} \quad \text{------ Equation 3-4}$$

Where:

K = intrinsic permeability (m^2)

P_1 = absolute applied pressure (bar)

P_2 = pressure at which the flow rate is measured (bar).

V = flow rate (cm^3/s)

l = length of specimen (m)

The concrete samples were cast in a PVC cylinder with (40 x 50 Ø mm) and cured for 28 days. The specimens test ages are 28, 56, and 112 and 180 days, these days were chosen because they give a good range of short and long-term permeability. After, the samples were removed from the curing room and put in the oven to dry at 40°C ±1°C to constant weight. This temperature was chosen because it was high enough to allow for pore water to be driven off in a reasonable time and not so high as to result in decomposition of the hydration products and create cracks.

Once the samples reached a constant weight, the ends of the cylinders were sanded to reveal the pore structure. The test used 1.5 bar for the input pressure and atmospheric (1 bar) outlet pressure. Before starting the test, the concrete sample (S) was weighed, and the diameter and height recorded. It was then put into the rubber cylinder (A) which was placed into the plastic ring (B). Before placing it into the Leeds cell and clamping the cell (H) into position. The clamp will ensure the cell is sealed correctly and ensures that gas only passes through the specimen. Once the cell is sealed, the nitrogen gas is forced through the specimen at the predefined pressure, flowing through the lid of the test cell (fl)

and exits at the gas outlet (L) at the bottom of the cell. Afterward, the flow needs to be become steady before taking any records, this usually takes 10-15 minutes. Then using the bubble form, the flowmeter, the time for a known volume of nitrogen gas to pass through the sample was recorded. This process has been repeated three times for each specimen, and each mix will have three specimens for each testing age, this supported a more reliable standard deviation.

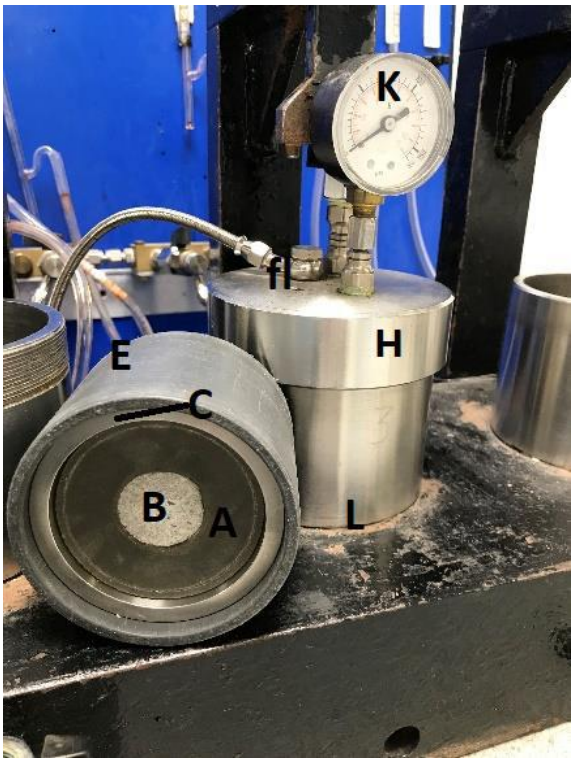

Figure 3-7 Setup for gas permeability test

3.6.6 **Calculating embodied carbon dioxide (eCO_2)**

Cement production has been shown there is different values of embodied carbon dioxide emission. There is no single fixed value for the embodied carbon of cement. Values of 0.88 $kgCO_2/kg$ have been reported in the US and 0.83 $kgCO_2/kg$ in Europe. These values are all high because the cement production is energy intensive process releasing CO_2 upon calcination of the limestone. The variability between figures depends on the methods used to reduce the carbon dioxide emissions, for example precalciners and the use of alternative fuels.

As part of this project, evaluation of the environmental impact of low carbon concrete should also be made by calculate the embodied carbon dioxide for each mix. The values of the embodied carbon dioxide (eCO_2), in $kgCO_2/Kg$ of the various components were those used by (Purnell and Black, 2012): cement = 0

.83; Slag = 0.052; PFA = 0.004; aggregate = 0 .005; superplasticiser = 0 .005; and water = 0 .001. Which takes into consideration the estimated eCO_2 for each component of the 18 concrete mixes, as in illustration in Equation 3.5.

$$ECO_2 = (\text{CEM I} \times 0.83) + (\text{GGBS} \times 0.052) + (\text{PFA} \times 0.004) + (\text{W} \times 0.001) + (\text{A} \times 0.005) + (\text{S.P} \times 0.005) \quad \text{-------- Equation 3-5}$$

Where:

CEM I = Portland cement

GGBS = Ground glass blast-furnace slag

FA = Fly ash

W = Water

A = Aggregates

Then, these calculations will be used to assess the eCO_2 of the low carbon concrete mixes in relation to the strength, permeation and durability properties in order to consider the environmental impact of different mix design variables.

3.7 **Paste sample preparation**

Paste samples were prepared by using the same proportions of water/binder ratio, binder content with the same replacement amount of supplementary cementitious materials, and % superplasticizers as was designed in concrete mixes Table 3-8.

The paste was prepared using a total of 1500g of cementitious materials to each mix which were blended for 3 hrs by using a ball mill to ensure homogeneity.

The measured water and superplasticizer were carefully added to the blended cement powder and mixed manually before filling into an 8mL plastic tube. Finally, these tubes were placed on sample rotator to spin 10 cycles per minute for 24 hrs to prevent the bleeding. The samples were then sealed in plastic bags and cured in a water bath with 20 C for 28 days.

Then, blended cement paste samples were placed in an isolated box which cured in equivalent conditions to concrete accelerated carbonation conditions at 28 and 90 days to realize environment conditions similar to the concrete circumstance.

Table 3-9 Blended cement paste proportions (%wt.)

No.	CEM I	W/B	Superplasticizer (%)	SCM-Type	SCMs (%)
1	100	0.35	0.2	PFA	0
2	85	0.45	0.6	GGBS	0.15
3	70	0.55	1	FS	0.3
4	85	0.35	0.2	GGBS	0.15
5	70	0.45	0.6	FS	0.3
6	100	0.55	1	PFA	0
7	70	0.35	0.6	PFA	0.3
8	100	0.45	1	GGBS	0
9	85	0.55	0.2	FS	0.15
10	85	0.35	1	FS	0.15
11	70	0.45	0.2	PFA	0.3
12	100	0.55	0.6	GGBS	0
13	100	0.35	0.6	FS	0
14	85	0.45	1	PFA	0.15
15	70	0.55	0.2	GGBS	0.3
16	70	0.35	1	GGBS	0.3
17	100	0.45	0.2	FS	0
18	85	0.55	0.6	PFA	0.15

3.7.1 **Hydration stopping**

Hydration stopping is a technique to remove the capillary water among the hydration products, which was activated after 28 days of curing. This technique has been applied to disc samples for SEM observations and to powdered samples for XRD and STA analysis. Paste samples were crushed for XRD and STA testing at 28 & 90 days which corresponding the concrete samples test ages, while discs were prepared by cutting 2mm thick (Isomet diamond blade).

Hydration stopping of paste samples was performed as follows: samples were immersed in isopropanol beakers with 200mL for 24 hours and then dried in a desiccator containing silica gel with low pressure until obtained the constant weight after 7 days, Figure 3.9 shows the stages of paste sample preparation for hydration stopping. This approach has relied on as the way to stop the hydration in blended cement paste which was executed under low pressure and temperature. This conditions of drying and solvent exchange will effect on microstructure and composition of cement paste caused by the most common drying techniques. Because there are many methods for this technique,

isopropanol exchange followed by ambient drying has been used which has a lower effect on the microstructure and the composition of the binder. (Zhang and Scherer, 2011).

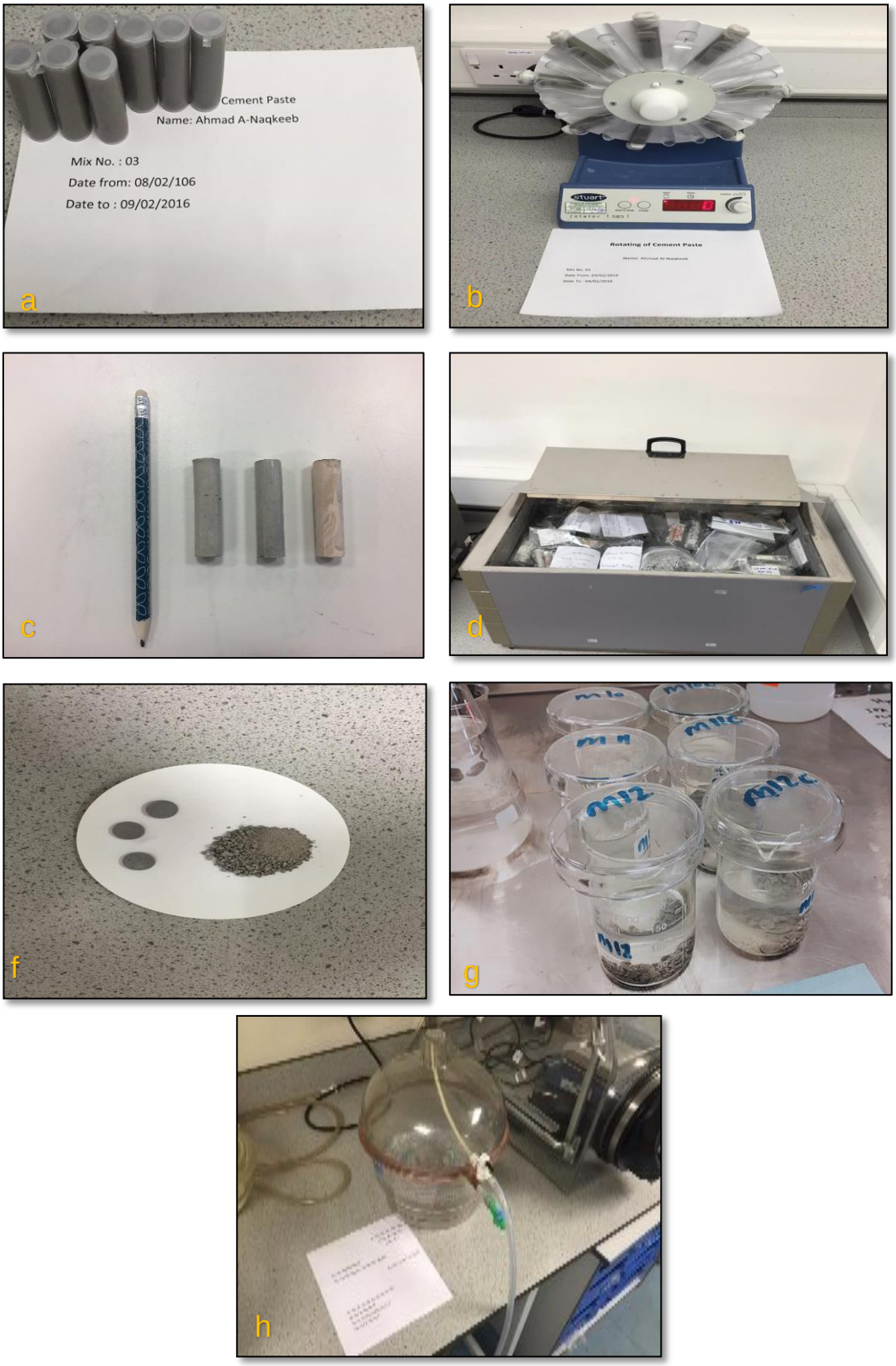

Figure 3-8 preparation paste samples for hydration stopping stages

3.8 **Isothermal conduction calorimetry**

Cement hydration is an exothermic reaction and isothermal conduction calorimetry can monitor heat evolution during the process. This, in turn, gives an insight into the kinetics of the reaction and the influence of variation in variables for each mix.

Calorimetry was performed on a TAM-Air eight channel calorimeter as shown in Figure 3-10. Paste samples were prepared as described earlier, with each of the eight channels containing 20ml plastic ampoules filled with 9g of paste mixed using a vortex shaker.

Experiments were run at 20°C for twelve days, collecting data on the rate of heat flow and cumulative heat over the test period. In addition to paste samples of the same composition as the equivalent concrete mixes, moreover, experiments were run replacing the SCMs with quartz of the same fineness, in order to examine the degree of SCM hydration.

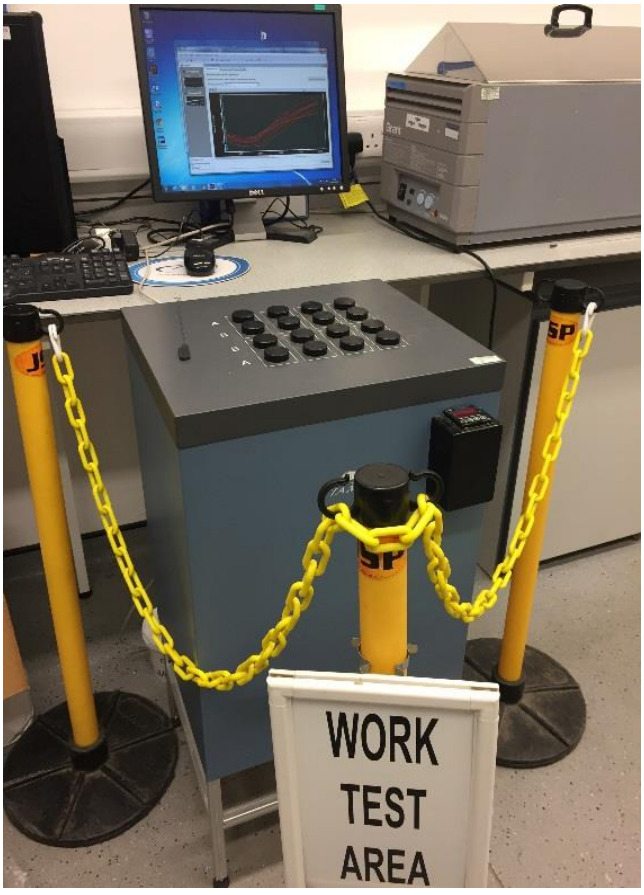

Figure 3-9 TAM air eight isothermal calorimeter

3.9 **Simultaneous thermal analysis (STA)**

Thermal analysis was adopted to understand hydration evolution. In this study an STA-780 machine as shown in Figure 3.11 was used, with nitrogen as a carrier gas. Approximately 15-18mg of powdered, hydration-stopped sample was added to a platinum crucible. The furnace temperature was increased at a rate of 20^0C per minute from room temperature to 1000^0C.

Mass loss was measured by using the tangent method (Figure 3.11), to determine portlandite content from the mass loss from 400°C to 550°C, Equation 3.7 and calcite from the mass loss at ~700°C, Equation 3.8 (Ogirigbo and Black, 2016). Furthermore, the chemically bound water content was determined as the mass loss from 50 to 550°C. Equation 3.10 was used to calculate a corrected CH content accounting for that which had carbonated.

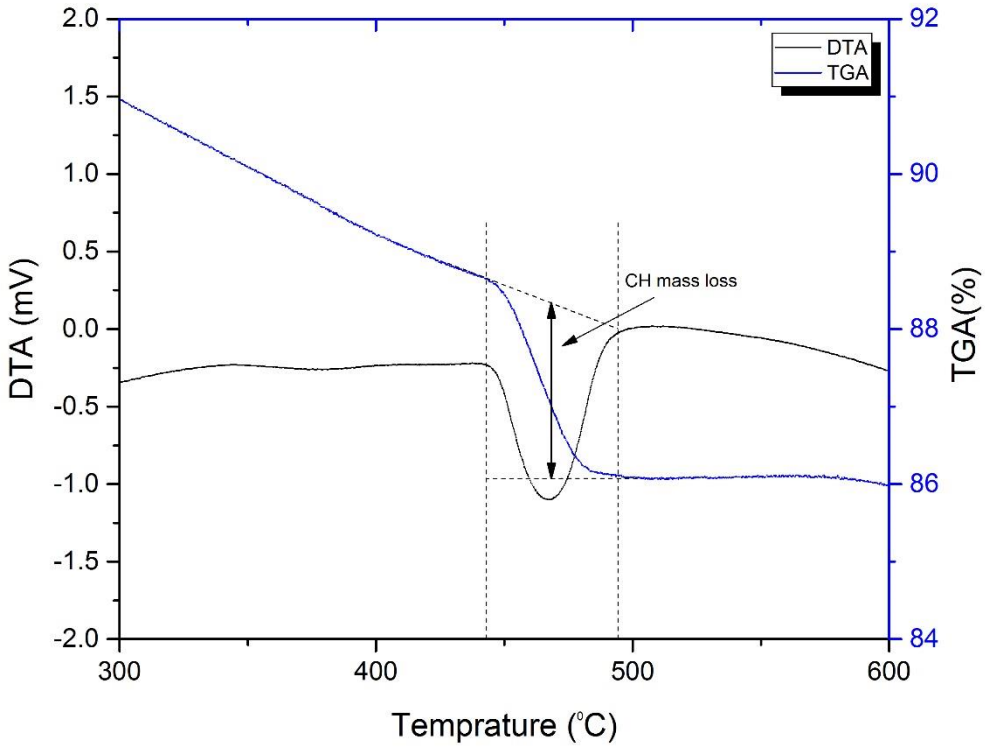

Figure 3-10 CH content calculation by tangent method

$$\%CH = \left(\frac{CHw \times \left(\frac{MCH}{MH2O}\right)}{W550}\right) \times 100$$ ------ Equation 3-6

$$Wb = \left(\frac{(W50 - W550)}{W550}\right) \times 100$$ ------ Equation 3-7

$$\%CaCO3\ (CC) = CaCO3 \times \left(\frac{mm.CaCO3}{mm.CO2}\right) \times 100$$ ------ Equation 3-8

$$\%CHcarb. = CC \times \frac{MCaCO3}{MCO2} \times \frac{Mch}{MCaCO3}$$------ Equation 3-9

Where:

C_{Hw} = mass loss of water bound to CH

M_{CH} = molar mass of CH, M_{CH} = 74 g.mol-1

M_{H2O} = Molar mass of water, M_{H2O} =18 g.mol-1

W_b= bound water

W50 = mass loss at 50°C

W550 = mass loss at 550°C

$CaCO_3$= weight loss associated with $CaCO_3$

mm. $CaCO_3$= molar mass of $CaCO_3$ (100 g.mol-1)

mm.CO_2= molar mass of CO_2 (44 g.mol-1)

3.10 Scanning electron microscopy

Scanning electron microscopy works by the principle of an electron beam accelerated onto a sample surface to produce secondary electrons (SE) and backscattered electrons (BSE). When electron accelerated onto the surface sample, it produces a number of interactions with the atom of the materials. These reflected electrons can be collected and analysed to produce outputs about the sample such as morphology and chemical compositions of the sample. These reflected electrons can be collected and analyzed to produce outputs which represented the sample details such as morphology and chemical compositions of the sample. The appearance of the compositions for the sample depends on the number of atoms that means the hydrated materials which have a lower atomic number appearing darker and a higher atomic number appearing brighter. A Carl Zeiss EVO MA 15 Scanning Electron Microscopy machine was used as shown in Figure 3.12 was used in this study.

Figure 3-11 Scanning Electron Microscope machine

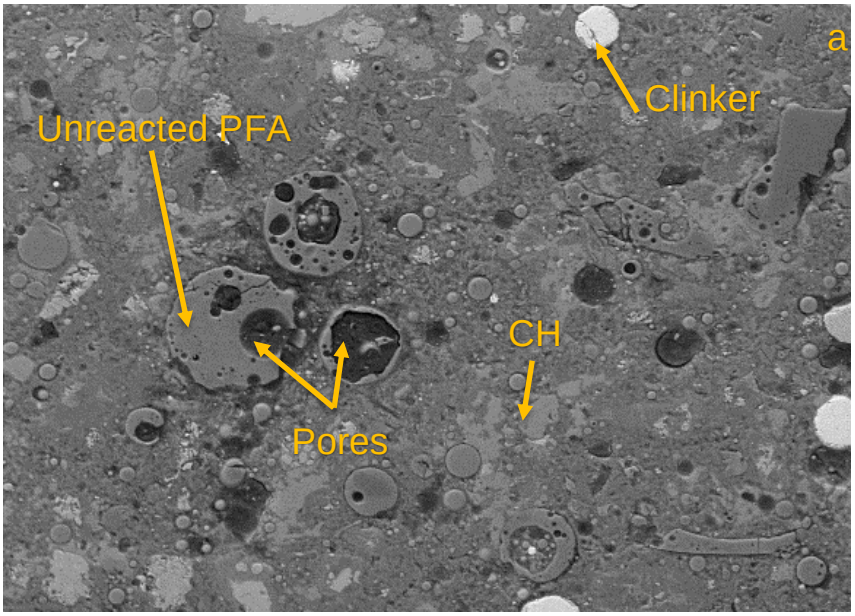

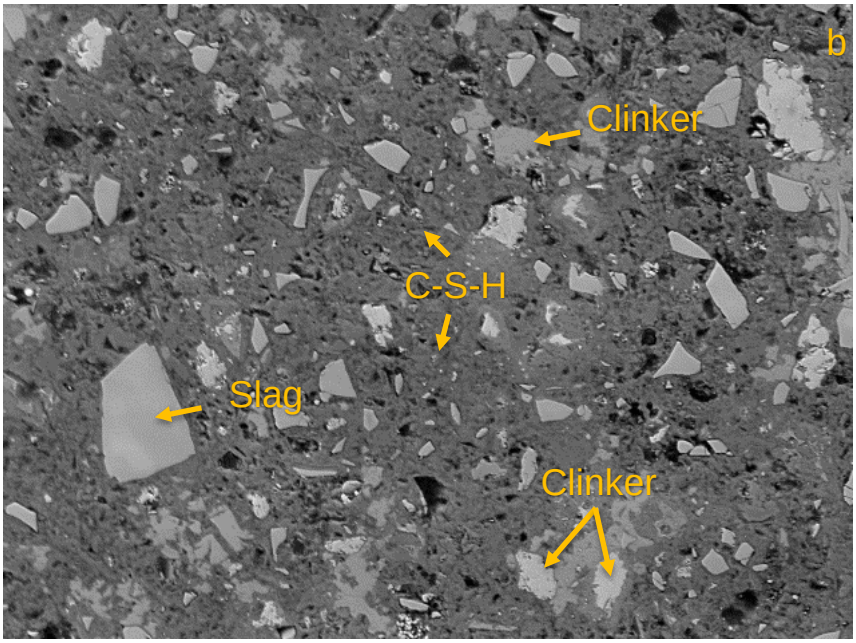

Figure 3-12 BSE micrograph of (a) 30% PFA blend and (b) 30% slag blend, hydrated for 28 days

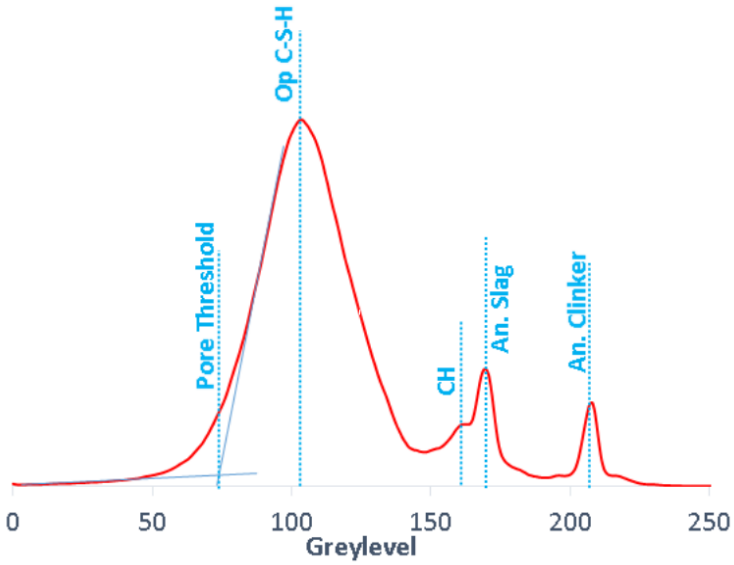

Figure 3-13 Typical constituents of a hydrated slag blended cement and pores(Whittaker, 2014)

Backscattered electron (BSE) images were analysed using ImageJ software to find the hydration degree of cement and the percentage of capillary porosity. Figure 3.13 shows typical binder phases and pores. Coarse pores were distinguished by separating the black spots as shown in Figure 3.14. Unreacted Portland cement was separated based on the light grey colour and quantified according to the Equation 3.10. The hydration of slag was calculated by using

BSE images with corresponding magnesium maps. Anhydrous slag threshold in BSE image was overlapped with the corresponding magnesium map. The degree of reaction of slag was calculated according to Equation 3.11. (Kocaba et al., 2012)

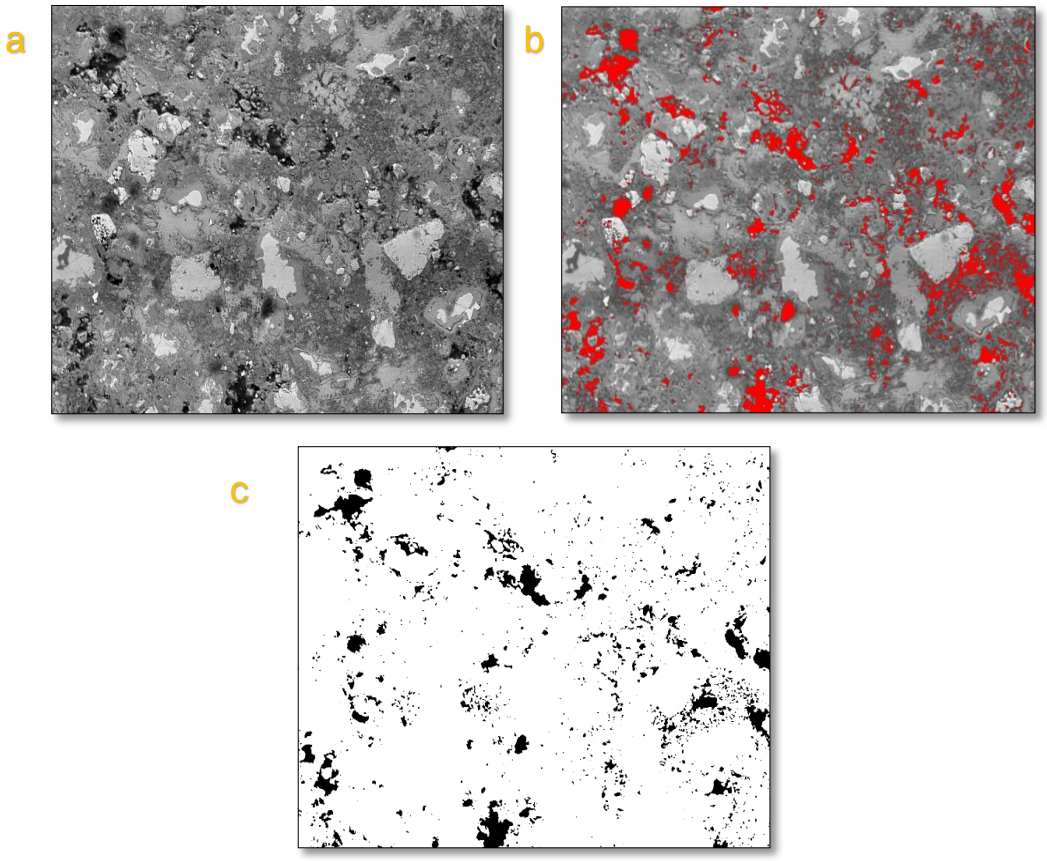

Figure 3-14 Determination of coarse pores from BSE image

$$DoH\ PC = \frac{Vanhydrous\ PC(t=0) - Vfanhydrous\ PC(t)}{Vfanhydrous\ PC(t=0)}$$ ------ Equation 3-10

Where:

DoH PC= degree of hydration of PC

$Vfanhydrous$ PC (t = 0) = Volume of initial anhydrous PC

$Vfanhydrous$ PC (t) = Volume of anhydrous PC at time t

$$DoH\ slag = \frac{Vanhydrous\ slag(t=0) - Vfanhydrous\ slag(t)}{Vfanhydrous\ slag(t=0)}$$ ------ Equation 3-11

Where:

DoH slag = degree of slag hydration

$Vfanhydrous\ slag$ (t = 0) = Volume of initial anhydrous slag

$Vfanhydrous\ slag$ (t) = Volume of anhydrous slag at time t

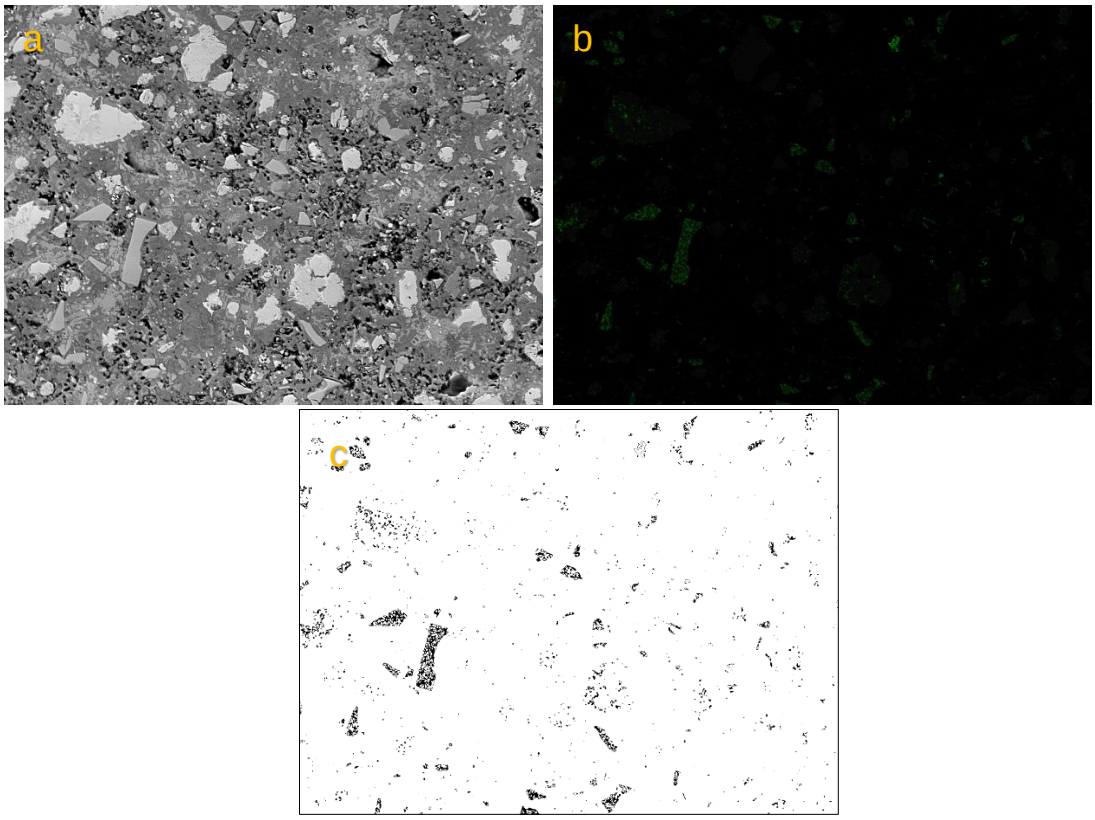

Figure 3-15 Determination of unreacted slag from BSE image and magnesium map by image analysis: (a) BSE image, (b) magnesium map, (c) unreacted slag

SEM-IA was used to determine the degree of hydration of the samples following specified curing periods (i.e. at t0). Hydration stopped sections were resin impregnated under vacuum and the sample surface was exposed using progressively finer grades of SiC paper (600, 1200, 2500). The samples were then polished using diamond paste up to a fineness of 0.25µm and carbon coated prior to analysis. 50 images at 800x magnification, a working distance of 8.5mm and an accelerating voltage of 15keV were collected for each sample on a Carl Zeiss EVO MA15 SEM. Mg maps were collected for the slag systems using an Oxford Instrument Xmax 800mm2 SDD detector with an acquisition time of 100s.

3.11 Statistical analysis

The main objective of many statistical investigations is to make predictions, preferably on the basis of a sound mathematical footing. Usually such predictions require the formula be found which relates the dependent variable to one or more independent variables.

Multiple linear regression techniques are very useful in performing the above target. It is in the construction of predictive model that (MLR) techniques have their greatest contribution.

In this chapter, MLR analysis has been adopted in building a group of models. The general form of the models will be as follows:

$\hat{Y}=b_1X_1+B_2X_2+\cdots+B_KX_K$------ Equation 3-12

$\hat{Y}$: Predicted concrete performance.

X1,X2,…,Xk: Included independent variables.

b1, b2,…,bk: The coefficients corresponding to the independent variables.

3.11.1 Statistical concepts

In order to get a better understanding to what follows, some statistical ideas have to be defined and explained. The analysis of variance, the coefficient of determination, and the residual statistics are the most necessary concepts with this respect.

3.11.2 Analysis of variance (ANOVA)

The analysis of variance (ANOVA) is the statistical treatment most commonly applied to the results of the experiment to determine the percent contribution of each factor and factor interactions. Study of the ANOVA table for a given analysis helps to determine which of the factors need control and which do not. ANOVA employs sums of squares which are mathematical abstracts that are used to separate the overall variance in the response into variances due to the processing parameters and measurement errors (Ayan et al., 2011). As such, ANOVA is a

statistical tool, which helps to minimize the errors of variance and quantifies the dominance of control factor. This analysis aids in justifying the effects of independent variables on the dependent variables in experiment.

This approach can be used for examining the significance of the factors considered for developing the responses model. In ANOVA, the statistical terminologies used are as follows:

Degree of Freedom (DF) is the number of values in the final calculation of a statistic that are free to vary. DF= n − 1, where n represents the number of groups.

Error (Residual) is the amount by which an observed variation differs from the value predicted by the assumed statistical model by the amount.

Sum of Squares (SS) is the squared distance between each data point (Xi) and the sample mean (X), summed for all n data points.

$SS=\sum(i=1)^n\{(Xi-X)\}^2$ ------ Equation 3-13

where, Xi represents the ith observation and X represents the sample mean.

Mean Square (MS) is the sum of squares divided by the degrees of freedom.

F-Ratio is ratio of MS of the concerned factor to the MS of the error. A higher F-ratio indicates a significant effect of the factor.

P-Valuet is a measure of acceptance or rejection of a statistical significance of a factor based on a standard that no more than 5% (0.05 level) of the difference is due to chance or sampling error. In other words, if the P value for a factor is 0.05 or more, it would not have effect on the dependent variable.

ANOVA provides a P value to measure the acceptance or rejection of statistical significance of a factor based on a standard that no more than 0.05 of the difference. That means if the P value for a factor is more than 0.05., it would not have an effect on a dependent variable. The contribution calculated by divided sum of square for each factor over the total.

3.11.3 **Regression model**

The relationship between the response variable and the factors is characterized by a mathematical model called a regression model. It provides a technique for building a statistical predictor of a response and places a bound on the error of prediction (Mendenhall et al., 1996).

The ANOVA table provides R^2 coefficient. It can be calculated as follows:

$R^2=SSR/SST$------ Equation 3-14

Where, R^2 compares the power of regression models that contain different number of predictors.

3.11.4 Confidence interval

Often when estimating the value of some parameter of a population, collecting the data for every member of a population is often infeasible. Instead, data values from a subset of the population are collected, the mean of the sample is calculated, and interpreted as an estimate of the population mean. Similarly, the variability in a population can be estimated by calculating the variance or standard deviation of a sample from that population (Petty, 2012). However, often the population standard deviation σ is not known. In this situation, the population standard deviation σ is estimated using the sample standard deviation s and the Student t distribution is used in place of the normal z distribution when calculating the confidence interval. The confidence interval for the population mean μ is:

$$\bar{x} - t_c \frac{s}{\sqrt{n}}, \bar{x} + t_c \frac{s}{\sqrt{n}}$$ ------ Equation 3-15

Where t_c is the critical value for the Student t distribution for confidence level c. The values for t_c, which can be found in statistical tables or generated by software or statistical calculators, depend not only on the confidence level c as with the z distribution, but also on the quantity n – 1, also known as the degrees of freedom (commonly abbreviated d.f.).

Chapter 4 : The significance of mix design variables on concrete performance

4.1 Introduction

In this chapter, the statistical analysis of the parameters describing concrete performance is discussed. Whereas, regression equations were implemented to find the correlation between these parameters and the variables considered and to analyse the relative importance of each variable on physical properties, transport permeation, and durability (carbonation resistance).

4.2 Slump test

The determined slump values are shown in Figure 4.1. The slump data also provides a visual indication as to harshness, stickiness, and bleeding. All concretes designed had an initial slump between 10-280 mm due to the variation in mix proportions for each mix, classified based on different groups (very low, low, medium, high, and very high).

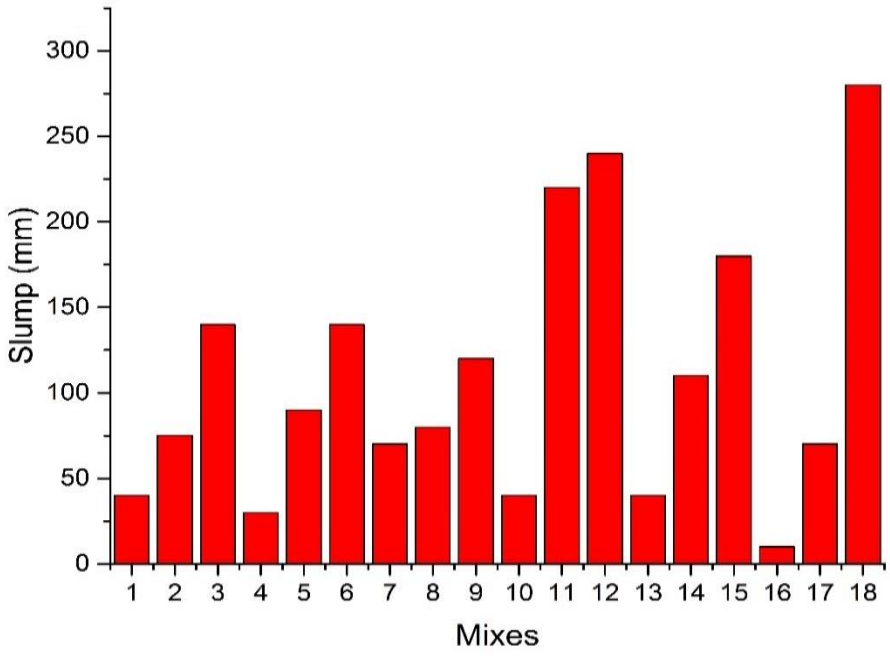

Figure 4-1 Slump values of 18 concrete mixtures

Table 4.2 shows the contribution percentage of each variable to slump. The dominant variable is w/b ratio, contributing 76.4% to the slump. The second most important variable is aggregate size with 11%, with SCMs type being the only other significant variable, with 6.8%. The workability can be expressed mathematically based on the regression model of the data, as shown in Table 4.1. The multiple coefficients of determination (R^2), indicates that 86.97% of observed variations in the slump values data may be explained by the adopted equation.

Table 4-1 Regression equations for slump values

Category	Response		Regression Equation
FS	slump	=	-411 + 4.17 Aggregate size + 0.292 Binder content + 721 w/b - 28.1 SP% + 0.500 SCMs%
GGBS	slump	=	-394 + 4.17 Aggregate size + 0.292 Binder content + 721 w/b - 28.1 SP% + 0.500 SCMs%
PFA	slump	=	-353 + 4.17 Aggregate size + 0.292 Binder content + 721 w/b - 28.1 SP% + 0.500 SCMs%

Table 4-2 Results of ANOVA for slump test values

Source	Adj SS	Adj MS	F-Value	P-Value	Significance	Contr%
Aggregate size	7812.5	7812.5	6.11	0.033	**significant**	**9.7**
Binder content	2552.1	2552.1	1.99	0.188	insignificant	3.2
w/b	62352.1	62352.1	48.74	0.000	**significant**	**77.8**
SP%	1518.7	1518.7	1.19	0.301	insignificant	1.9
SCMs%	675.0	675.0	0.53	0.484	insignificant	0.8
SCMs type	10502.8	5251.4	4.10	0.050	**significant**	**6.6**

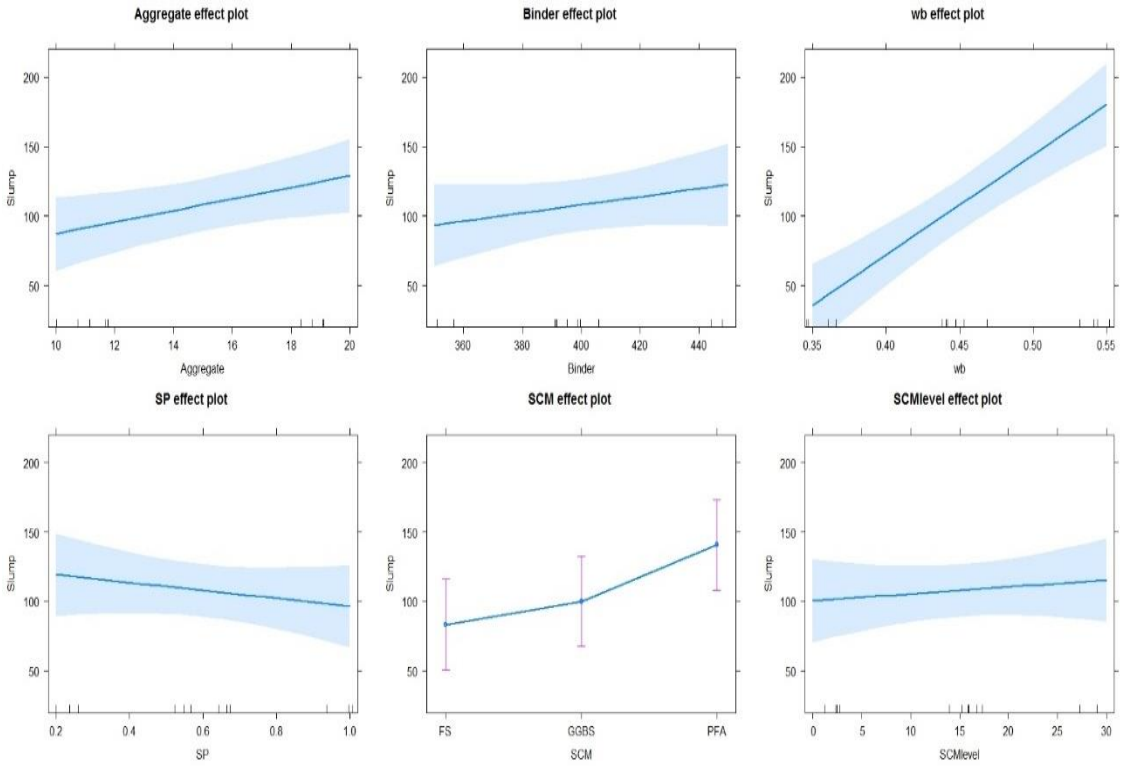

Figure 4-2 Main effects Plot for slump test values

The residual plots of this model are given in Figure 4.3. As with the data for concrete slump, it indicates the validity of the model.

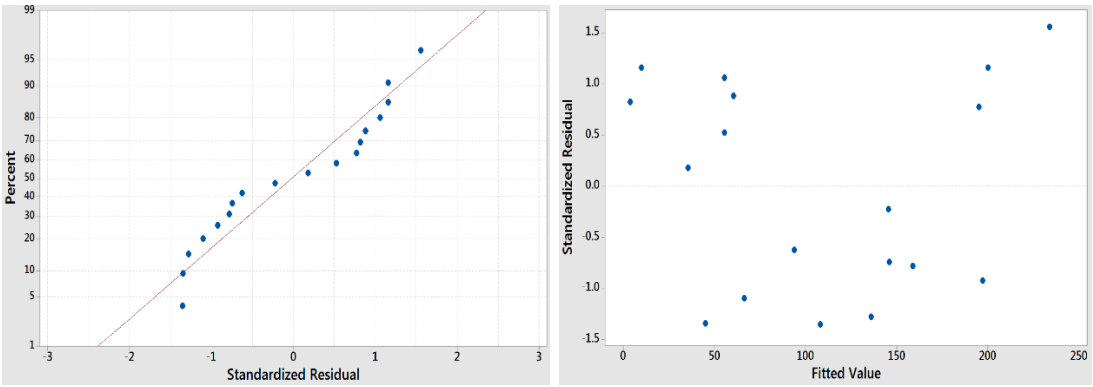

Figure 4-3 Residual plots of regression model generated for concrete slump

Figure 4.2 shows the main effects of significant variables on slump value. Concrete mixes containing fine slag with 30% replacement were sticky and needed a higher w/b ratio to be workable, due to the large fineness and small particle sizes compared with PFA mixes (Zhou et al., 2012). However, the smooth surface and fine texture for slag particles are responsible partly for lower water required and better workability when compared with PC. Fly ash concretes increased workability due to PFA particles having a smooth spherical shape

which leads to low friction between particles (Uysal and Sumer, 2011). These findings agree with the literature (Zhou et al., 2012, Lee et al., 2003, Mehta, 1989).

In addition, the increase in the aggregate size increases the slump value. Higher aggregate size will mean an effectively lower specific surface area and less paste content and water demand, which leads to improved workability (Shetty, 2005). As for w/b ratio, the increasing of water content led to increasing the workability, as expected.

4.3 **Compressive strength development**

Mean compressive strengths were obtained from the 18 concrete mixes at each age, as shown in Figure 4.3. Of all of these samples, at each age the highest compressive strength result was in mix 16, the lowest was 6.

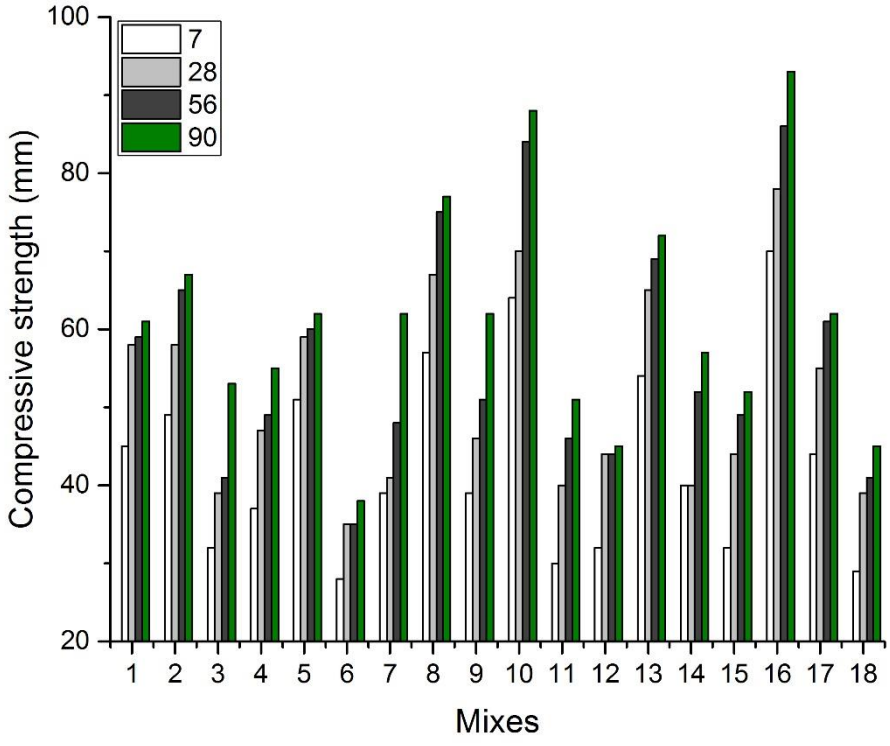

Figure 4-4 Compressive strength development over time

Statistical analysis of the data was undertaken using Minitab to obtain a regression equation. Multiple linear regression (MLR) is suitable to make a correlation between mix design variables and the compressive strength, giving a

more accurate representation based on designed experiment result (Draper and Smith, 1998). The multiple coefficients of determination (R^2), indicate that 78.24% and 77.9% of the observed variations in the compressive strength data may be explained by the adopted equation. The ANOVA results for the compressive strength are shown in Table 4.3 and 4.4, which used the strength data at ages 28 and 90 days, respectively. Table 4.5 presents the multiple linear regression equations for compressive strength.

The data selection of 28 and 90 days were chosen to represent the performance of concrete at the age at which concrete performance is typically measured in standards and at 90 days to represent long-term performance

Also, the paste and concrete samples were tested at the same ages to allow comparison between the two. The other data of concrete properties are presented in annex section.

Table 4-3 Results of ANOVA for compressive strength at 28 day

Source	Adj SS	Adj MS	F-Value	P-Value	Significance	Contr.%
Aggregate size	18	18	0.32	0.586	insignificant	1.8
Binder content	8.33	8.33	0.15	0.71	insignificant	2.9
w/b	1140.75	1140.75	20.03	0.001	**significant**	63.8
SP%	341.33	341.33	5.99	0.034	**significant**	14.9
SCMs%	3	3	0.05	0.823	insignificant	1.1
SCMs type	540.78	270.39	4.75	0.036	**significant**	15.5

Table 4-4 Results of ANOVA for compressive strength at 90 day

Source	Adj SS	Adj MS	F-Value	P-Value	Significance	Contr.%
Aggregate size	34.72	34.72	0.5	0.496	insignificant	2.0
Binder content	30.08	30.08	0.43	0.525	insignificant	1.7
w/b	1045.33	1045.33	15.05	0.003	**significant**	59.2
SP%	126.75	126.75	1.82	0.206	**significant**	12.9
SCMs%	44.08	44.08	0.63	0.444	insignificant	2.5
SCMs type	766.78	383.39	5.52	0.024	**significant**	21.7

Table 4-5 Regression equations for compressive strength at 28 and 90 days

Category	Response	Regression Equation
FS	Strength	= 74.0 + 0.200 Aggregate size + 0.0167 Binder content - 97.5 w/b + 13.33 SP% - 0.033 SCMs%
GGBS	Strength	= 72.9 + 0.200 Aggregate size + 0.0167 Binder content - 97.5 w/b + 13.33 SP% - 0.033 SCMs%
PFA	Strength	= 61.9 + 0.200 Aggregate size + 0.0167 Binder content - 97.5 w/b + 13.33 SP% - 0.033 SCMs%

Category	Response	Regression Equation
FS	Strength	= 84.1 + 0.311 Aggregate size + 0.0483 Binder content - 113.3 w/b + 13.12 SP% + 0.100 SCMs%
GGBS	Strength	= 82.5 + 0.311 Aggregate size + 0.0483 Binder content - 113.3 w/b + 13.12 SP% + 0.100 SCMs%
PFA	Strength	= 70.0 + 0.311 Aggregate size + 0.0483 Binder content - 113.3 w/b + 13.12 SP% + 0.100 SCMs%

Equations and ANOVA results derived for the 28 and 90 day data both identified three significant factors on compressive strength, (where the values of P are less than 0.05), namely w/b ratio, superplasticizer % and the type of SCM.

It can be inferred form Figures 4.4 and 4.5, that both cases, w/b ratio is identified as the dominant factor, contributing 63.8% at 28 days and 59.2% at 90 days. The SCM type was identified as the second most important determinant. Furthermore, the contribution was greater at 90 days (21.7%) than at 28 days (15.5%). It is interesting that the contribution from SCM becomes more significant with time, reflecting the continued, more gradual, hydration of SCMs than cement clinker. The superplasticizer content was found to be the third significant contributor that this may be because the use of a plasticizer has allowed a lower w/b ratio

At 90 days, all variables gave the same trend regarding compressive strength performance, albeit with slightly different contribution percentages compared with the results at 28 days. Meanwhile, the effect of addition GGBS, PFA, and fine slag and replaced at both level (15% and 30% WoB), were almost lower than Portland concretes at age 28 days, while the SCMs concretes have a clear effect value on strength development at age 90 days compared with CEMI concretes.

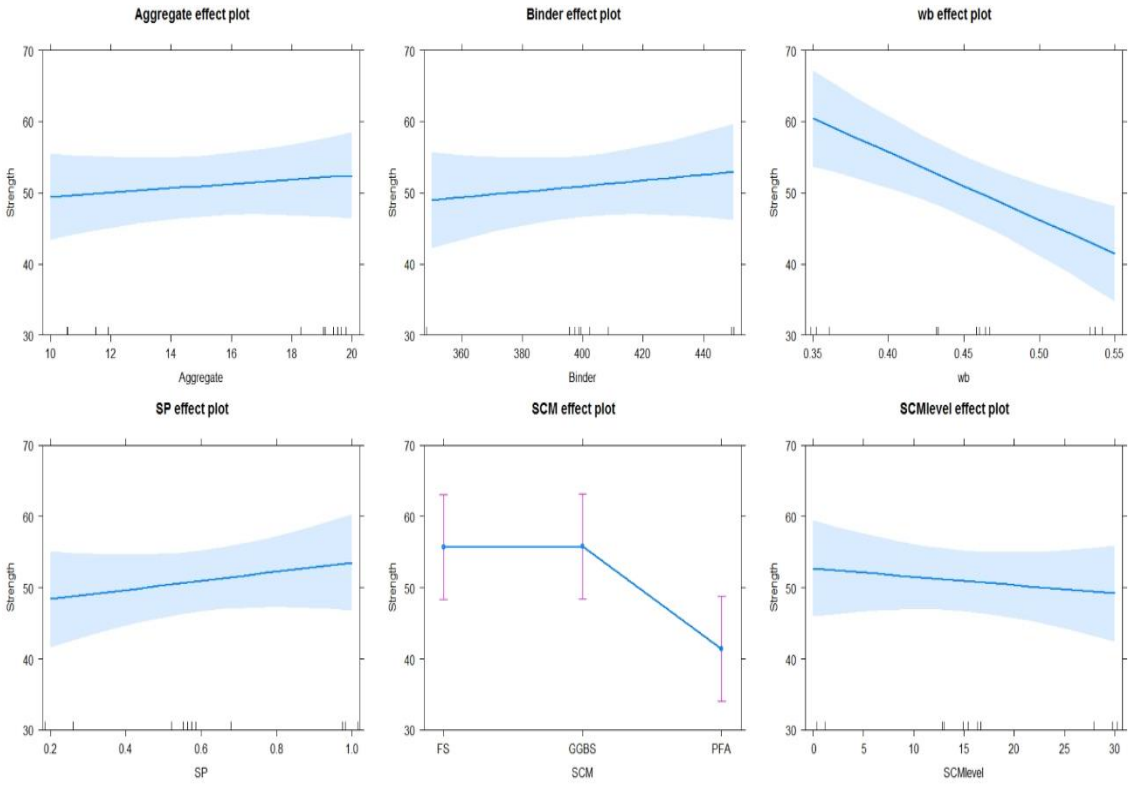

Figure 4-5 Main effects plot for compressive strength at 28 day

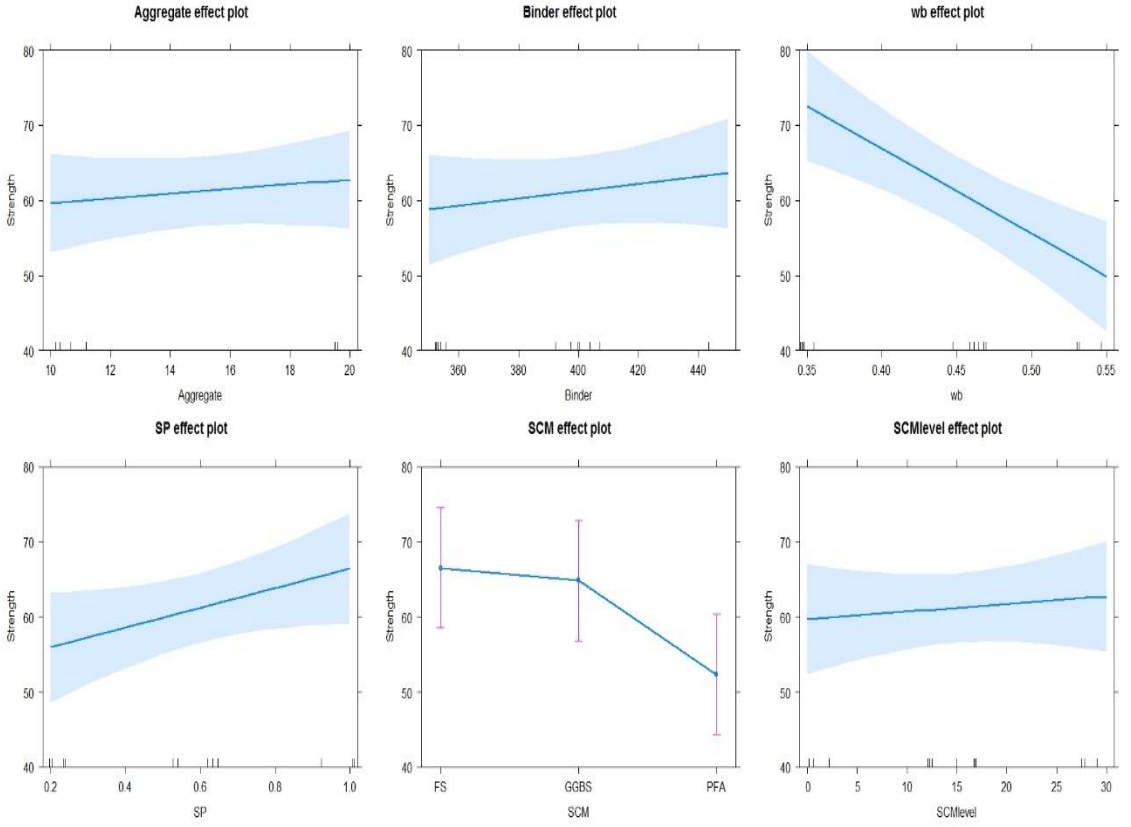

Figure 4-6 Main effects plot for compressive strength at 90 day

The correct specification of the models represented by the equations above was verified by carrying out the usual diagnostics on the residuals, to confirm they

followed a normal distribution, were centered in zero, and showed constant variance. The normal probability and versus fit for residuals are presented in Figure 4.6.

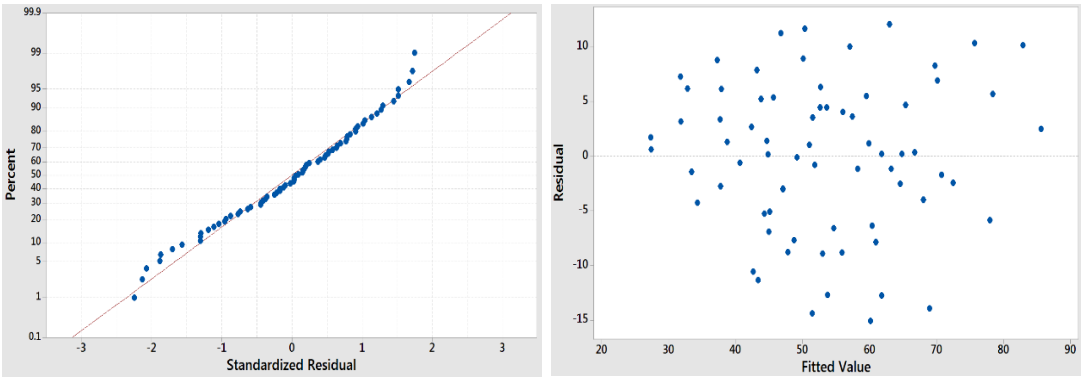

Figure 4-7 Residual plots of regression model generated for mean compressive strength

This indicates that the dispersion of residuals are around their mean and the residuals plots confirm the regression analysis assumptions. As stated (Al-Rawi, 1987), that the residuals, when plotted versus the predicted value, should be gathering around zero concentrically in order to confirm the regression analysis assumptions. When plotting the normal probability, they should show a straight line. Thus, the model can be considered to accurately describe the data.

4.3.1 **Effect of SCMs type**

The effects of SCMs type on the compressive strength at 7, 28, 56 and 90 days are discussed in the following sections. In general, the compressive strength of concrete when containing PFA, GGBS, and fine slag increased with the age of the concrete, as shown in Figure 4.7. It is interesting that the contribution from the SCM became more significant with time, reflecting the SCM's gradual hydration compared with clinker. This is consistent with the literature (Shariq et al., 2010, Bai et al., 2000).

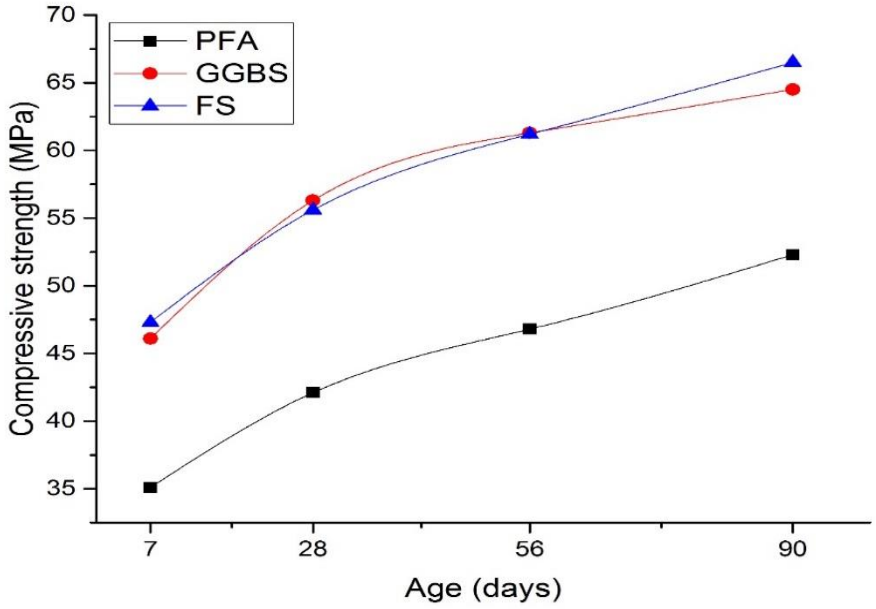

Figure 4-8 Development of compressive strength over time as a function of SCMs

As seen from Table 4.3 and 4.4, the second most influencing variable was SCM type with a contribution of 15.5% & 21.7% based on the statistical analysis at 28 and 90 days. Furthermore, Figure 4.8 shows that the different SCMs (PFA, GGBS, and FS) all behaved differently at all ages. Replacing cement with PFA by 15% and 30% leads to a lower strength at age 28 days, but increased compressive strength at 90 days. This is due to that PFA hydration being more gradual and being reliant on the presence of CH, produced during clinker hydration. Nevertheless, the increased 90 day strength was as a result of C-S-H production, which improves the microstructure. This is consistent with the findings (Luke, 2002, Taylor et al., 2010, Kosior-Kazberuk and Lelusz, 2007). In addition, mixes containing PFA produced lower compressive strengths, possibly a result of the low CaO content (as mentioned in section 3.3.2), indicating that compressive strength development relies on the CaO content (Khale and Chaudhary, 2007, Li et al., 2010).

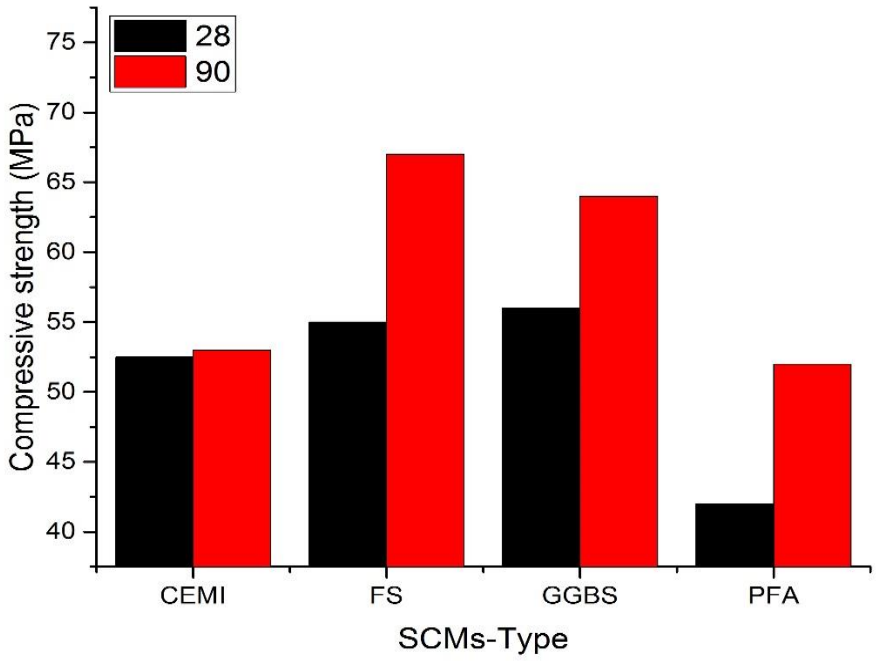

Figure 4-9 The effect of SCMs on strength compared with CEMI at 28 and 90

Slag (fine & coarse) had a great effect on 28 and 90-day strengths. While slag is latently hydraulic, by 28 days the depressive impact on early-age strength is no longer visible and so only the beneficial impact on later-age strength was seen. The improved later-age strength was due to the continued reactivity of slag compared with cement reaction (Oner and Akyuz, 2007). Also, addition of slag causes acceleration in hydration (Stark et al., 2007). Moreover, the slag fineness has a good impact, which seems to go correspond common belief that hydration accelerate because of the surface area, which where slag has given higher reactivity than cement and more stability, this is probably because of fine slag has a greater surface area, so is more reactive and provides more nucleation sites (Deboucha et al., 2018).

The significant effect of SCM replacement on compressive strength is consistent with the results obtained on cumulative heat flow [5.1]. The presence of slag was found to increase heat flow, particularly when using fine slag. This reflects the greater degree of hydration and hence the greater strength. Similarly, the strength data correlate well with bound water contents [5.3], with slag (particularly fine slag) mixes showed higher bound water contents.

4.3.2 Effect of w/b ratio

According to the ANOVA results of compressive strength (Tables 4.3. and 4.4), the most significant factor is w/b ratio, contributing 59.2% & 63.8% at 28 and 90 days, respectively, while Figure 4.9 illustrates that w/b ratio has a great impact on the compressive strength at all ages. This agrees with (Wassermann et al., 2009, Mindess et al., 2003, Mehta and Monteiro, 1993), who reported that compressive strength at all ages is a function of w/b. Compressive strength decreased when w/b ratio increased, as has been known for some time (Neville, 2011). Specifically, the higher the w/b ratio, the lower the strength of concrete. Therefore, the variation in compressive strength due to the different ratio of w/b (0.35 and 0.45) was smaller than 0.55, whereas, increasing the w/b ratio by 0.55 had a big effect on concrete strength reduction.

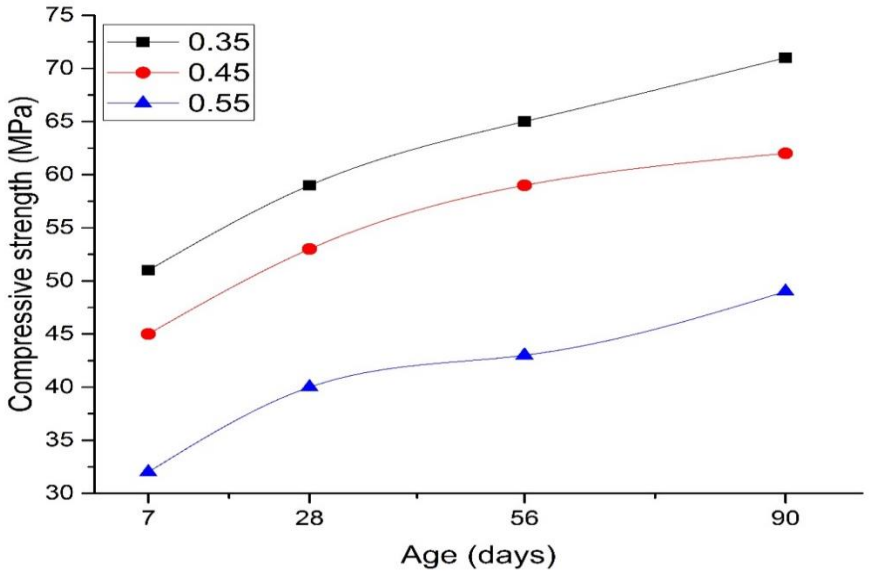

Figure 4-10 Development of compressive strength over time as a function of w/b

Moreover, the hydration of cementitious materials starts when the water touches cementitious particles to form the hydration products which in turn reduce the voids and pores by filling these pores with hydration products. But, any additional amount of water leads to paste dilution and forms more water-filled pores, which results in high porosity when the concrete hardens (Wassermann et al., 2009, Taylor et al., 2006, Schulze, 1999). The effect of w/b ratio on concrete strength is consistent with the results found for blended cement paste. Both heat flow and bound water contents, as determined on pastes, decreased with increasing w/b

ratio, as mentioned in chapter five section 5.1 and 5.3. On the other hand, the coarse capillary porosity determined by SEM image analysis supported the strength data which decreased as the result of w/b ratio increasing, as measured in chapter five section [5.6].

4.3.3 **Effect of superplasticizer**

ANOVA showed that use of SP had a significant impact on strength (Table 4.3 and 4.4). At all ages, increasing SP dosages led to increased strength, as shown in Figure 4.10. This agrees with (Kosmatka et al., 2011, Mindess et al., 2003) who concluded that compressive strengths increase with SP dosage due to a w/b ratio reduction. The use of a plasticizer allows a lower w/b ratio (Pereira et al., 2012 and so a higher strength. In addition, the presence of SP enhances the compaction effectiveness which in turn produces a high density concrete (Alsadey, 2013). The SP enables deflocculation of the water which in turn allows more water to hydrate the cementitious materials and develop the strength.

It can be inferred from Figure 4.10, that SP dosage with 0.2% and 0.6% gave a slight variation regarding concrete strength, but 1.0% had a high impact on concrete strength.

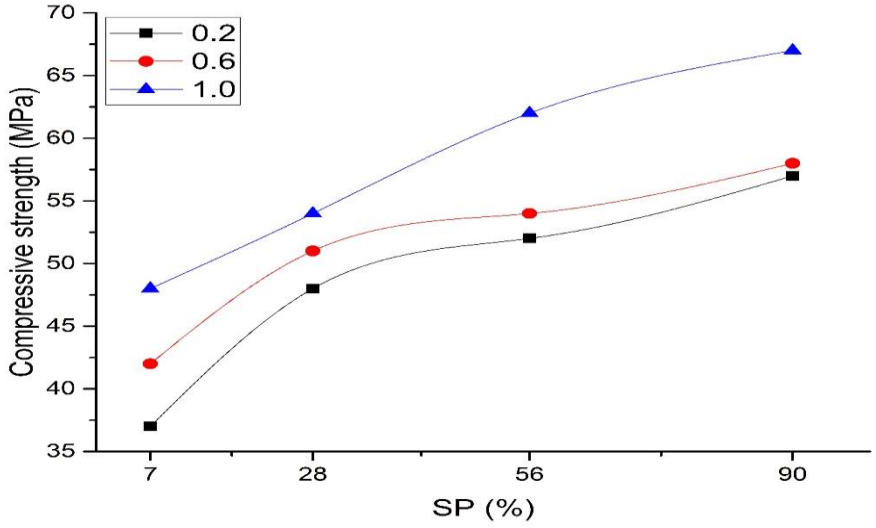

Figure 4-11 Relationship between compressive strength and SP% at 28 and 90 days

4.4 **Gas permeability**

Mean gas permeability was obtained from the 18 mixes at 28, 56, 90 and 180 days, as shown in Figure 4.11. For all samples, permeability decreased with increased curing duration, but at each age, highest permeabilities were seen for mixes 6 and 18, while the lowest were 2, 8, 10, 13 and 16.

Statistical analysis of the gas permeability data at 28 and 90 days was undertaken using Minitab to obtain a multiple liner regression equation (Table 4.8). The multiple coefficients of determination (R^2), indicate that 86.57% and 81.4% of observed variations in the gas permeability data, could be explained by the adopted equation. The ANOVA results for the gas permeability are shown in Tables 4.6 and 4.7, which represented the statistical analysis outputs of gas permeability data at ages 28 and 90 days, respectively. Three factors had a significant impact, i.e. P values less than 0.05, on gas permeability. The significant variables were: w/b ratio, aggregate size and type of SCM. According to the main effects plot of gas permeability for short and long term in Figure 4.12 and 4.13 shows that the gas permeability influenced significantly as mix variables of the concrete changed.

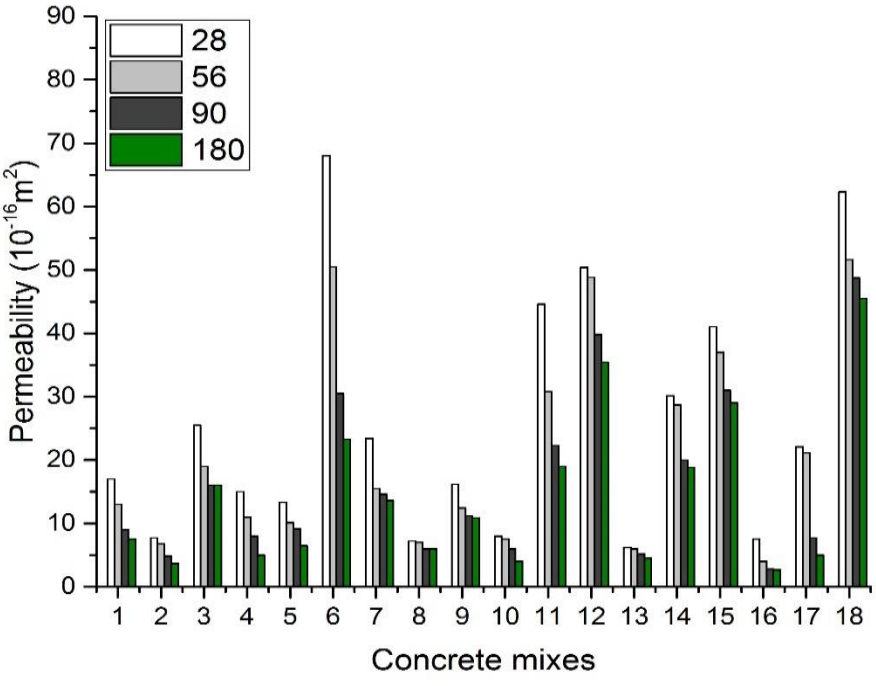

Figure 4-12 Gas permeability results over time

Table 4-6 Results of ANOVA for gas permeability at 28 day

Source	Adj SS	Adj MS	F-Value	P-Value	Significance	Contr.%
Aggregate size	306.36	306.36	5.5	0.041	**significant**	5.9
Binder content	2.86	2.86	0.05	0.825	insignificant	2.6
w/b	1443.21	1443.21	25.9	0	**significant**	32.7
SP%	5.2	5.2	0.09	0.766	insignificant	0.2
SCMs%	0.48	0.48	0.01	0.928	insignificant	29.2
SCMs type	680.11	340.05	6.1	0.019	**significant**	29.4

Table 4-7 Results of ANOVA for gas permeability at 90 day

Source	Adj SS	Adj MS	F-Value	PValue	Significance	Contr.%
Aggregate size	284.09	284.09	5.9	0.035	**significant**	15.0
Binder content	0.19	0.19	0	0.951	insignificant	0.1
w/b	1256.65	1256.6	26.2	0	**significant**	36.3
SP%	2.61	2.61	0.05	0.82	insignificant	0.3
SCMs%	2.13	2.13	0.04	0.837	insignificant	31.8
SCMs type	548.13	274.07	5.72	0.022	**significant**	16.6

Table 4-8 Regression equations for gas permeability at 28 and 90 days

Category	Response		Regression Equation
FS	Permeability	=	-47.4 + 0.825 Aggregate size - 0.0098 Binder content + 109.7 w/b - 1.65 SP% - 0.013 SCMs%
GGBS	Permeability	=	-41.2 + 0.825 Aggregate size - 0.0098 Binder content + 109.7 w/b - 1.65 SP% - 0.013 SCMs%
PFA	Permeability	=	-32.4 + 0.825 Aggregate size - 0.0098 Binder content + 109.7 w/b - 1.65 SP% - 0.013 SCMs%

Category	Response		Regression Equation
FS	Permeability	=	-48.0 + 1.003 Aggregate size - 0.0291 Binder content + 135.3 w/b - 1.79 SP% - 0.167 SCMs%
GGBS	Permeability	=	-41.6 + 1.003 Aggregate size - 0.0291 Binder content + 135.3 w/b - 1.79 SP% - 0.167 SCMs%
PFA	Permeability	=	-29.0 + 1.003 Aggregate size - 0.0291 Binder content + 135.3 w/b - 1.79 SP% - 0.167 SCMs%

As with compressive strength, w/b ratio was found to be the most significant factor, contributing 59.7 and 68.8% at 28 and 90 days respectively. This was followed by SCM type, contributing 28.3 and 16.2% respectively. At 90 days (but

not at 28 days) aggregate size was also seen to be significant, contributing 14.6%.The other factors were all found to be insignificant.

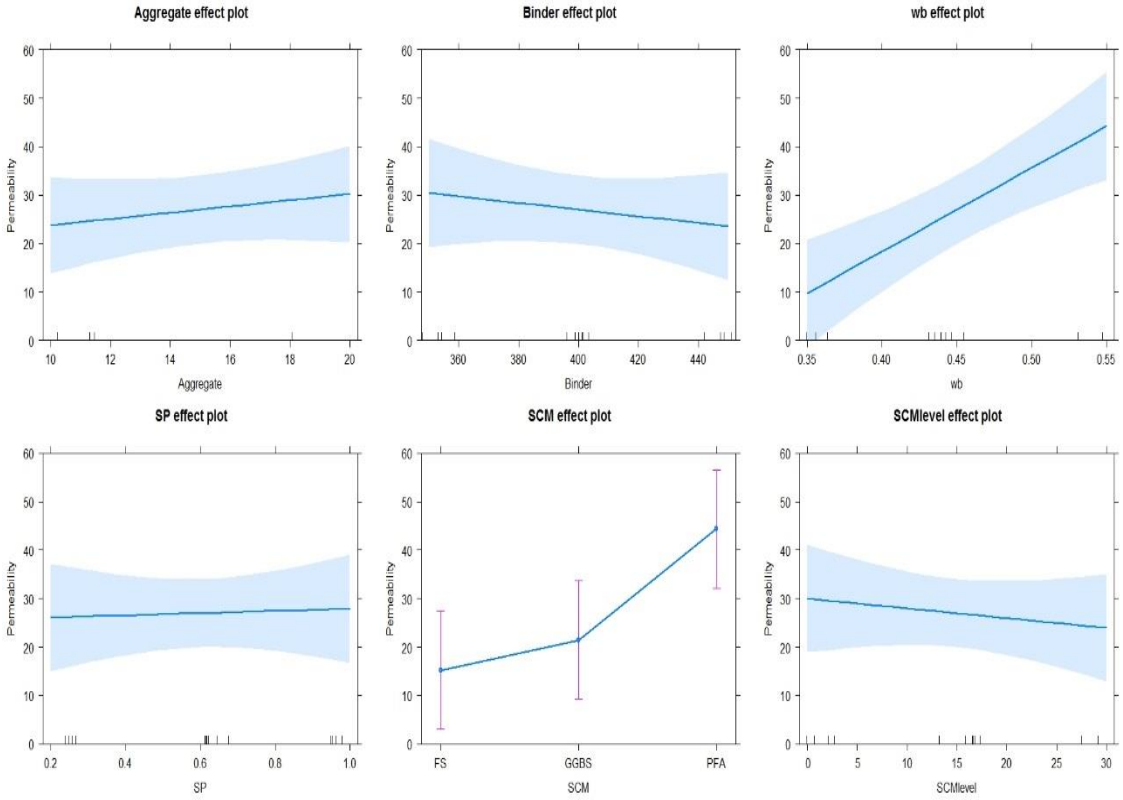

Figure 4-13 Main effects plot for gas permeability at 28 day

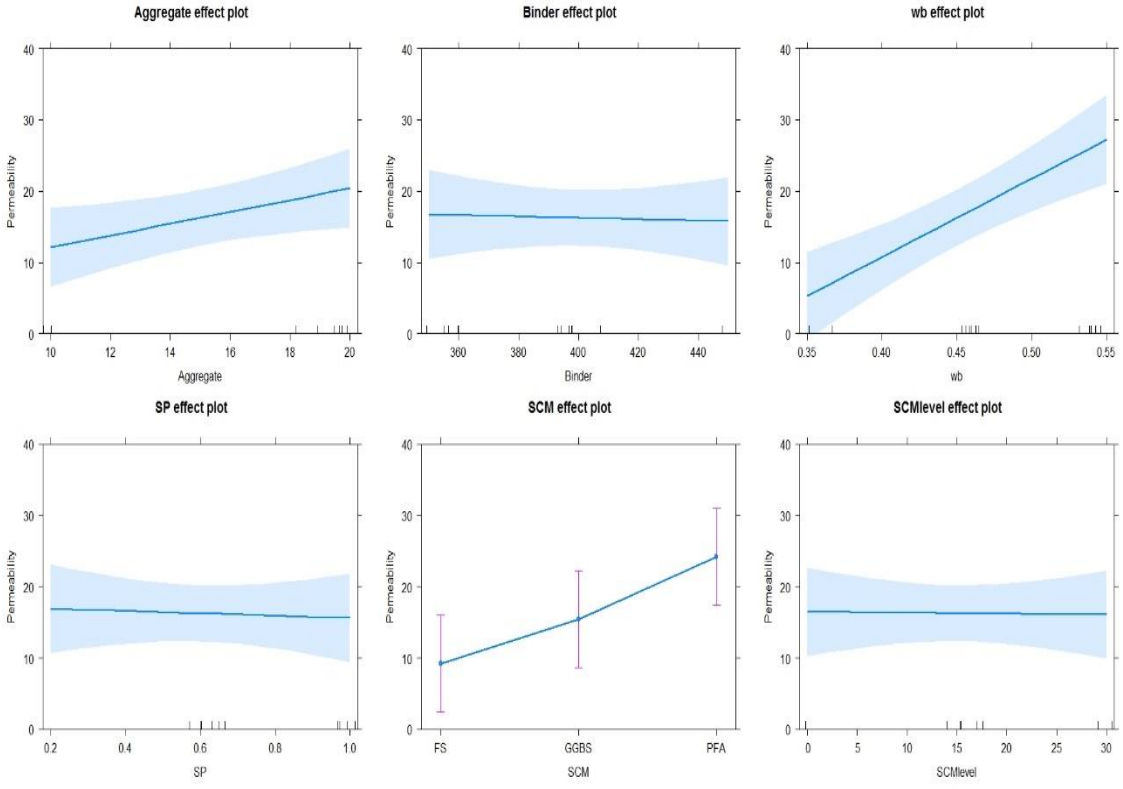

Figure 4-14 Main effects plot for gas permeability at 90 day

The residual plots of this model are given in Figure 4.14. As with the data for gas permeability, they indicate the validity of the model.

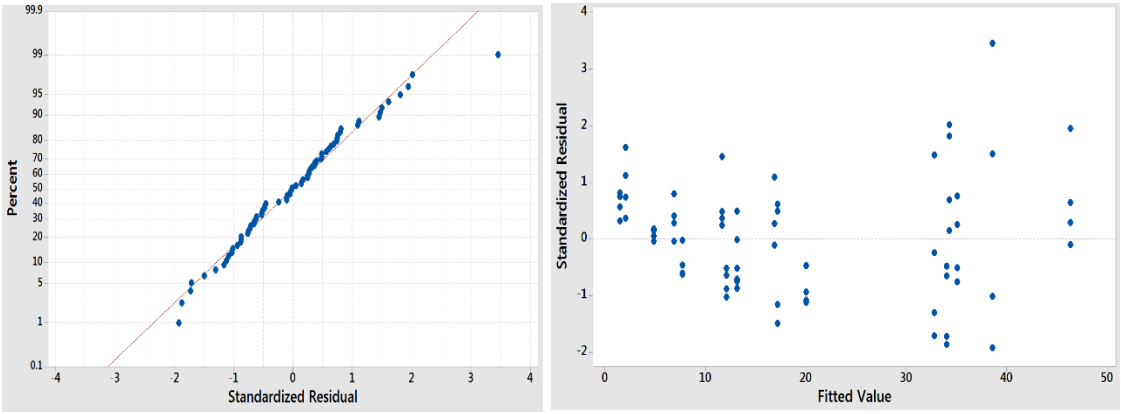

Figure 4-15 Residual values plot of regression model generated for mean gas permeability values.

4.4.1 **Effect of SCMs type**

SCM mixes showed low permeability with age at 28 to 90 days (Figure 4.15). This reduction in permeability may due to the progressive hydration over time which led to filling of the pores with hydration products which in turn block the path of capillary pores and increased tortuosity of the pores. These results agree with literature (Shi et al., 2009, Hadjsadok et al., 2012, Elahi et al., 2010). Slag mixes shows lower permeability than CEMI concrete. Meanwhile, PFA mixes show higher permeability than CEMI concrete at 28 and 90 days.

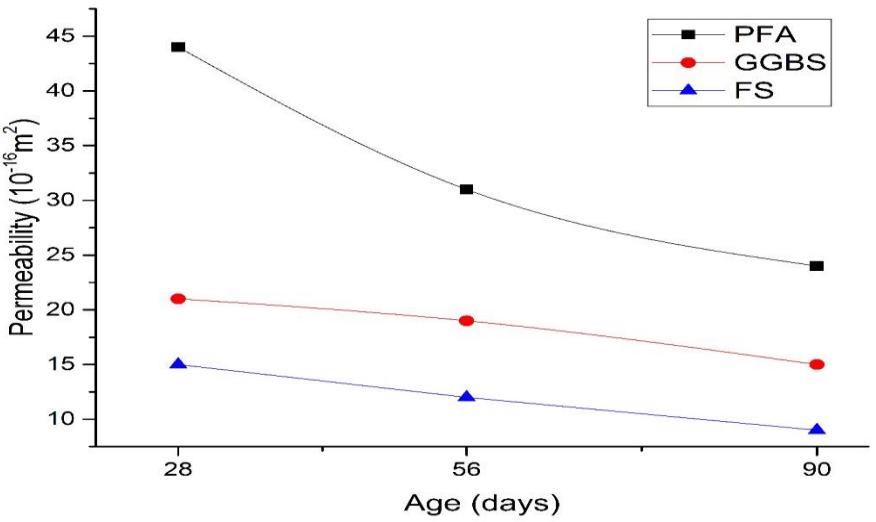

Figure 4-16 Gas permeability over time as a function of SCMs

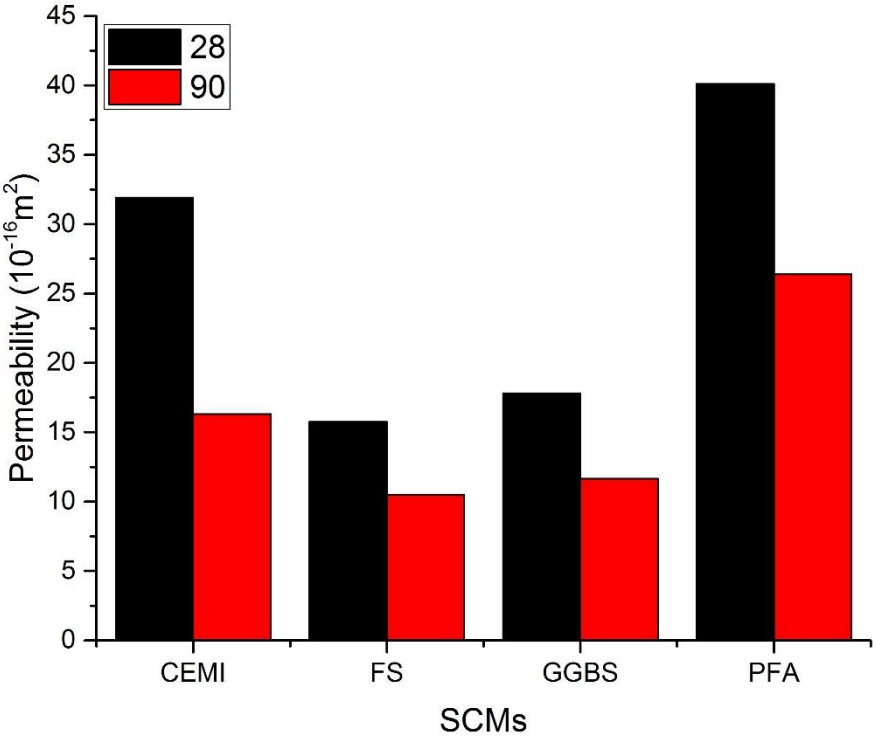

Figure 4-17 Effect of SCMs on permeability compared CEMI at 28 and 90 days

As can be seen from Tables 4.6 and 4.7, the second most influencing variable is SCM type, with a contribution of 28.3% and 16.2 % at ages 28 and 90 days, respectively. Furthermore, it's clear from Figure 4.16 that replacement with slag (fine & coarse) decreases gas permeability. Supplementary cementitious materials are known to improve microstructure, reducing capillary porosity and increasing tortuosity (Obla et al., 2003, Barbhuiya et al., 2009). Furthermore, the addition of SCMs leads to a change in the C-S-H structure, from fibrillar to foil-like, further reducing permeability (Richardson et al., 1994), and that makes the concrete structure dense according to filler effect which leads to better performance in term of transport properties. (Sharma and Khan, 2016, Shi et al., 2009). Nevertheless, PFA concrete shows higher permeability than CEM I concretes. This due to the lower reactivity of PFA which delays the pozzolanic reactions, hence, these mixes show lower permeability (Ortega et al., 2017). Also, because of high fineness of slag particles that making fills the spaces between cement particles and forms the concrete with high density. In addition, fly ash increase the total porosity in paste which in turn increase the permeability due to

the increasing of pore size and make it connected, this results agrees with literature (Wawrzeńczyk et al., 2016, Yu et al., 2017, Yu and Ye, 2013).

The effect of SCM on gas permeability is consistent with the degree of hydration as assessed by chemical bound water from STA and paste porosity from SEM analysis, as shown in section 5.6. The PFA mixes had a higher permeability than the slag mixes at 28 and 90 days, due to the more gradual hydration of PFA . The permeability is affected by the degree of hydration of paste, the more the hydration progresses the lower the permeability. This is consistent with literature (Tracz and Zdeb, 2019, Banthia and Mindess, 1989, Mehta and Monteiro, 1993), who concluded that the coefficient of permeability decreased with an increase in the degree of hydration, as a result of reduced pore size and lowered interconnection.

4.4.2 **Effect w/b ratio**

According to the results in Tables 4.6 and 4.7, the most significant contribution to permeability is w/b ratio, contributing 59.7% and 68.8% at 28 and 90 days respectively. Figure 4.17 illustrates the reduction in average gas permeability with increasing w/b ratio at all ages (28, 56 and 90 days). In addition, permeability decreases with prolonged hydration, as hydration products fill the capillary porosity. This behaviour agrees with literature (Dhir et al., 2006, Mehta and Monteiro, 1993). The permeability of concrete has been influenced by increasing the w/b ratio from 0.35 to 0.55. the presence of water is responsible for hydration of the cementitious materials and any additional water which leads to increase in the content of evaporable water, then produce more pores (Buenfeld and Okundi, 1998, Dinku and Reinhardt, 1997). It is also that the w/b ratio defines the spacing between adjacent cement particles in the fresh paste, so a greater w/b ratio will lead to a greater space between particles and so a greater porosity upon hardening.

This significant contribution of w/b ratio is consistent with the negative influence of w/b ratio increase on the hydration of paste and the formation of pores. Capillary porosity was high with increasing w/b ratio and the hydration progress was slow when adding an additional amount of water. Hence, high water content leads to increase the permeability, this agrees with previous findings (Liu et al., 2016, Yang et al., 2018). The effect of w/b on permeability was consistent with

the influence of w/b on paste behaviour in terms of porosity as discussed in chapter 5.

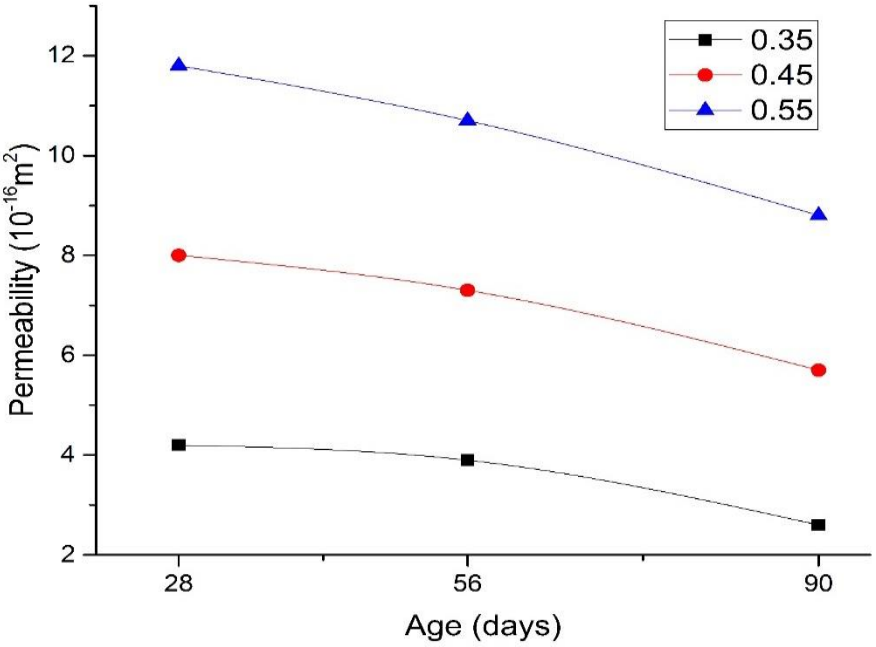

Figure 4-18 the gas permeability behaviour over time as a function of w/b

4.4.3 **Effect of aggregate size**

According to the ANOVA results shown in Tables 4.6 and 4.7, aggregate size contributes 14.6% to permeability at 90 days. Figure 4.18 illustrates that permeability decreases with curing duration. In addition, 20mm aggregate leads to higher gas permeability than 10mm. Larger aggregate leads to heterogeneity and a weak transition zone due to internal bleeding, which leads to more microcracks and thus to greater permeability (Shetty, 2005). These observed results are consistent with the literature (Sriravindrarajah et al., 2012; Jain et al., 2011), who reported that increasing maximum aggregate size leads to increased permeability because the coarse aggregate has a main role to widen the interfacial zone, which in turn influences the microcracks there.

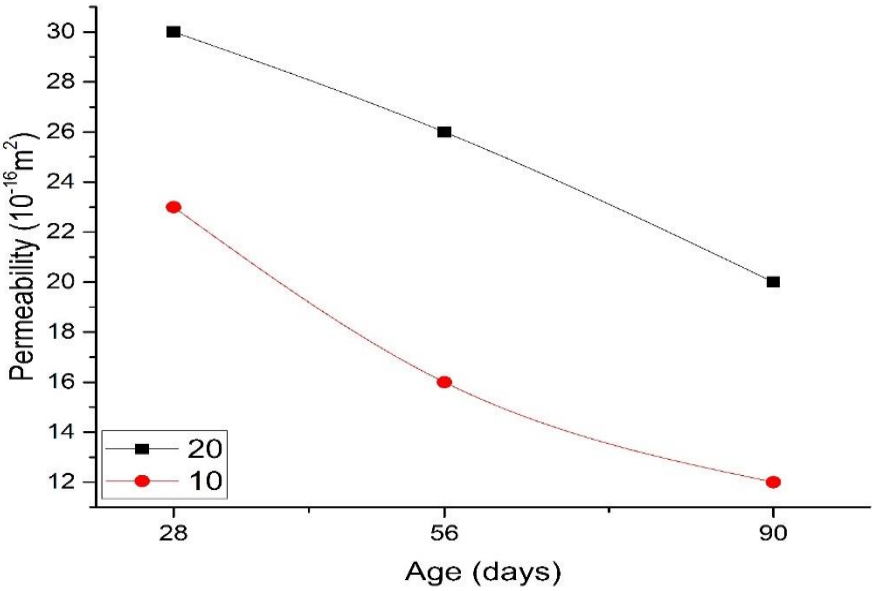

Figure 4-19 The influence of aggregate size on gas permeability overtime

4.5 **Water sorptivity**

Mean water sorptivity were obtained from the 18 concrete mixes for each age, (Figure 4.19). Of all of these samples, at each age the highest sorptivity value was in mix 6 and 18, the lowest was 10 and 16. Sorptivity reduced with age, illustrating the role of hydration, replacing the voids formed at the beginning with hydration products which in turn control uptake of water (Idowu, 2017).

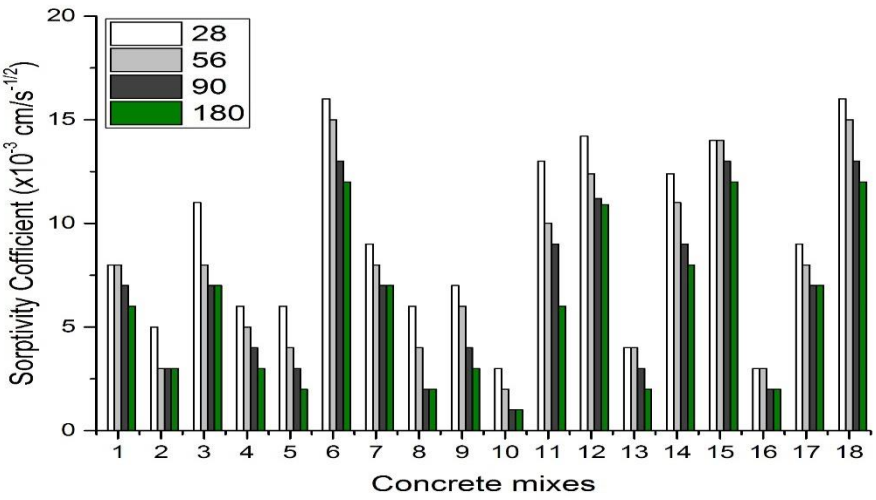

Figure 4-20 Water sorptivity results over time

Statistical analysis of the data was undertaken using Minitab to obtain a regression equation. The R^2 coefficient are 82.68% and 89.18% for 28 and 90 days results, respectively. i.e. This proportion of observed scatter in the data is explained by the adopted equation. The ANOVA results for water sorptivity are shown in Tables 4.9 and 4.10, which used the sorptivity data at ages 28 and 90 days, respectively. Table 4.11 presents the multiple linear regression equations for water sorption at 28 and 90 days results.

Table 4-9 Results of ANOVA for water sorptivity at 28 day

Source	Adj SS	Adj MS	F-Value	P-Value	Significance	Contr.%
Aggregate size	44.18	44.18	6	0.034	**significant**	4.9
Binder content	23.52	23.52	3.19	0.104	insignificant	0.6
w/b	115.32	115.32	15.65	0.003	**significant**	70.9
SP%	0	0	0	1	insignificant	1.1
SCMs%	0.403	0.403	0.05	0.82	insignificant	0.0
SCMs type	168.271	84.136	11.42	0.003	**significant**	22.4

Table 4-10 Results of ANOVA for water sorptivity at 90 day

Source	Adj SS	Adj MS	F-Value	P-Value	Significance	Contr.%
Aggregate size	18.809	18.809	5.56	0.04	significant	16.5
Binder content	7.68	7.68	2.27	0.163	insignificant	8.8
w/b	136.013	136.013	40.22	0	significant	43.1
SP%	5.333	5.333	1.58	0.238	insignificant	0.0
SCMs%	1.613	1.613	0.48	0.505	insignificant	0.2
SCMs type	109.373	54.687	16.17	0.001	significant	31.4

Table 4-11 Regression equations for water sorptivity at 28 and 90 days

Category	Response	Regression Equation
FS	Sorptivity	= -3.10 + 0.313 Aggregate size - 0.0280 Binder content + 31.00 w/b+ 0.00 SP% - 0.0122 SCMs%
GGBS	Sorptivity	= -1.40 + 0.313 Aggregate size - 0.0280 Binder content + 31.00 w/b+ 0.00 SP% - 0.0122 SCMs%
PFA	Sorptivity	= 4.07 + 0.313 Aggregate size - 0.0280 Binder content + 31.00 w/b + 0.00 SP% - 0.0122 SCMs%

Category	Response		Regression Equation
FS	Sorptivity	=	-5.12 + 0.2044 Aggregate size - 0.0160 Binder content + 33.67 w/b - 1.67 SP% - 0.0244 SCMs%
GGBS	Sorptivity	=	-3.55+ 0.2044 Aggregate size- 0.0160 Binder content + 33.67 w/b - 1.67 SP% - 0.0244 SCMs%
PFA	Sorptivity	=	0.72 + 0.2044 Aggregate size - 0.0160 Binder content + 33.67 w/b - 1.67 SP% - 0.0244 SCMs%

Based on the produced regression equation and ANOVA results, three factors have a significant impact on water sorptivity: w/b ratio, the type of SCMs and aggregate size. As the main effects plot of water sorptivity for short and long term in Figure 4.20 and 4.21 show, sorptivity changed significantly with mix variables. In addition, the contribution percentages clarify the degree of influence of these variables and the optimal level for each significant variable through which lower water sorptivity may be achieved. At 28 days, the most important contributions is the w/b ratio with 70.9%, followed by supplementary cementitious materials and aggregate size with 31.4% and 16.5%, respectively. The trends were the same at 90 days, although with slightly different contributions from the different variables.

The residual plots of this model are given in Figure 4.22, which included normal probability and versus fits. It is concluded that there is not any indication of the violation of the assumptions of the error.

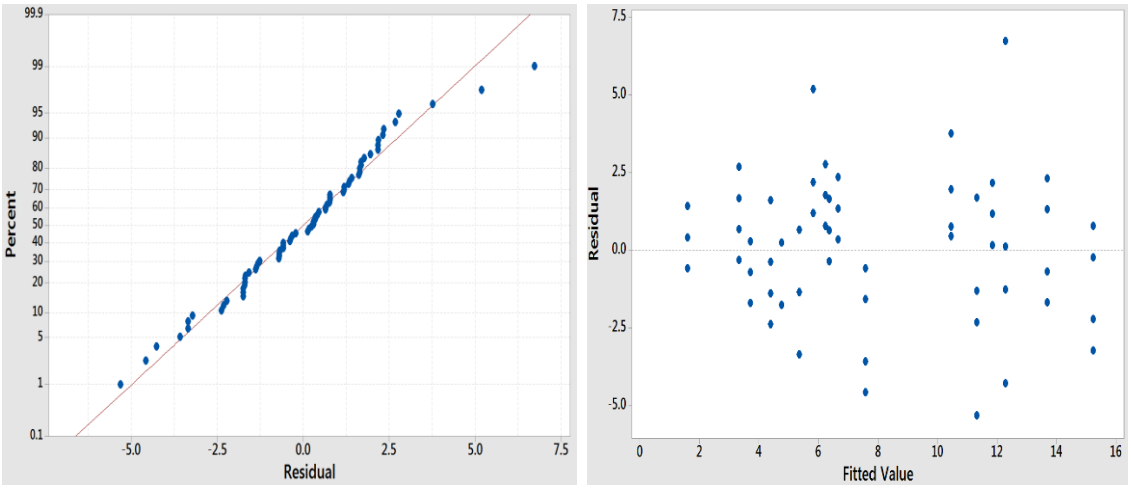

Figure 4-21 Residual values plot of regression model generated for mean water sorptivity values.

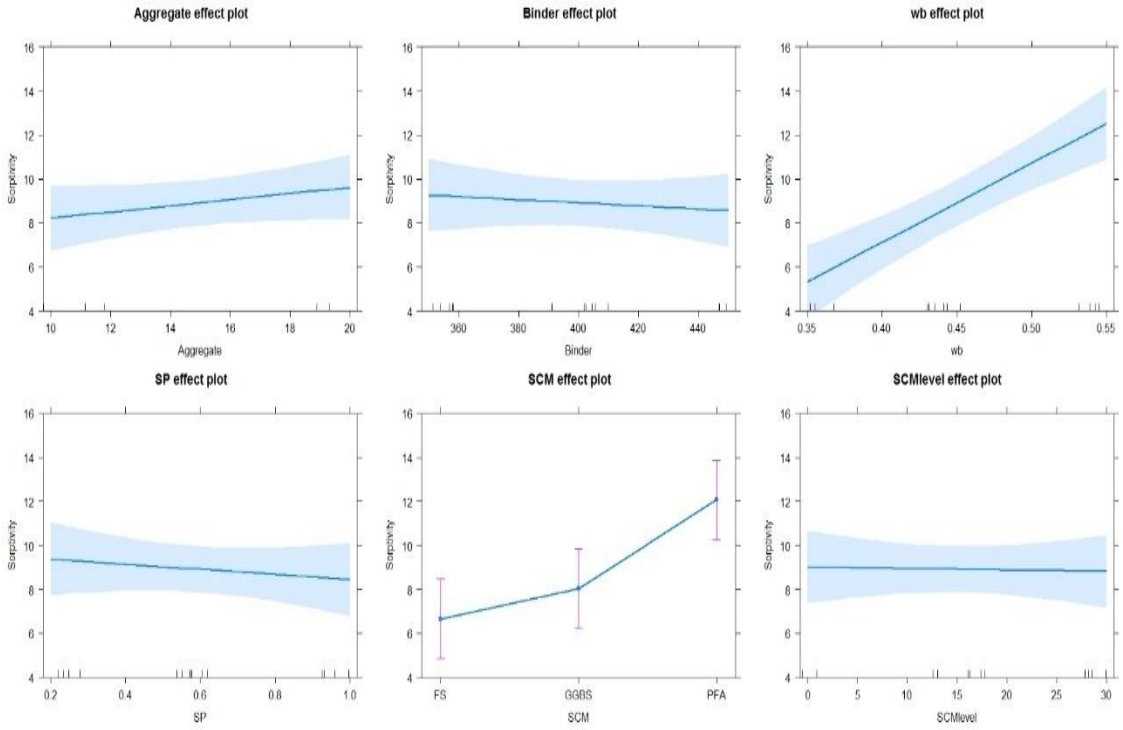

Figure 4-22 Main effects plot for water sorptivity at 28 day

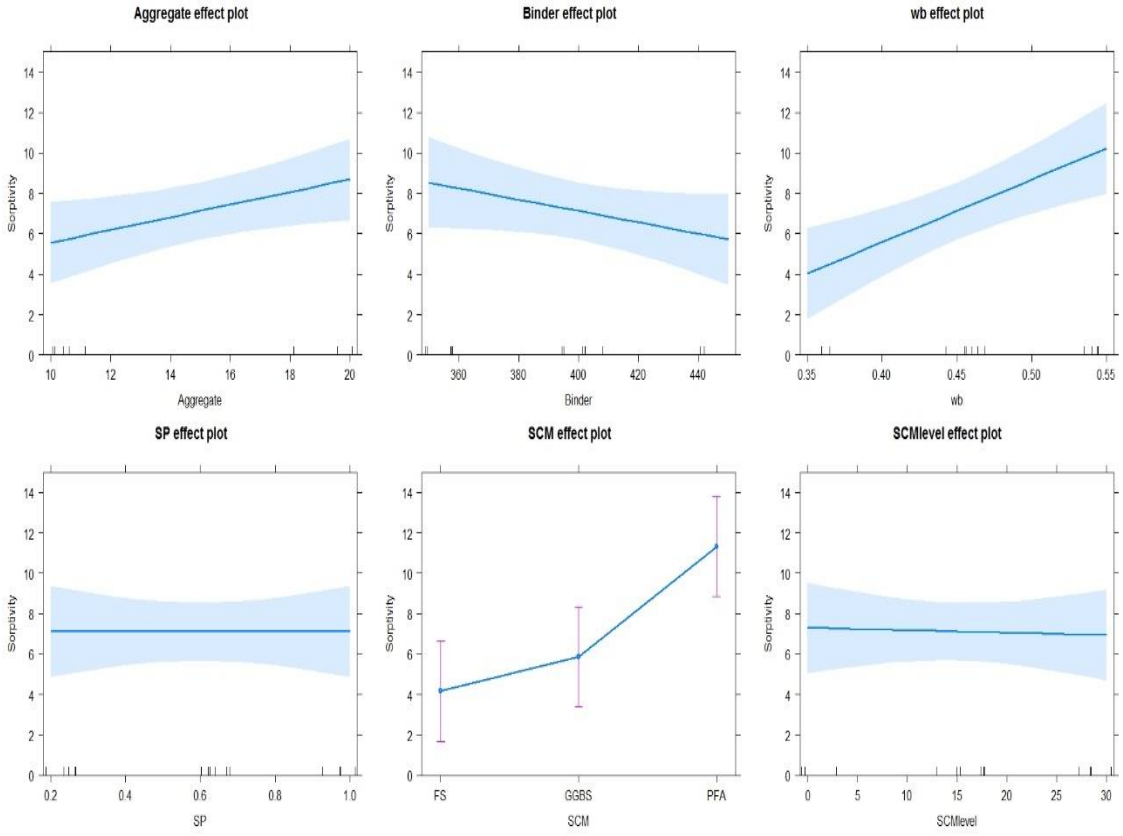

Figure 4-23 Main effects plot for water sorptivity at 90 day

4.5.1 1Effect of SCMs type

The effects of SCMs type on the water sorptivity at 28, 56 and 90 days are discussed in the following section. In general, the sorptivity of concrete decreases when the age increased as shown in Figure 4.23.

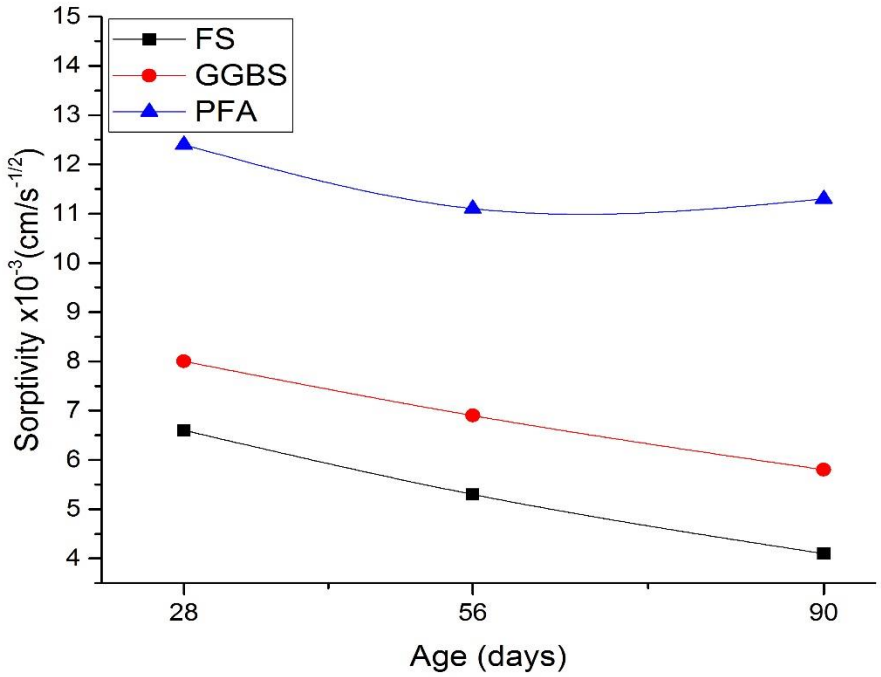

Figure 4-24 Water sorptivity over time as a function of SCM

The second most influencing variable is SCMs type with a contribution of 22.4% and 31.4% at 28 and 90 days, respectively (Tables 4.9 and 4.10). Fine slag with 30% (WoB) replacement showed lower sorptivity than PFA and GGBS at 28 days, but at 90 days the fine and coarse slag showed similar sorptivity. The low water sorption for fine slag concretes were as results of the fineness of fine slag compared with other replacements and the high reactivity. This feature made the fine slag had the capability for improving the hydration progress which in turn filled the pores that blocked the path of water flow. Figure 4.24 shows the effect of using different SCMs on water sorptivity of concrete samples at 28 and 90 days with 30% replacement ratio. PFA mixes showed higher sorptivity that other binders.

Sorptivity is related to porosity, so higher sorptivity arises due to greater spacing of cement particles in the fresh paste..Then, lower degrees of hydration in the PFA blends (because PFA is less reactive than either the cement or the slag) leads to higher sorptivity. Similarly, fine slag leads to lower sorptivity because it is more reactive than coarse slag. This relates to the bound water data and the calorimetry.

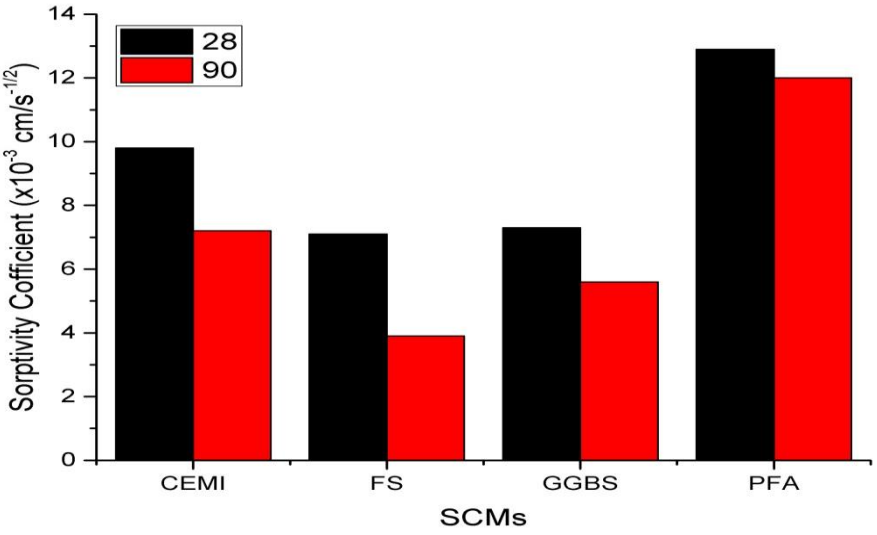

Figure 4-25 Effect of SCMs on sorptivity compared CEMI at 28 and 90 days

4.5.2 **Effect of w/b ratio**

According to the ANOVA results of water sorptivity as tabulated in Tables 4.9. and 4.10, the most significant contribution is by w/b ratio, contributing 70.9% and 43.1% at 28 and 90 days, respectively. Figure 4.25 illustrates that water sorptivity is greatly reduced at all ages by reducing w/b ratio from 0.55 to 0.35.

The water sorption of concrete mixtures have increased with increasing the w/b ratio due to the reducing of concrete density when the content of water high, which in turns increased the porosity (Misra et al., 2007).

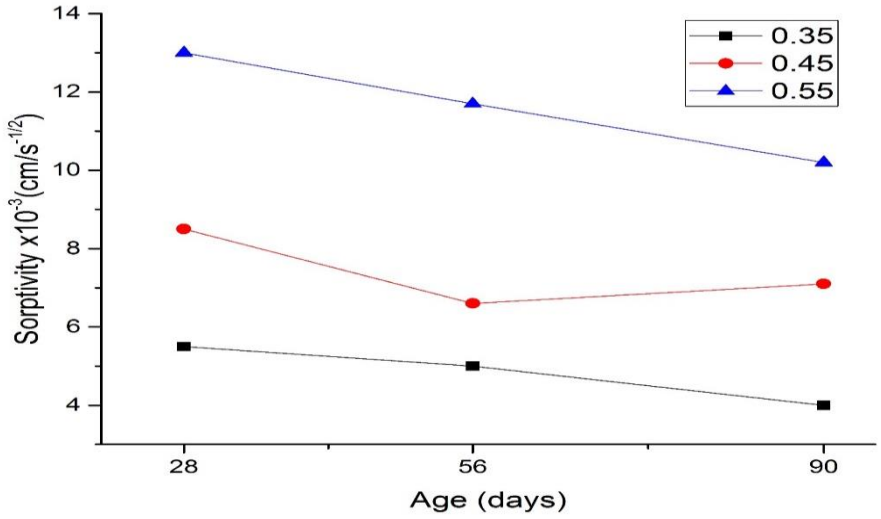

Figure 4-26 The water sorptivity behaviour over time – w/b

4.5.3 **Effect of aggregate size**

According to the ANOVA results for gas permeability, as tabulated in Tables 4.9 and 4.10., shows that the maximum aggregate size had the third significant contribution with 16.5%. Figure 4.26 illustrates that sorptivity decreases with curing duration. In addition, 20mm aggregate gave higher water sorptivity than 10mm. The higher aggregate size gives heterogeneity and weak transition zone due to the internal bleeding which leads to more microcracks which helps to penetrate more water through the concrete (Shetty, 2005). These observed results are consistent with the literatures (Sriravindrarajah et al., 2012, Jain et al., 2011).

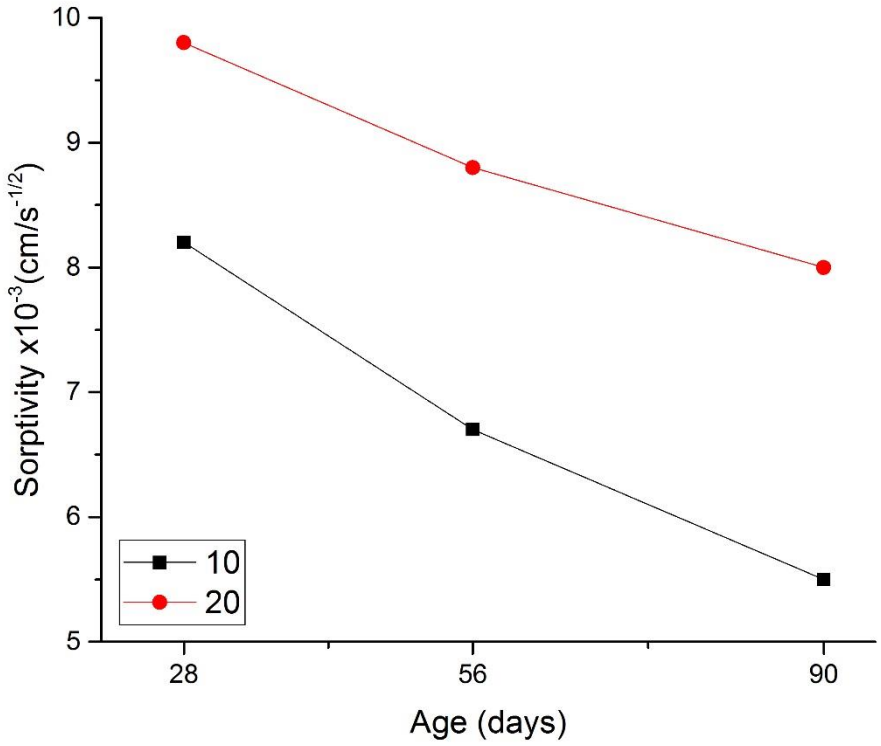

Figure 4-27 The influence of aggregate size on water sorptivity overtime

4.6 **Shrinkage**

Mean shrinkages were obtained from the 18 concrete mixes for 28 and 90 days, which shown in Figure 4.27. The readings of shrinkage were measured after curing for 28 days, then cured in a control room under dry condition for 28 and 90 days. The shrinkage is increased with time increasing as the result of drying circumstance which leads to loss of water from the concrete which exists in pores (Ayub et al., 2014, Kosmatka et al., 2011) . Of all of these samples, at each age the highest shrinkage was mix 3, the lowest was 11.

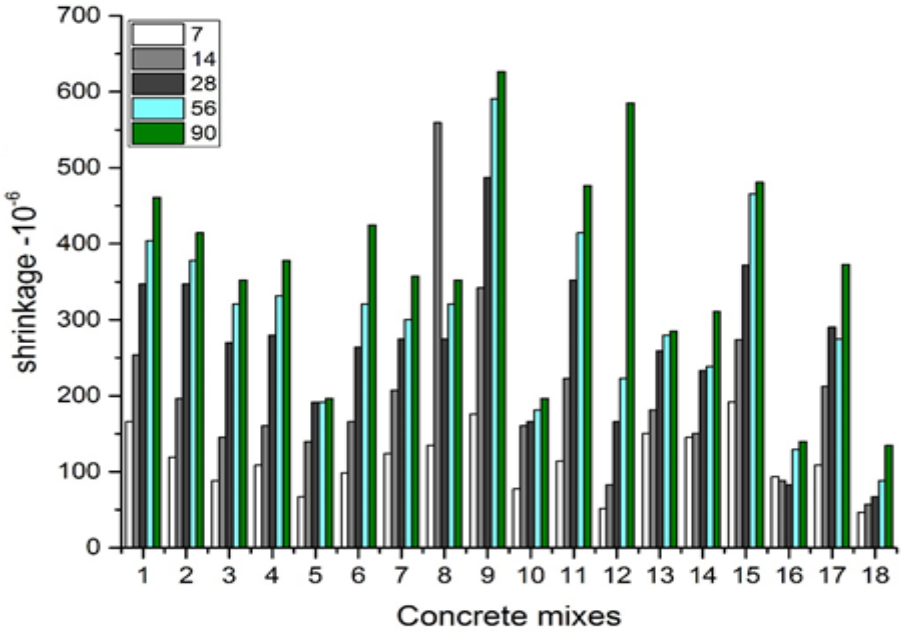

Figure 4-28 Shrinkage over following curing for 28 or 90 days

Statistical analysis of the data was undertaken using Minitab to obtain a regression equation. The multiple linear regression (MLR) is suitable to make a correlation between mix design variables and the shrinkage, where gives a more accurate representation based on designed experiment results (Draper and Smith, 1998). The multiple coefficients of determination (R^2), indicates that 71.11% and 72.22% of observed variations in the shrinkage data is explained by the adopted equation. The ANOVA results for the shrinkage readings are shown in Tables 4.10 and 4.11, which used the shrinkage data at ages 28 and 90 days, respectively. The regression equation relating to 28 and 90 days shrinkages is given in Table 4.12.

Table 4-12 Results of ANOVA for shrinkage at 28 day

Source	Adj SS	Adj MS	F-Value	P-Value	Significance	Contr.%
Aggregate size	16928	16928.0	3.77	0.058	significant	**18.3**
Binder content	12	12.0	0.00	0.960	insignificant	0.0
w/b	22533	22533.3	5.02	0.049	significant	**24.3**
SP%	21084	21084.1	4.69	0.075	insignificant	17.7
SCMs%	14352	14352.1	3.20	0.104	insignificant	15.5
SCMs type	35659	17829.4	3.97	0.054	significant	**19.2**

Table 4-13 Results of ANOVA for shrinkage at 90 day

Source	Adj SS	Adj MS	F-Value	P-Value	Significance	Contr.%
Aggregate size	21494	21493.6	4.12	0.050	significant	**20.6**
Binder content	1	0.7	0.00	0.991	insignificant	0.0
w/b	25669	25668.8	4.92	0.051	significant	**23.3**
SP%	24120	24120.3	4.63	0.077	insignificant	18.9
SCMs%	13002	13002.1	2.49	0.145	insignificant	11.8
SCMs type	51302	25651.1	4.92	0.033	significant	**23.3**

Table 4-14 Regression equations for shrinkage at 28 and 90 days

Category	Response	Regression Equation
FS	Shrinkage	= 251 - 6.13 Aggregate size + 0.020 Binder content + 433 w/b + 104.8 SP% + 2.31 SCMs%
GGBS	Shrinkage	= 242 - 6.13 Aggregate size + 0.020 Binder content + 433 w/b + 104.8 SP% + 2.31 SCMs%
PFA	Shrinkage	= 152 - 6.13 Aggregate size + 0.020 Binder content + 433 w/b + 104.8 SP% + 2.31 SCMs%

Category	Response	Regression Equation
FS	Shrinkage	= 383 - 6.91 Aggregate size - 0.005 Binder content + 462 w/b + 112.1 SP% + 2.19 SCMs%
GGBS	Shrinkage	= 367 - 6.91 Aggregate size - 0.005 Binder content + 462 w/b + 112.1 SP% + 2.19 SCMs%
PFA	Shrinkage	= 263 - 6.91 Aggregate size - 0.005 Binder content + 462 w/b + 112.1 SP% + 2.19 SCMs%

At both ages, three factors were found to be significant on shrinkage; w/b ratio, superplasticizer % and SCM type. The effect of each of these variables is shown in the main effects plots (Figures 4.27 and 4.28), while the contribution percentage (Tables 4.10 and 4.11) clarify the degree to which these variables affect shrinkage, and help to identify the factors which can limit shrinkage .The most important contribution is w/b ratio, with 23.3%, followed by supplementary cementitious materials and superplasticizer with 23.3% and 21.9%, respectively. However, at age 90 days, all variables have given the same trend whether an increment or decreases regarding compressive strength performance with a bit different contribution percentage compared with results at 28 days.

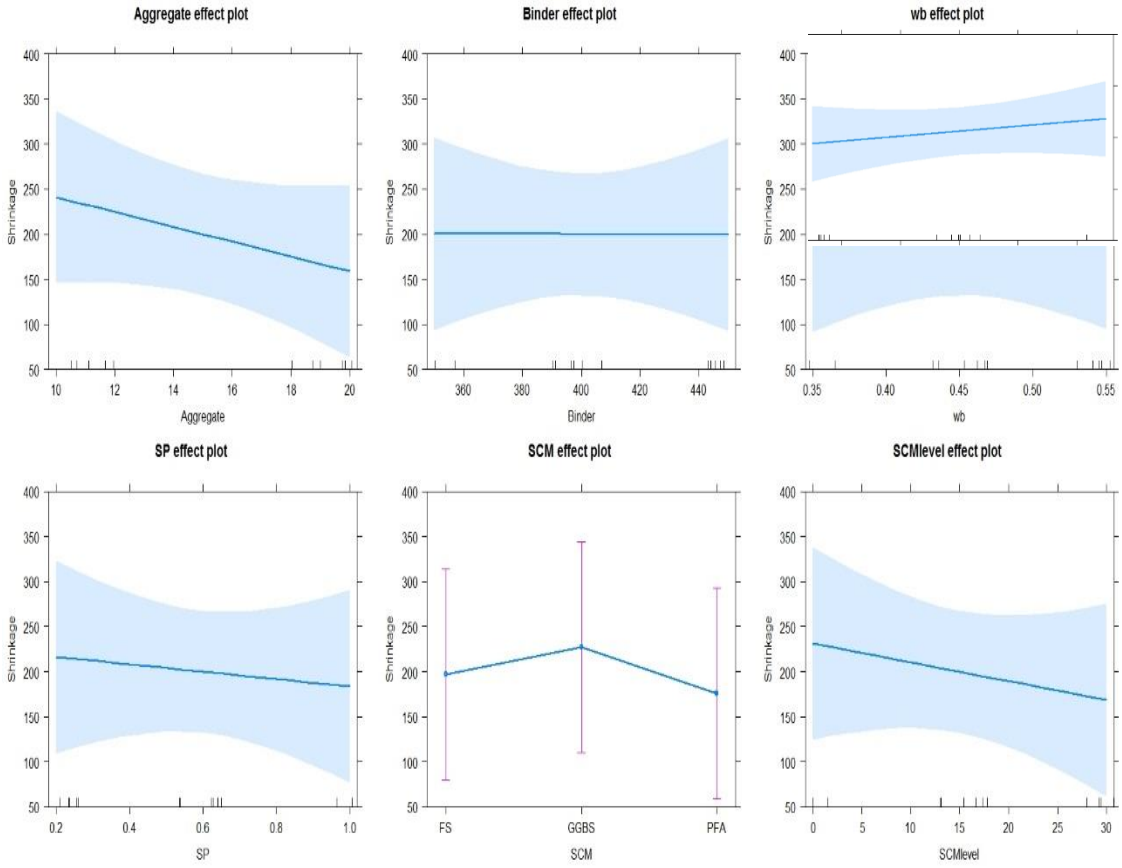

Figure 4-29 Main effects plot for shrinkage at 28 day

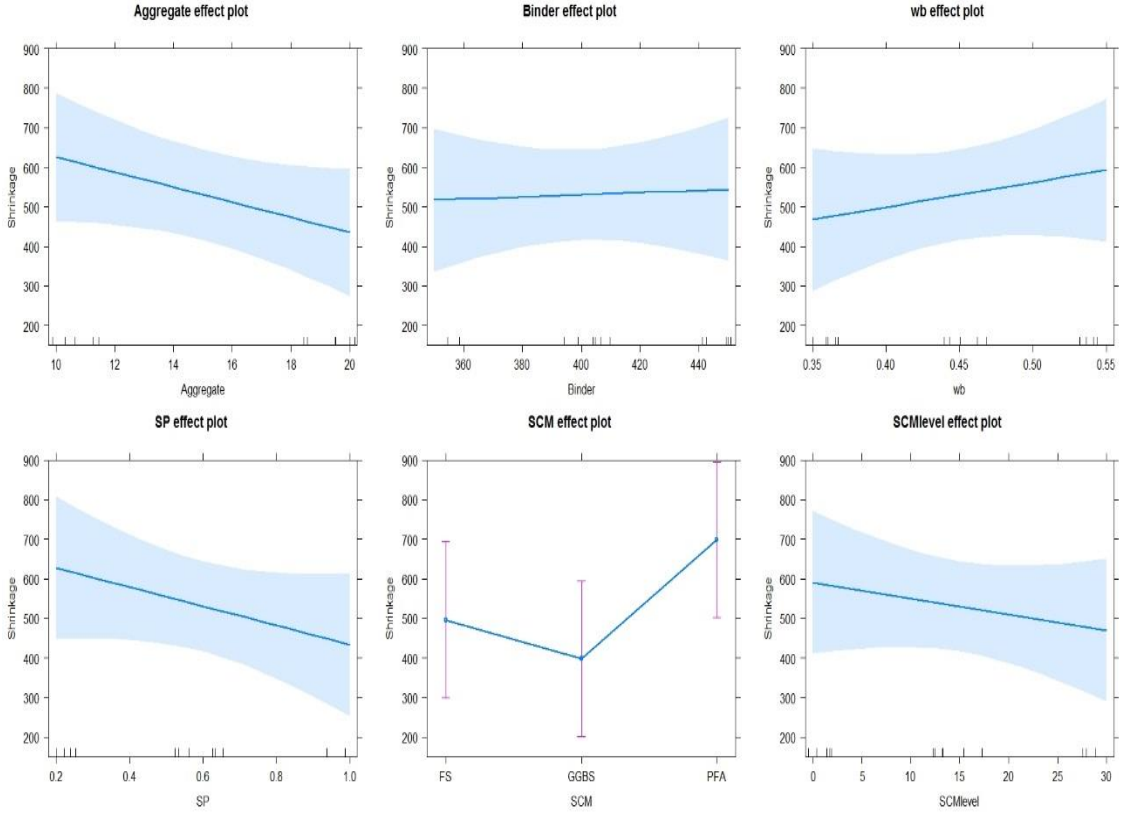

Figure 4-30 Main effects plot for shrinkage at 28 day

Examining the conditions of normality and quality of variance (Figure 4.30), the model accurately describes the design mixes. According to the model, all three factors make a comparable contribution to shrinkage.

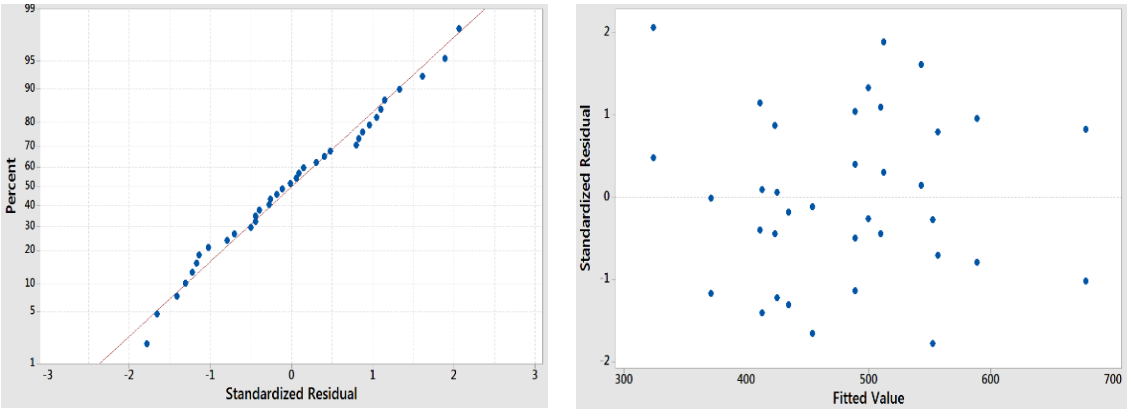

Figure 4-31 Residual plots of regression model generated for mean shrinkage readings

4.6.1 **Effect of SCMs**

Figure 4.31 shows the effect of SCM on concrete strains (shrinkage) to 90 days for concrete mixtures which contained PFA, GGBS, and FS. The presence of SCM led to decreased shrinkage compared with Portland cement mixes. This due to the role of the less reactive supplementary cementitious materials as fillers which restrain the shrinkage at an early age (Bisaillon et al., 1994, Zhang, 1995, Güneyisi et al., 2010). Nevertheless, the PFA mixes showed higher shrinkage values than slag (fine & coarse) and similar values to CEM I mixtures at 90 days. The shrinkage behaviour of PFA mixtures is consistent with the high permeability values and low strength as seen in earlier sections. Also, these results are consistent with the coarse porosity in PFA paste, with increased shrinkage with increasing porosity, whereby there was more water loss from pores, which increased shrinkage (Mokarem et al., 2005). This agrees with the literature (Tongaroonsri and Tangtermsirikul, 2009, Chindaprasirt et al., 2004)..

On the other hand, slag mixes (especially the fine slag) showed low shrinkage. This is due to the low coarse porosity in slag paste as found by SEM analysis. The fine slag generally increases pore refinement of paste and reduces the water content in the pores, causing low shrinkage as the result of low water content lost from capillaries (Zhou et al., 2012). In addition, the high degree of hydration, as seen by strength and bound water content, leads to C-S-H formation, increasing

the density and enhancing resistance against length change (shrinkage strain) (Li and Yao, 2001). This behaviour agrees with the literature (Almutairi, 2017).

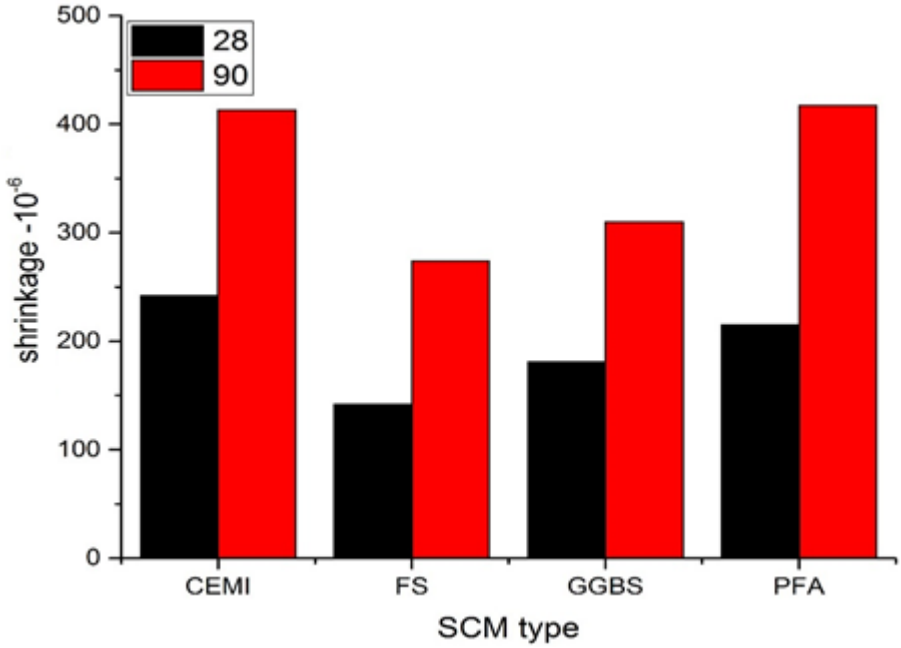

Figure 4-32 The effect of SCMs on shrinkage compared with CEMI at 28 and 90 days

4.6.2 **Effect of w/b ratio**

Tables 4.10 and 4.11 shows that w/b ratio influenced the degree of shrinkage. Figure 4.32 shows that shrinkage increases with w/b ratio. This reflects the increased water content in the capillary pores as the result of increasing the amount of evaporable water (Zhang et al., 2013b).

This is consistent with the effect of w/b ratio on the strength properties and permeation properties which concluded that the increasing w/b ratio increase the permeability and sorptivity and decrease the strength development.

Moreover, microstructural features supported this. The bound water, which gives an indication about the degree of hydration, decreased with increasing w/b. Meanwhile, the porosity determined by SEM image analysis increased with increasing w/b. This is agrees with literature (Neubauer et al., 1997, Zhang et al., 2013b, Zhu et al., 2017) who reported that increasing w/b ratio led to increase the shrinkage.

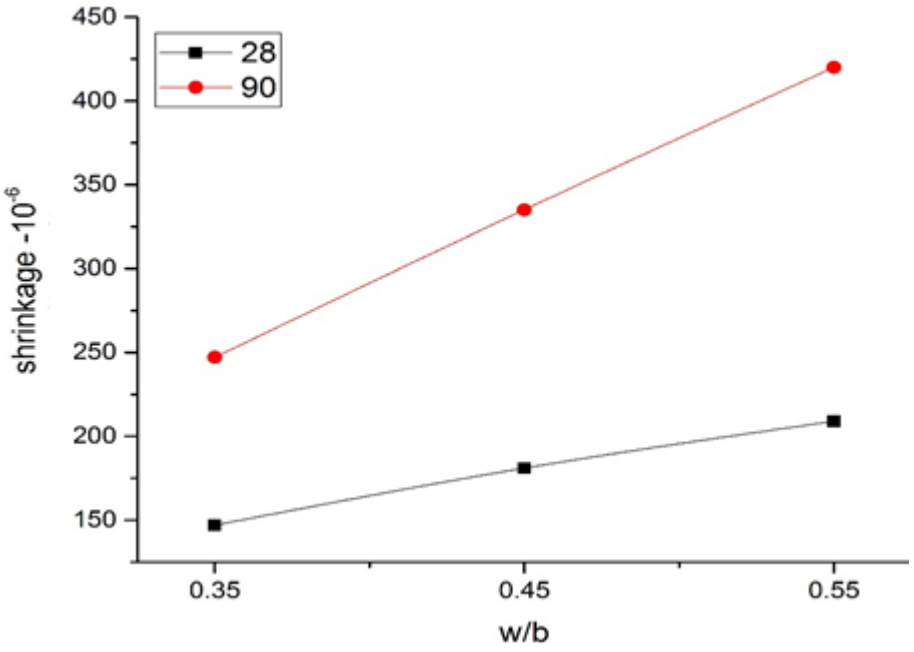

Figure 4-33 The effect of w/b ratio on shrinkage behaviour

4.6.3 **Effect of aggregate size**

Figure 4.33 shows that increasing the aggregate size decreases shrinkage. The aggregate is known to restrain shrinkage because of a high modulus of elasticity, thus there is shrinkage reduction when using larger aggregate, where the paste content will be reduced and replaced with aggregate (Dyer, 2014). Also, that increasing aggregate content will lead to lower water content, so less binder and less C-S-H. These results are consistent with earlier findings (Wassermann et al., 2009; Kosmatka et al., 2011; Mehta and Monteiro, 1993). It can be observed from figure 4.33, that the effect of aggregate size is much clear at 90 days than at 28 days. This may be due to the presence of pozzolanic materials which hydrate slowly producing hydration product in the long term. Therefore, the shrinkage gets in this period (90 days) and the role of aggregate resistant against paste shrinkage be activating.

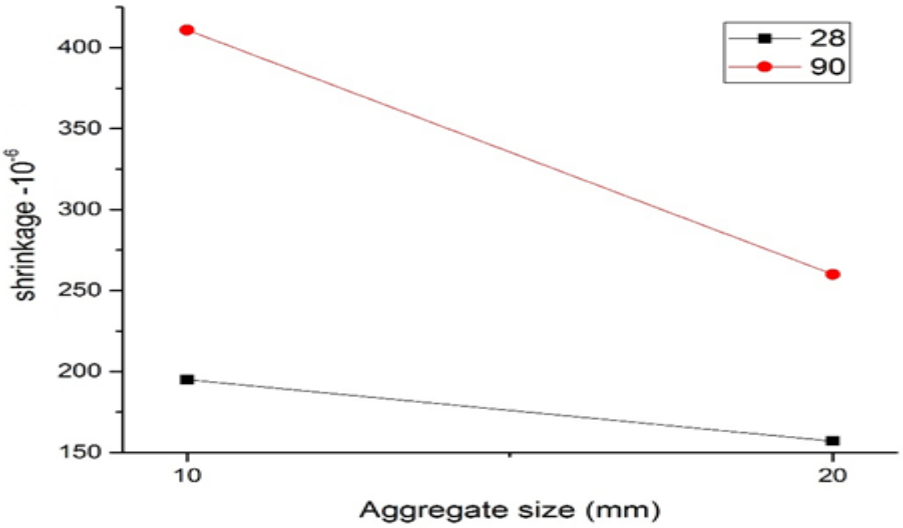

Figure 4-34 The effect of aggregate size on shrinkage

4.7 Carbonation depth

Figure 4.34 displays the average carbonation depth, as determined by sprying phenolphthalein for 18 concrete samples exposed to 4% carbon dioxide (60% RH, 20°C) for 28, 56, 90, and 180 days. In all 18 mixes, carbonation progressed the least in mixes 1, 5, 10 and 16, whereas it was greatest in mixes 6, 11 and 18.

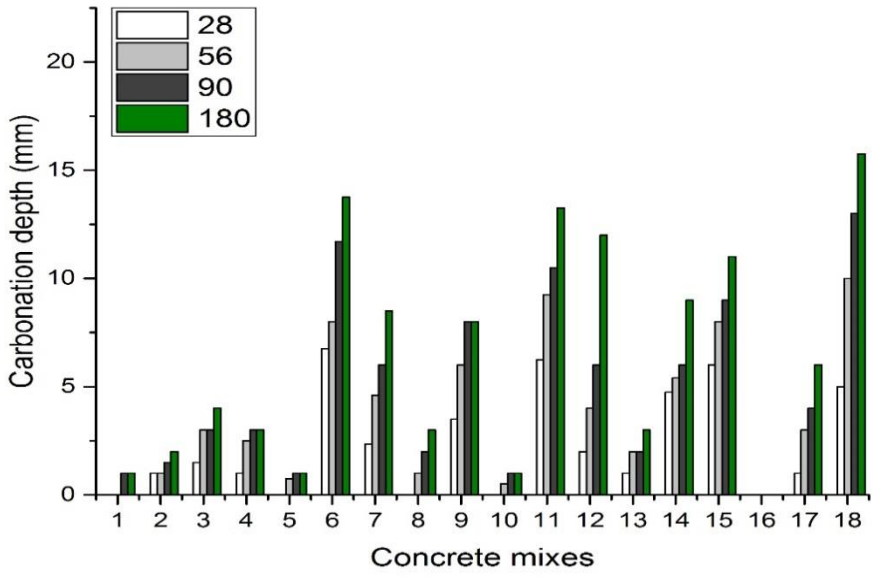

Figure 4-35 Carbonation depth of 18 concrete mixes exposed to CO_2 for different age.

Carbonation depth was converted to a carbonation coefficient (k), obtained from a linear fit of carbonation depth data at 28, 56, 90 and 180 days (Figure 4.34) as a function of the square root of time as calculated in Equation 4.13.

$$x(t) = k\sqrt{\mathrm{t}}$$ --------- Table 4-15 (Kropp et al., 1995)

Where:

x = carbonation depth (mm)

t = time (s)

k = carbonation coefficient

Statistical analysis (ANOVA), as shown in Table 6-1, indicates the existence of three significant variables: binder content, w/b ratio, and SCM type. Of these, w/b ratio is the most significant, contributing 28.3%. SCM type is the second most influencing variable and binder content the third significant variable with 23.3%.

Table 4-16 Results of ANOVA for carbonation coefficient (k)

Source	Adj SS	Adj MS	F-Value	P-Value	Significance	Contr.%
Aggregate size	0.057	0.0571	1.52	0.245	insignificant	2.6
Binder content	0.131	0.1315	3.51	0.059	**significant**	**15.9**
w/b	0.918	0.9182	24.47	0.001	**significant**	**31.4**
SP%	0.103	0.1036	2.76	0.128	insignificant	4.7
SCMs%	0.000	0.0003	0.01	0.925	insignificant	0.0
SCMs type	1.007	0.5038	13.43	0.001	**significant**	**45.4**

Table 4-17 Regression equations for carbonation coefficient

Category	Response		Regression Equation
FS	Carbonation Coefficient	=	-0.126 + 0.01127 Aggregate size - 0.00209 Binder content + 2.766 w/b - 0.232 SP% - 0.00036 SCMs%
GGBS	Carbonation Coefficient	=	-0.063 + 0.01127 Aggregate size - 0.00209 Binder content + 2.766 w/b - 0.232 SP% - 0.00036 SCMs%
PFA	Carbonation Coefficient	=	0.404 + 0.01127 Aggregate size - 0.00209 Binder content + 2.766 w/b - 0.232 SP% - 0.00036 SCMs%

The normal probability and versus fit for residuals are presented in Figure 6.5 and indicate that the model accurately describes the design mixes, while Figure 4.36 shows the main effects of significant mix design variables which influence the progression of carbonation.

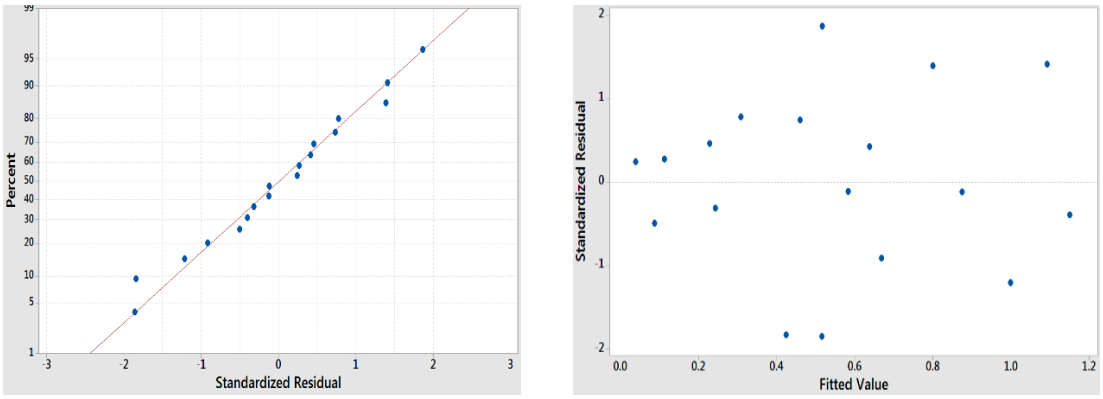

Figure 4-36 Residual values plot of regression model generated for mean gas permeability values.

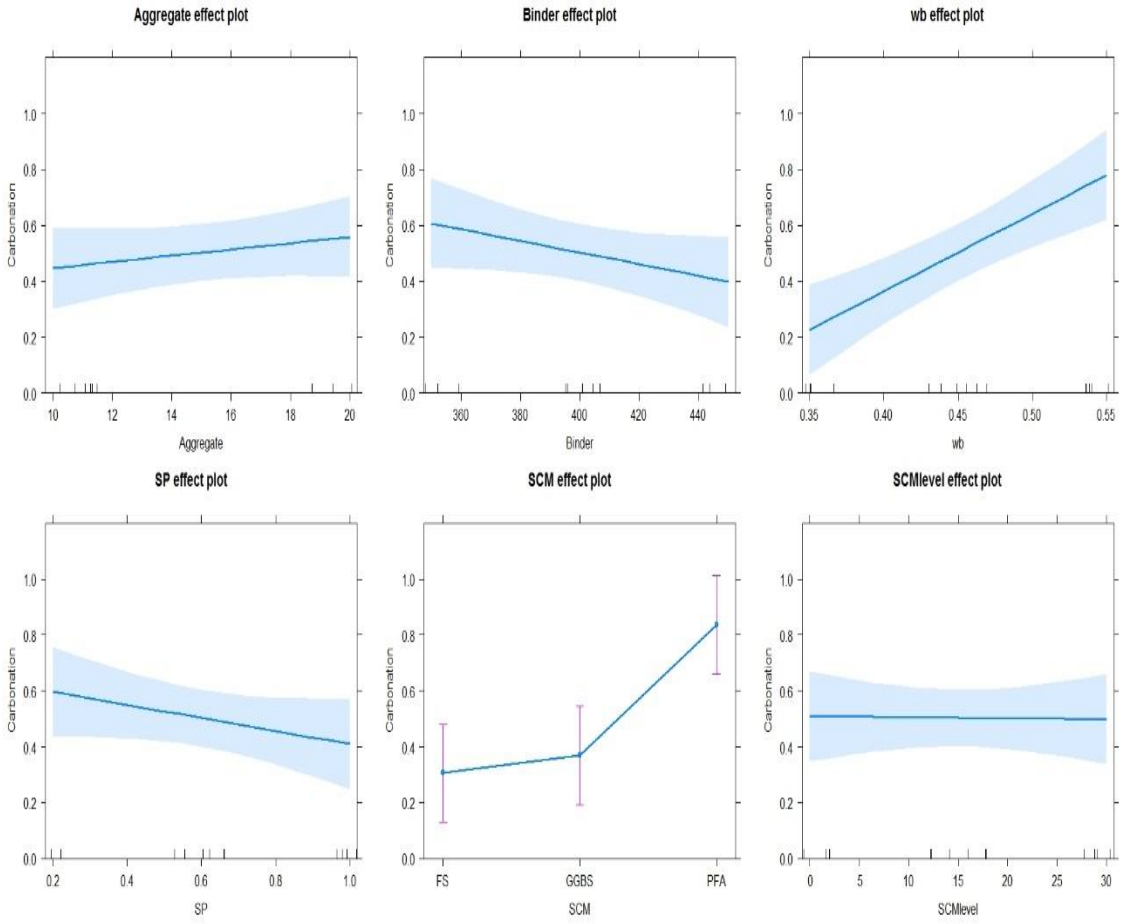

Figure 4-37 Main effects plot for carbonation coefficient (k)

4.7.1 **Effect of w/b ratio**

Mean effects plot for carbonation coefficient (k) in Figure 4.32 indicates that w/b ratio was significant regarding the rate of carbonation. The carbonation depth for w/b 0.55 was 73% higher than for w/b 0.35. (Ho and Lewis, 1987) found that the

w/c ratio is the most controlled variable which determines the carbonation resistance process because of its role in defining porosity and thus the path by which CO_2 ingresses the concrete. Where the carbonation is proportional to the permeability and inversely proportional to the amount of carbonatable matter. This is consistent with permeability findings for concrete and the porosity for blended cement paste samples which concluded that the permeability and coarse porosity increased with w/b ratio increasing. This behaviour agrees with literature (Khunthongkeaw et al., 2006, Herterich, 2017).

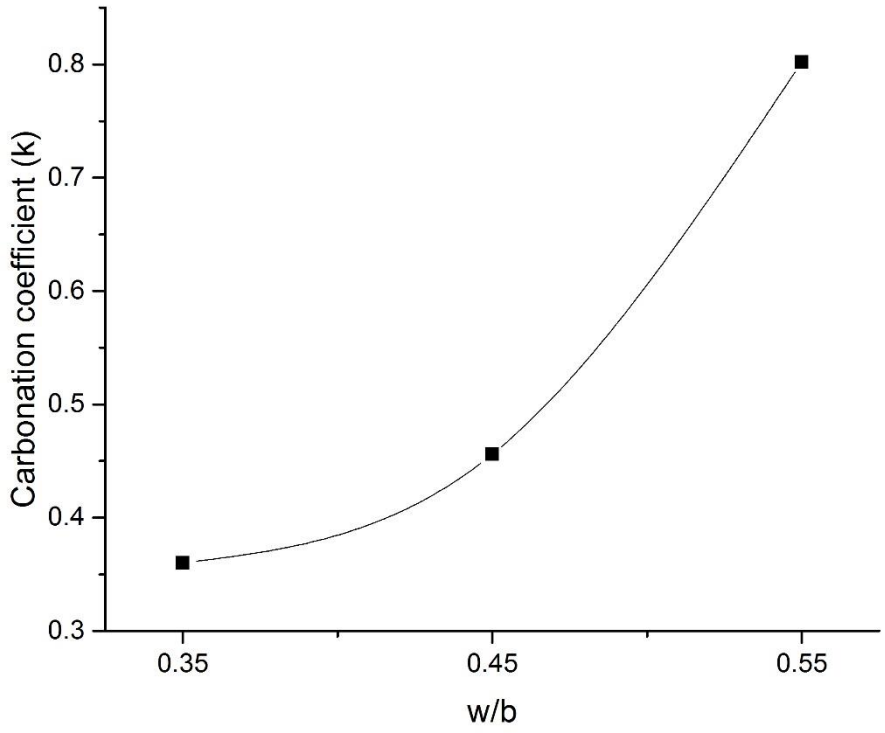

Figure 4-38 Effect of w/b ratio on concrete carbonation

4.7.2 **Effect of SCMs type**

The second significant variable influencing the rate of carbonation is SCM type. Figure 4.39 shows the effect of SCMs type (30% WoB) on carbonation compared with CEM I. As can be seen, the slag cement outperforms the CEM I in terms of carbonation resistance, with the fine slag slightly outperforming them still. This is to be expected since the slag is known to react to a considerable degree, plus it

induces a change in C-S-H structure from fibrillar to foil-like (Richardson, 2014), which reduces paste diffusivity and permeability (Ngala and Page, 1997, Morandeau et al., 2014). This result is consistent with the effect of slag on strength development and reduction of the permeation properties of concrete as earlier discussed. In addition, the hydration progress of blended cement paste mixes (bound water & heat flow) showed a similar trend, which explains the effect of hydration degree of SCM on carbonation resistance. Also, fine slag outperforms GGBS because it is finer so hydrates more rapidly.

The PFA blends did not perform as well as the CEM I blends. This is because the PFA hydrates more slowly than the clinker so the hydrated cement paste is more porous, as was shown in the permeability results. Furthermore, the PFA consumes more CH during the pozzolanic reaction, so there is a reduced amount of carbonatable matter (Deschner et al., 2012, Papadakis and Tsimas, 2002). Figure 4.39 shows the concrete samples which were exposed to carbon dioxide for 180 days.

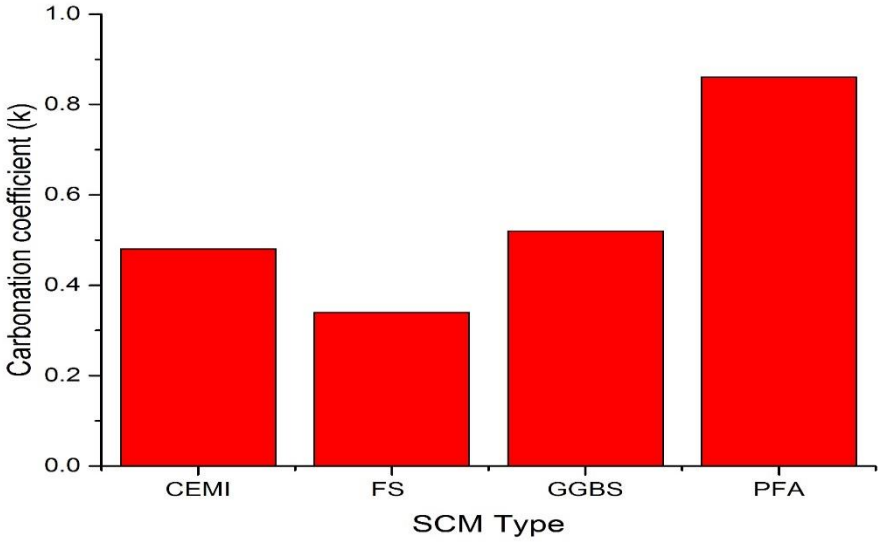

Figure 4-39 The effect of SCMs type compared with CEMI at different age

These results, on the effect of SCMs on the progression of carbonation are consistent with data on the degree of clinker hydration and the CH content, as reported in Chapter 5. The CH content was greater in mixes containing PFA than in those containing slag. This would be assumed to reduce carbonation, but because the rate of PFA hydration is less than that of slag, this leads to a more open pore structure, thus increasing the diffusion of carbon dioxide. As for slag,

the greater consumption of CH led to further C-S-H formation, thus reducing porosity and so carbonation. This is all consistent with the results of paste mentioned in Chapter 5, specifically the coarse pores content, the CH content and the CH consumed. The progress of carbonation according to route equation relied on the CH content and the diffusion, and to reduce the carbonation depth should assuring provide these two factors.

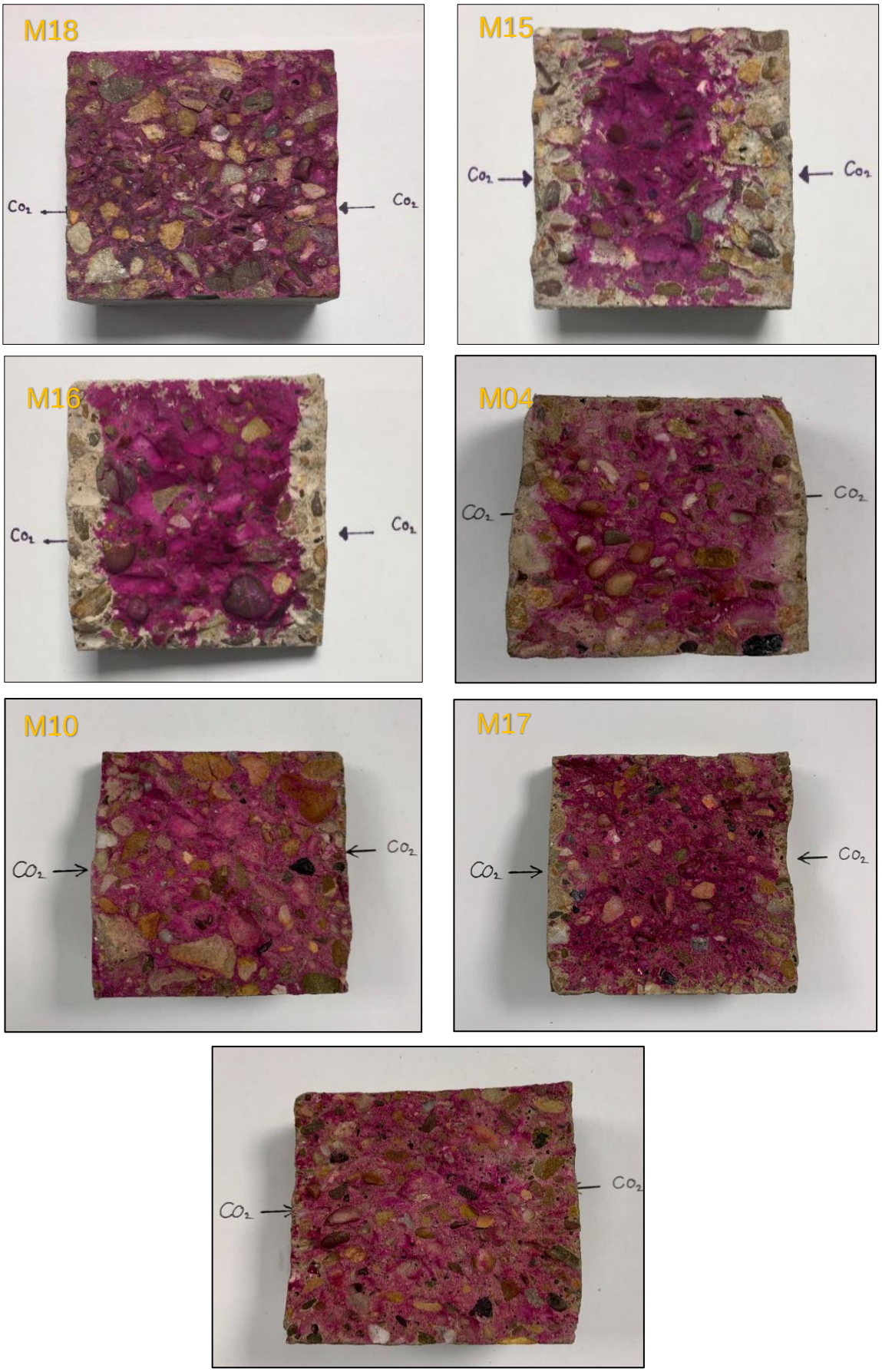

Figure 4-40 Concrete samples exposed to CO_2 for 180 days sprayed with phenolphthalein.

4.7.3 Effect of binder content

In addition, the mean effect of carbonation coefficient (k) highlights the positive effect of increasing the binder content on carbonation resistance, where samples with a high binder content (450-400) kg/m^3 exhibited high carbonation resistance as compared with low binder content. (Kosmatka et al., 2011) reported that increasing cement content will reduce carbonation depth as the result of increasing the concrete dense and reducing the permeability. Carbonation rate decreases with increasing binder content. It is worth noting that w/b ratio and SCM type both influenced permeability, but binder content didn't. However, binder content did influence carbonation. This is because of the amount of carbonatable matter, i.e. more cement will lead to the formation of more portlandite. Whereas, much of CH increases the ability to buffer pore solution and more ability of CO_2 binding. (Helene and Castro-Borges, 2009, Katz et al., 2015)

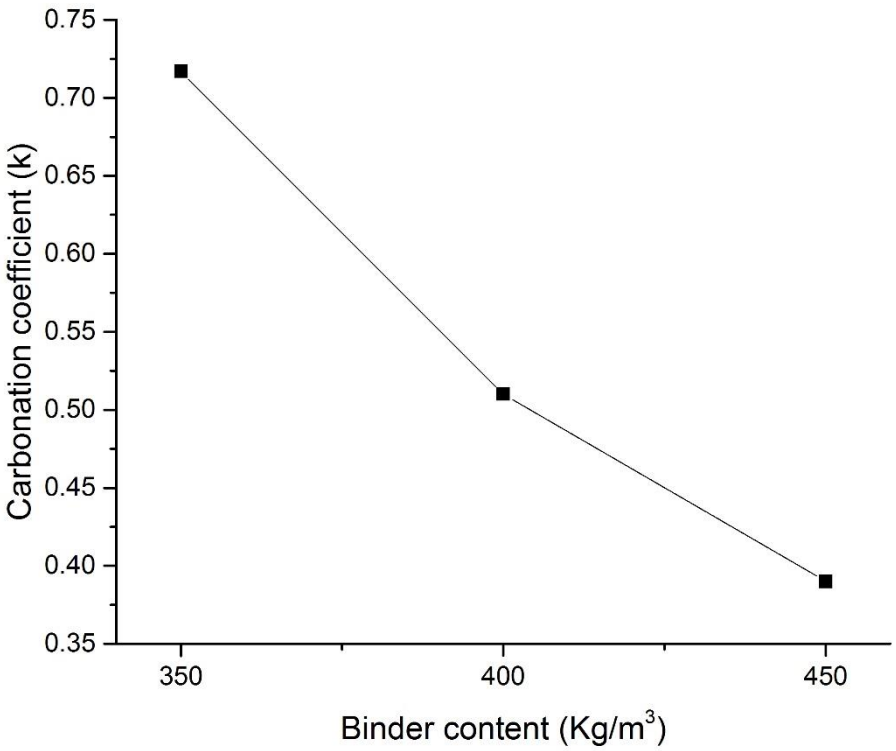

Figure 4-41 The effect of binder content on carbonation depth

4.8 **Effect mix design variables of concrete on eCO_2**

The embodied carbon dioxide (eCO_2) of concrete was determined as the mass of CO_2 by kg for every m^3, based on the carbon footprint of each component and the mass of component per cubic metre of concrete, as shown in Figure 4.41.

The statistical detailed (ANOVA) of the mix design variables which illustrates the effect of concrete constituents on eCO_2 is given in Table 4.10. There is a good correlation between the eCO_2 and mix design variables, as indicated by a value of 0.98 for the coefficient of determination.

As can be seen from Figure 4.42 that the significant variables are the SCMs type and the content of binder with 62% and 36.7%, respectively. Binder content increased the embodied carbon dioxide, while increasing replacement level decreased embodied carbon dioxide.

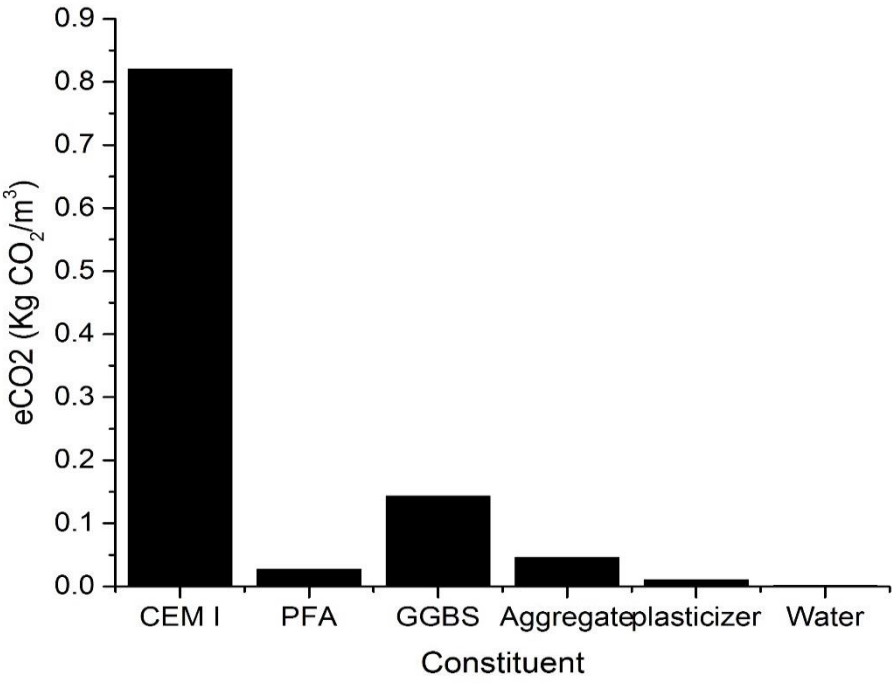

Figure 4-42 eCO_2 emissions of concrete constituents

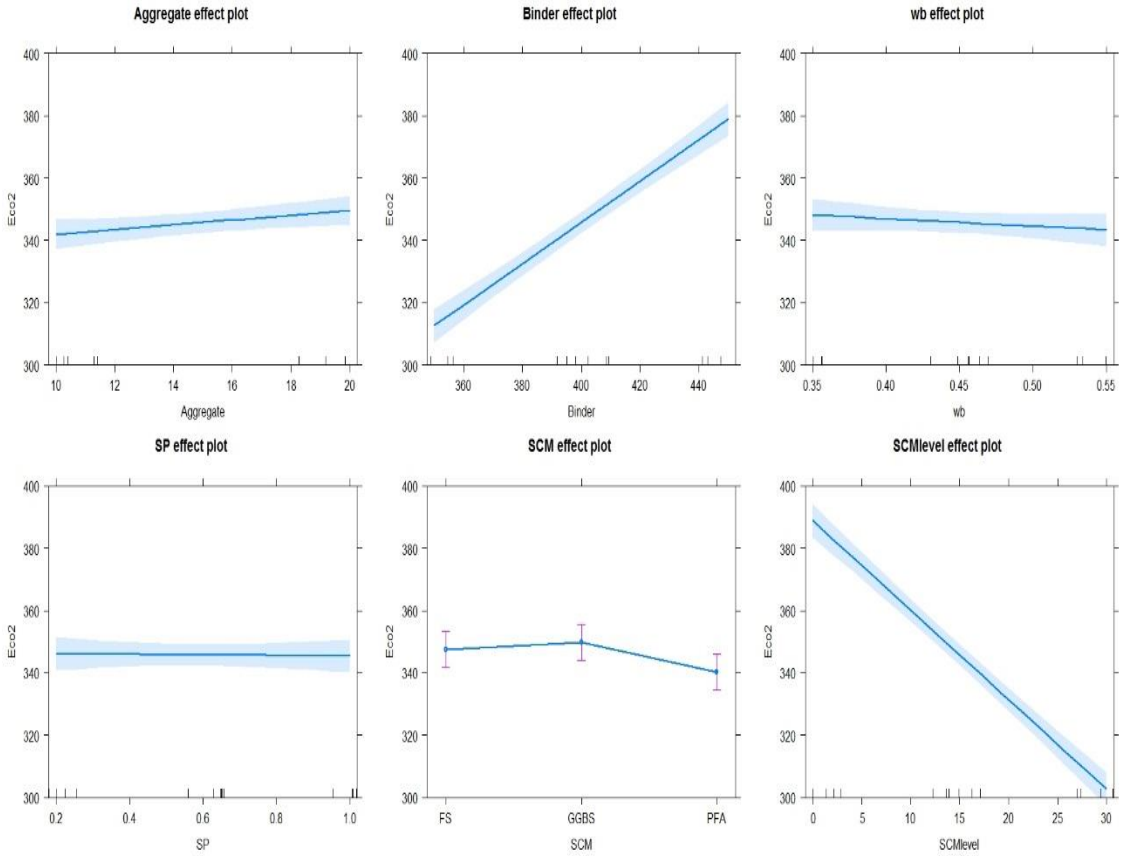

Figure 4-43 Mean effect plot of embodied carbon dioxide (eCO_2)

Table 4-18 Results of ANOVA for embodied carbon dioxide (eCO_2)

Source	Adj SS	Adj MS	F-Value	P-Value	Significance	Contr.%
Aggregate size	269.7	269.7	6.65	0.127	insignificant	0.8
Binder content	13165.6	13165.6	324.91	0.000	**significant**	**36.7**
w/b	67.7	67.7	1.67	0.225	insignificant	0.2
SP%	1.4	1.4	0.03	0.856	insignificant	0.0
SCMs%	22259.1	22259.1	549.32	0.000	**significant**	**62.0**
SCMs type	291.8	145.9	3.60	0.166	insignificant	0.4

The residual plots of this model are given in Figure 4.37, which included normal probability and versus fits. It is concluded from the residual plots that there is not any indication of the violation of the assumptions of the error.

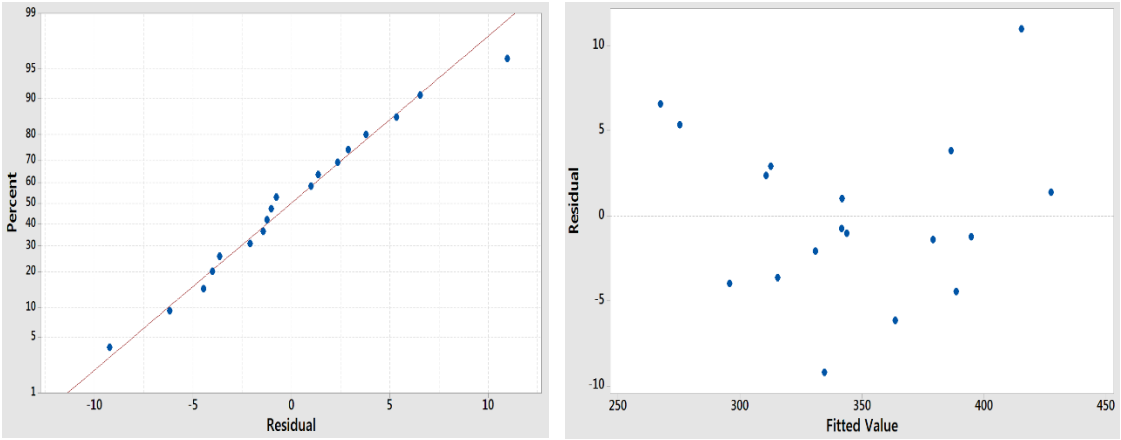

Figure 4-44 Residual values plot of regression model generated for mean eCO_2

4.8.1 Effect of SCMs type and percentage

The embodied carbon dioxide of concrete is affected significantly by using SCMs, the extent of which depending on the type of replacement, as shown in Figure 3.44. When fine slag is used there is an almost 16% reduction in eCO_2, while there is a slightly greater reduction in embodied carbon dioxide with GGBS with 20% and 22% for fly ash.

Increasing the level of replacement had a significant impact, as shown in Figure 4.44. The trend of decreasing eCO_2 is proportionate to the SCM content. For 15% replacement proportion, the reduction in eCO_2 is approximately 12% and 22% for 30% replacement proportion, compared with neat Portland cement.

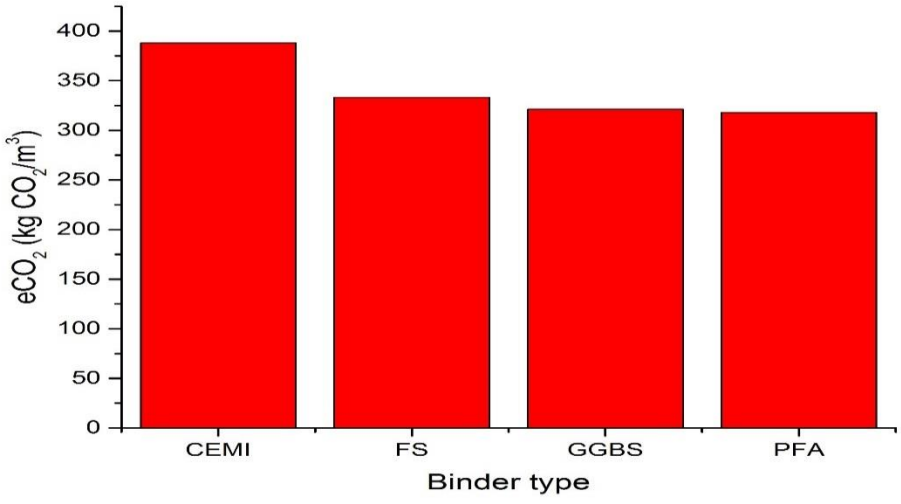

Figure 4-45 eCO_2 of concrete with different cementitious materials

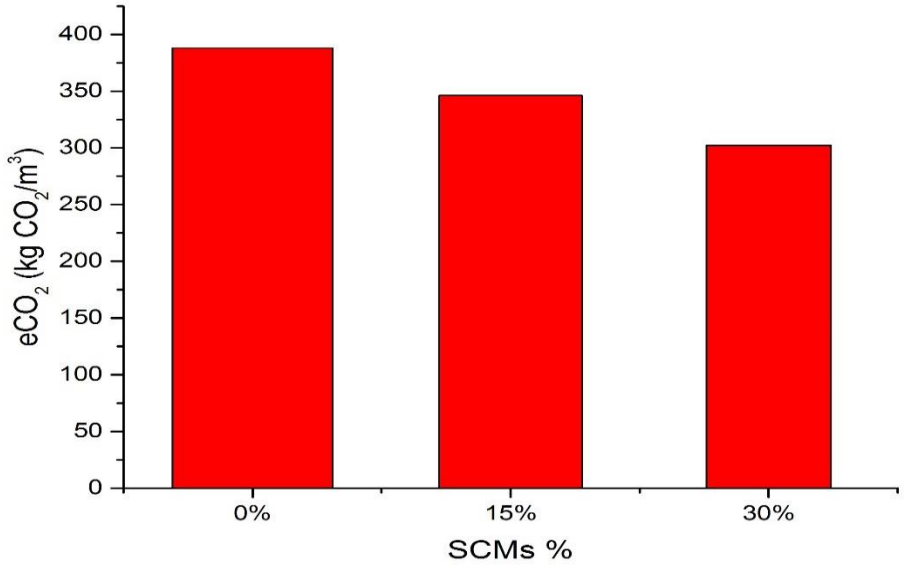

Figure 4-46 eCO_2 of concrete with different cementitious materials proportions

4.8.2 Effect of binder content

The effect of binder content on embodied carbon dioxide of concrete can be seen from Figure 4.46. Increasing the binder content increases embodied carbon dioxide as a result of Portland cement having a carbon footprint significantly greater than any of the other components. Increasing the binder content from 350 to 400 (Kg/m^3) increased the eCO_2 by 12.5%.

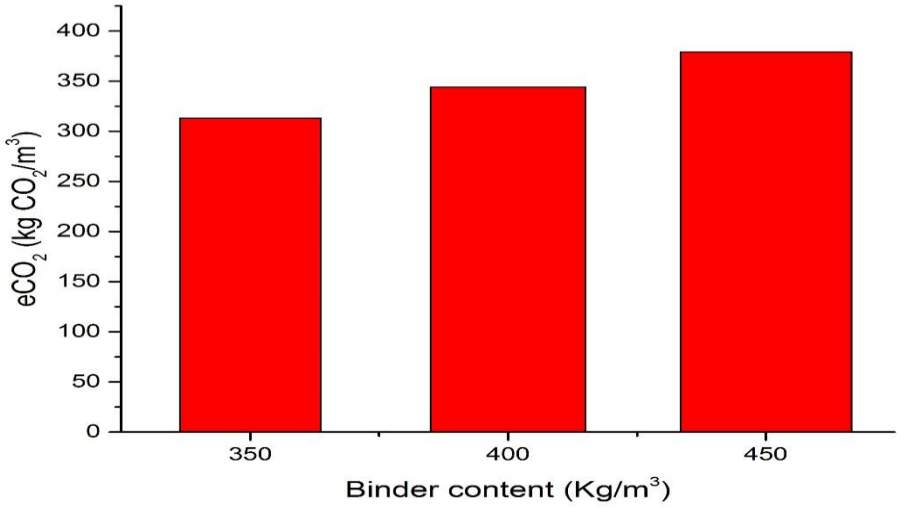

Figure 4-47 eCO_2 of concrete with different proportion of binder Summary

In this chapter, the impact of concrete mix design variables on mechanical properties, permeation indices, and durability (carbonation resistance) have been studied. Furthermore, environmental performance has been determined by calculating the embodied carbon dioxide for each of these 18 concrete mixes and studied the effect of concrete mix design variables variation on their eCO_2 has been studied. In addition, multiple linear regression techniques were implemented to build up a relationship between the concrete properties (independent variables) and mix design variables (dependent variables) to understand the significance for each variable in relation to concrete performance. Evaluation of the model was made according to certain statistical procedures, including analysis of variance (ANOVA), using MINITAB. The results are summarized in Table 4.18.

Table 4-19 Concrete performance evaluation

Independent variables		Dependent variables					
		Slump	Compressive strength	Permeability & Sorptivity	Shrinkage	Carbonation resistance	eCO_2
Aggregate size	10	↓	N	↓	↑	N	N
	20	↑		↑	↓		
Binder content	350	N	N	N	N	↓	↓
	400					↓	↑
	450					↑	↑
w/b ratio	0.35	↓	↑	↓	↓	↑	N
	0.45	↓	↓	↑	↑	↓	
	0.55	↑	↓	↑	↑	↓	
SCM Type	PFA	↑	↓	↑	↑	↓	↓
	CS	↓	↑	↓	↑	↓	↓
	FS	↓	↑	↓	↓	↑	↓
SP%	0.2	N	↓	N	N	N	N
	0.6		↓				
	1.0		↑				

Green arrows: Improving performance

Red arrows: Decreasing performance

Based on a series of evaluation criteria covering mechanical properties, permeation properties, carbonation resistance, and sustainability, a mix with low w/b of 0.35 showed improved performance, which means improved strength, reduced permeability and increased carbonation resistance. The incorporation of

fine slag at either 15 or 30% generally performed well in terms of increasing the compressive strength and improving permeation properties.

The 18 concrete mixtures showed variation in slump based on the effects of significant variables such as increasing w/b ratio and increasing the aggregate size. As for using SCMs, concretes contains slag were very sticky, while the PFA concretes were more workable. This workability was due to the specific surface area of the slag being higher than that of PFA.

High w/b ratio (0.55) mixes showed low compressive strengths, due to the dilution of hydration products leading to higher porosity. Concretes containing SCMs showed lower 28 day strengths than CEM I concretes. By 90 days slag cements showed higher strengths, while PFA cements still gained less strength. For instance, the average 90 day compressive strength of concrete when the OPC replaced by PFA, GGBS, and FS with 30% was 53, 67, and 66 MPa, respectively, compared with 59 MPa for OPC. SCMs react with $Ca(OH)_2$ to form C-S-H gel which is responsible for strength development. This reaction is slow so SCM concretes showed lower strengths at early ages. It may also be considered that slag has a higher CaO content and this oxide is able to influence strength. Also, slag fineness influences reactivity and works as a filler reducing interparticle spaces and increasing strength. Use of superplasticizer had a positive impact on concrete strength, since the higher SP% (1.0 WoB) achieves a high strength due to superplasticizer's ability to disperse the binder (Mbadike, 2011). However, compressive strength was not influenced by all factors. For example, both the aggregate size and binder content were found to be not statistically significant.

As for transport properties (gas permeability & water sorptivity), mix design variables had a significant effect at both 28 and 90 days. The key variables were w/b ratio, aggregate size, SCMs type, and replacement level. A low permeability concrete could be designed by reducing the w/b ratio (0.35), using smaller large aggregate and incorporating slag (fine or coarse). These variables were also found to influence water sorption, but to slightly different extents.

Water and gas diffusion through the concrete relied on the paste microstructure, particularly the capillary porosity. Increasing the w/b ratio (0.55) led to increasing porosity as a result of hydration products distribution. In slag concrete, water & gas permeability was reduced as the result of slag hydration and the filler effect

increasing the volume of hydration products and densifying the concrete structure. In contrast, fly ash increased the permeability, in spite of the role of fly ash to reduce the heat flow and subsequently shrinkage. This is because of the slow reaction which reduced the volume of hydration products and increased the porosity (Sharma and Khan, 2016). The third significant factor is aggregate size which showed negative impact on the permeability with increasing aggregate size. This was due to the action of fine aggregate size which reduces the voids as the result of space filling (Chen et al., 2008). In addition, permeation properties were not influenced by all factors, with both the superplasticizer and binder content being found to be not statistically significant.

It can be concluded from the shrinkage readings, that the most influencing variables at ages 28 and 90 days were w/b ratio, SCMs type, and the use of a superplasticizer. Whereas, the shrinkage could be reduced by selecting optimal concrete mix proportions via reducing the w/b ratio and increasing the SP dosage (0.2% Wob) and using 30% PFA replacement.

With shrinkage relying on the amount of water loss from capillaries pores (Güneyisi et al., 2010), a high water content (0.55) causes increased drying shrinkage, due to the higher w/b ratio increasing the pore content. Slag samples showed a reduction in shrinkage due to the slow pozzolanic reaction and because of the high fineness which in result reduction in pore size. In contrast, PFA showed higher shrinkage because the fineness decreased. With a high dosage of superplasticizer shrinkage was increased. This was attributed to increasing the porosity which resulted in more pore fineness that's mean increasing the divergence inside the paste (Ma et al., 2007). ANOVA results showed that shrinkage was not influenced by aggregate size and binder content.

Carbonation depths depended on mix design variables and the permeation properties as discussed in Chapter 6. Concrete containing slag (fine & coarse) showed better carbonation resistance than PFA concrete. This is due to the disjointed microstructure of the paste as the result of slow PFA hydration. In addition, the fine slag particles acted as a filler and led to a dense microstructure. The carbonation resistance of concrete was relatively higher when the binder content increased, perhaps the improving microstructure due to the presence of the additional binder particles. ANOVA showed that carbonation resistance was not influenced by the aggregate size or the presence of superplasticizer.

On the other hand, some variables did not affect the concrete properties and had an insignificant statistical impact on the independent variables (strength, permeation properties, shrinkage, and carbonation resistance). The binder content, which ranged from 350 Kg/m^3 to 450Kg/m^3, did not show a significant effect on concrete properties. This insignificance of binder content is due to this parameter not changing individually, which means the other variables, such as w/b ratio, may also have changed based on the orthogonal array. Also, it was found that the SCM replacement level (0%, 15% & 30%) was statistically insignificant, while the type of SCM was significant. The type of SCM has a significant impact on concrete performance over the short and long term. As mentioned in chapter five, the microstructure of the fine slag cement is greatly refined compared with mixtures containing PFA and based on that the concrete performance changed when using these supplementary cementitious materials. The fineness and the reactivity controlled the behaviour of concrete performance by improving the microstructures of blended cement with slag. On contrast of that, PFA showed negative effect on concrete performance as the result of low reactivity and low fineness which increased the permeability and increased the carbonation depth. While the percentage of SCM was not statistically significant seems counterintuitive and may be a result of using too low replacement levels, i.e. the difference between 0%, 15% & 30% were insufficient to be significant. Many researchers mentioned about limitation of using these materials up to 80% for slag and 40% for PFA (Bouikni et al., 2009) (Khunthongkeaw et al., 2006) (Pacheco-Torgal et al., 2013)

It would have instinctively have been expected that the superplasticizer would have an impact on the slump. However, it didn't and the possible reason for this is because the superplasticizer was present in every mix, so the level of SP was insignificant.

This chapter has shown that a set of durable low-carbon concretes could be achieved with reduced Portland cement content by incorporating fine slag and coarse slag with 15% and 30% replacement, reduced w/b ratio with 0.35 and reduced water content by using 1.0% SP. These findings confirm what has been done before, but the impact of these parameters on carbonation resistance and microstructural development is novel.

Finally, The Taguchi method and ANOVA approach only tells about the significance of variables, it does not tell why. Also, the methodology of Taguchi method means that not be able to optimize particular levels and steak with rigid matrix and that the limitations of Taguchi method. Other thing, have ignored the interaction between variables. For example, SP are known interact differently with cement and PFA.

Chapter 5 : Microstructural investigation on blended cement paste

Microstructural investigations have been performed in order to understand how the hydration products at different ages relate to concrete performance. Based on that, cement pastes were prepared controlling the different variables in the same proportions as in concrete samples. Samples were then characterised by isothermal calorimetry, thermogravimetry (Montgomery) and scanning electron microscopy.

5.1 Heat flow of hydration by calorimetry

Isothermal calorimetry was used to follow total heat evolution, to give an indication about the degree of hydration. Figure 5.1 shows the main effects of significant mix variables which influence the heat flow, while Figure 5.2 shows the cumulative heat over the first 10 days of hydration for SCM mixes. The heat evolution results have been analyzed according to the peak value of the calorimetry curves, i.e. the maximum heat releases rate (García-Taengua et al., 2015).

Table 5-1 Results of ANOVA for heat evolution

Source	Adj SS	Adj MS	F-Value	P-Value	Significance	Contr.%
Binder content	3008.3	3008.33	6.78	0.023	significant	**48.5**
w/b	1976.3	1976.33	4.46	0.056	significant	**31.9**
SP%	80.1	80.08	0.18	0.678	insignificant	1.3
SCMs Type	2275.1	1137.56	2.57	0.118	significant	**18.3**

Statistical analysis provided a regression model for paste variables, as shown in Equation 4.2, for which the R^2 is 80.71%, while the ANOVA results are shown in Table 5.1. The results show that binder content, water-binder ratio, SCM type, and SCM replacement level influence the heat of hydration.

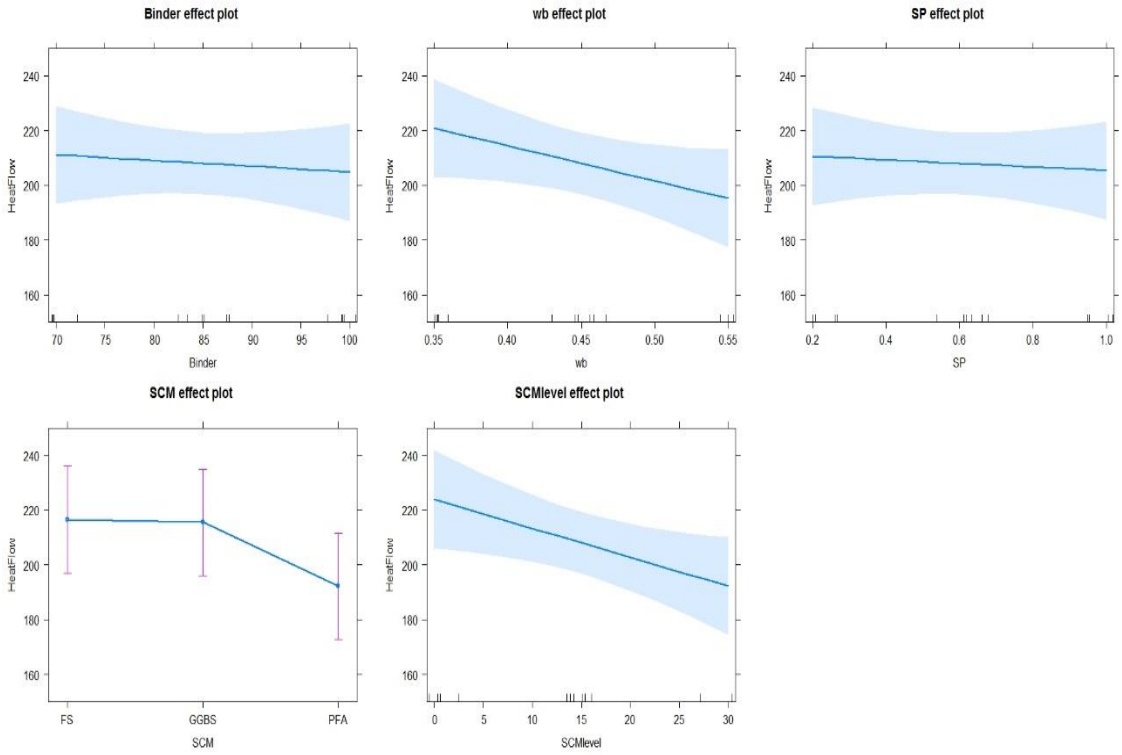

Figure 5-1 Main effects plot for heat evolution

Heat evolution decreased with increasing replacement level, indicating that all of the SCMs released less heat than the cement clinker. Hydration processes are exothermic, releasing CH in the process, but any replacement of CEM I with SCM leads to reduced hydration and a decrease in heat flow (Bougara et al., 2010). Of the three SCMs, PFA released the least heat, while finer grinding of the slag led to greater heat evolution, i.e. more hydration. This is reflected in the k-factors for PFA (0.3) and slag (1.0) (Klemczak and Batog, 2016, Bougara et al., 2010). Figures 5.2 shows the effect of replacing SCM with CEM I on heat flow.

The cumulative heat release curves for selected cement and blended cement pastes are shown in Figure 5.3. The plots also show traces for equivalent mixes where inert quartz with similar fineness to the pozzolanic materials has been used in the paste in an attempt to find the contribution of SCMs. This slowing of CEM I hydration accounted for by the effect of SCM incorporation as filler materials, The filler effect accelerates cement hydration. There are surfaces on which the cement hydrates can precipitate and there is an increase in effective water/cement ratio (Bentz et al., 1999, Bentz et al., 2013).

The degree of SCM reaction was determined by running each mix with the SCM replaced by quartz of similar fineness. The heat evolution due to SCM hydration was obtained by subtracting the heat flow for SCM mixes from replaced quartz

mixes (Kocaba et al., 2012). Figure 5.4 shows the effect of hydration due to SCM with 30%. This results are consistent with the effect of SCM on bound water content which calculated from STA results which discussed later in this chapter.

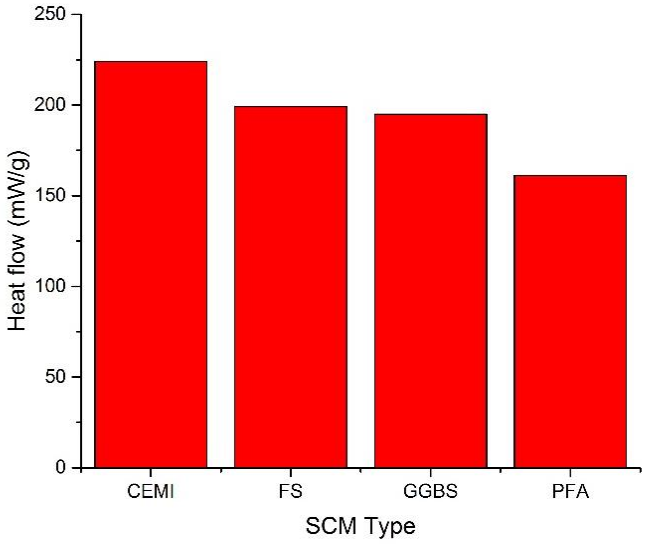

Figure 5-2 Total heat flow as a function of SCM

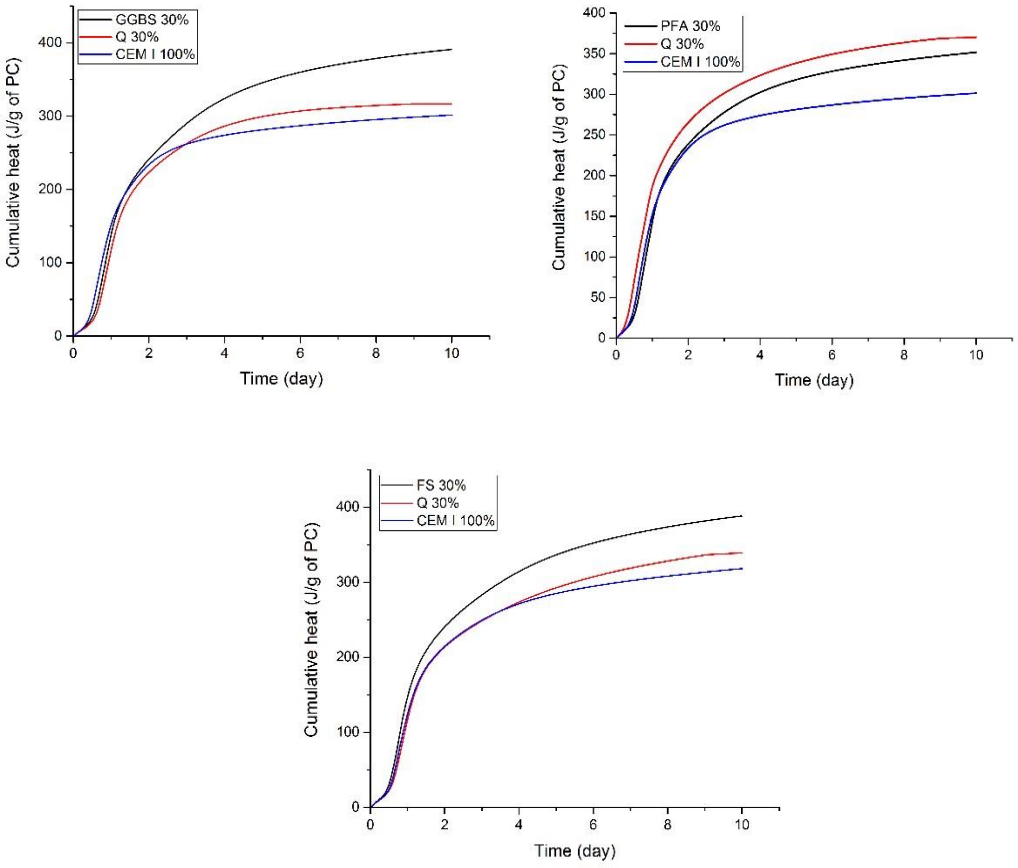

Figure 5-3 Cumulative heat of CEM I and 30% GGBS, PFA and FS

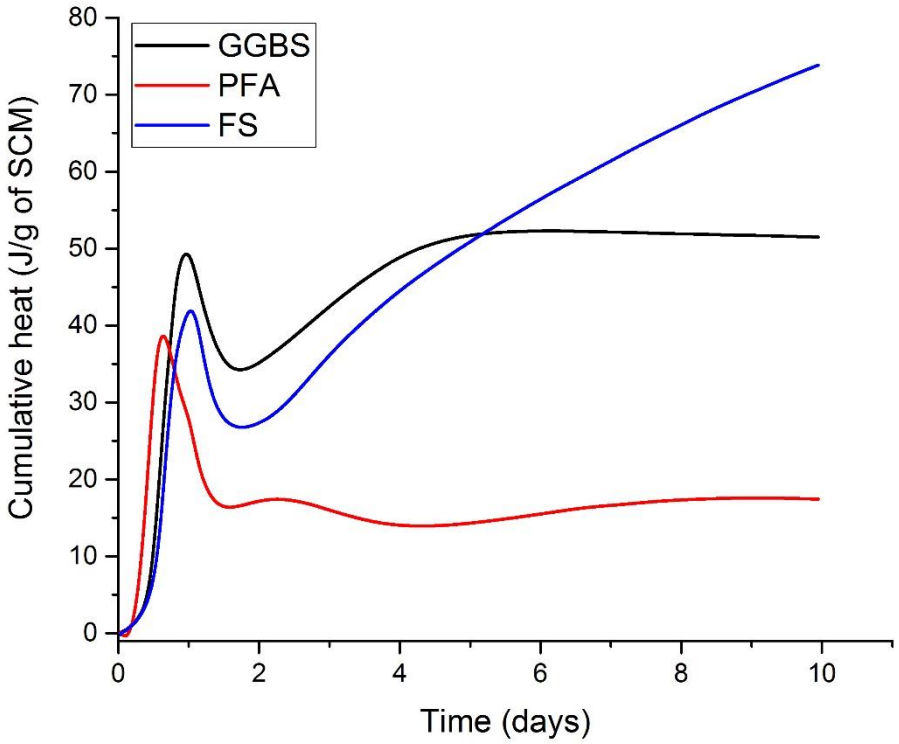

Figure 5-4 Cumulative heat flow from SCM hydration with 30% replacement

This results are consistent with the effect of SCM on bound water content which calculated from STA results which discussed later in this chapter.

As for binder content, there is less heat release when reducing the binder content because less binder releases less heat per gram as the cement clinker decreasing which represents the main component responsible about the hydration.

Meanwhile, with the increasing the w/b ratio (from 0.35 to 0.45) in blended pastes are shown high heat release according to the more viscous paste exist, which might produce a better dispersion (deflocculation) of the cement paste particles and a greater rate of initial hydration (Berodier and Scrivener, 2014). But increasing w/ b ratio (from 0.45 to 0.55) reduces the heat flow. The explanation for this behavior that a high w/c causes a higher degree of dilution of cement in the cement paste, which leads to a lower rate of hydration (Bentz et al., 2009).

5.2 **Degree of hydration of clinker and GGBS by SEM-IA**

The degree of hydration of clinker was measured by using SEM-IA. Statistical analysis for clinker hydration results provided a regression model for blended cement paste variables for which the R^2 is 53.6%, while the ANOVA results are shown in Table 5.2. The results show that binder content, SCM type, and SCM replacement level influence the clinker hydration kinetics. Figure 5.5 and 5.6 gives an indication of the extent to which mix variables affect clinker hydration kinetics, while Figure 5.7 shows the average degree of clinker hydration for the various binder types.

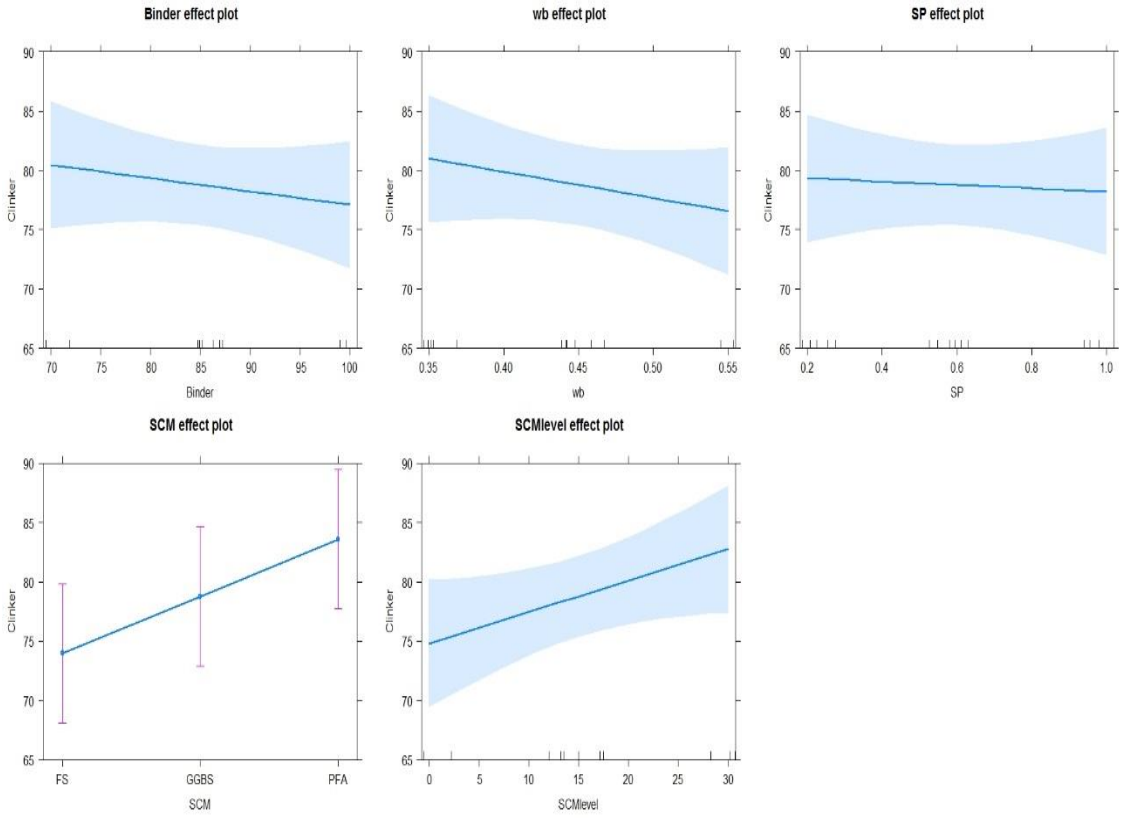

Figure 5-5 The effect of mix variables on degree of hydration of clinker by SEM-IA at 28 days

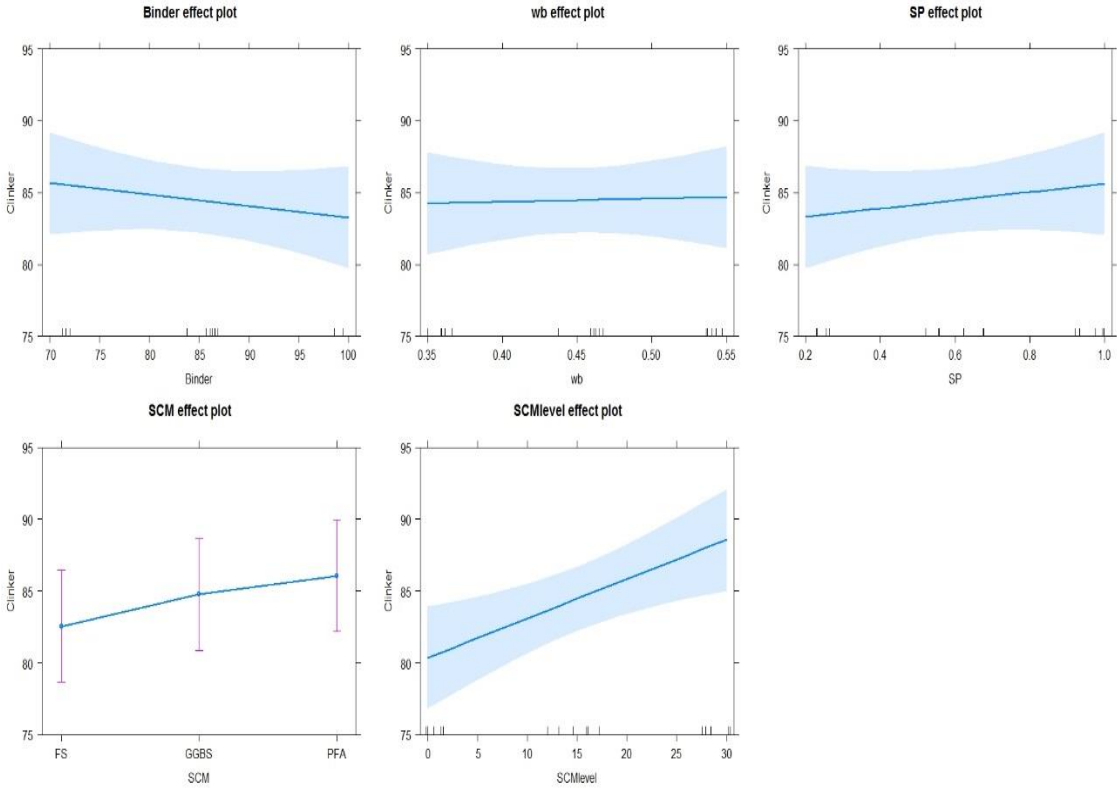

Figure 5-6 The effect of mix variables on degree of hydration of clinker by SEM-IA at 90 days

Table 5-2 Results of ANOVA for DoH of clinker at 28 days

Source	Adj SS	Adj MS	F-Value	P-Value	Significance	Contr.%
Binder	190.64	190.642	4.53	0.055	significant	**46.3**
w/b	58.21	58.212	1.38	0.262	insignificant	14.1
SP%	3.89	3.887	0.09	0.766	insignificant	0.9
SCMs%	278.31	139.154	3.31	0.042	significant	**33.8**
SCMs type	39.803	19.9017	10.60	0.072	significant	4.8

Figure 5.7 shows that the degree of clinker hydration is affected by SCM replacement. PFA mixtures showed the highest degree of hydration, flowed by coarse then fine slag, and finally CEM I. This trend is attributed to the slower reaction of PFA, whereas the slag has the ability to consume CH, in turn reducing the clinker hydration kinetics. This is in line with measured CH contents and will be discussed further in section 5.4. This agrees with other studies published (Herterich, 2017, De Weerdt et al., 2011). Meanwhile, increasing the SCM replacement level from 15% to 30% led to increased clinker hydration due to the role of SCM as filler which promotes the nucleation site and provides additional space for more cement reaction (Lothenbach et al., 2011).

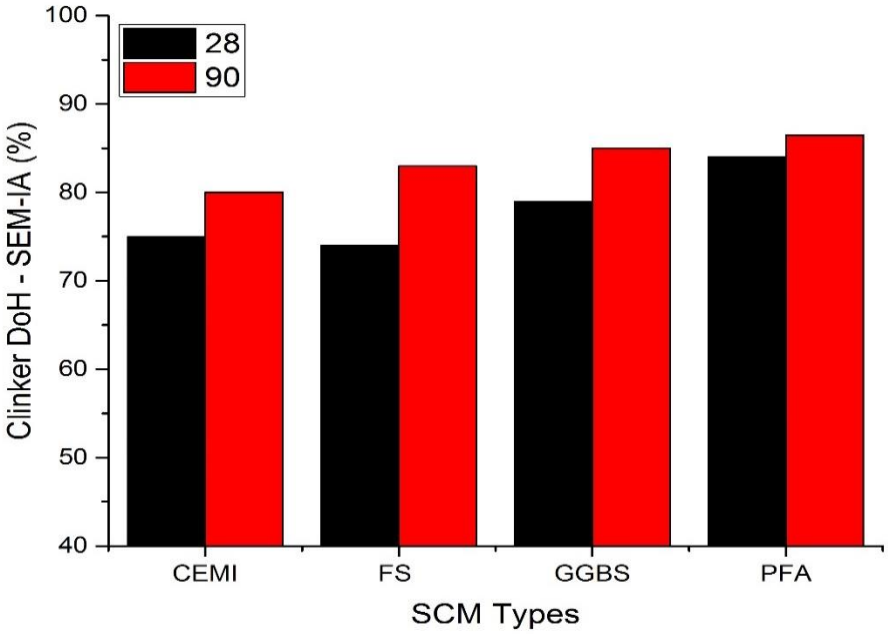

Figure 5-7 Hydration degree of clinker as a function of SCM

As for w/b ratio, increases in w/b lead to more clinker hydration as the result of providing more space for the hydration reaction. This agrees with previous studies (Herterich, 2017, Gutteridge and Dalziel, 1990). Figure 5.8 illustrates the effects of slag reaction, illustrating how fine slag resulted in greater reaction than coarse slag. Figure 5-9 showing the microstructural variations for the 18 paste samples which cured at 28 days.

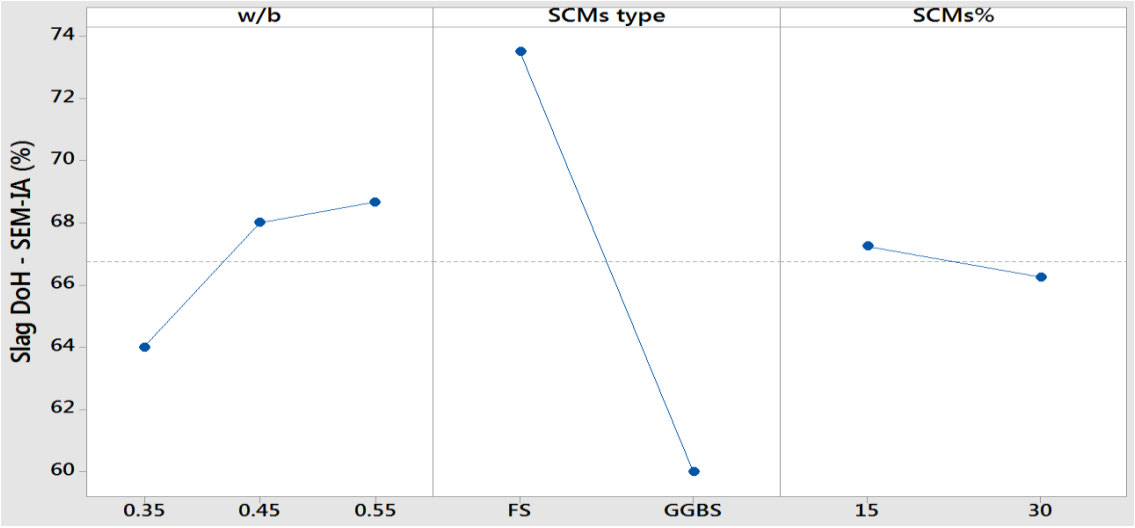

Figure 5-8 Degree of hydration of the slag (coarse & fine) measured by SEM-IA at 28 days

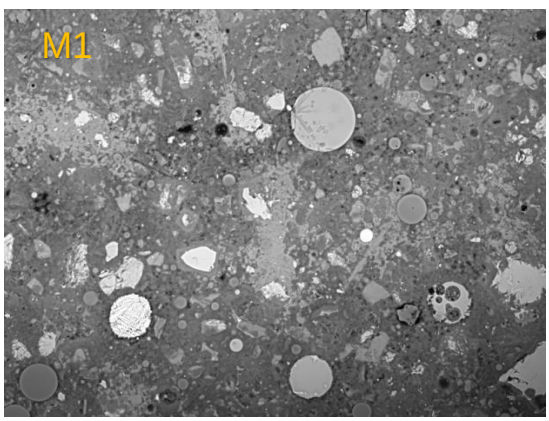
M1

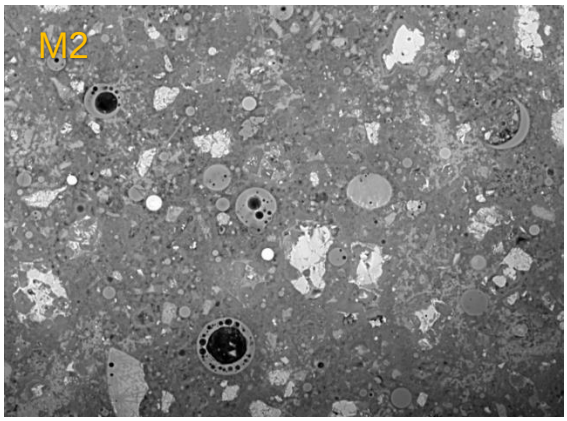
M2

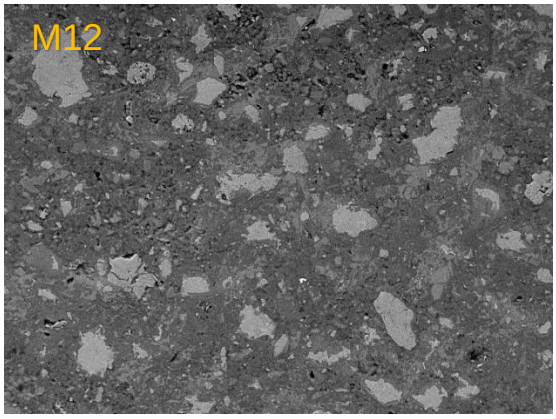
M12

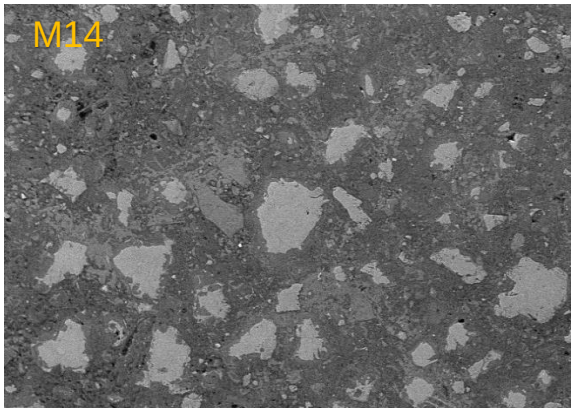
M14

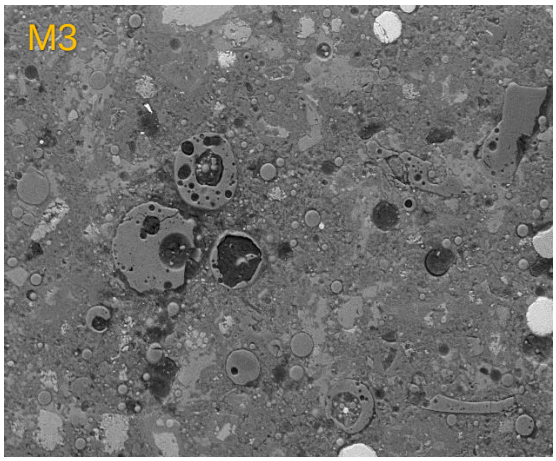
M3

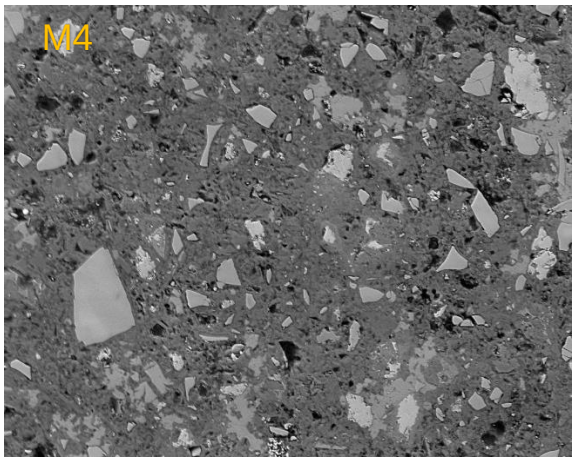
M4

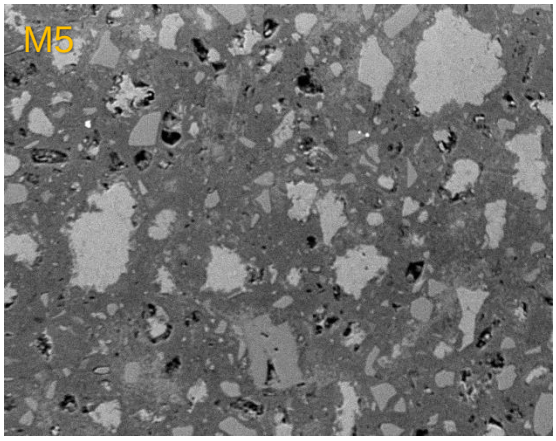
M5

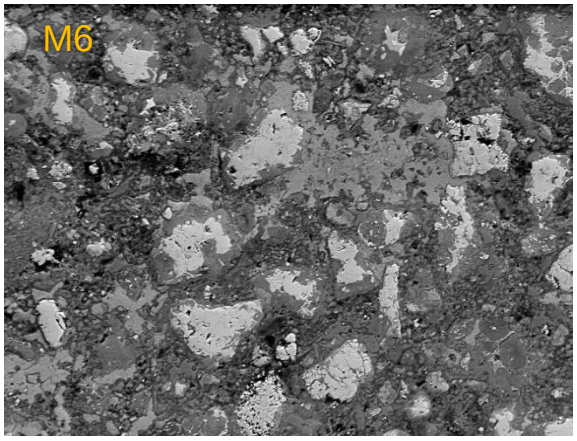
M6

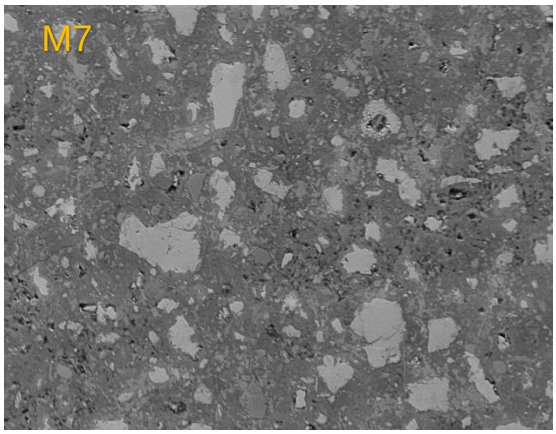
M7

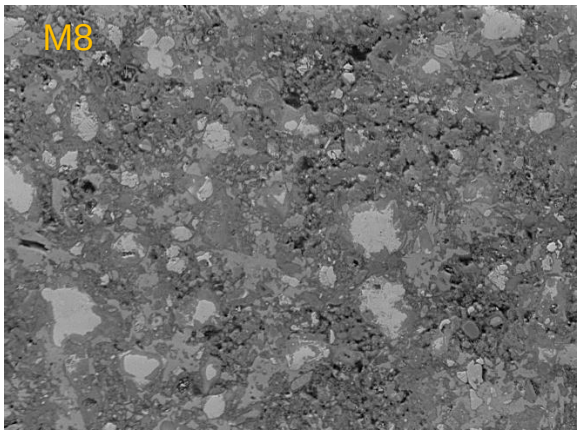
M8

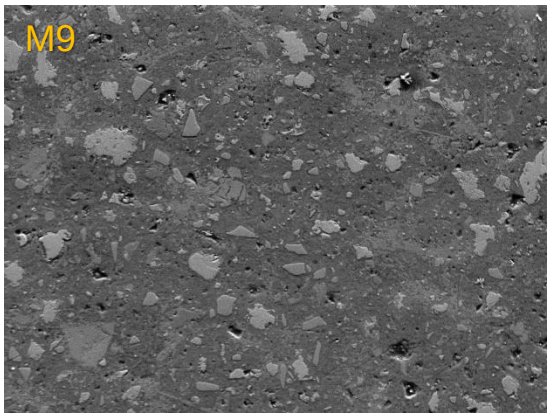
M9

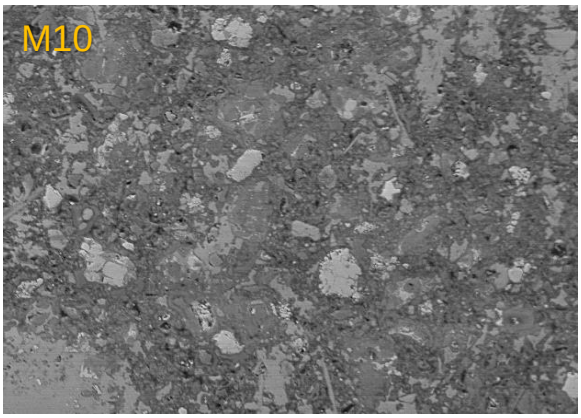
M10

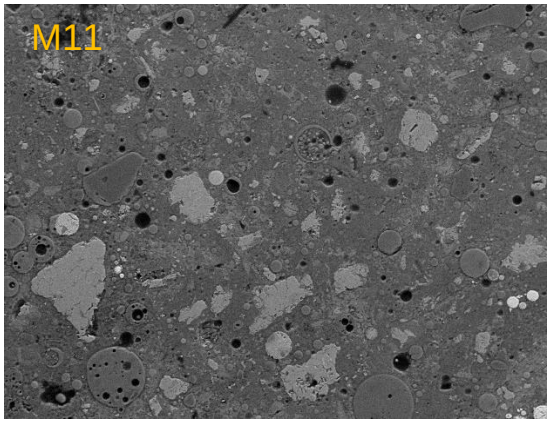
M11

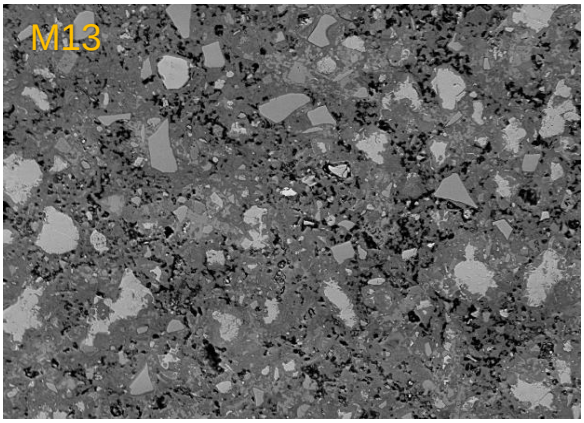
M13

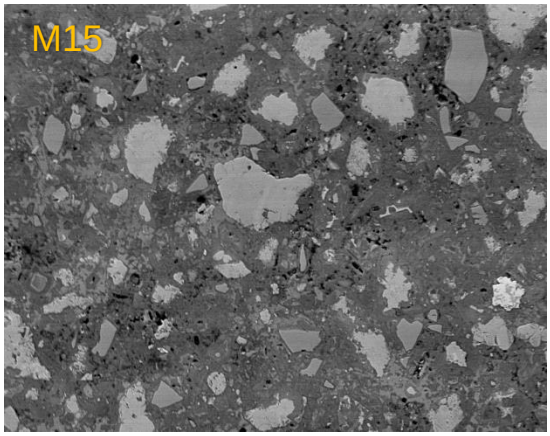
M15

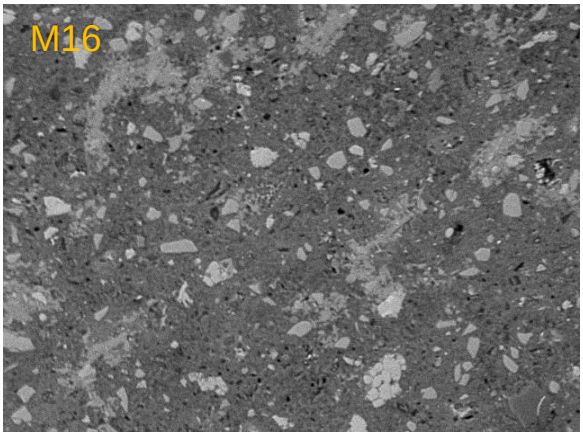
M16

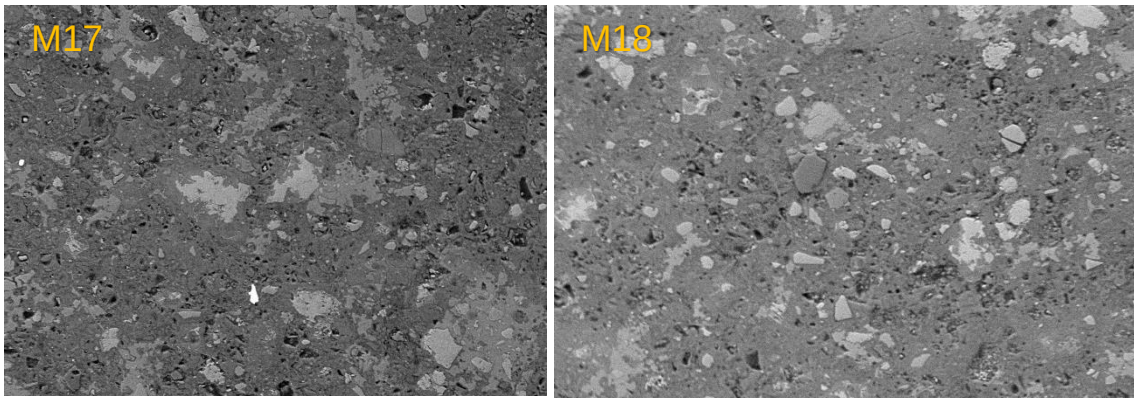

Figure 5-9 SEM-BSE images of 18 paste samples cured at 28 days

5.3 **Bound water**

The chemical bound water content reflects the progress of hydration of cementitious materials (Whittaker et al., 2014, Scrivener et al., 2018, Prochon and Piotrowski, 2016). Figures 5.10 and 5.11 show the bound water content at 28 and 90 days respectively reflecting the influence of each variable on paste hydration. Statistical analysis provided a regression model for blended cement paste variables for which the R^2 is 89.04%, while the ANOVA results are shown in Table 5.3. The results show that binder content, water-binder ratio, SCM type, and replacement level influence the chemical bound water content. The results are consistent with cumulative heat flow of paste mixes and strength development for concrete samples as discussed earlier.

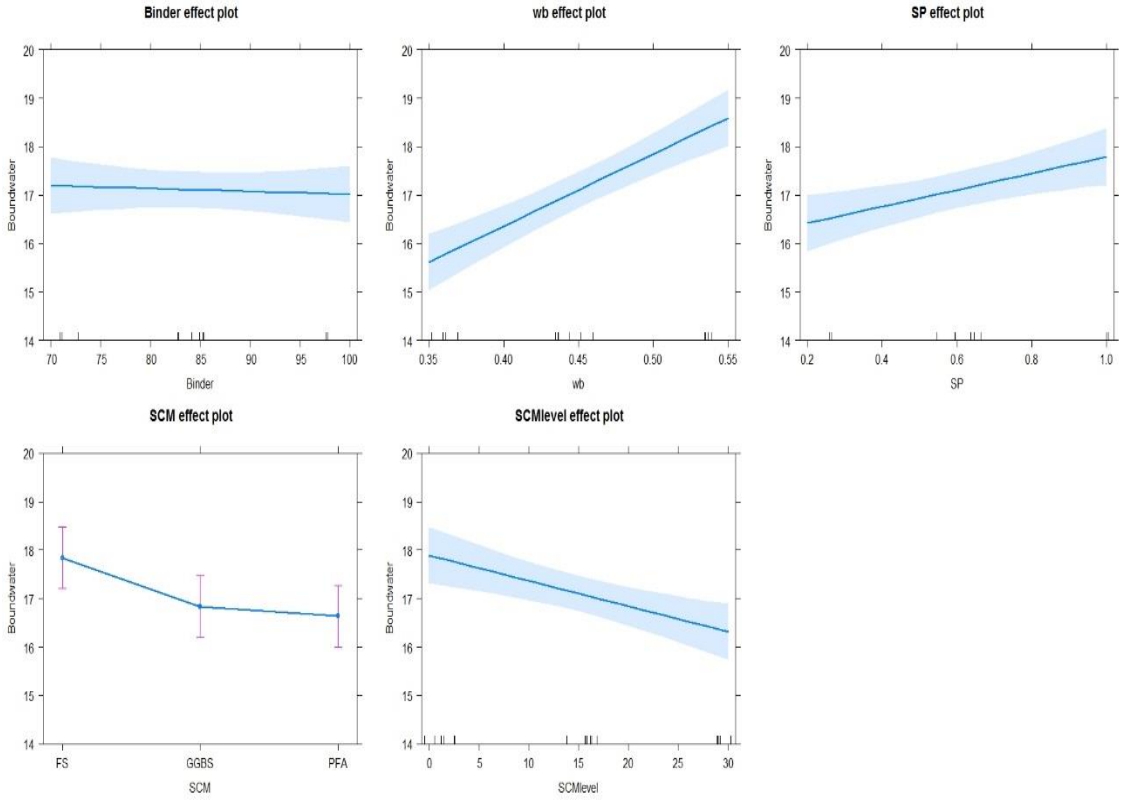

Figure 5-10 Effect of mix ingredients on bound water content at 28 days

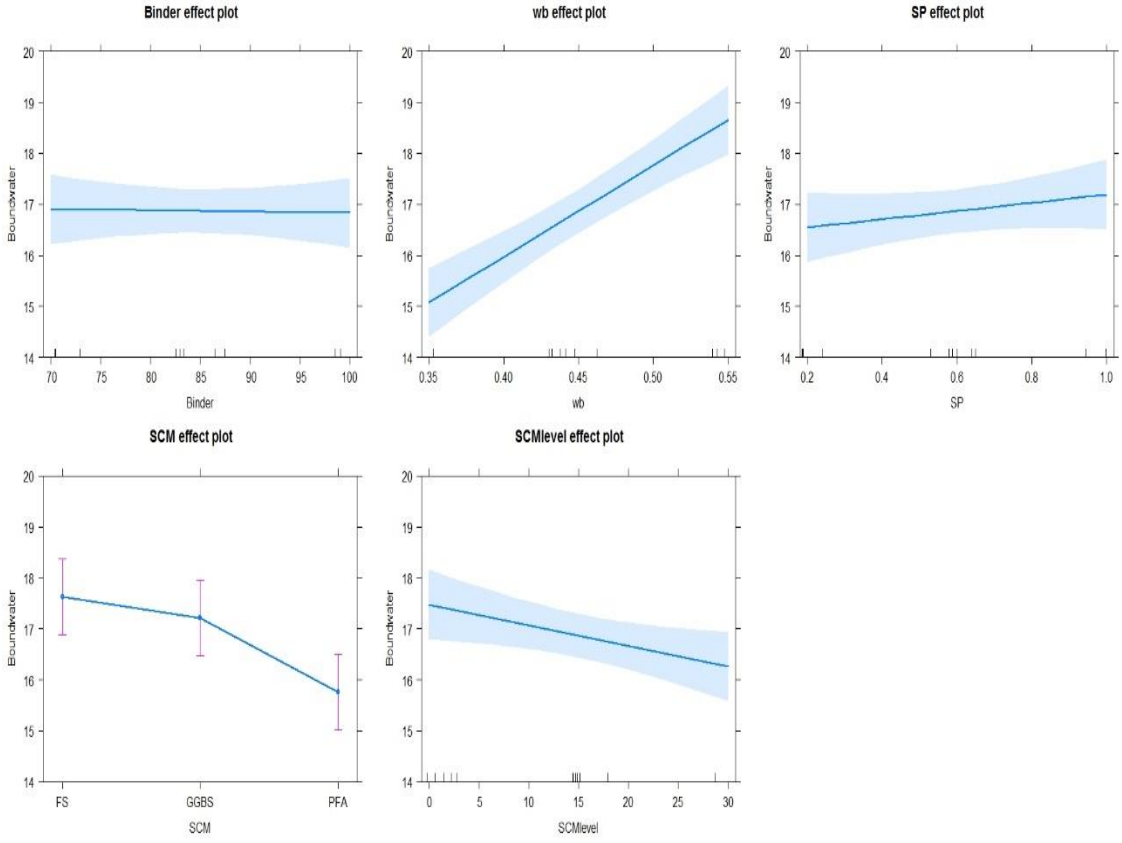

Figure 5-11 Effect of mix ingredients on bound water content at 90 days

Table 5-3 Results of ANOVA for bound water content at 28 days

Source	Adj SS	Adj MS	F-Value	P-Value	Significance	Contr.%
Binder content	7.442	7.4419	15.95	0.002	significant	**12.0**
w/b	26.522	26.5221	56.84	0.000	significant	**42.8**
SP%	5.644	5.6444	12.10	0.005	significant	**9.1**
SCMs%	4.993	2.4967	5.35	0.022	significant	**4.0**
SCMs type	39.803	19.9017	10.60	0.002	significant	**32.1**

Table 5-4 Results of ANOVA for bound water content at 90 days

Source	Adj SS	Adj MS	F-Value	P-Value	Significance	Contr.%
Binder content	1.9927	1.9927	6.21	0.028	insignificant	**4.1**
w/b	21.8700	21.8700	68.17	0.000	significant	**45.5**
SP%	0.9296	0.9296	2.90	0.114	insignificant	**1.9**
SCMs%	6.8358	3.4179	10.65	0.002	significant	**7.1**
SCMs type	39.803	19.9017	10.60	0.002	significant	**41.4**

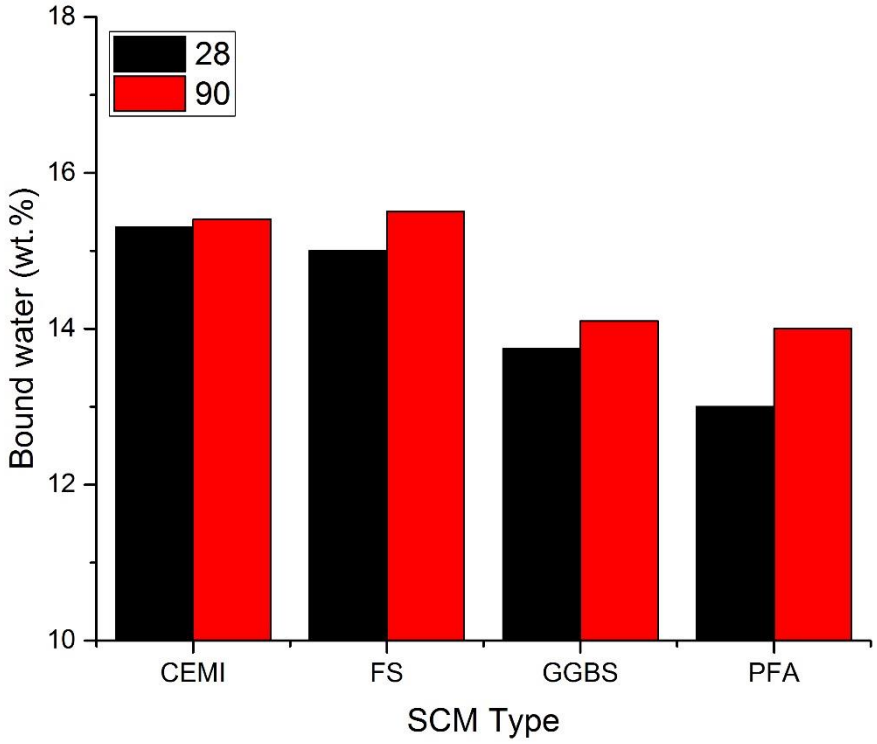

Figure 5-12 Bound water content in SCM mixes compared with CEM I mixes

All the blended pastes showed a lower bound water content than CEM I at 28 days, with PFA at 30% replacement showing the lowest, as shown in Figure 5.12.

The bound water content in SCM blends showed a clear increase with time as a result of the gradual pozzolanic reaction. Meanwhile, CEM I showed little change from 28 days to 90 days, due to the hydration of clinker being almost complete by 28 days (Whittaker et al., 2014). Meanwhile, fine slag shows a higher bound water content than coarse slag, due to particle fineness (Hewlett, 2003), as illustrated by the cumulative calorimetric heat flow results. In addition, increasing the SCM content from 15% to 30% led to decreased bound water contents, in line with the more gradual hydration, in line with the calorimetry results (chapter five, section 5.1).

The bound water content was dependent on the water/binder ratio, where the chemical bound water increases with water content. The increased water content enhanced hydration as the result of nucleation sites added. (Berodier, 2015) reported that higher water content promotes more spaces for hydration products which in turn increase the bound water content. This finding agrees with literature (Gutteridge and Dalziel, 1990, Berodier and Scrivener, 2014).

5.4 **Portlandite content by TGA**

The $Ca(OH)_2$ content was determined by TGA analysis with statistical analysis undertaken using Minitab to obtain a regression equation, with an R^2 equal to 83.96% and 79.17% at 28 and 90 days respectively. The ANOVA results for the Portlandite content at 28 and 90 days is shown in Tables 5.5 and 5.6. Figures 5.13 and 5.14 shows the effect of significant paste variables on CH content.

Table 5-5 Results of ANOVA for CH content at 28 days

Source	Adj SS	Adj MS	F-Value	P-Value	Significance	Contr.%
Binder content	23.019	23.0187	14.84	0.002	significant	**22.7**
w/b	42.526	42.5257	27.42	0.000	significant	**41.9**
SP%	0.032	0.0320	0.02	0.888	insignificant	0.0
SCMs%	31.864	15.9322	10.27	0.003	significant	**15.7**
SCMs type	39.803	19.9017	10.60	0.002	significant	**19.6**

Table 5-6 Results of ANOVA for CH content at 90 days

Source	Adj SS	Adj MS	F-Value	P-Value	Significance	Contr. %
Binder content	80.445	80.4454	23.04	0.000	significant	**49.7**
w/b	43.320	43.3200	12.40	0.004	significant	**26.8**
SP%	0.750	0.7500	0.21	0.651	insignificant	0.5
SCMs%	34.764	17.3822	4.98	0.027	significant	**10.7**
SCMs type	39.803	19.9017	10.60	0.002	significant	**12.3**

Three factors were significant with regards to $Ca(OH)_2$ content: w/b ratio, SCM replacement level, and the type of SCM. The most important contribution is made by the w/b ratio at 52.2%, followed by SCM replacement level and the type of supplementary cementitious material at 27.4% and 20.2%, respectively.

It can be observed, that total content of $Ca(OH)_2$ was high where SCMs were not used, and fell as the SCM content increased. This is attributed to a combination of dilution and the pozzolanic reaction. As for the type of SCM as shown in Figure 5.15, PFA had a much higher CH content than either coarse or fine slag. The consumption of CH by slag reflects its higher reactivity compared to PFA (Fraay et al., 1989, Escalante et al., 2001). Meanwhile, increasing the w/b ratio led to an increased CH content. This was due to more water leading to more space for clinker hydration and so higher CH content (Herterich, 2017).

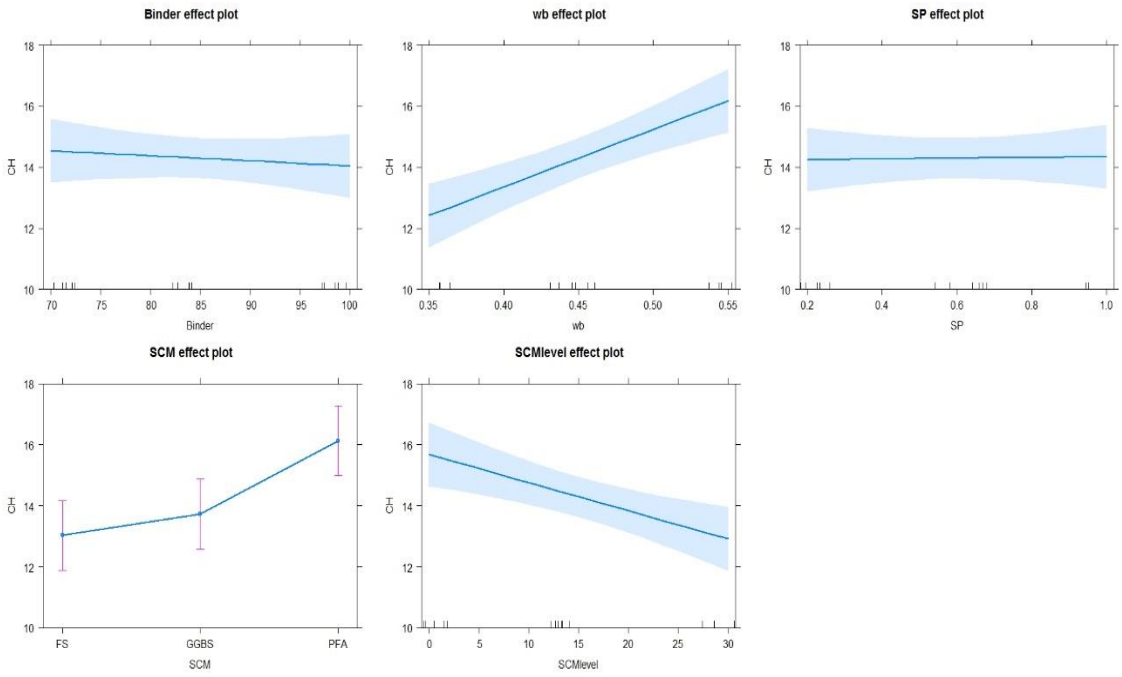

Figure 5-13 CH content determined from TGA data at 28 days

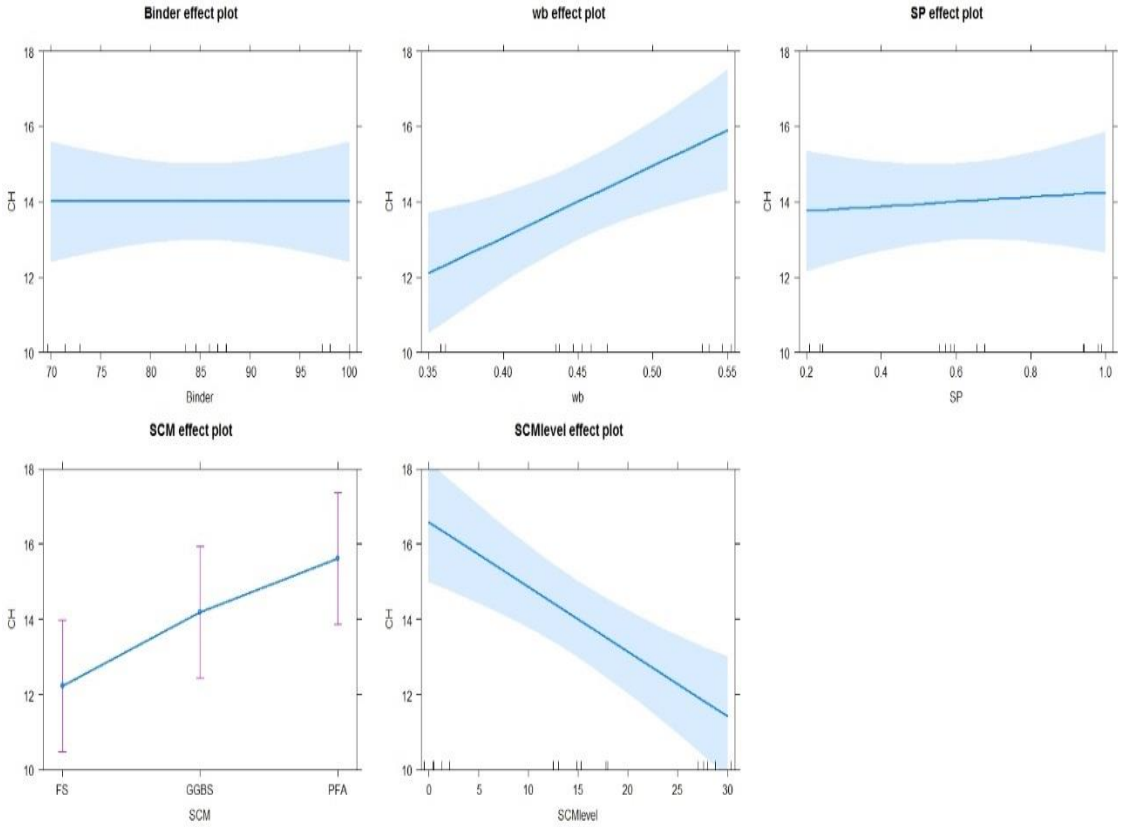

Figure 5-14 CH content determined from TGA data at 90 days

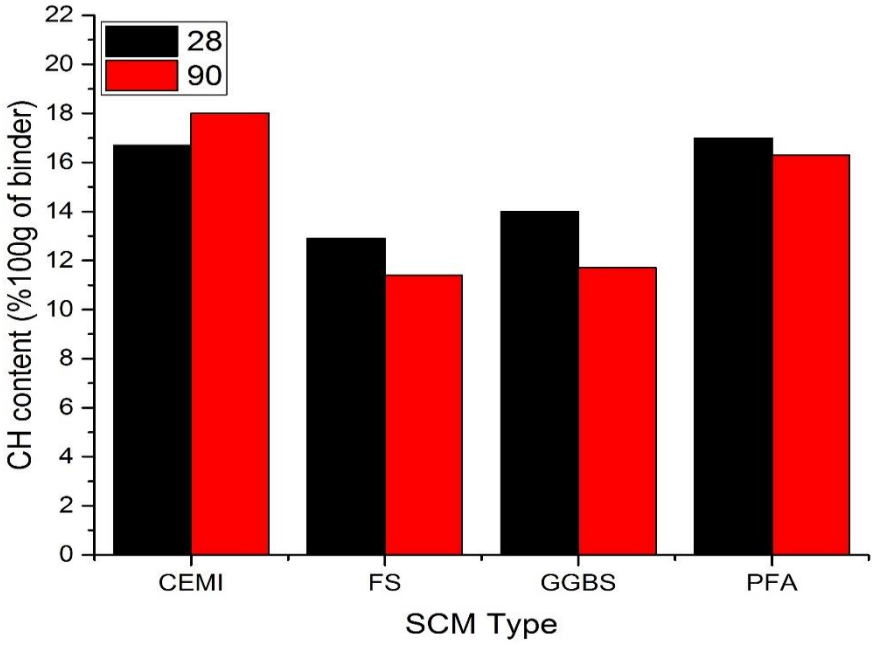

Figure 5-15 CH content determined from TGA data as a function of cementitious materials at 28 days

5.5 Calcite content by TGA

The proportion of calcite is calculated by considering the relative atomic number of individual components as mentioned in chapter 3, section 3.12. Then, this calcite content calculated used it to correct the carbonation of portlandite. This involved working out how much calcite is in each paste from the mass of calcite in the anhydrous cement, subtracting that from the calcite content in each paste and then converting the result to an equivalent mass of portlandite.

Statistical analysis of the CC content data was undertaken using Minitab to obtain a regression equation. Whereas, the regression model with an R^2 equal to 80.38%. The ANOVA results for the calcite at 28 days is shown in Table 5-7.

Table 5-7 Results of ANOVA for calcite content at 28 days

Source	Adj SS	Adj MS	F-Value	P-Value	Significance	Contr.%
Binder content	30.08	30.08	0.43	0.525	insignificant	40.4
w/b	22.9750	22.9750	25.44	0.000	significant	30.9
SP%	0.0645	0.0645	0.07	0.794	insignificant	0.1
SCMs%	4.4664	4.4664	4.95	0.046	significant	6.0
SCMs type	16.8820	8.4410	9.35	0.004	significant	22.7

Three factors are a significant impact on producing $Ca(OH)_2$, where the values of P are less than 0.05 (w/b ratio, SCMs% and the type of SCMs). In addition, the contribution percentage clarifies the degree of influence for these variables on CH content and shows the optimal level for each significant variable through which CH content be changed. Whereas the most important contributions centric on the w/b ratio at 63.9%, followed by supplementary cementitious materials type and SCMs% at 23.5% and 12.4%, respectively.

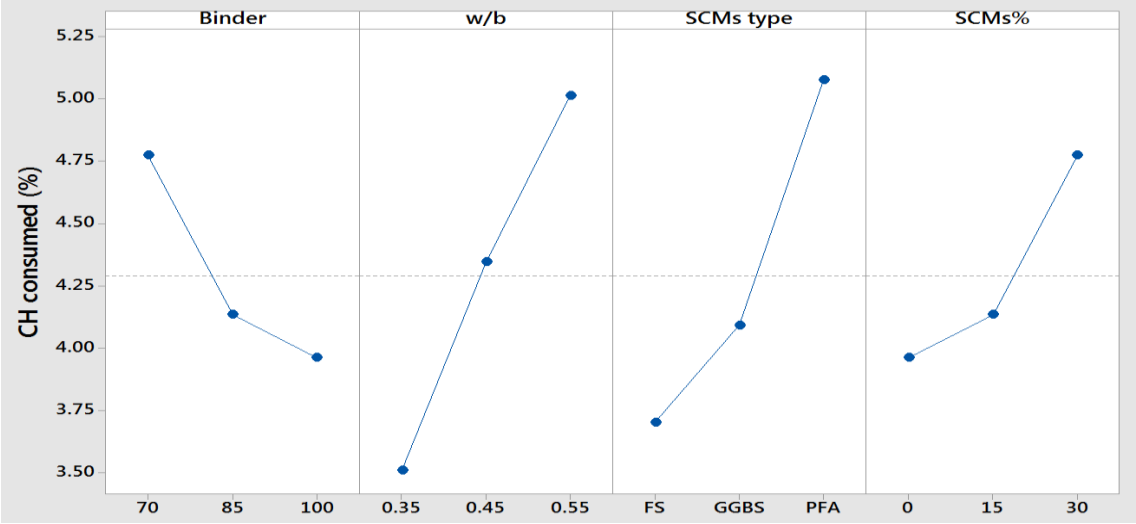

Figure 5-16 $CaCO_3$ content determined from TGA data for 28 days

It can be observed from Figure 5.16, that the calcite formation for Portland cement lower than when replacing the CEM I with SCMs. This process due to as neat cement has a high content of CaO (as mentioned in chapter 3 , section 3.3.2) which means it's an ability to catch more quantity of CO_2.

As for blended cement has lower CaO content which in turn reduces the ability to bind the CO_2 (Leemann et al., 2015). In addition, the fine slag enhanced the carbonation resistance compared with CEM I and PFA as shown in Figure 5.17. despite the fact that the ability of binding for CEM I, but fine slag showed higher carbonation resistance than Portland cement as results of this fine material to reduce the porosity and fill the pores with hydrated production as much as it can (Shi et al., 2016).

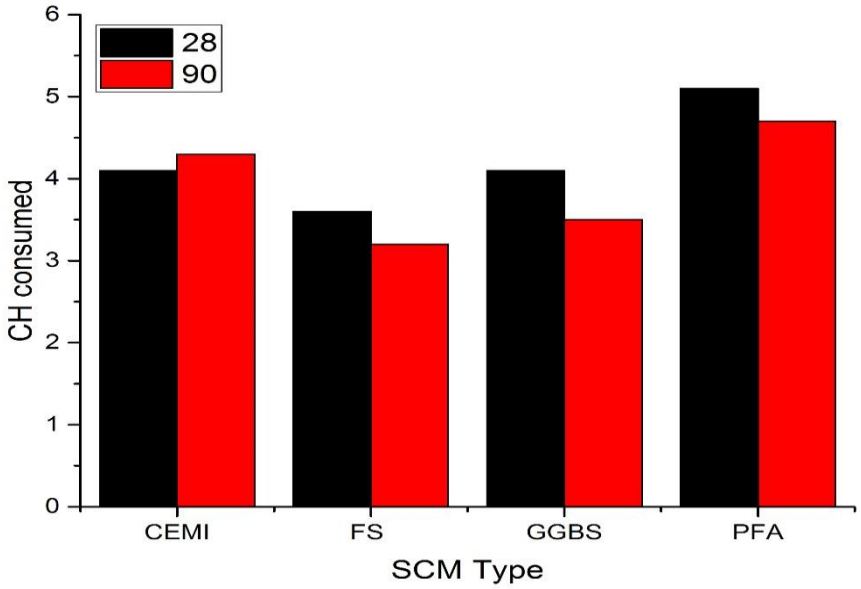

Figure 5-17 $CaCO_3$ content determined from TGA data

5.6 **Porosity by using SEM image analysis**

Both strength development and durability are influenced by the paste microstructure, where the porosity of the system is one of the most important components of paste microstructure, with the ingress of gases and liquids relying on the porosity of the paste (Mindess et al., 2003, Bentz and Stutzman, 2006).

The effect of paste variables on capillary porosity, as derived from SEM image analysis is shown in Figure 5.18 and 5.19 at 28 and 90 days respectively. This approach was used to assess the coarse capillary porosity, where the large pores (>0.03µm), as determined in this method (Ogirigbo and Black, 2016). Statistical analysis was undertaken using Minitab to obtain a regression equation. Whereas, the regression model with an R^2 equal to 51.38%. The ANOVA results for the coarse porosity at 28 and 90 days are shown in Tables 5.8 and 5.9. Three factors had a significant impact on capillary porosity: w/b ratio, plus both SCM type and replacement level. w/b ratio was found to contribute 63.9%, followed by SCM type and replacement level at 23.5% and 12.4%, respectively.

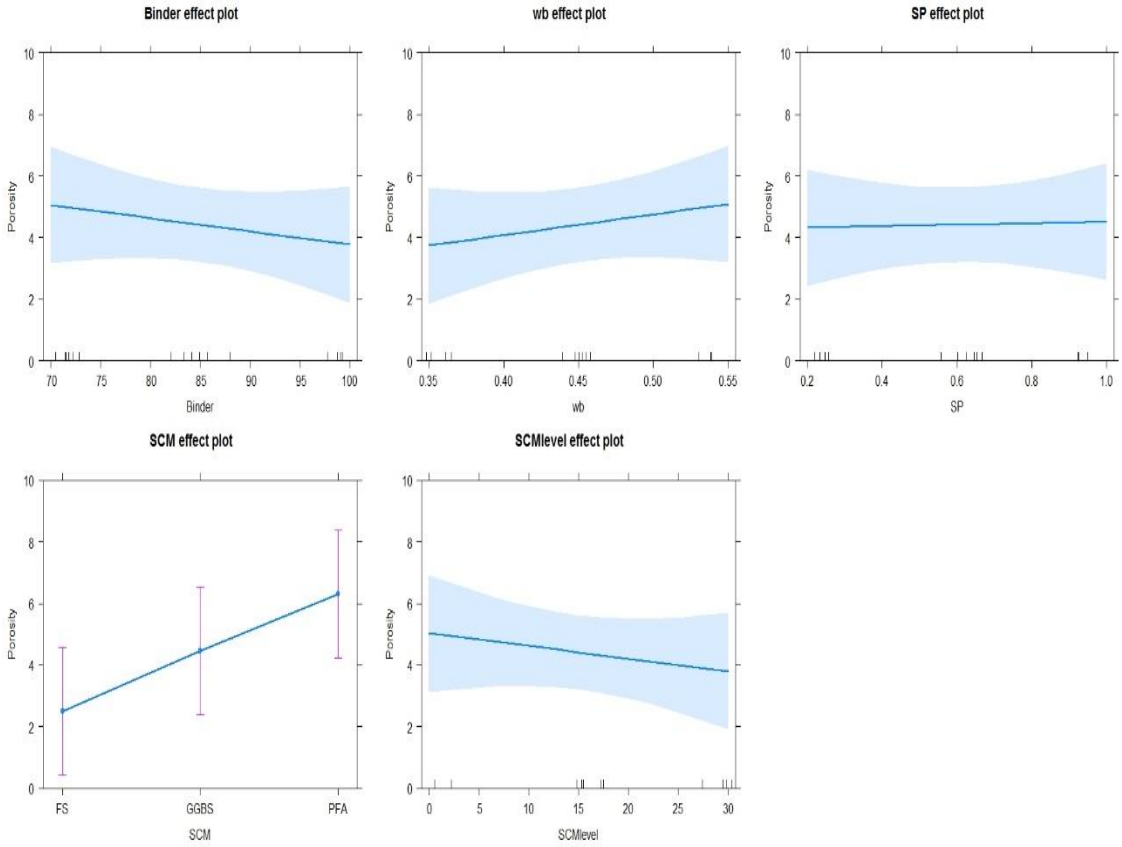

Figure 5-18 Capillary porosity content determined from SEM analysis for 28 days

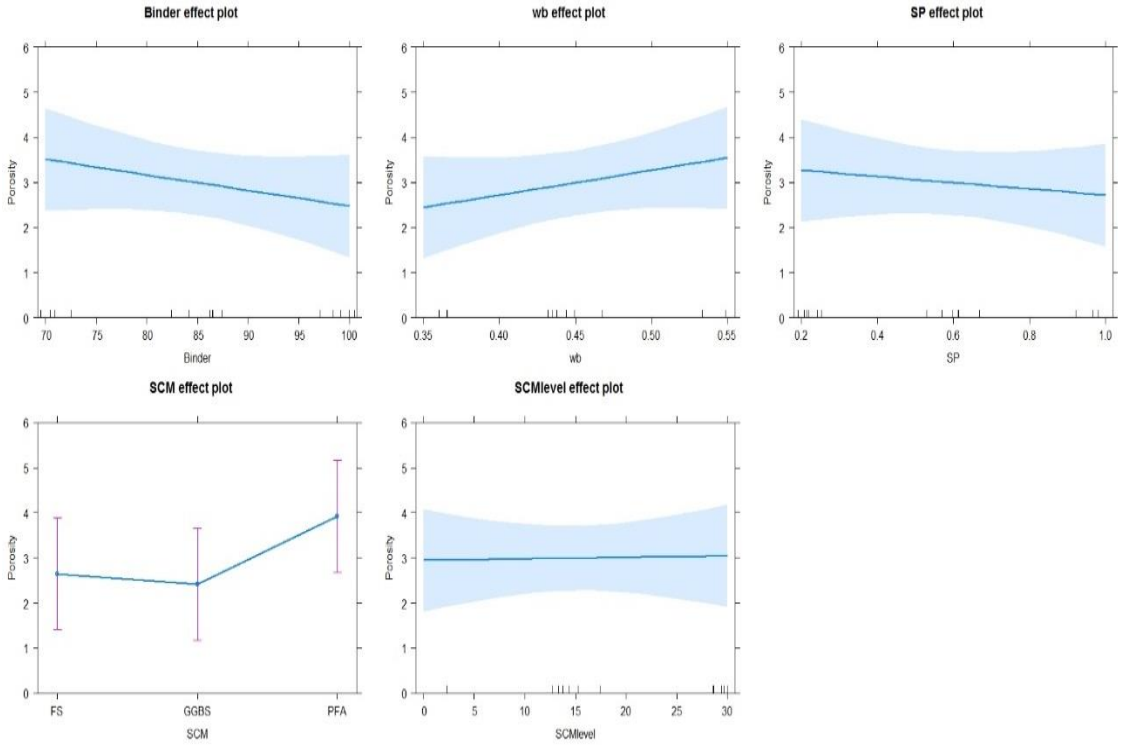

Figure 5-19 Capillary porosity content determined from SEM analysis for 90 days

Table 5-8 Results of ANOVA for coarse porosity at 28 days

Source	Adj SS	Adj MS	F-Value	P-Value	Significance	Contr.%
Binder content	3.101	3.1008	0.64	0.440	insignificant	5.4
w/b	12.403	12.4033	2.55	0.136	significant	**21.4**
SP%	0.801	0.8008	0.16	0.692	insignificant	1.4
SCMs%	43.391	21.6956	4.46	0.036	significant	**37.5**
SCMs type	39.803	19.9017	10.60	0.002	significant	**34.4**

Table 5-9 Results of ANOVA for coarse porosity at 90 days

Source	Adj SS	Adj MS	F-Value	P-Value	Significance	Contr.%
Binder content	0.2408	0.2408	0.09	0.770	insignificant	1.8
w/b	7.0533	7.0533	2.63	0.131	significant	**53.4**
SP%	0.1200	0.1200	0.04	0.836	insignificant	0.9
SCMs%	11.5433	5.7717	2.15	0.159	significant	**43.7**
SCMs type	0.0300	0.0300	0.01	0.907	significant	0.2

In general, coarse porosity decreased with prolonged hydration, from 28 to 90 days, for all samples, as the result of hydration, with hydration products gradually filling the porosity. Fine slag mixes showed lower coarse porosity than coarse slag or PFA blends. This due to the increased rate of slag hydration, refining the pores and reducing the coarse porosity (Bijen, 1996, Divsholi et al., 2014). Fly ash mixes showed higher porosities compared with slag and CEM I at 28, but lower than CEM I at 90 days as shown in Figure 5.20. This is attributed to the slow, gradual pozzolanic reaction such that at 90 days (later age) the pozzolanic reaction has been active and produced a refined pore structure (Yu and Ye, 2013).

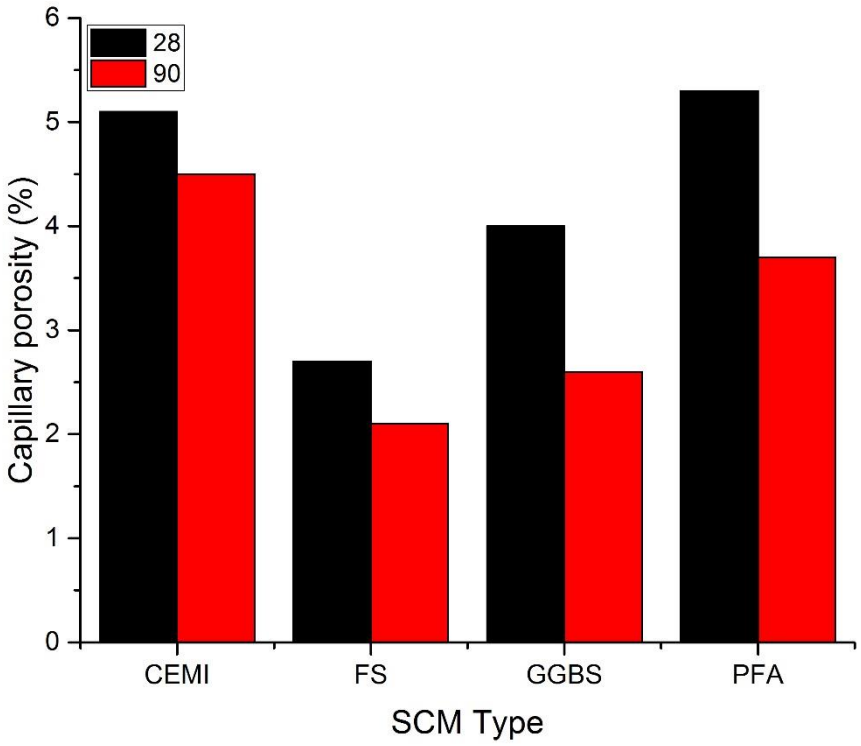

Figure 5-20 Capillary porosity from SEM images as a function of SCM

It can be observed from Figure 5.18 and 5.19, that the increasing the w/b ratio from 0.35 to 0.55 increased the coarse porosity. This result is consistent with transport properties (gas permeability and water sorptivity). Whereas, changing the w/b ratio from 0.35 to 0.45 didn't show a clear or significant effect on porosity. These results are consistent with the literature (Cook and Hover, 1999, Lam et al., 2000), who reported that increasing w/b ratio leads to increase the pore structure which includes the pore size and pore volume. This is also consistent with the permeability and sorptivity findings illustrated in chapter 4.

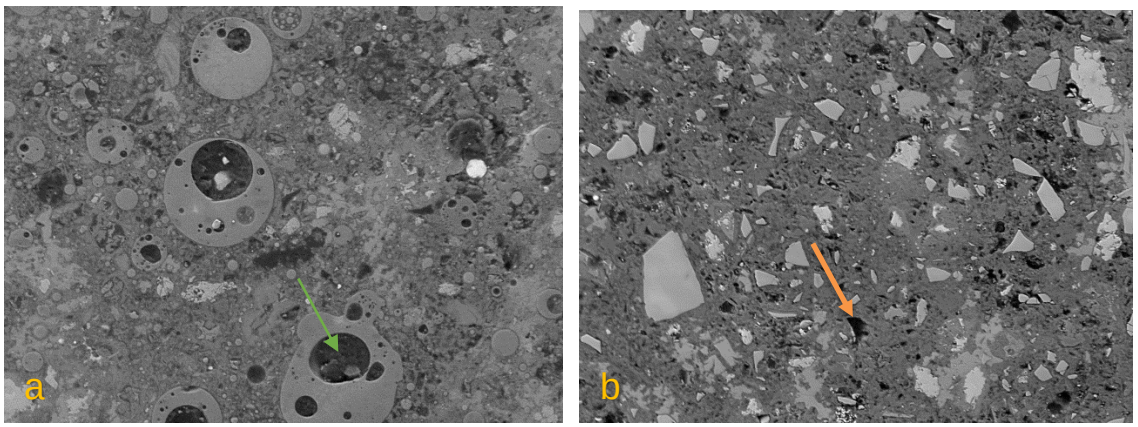

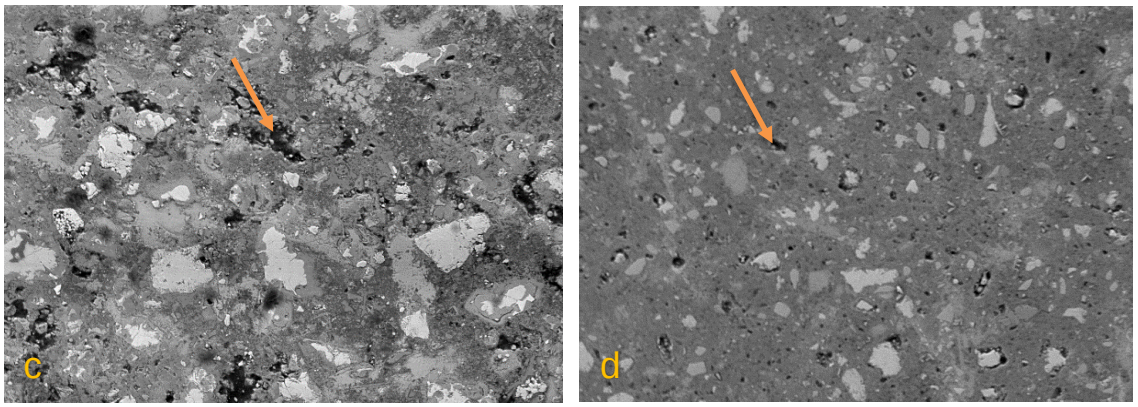

Figure 5-21 Microstructures of blended cement paste mixes after 90 days. (a) PFA ; (b) GGBS ; (c) CEM I (d) FS: Images recorded at 800x magnification and 15 KeV accelerating voltage

5.7 **Summary**

The portlandite content was higher in pastes containing pure Portland cement compared with blends containing SCMs. This is because the use of SCMs reduces the cement content and consumes portlandite during the pozzolanic reaction. For the blended cements, the PFA-bearing mixes had higher portlandite contents than the mixes containing slag as a result of slag's greater reactivity consuming the $Ca(OH)_2$. In addition, the production of calcite was lower with pastes containing slag than PFA and CEMI, as the carbonation process relying on CH content, which means the extent of carbonation was lower for slag blends because there was lower porosity

SEM image analysis of the different combination of pastes at both 28 and 90 days revealed that the pastes containing slag (coarse & fine) showed a more dense microstructure with low porosity compared with PFA and CEMI pastes. The microstructure of fly ash was porous mainly due to unreacted particles of fly ash and its slow reaction.

Pure Portland cement pastes contained large capillary pores compared to blended cements demonstrating the production of additional hydration products due to the pozzolanic reaction.

Chapter 6 Relationship between concrete performance, binder microstructure and carbonation resistance

6.1 Dependence of carbonation depth on concrete strength and porosity

Concrete strength is considered a good indicator of carbonation resistance, with carbonation resistance increasing with increasing strength (Sulapha et al., 2003). The results in this study confirm this concept in Figure 6.1, with an inverse correlation between compressive strength and carbonation depth (R^2 0.805), as shown in Figure 6.1. As both w/b ratio and SCM replacement are the main contributors to both compressive strength and carbonation depth, a reduction in w/b ratio has a direct effect on both increasing compressive strength and decreasing the carbonation depth. In addition, the increase in strength is due to the reduced capillary porosity and that capillary porosity also defines transport properties (Glinicki et al., 2016, BASHEER et al., 1999).

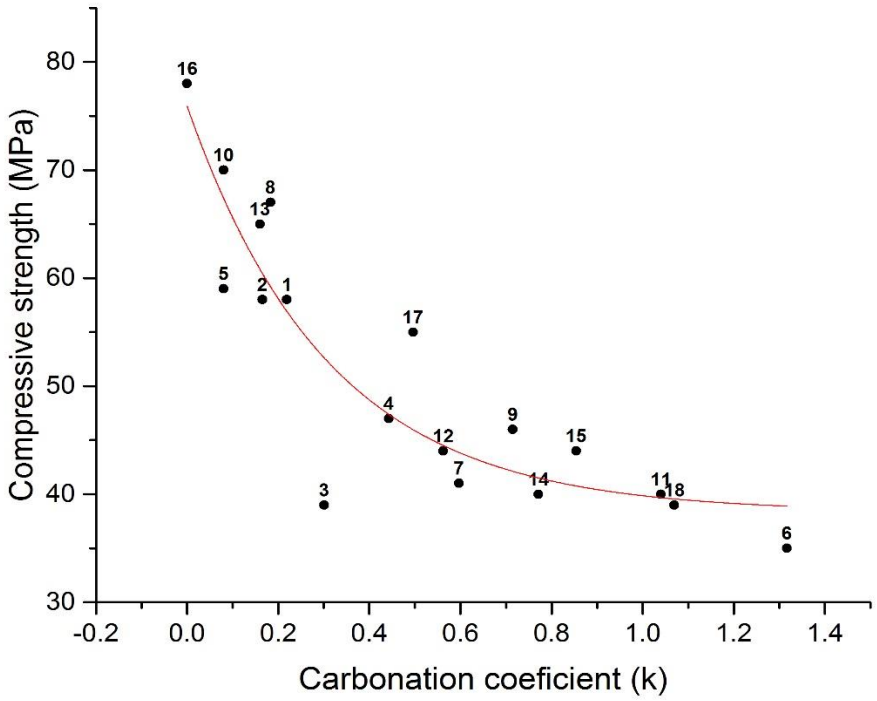

Figure 6-1 Carbonation depth vs compressive strength at 28 days

The relationship between strength and carbonation resistance was reflected in the relationship between concrete permeability and compressive strength. This relationship at 28 days is shown in Figure 6.2. The correlation between gas permeability and coarse porosity is strong, as indicated by a value of 0.774 for the coefficient of determination. (Bakhshi et al., 2006, Jaya et al., 2011) who concluded that negative correlation is attributed to the fact that the strength and permeability are related to the pore structure of the paste.

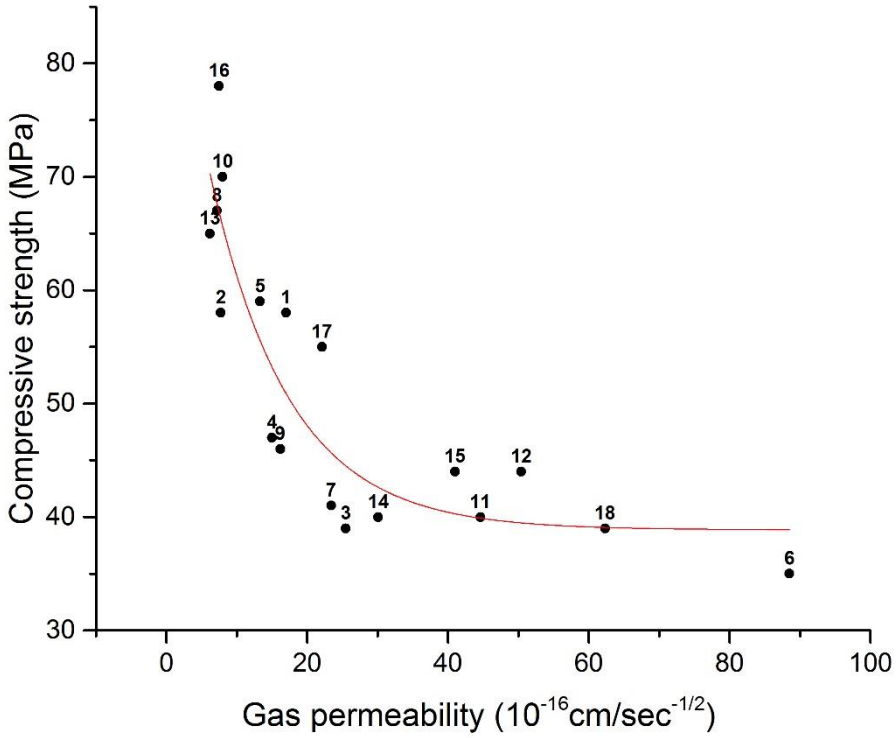

Figure 6-2 Gas permeability vs compressive strength at 28 days

The relationship between compressive strength and coarse porosity for 18 concrete mixes is presented in Figure 6.3, indicating the inverse correlation between coarse porosity and strength. This trend agrees with literature (De Weerdt et al., 2011, Igarashi et al., 2004). As was observed, (The ANOVA Tables in chapter 4, section 4.5 and 4.6 and chapter 5 section 5.6), the second variable affecting the permeation properties and coarse porosity is replacing Portland cement with GGBS (fine and coarse), which results in low gas permeability and low coarse porosity. This low porosity is a result of the pozzolanic reaction and the formation of additional C-S-H. This thus explains the trend of compressive

strength and carbonation resistance which relied on the microstructure of the paste (pore structure).

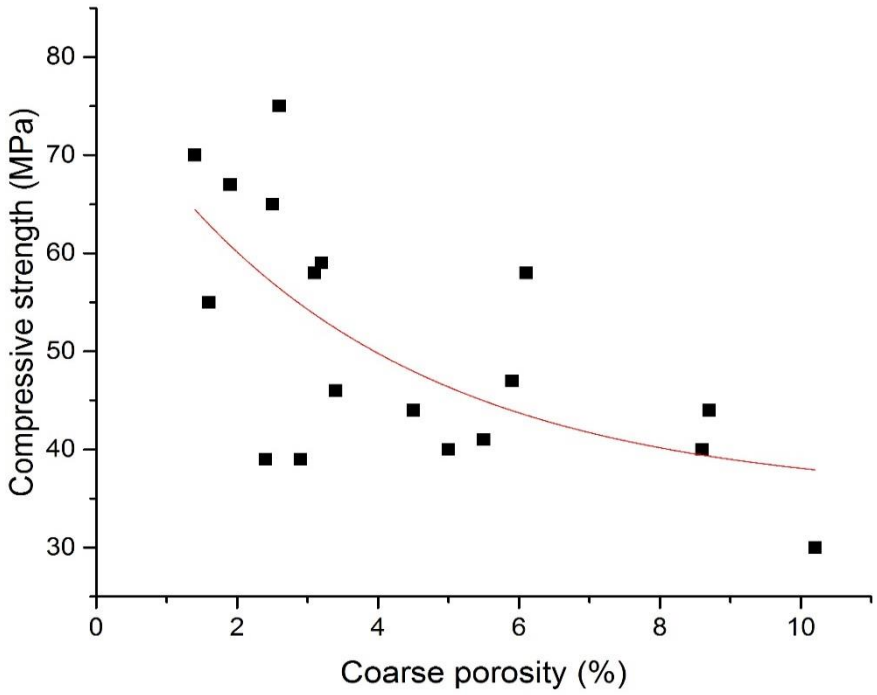

Figure 6-3 The relationship between compressive strength and porosity at 28 days

Mixes 2, 8, 10, 13, and16, as shown in Figure 6.1, have higher compressive strengths and lower carbonation depths compared to other concrete mixes, while mixes 6, 11, 15, and 18 showed lower compressive strengths and carbonation resistance. These well-performing mixes all show the common characteristics of low w/b ratios and the incorporation of slag.

Although the relationship was strong some mixes showed very similar strengths yet dissimilar carbonation resistance. For example in Figure 6.1, mix 3 and mix 11 both had strengths of ~52 MPa, but their carbonation depths ranged from 3 to 11mm. This indicates the role of other significant variables (binder content and superplasticizer) which impact on compressive strength but have different effects on carbonation depth. In addition, concretes with variables such as using PFA, higher w/b ratios or high Portland cement contents had acceptable compressive strengths but low carbonation resistance.

6.2 Dependence of carbonation depth on gas permeability and porosity

Air permeability is a good predictor of carbonation resistance, since CO_2 diffusion through the concrete relies on the porous microstructure of the concrete. (Salvoldi et al., 2015). There is an inverse correlation between gas permeability and carbonation resistance (Figures 6.4 and 6.5), with R^2 values of 0.802 and 0.707 at 28 and 90 days respectively.

As the w/b ratio and presence of SCMs are the main contributors to both compressive strength and carbonation depth, reduction w/b ratio has a direct effect on reducing gas permeability and decreasing the carbonation depth. Reducing the w/b ratio leads to reduced capillary porosity (and so increased strength, as shown before), with a significant effect on carbonation resistance.

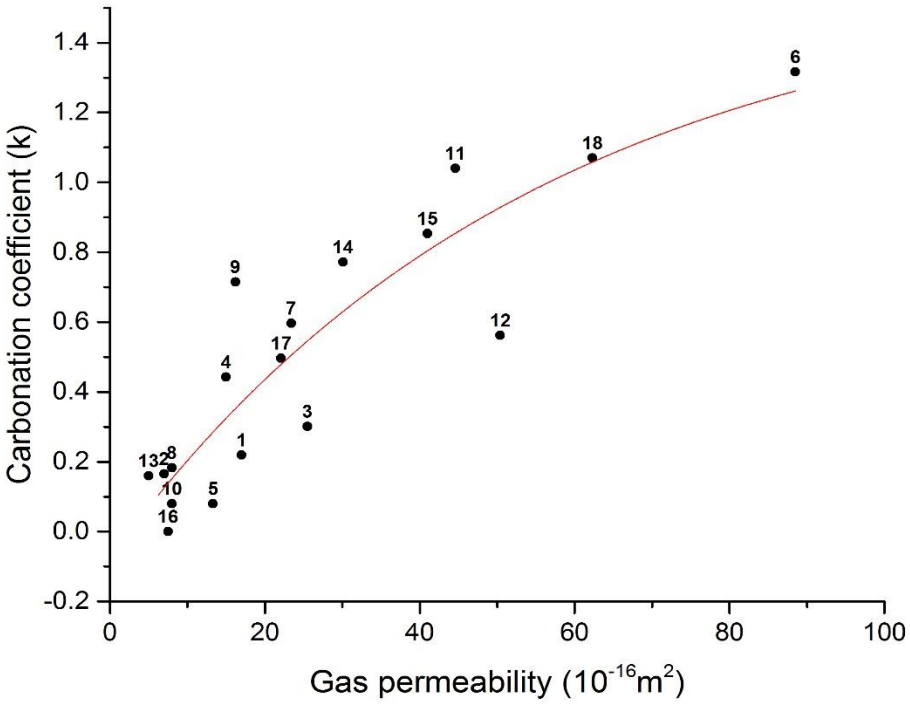

Figure 6-4 Carbonation depth vs gas permeability at 28 days

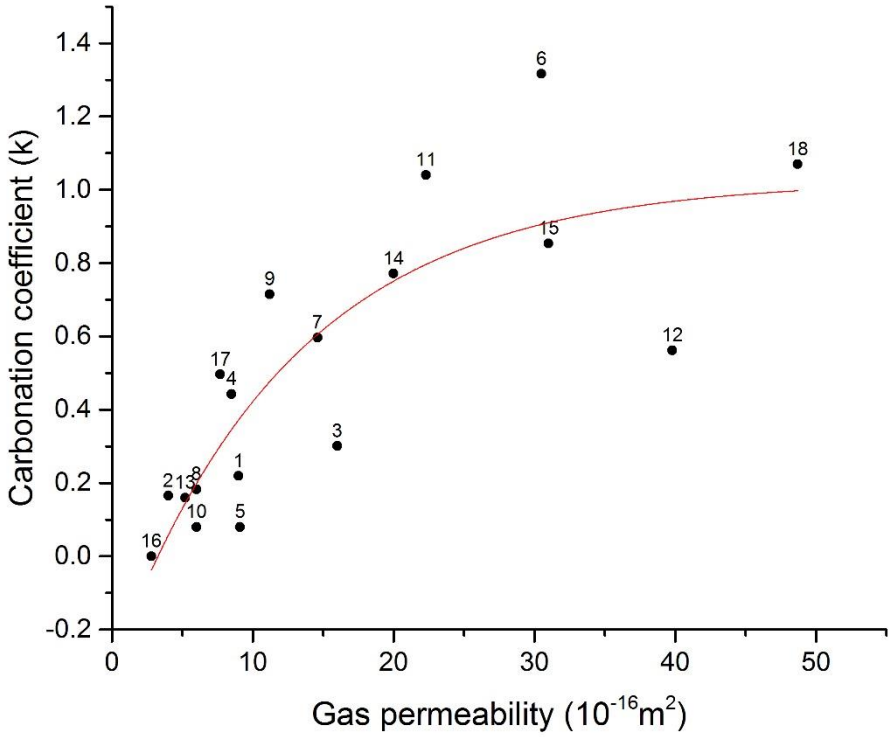

Figure 6-5 Carbonation depth vs gas permeability at 90 days

Therefore, with decreased gas permeability due to the lower ratio of w/b, the carbonation depth decreases. Reducing w/b ratio is known to lead to reduced capillary porosity (and so increases strength, as shown before). This reduction in capillary porosity has a significant effect on carbonation resistance, with a significant decrease in carbonation depth seen with decreasing w/b ratio.

This agrees with the relationship between concrete permeability and coarse porosity for pastes at 28 days as shown in Figure 6.6. The correlation between gas permeability and coarse porosity is good but not strong, as indicated by a value of 0.54 for the coefficient of determination. The weak correlation between the gas permeability for concrete and coarse porosity for paste as the results of variation between the factors which controlled the trend each of them. For example, the aggregate size had a significant effect on the permeability but not on coarse porosity, because the aggregate was not present in the paste.

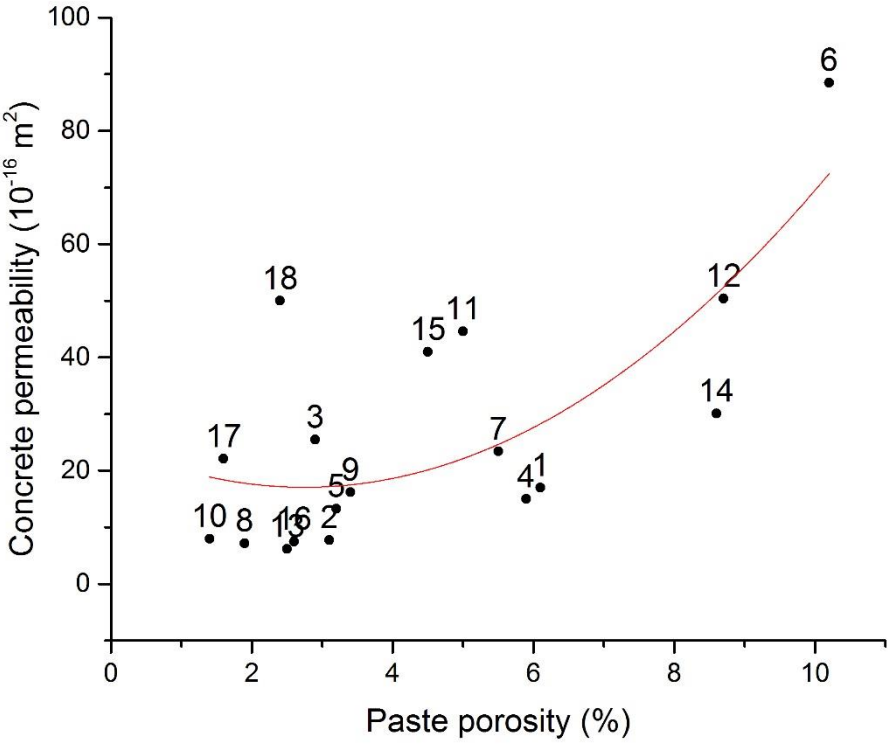

Figure 6-6 Relationship between the gas permeability and coarse porosity at age 28 days

As observed in the ANOVA tables in chapter 4, section 4.4 and 4.5, the addition of GGBS (either fine or coarse) reduced gas permeability and improved carbonation resistance. Mixes 1, 2, 5, 8, 10, and 16 (Figure 6.3), have both lower gas permeability and carbonation depths, while mixes 11, 12, 15, and 18 showed higher gas permeability and lower carbonation resistance. This is due to the latent hydraulic behaviour of GGBS in promoting the formation of additional C-S-H and also changing the nature of the C-S-H from fibrillary to foil-like, further improving permeability.

This behaviour as results of the main contribution of significant variables on carbonation depth and compressive strength which lies in reducing the w/b ratio and using the slag replacements which ranged from 15% and 30 %. Although the relationship was strong some mixes show a poor correlation as the result of the variable which impacts the carbonation depth negatively (binder content), but on the other hand, have a negligible effect on gas permeability. For example in Figure 6.3, mixtures 4, 9, and 17 had an approached gas permeability (10^{-16} m^2), while the carbonation depth measurements were ranged from 4.5 to 8 mm. This

is attributed to the negative effect of reducing the binder content which was 350 kg/m^3. Also, there are other significant variables (aggregate size and superplasticizer) which impact on gas permeability but differs effect theirs on carbonation depth. In addition, that derivation of the carbonation equation, i.e. rate = k.t 0.5 where k is proportional to the diffusion coefficient and inversely proportional to the amount of carbonateable matter.

6.3 Dependence of carbonation depth on sorptivity and porosity

Water sorption defines the ability of water to flow through the concrete according to the capillary absorption as a result of pressure. Figure 6.7 shows that while there is a positive correlation, it is weak with R^2 of 0.673 and 0.761 at 28 and 90 days respectively. This reverse trend refers that the variation of mix design variables impacts each properties (carbonation & sorptivity) where can affect the performance greatly or poorly. Whereas, the significant variables not similar for both properties such as the aggregate size insignificant for carbonation resistance but were considered significant for water sorptivity.

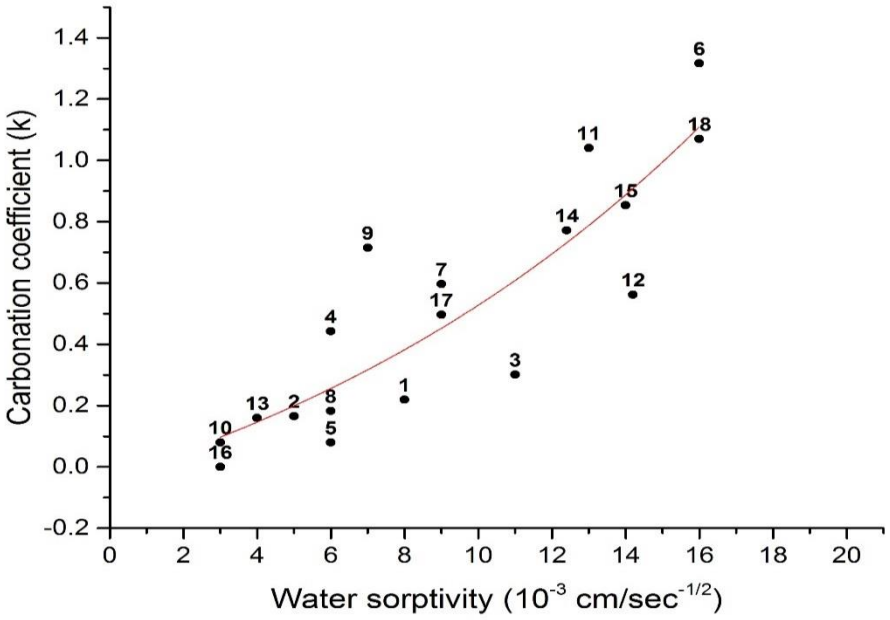

Figure 6-7 Carbonation coefficient vs water sorptivity at 28 days

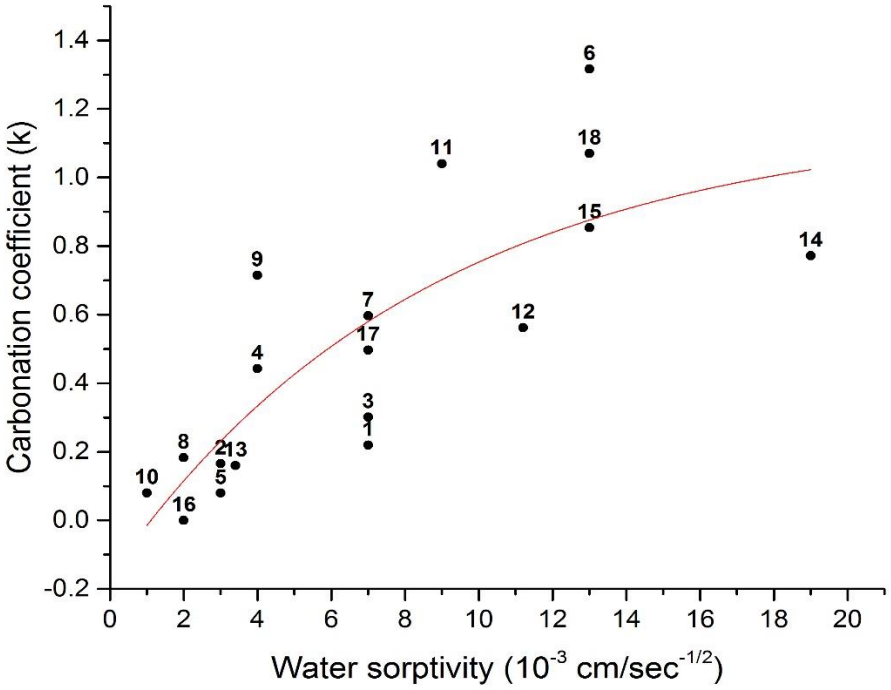

Figure 6-8 Carbonation coefficient vs water sorptivity at 90 days

As with strength and permeability, the principal factors determining sorptivity were w/b ratio and SCM replacement. Therefore, reducing w/b led to lower capillary porosity. Lower porosity was shown by Powers to lead to lower sorptivity . Referring back to the ANOVA Tables in Chapter 4, section 4.6 and 4.7, replacement of cement with either coarse or fine GGBS was shown to be a significant factor. This resulted in low concrete sorptivity and thus low carbonation depth. The carbonation depth of mixes 2, 5, 8, 10, and 16, as shown in Figure 6.5, correlated with lower water sorptivity.

This behaviour results from a combination of the main contributing variables on carbonation depth and water sorptivity, namely reducing the w/b ratio and using either 15 or 30% slag replacement. Although the relationship on the whole was strong, some mixes showed a deviation from the trend as a result of influencing variable which have a negative impact on carbonation depth but a positive effect on water sorptivity, or vice versa. For example in Figure 6.8, mixes 4, 9, and 13 had a low water sorptivity (4-16cm/s-1/2), while the carbonation depths ranged from 4.5 to 8 mm. This was due to aggregate size which had an impact on water sorptivity but an insignificant effect on carbonation depth. Conversely,

superplasticizer was considered a significant variable affecting carbonation, but with an insignificant effect on water sorptivity. Figure 6.9 shows the correlation between water sorptivity and paste coarse porosity, where the R2 equal to 0.4. This relationship gives a significant indication about the responsibility of paste microstructure regarding the concrete permeation properties, where any increase in pore content leads to an increase the concrete permeability.

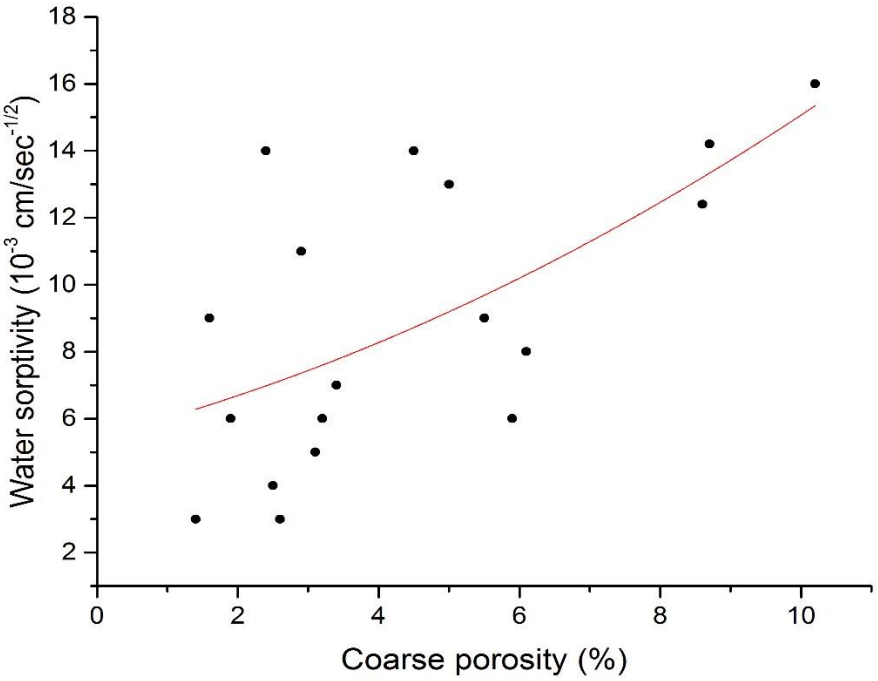

Figure 6-9 Relationship between the water sorptivity and coarse porosity at age 28 days

6.4 **Dependence of carbonation on Portlandite content**

Carbonation progression in concrete relies on two aspects: the presence of carbonatable matter (portlandite) and the diffusion of carbon dioxide, where these two factors combine to give a square root relationship:

$$x^2 = \frac{2DCt}{A}$$

As a result of these two phenomena, it is not possible to assess the resistance of blended cement paste to carbonation that means the two compete against one another so it is difficult to isolate the effects of each one (Šavija and Luković, 2016). As a result of carbonation coefficients for 18 concrete mixes (chapter 4,

section 4.7), the main contributor was w/b ratio which governs the carbonation rates. As can be seen in Figure 6.11, low w/b ratio showed high carbonation resistance, this attributed to pore structure densification which reduced the carbon dioxide diffusion, as indicated by permeation properties for concrete samples and capillary porosity for paste samples (Figures 6.4, 6.5 and 6.6). This finding of the effect low w/b on carbonation resistance similar to the literature (Houst and Wittmann, 1994, Sulapha et al., 2003, Wee et al., 1999)

On the other hand, high w/b pastes showed a high CH content compared to low w/b as seen in Figure 6.10, which means more carbonateable materials available to react with carbon dioxide which in turn lower carbonation coefficient. However, if the CH content does not govern the pore structure which reduces the carbon dioxide diffusion, the carbonation may progress faster as the result of more capillary porosity content according to the effect of significant variables w/b ratio and using SCM.

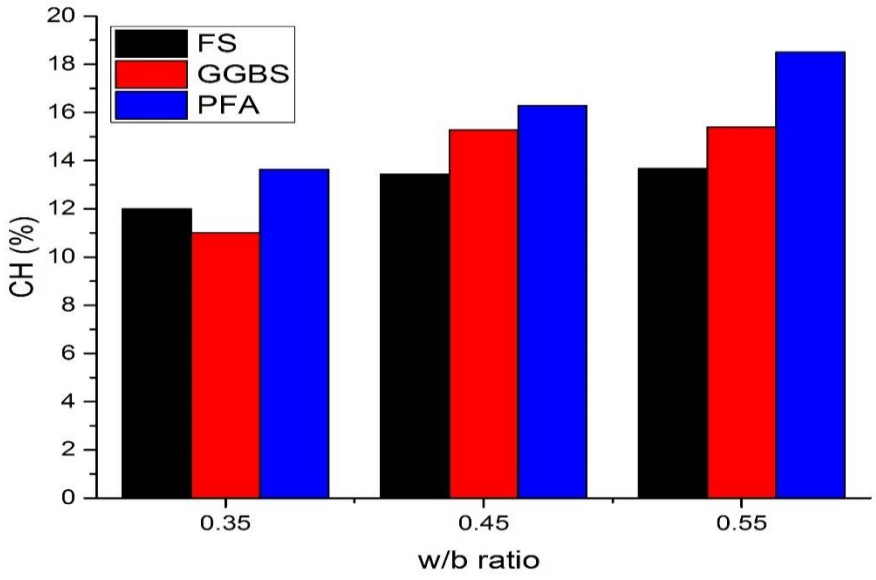

Figure 6-10 Portlandite content for different paste mixtures with different w/b ratio and SCM at 28 days

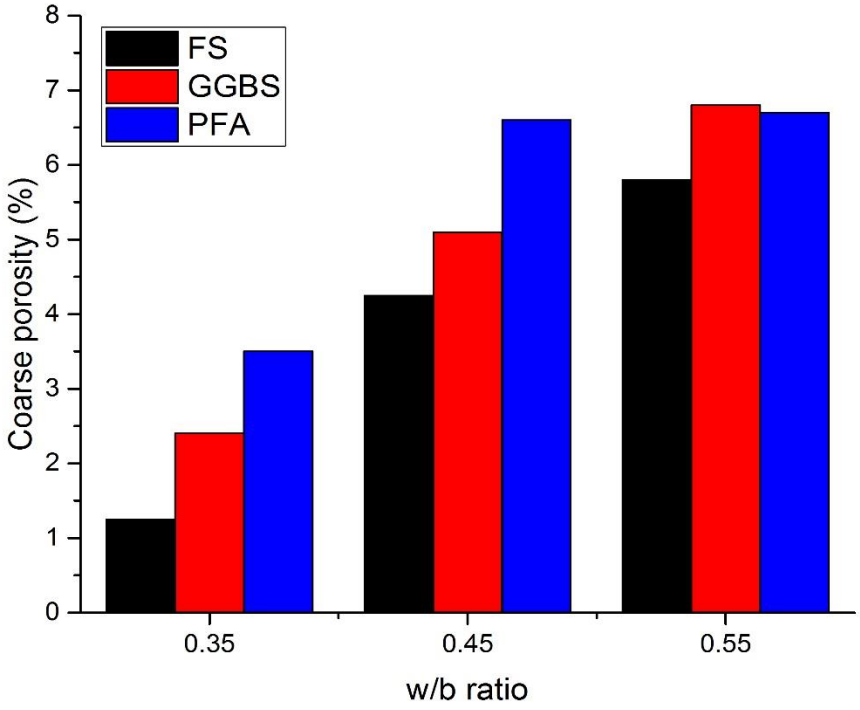

Figure 6-11 Coarse porosity with different w/b ratio and SCM at 28 days

6.5 **Dependence of carbonation on shrinkage**

Based on the effect of mix design variables which affected by significant variables (w/b, SCM and aggregate size), it indicates that the shrinkage and gas permeability was obviously proportional as shown in Figure 6.12. Moreover, there is a good correlation between the shrinkage and capillary porosity as shown in Figure 6.13. This explains the role of concrete shrinkage to increase the porosity of paste which in turn led to increased diffusion of carbon dioxide. Hence, the carbonation progress as indicated in Figure 6.15 increased with shrinkage increasing. The main reason for increasing the shrinkage as the result of losing the water from the capillaries which in turn led to tension which causes this shrinkage. In addition, this loss of water results in more pores content which make the CO_2 diffusion faster and increase the carbonation reaction.

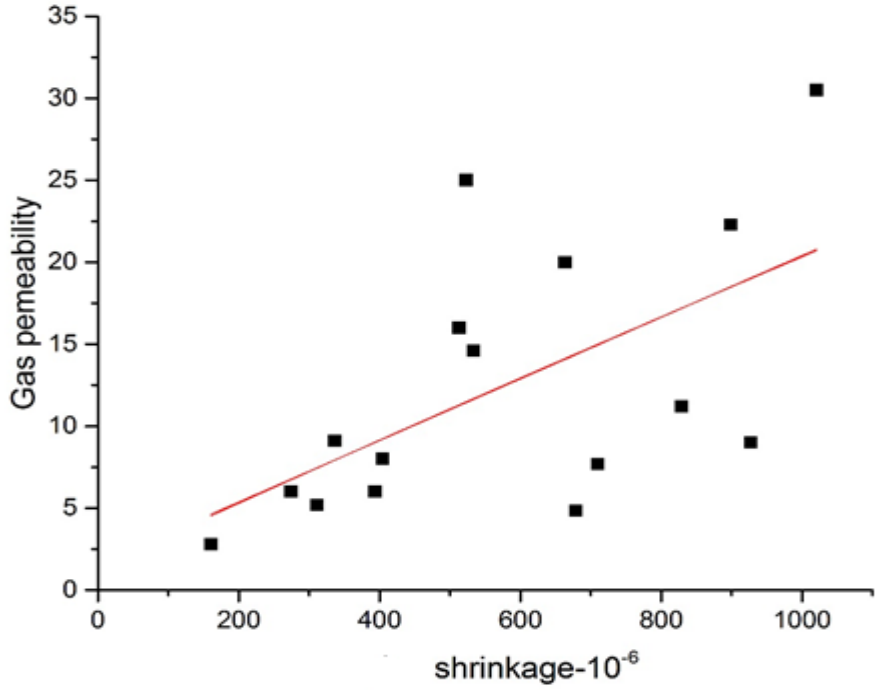

Figure 6-12 Gas permeability vs shrinkage at 90 days

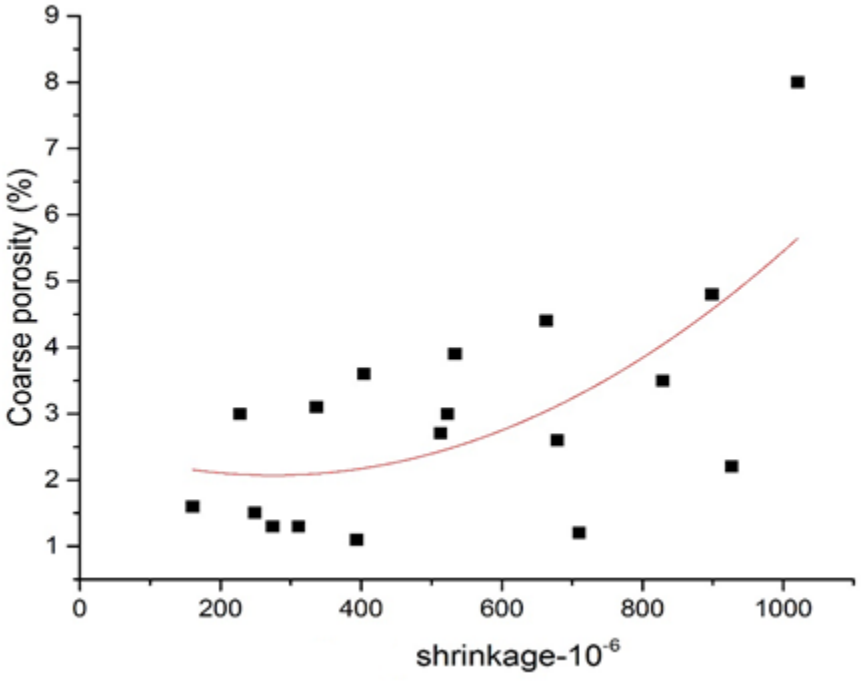

Figure 6-13 Capillary porosity vs shrinkage at 90 days

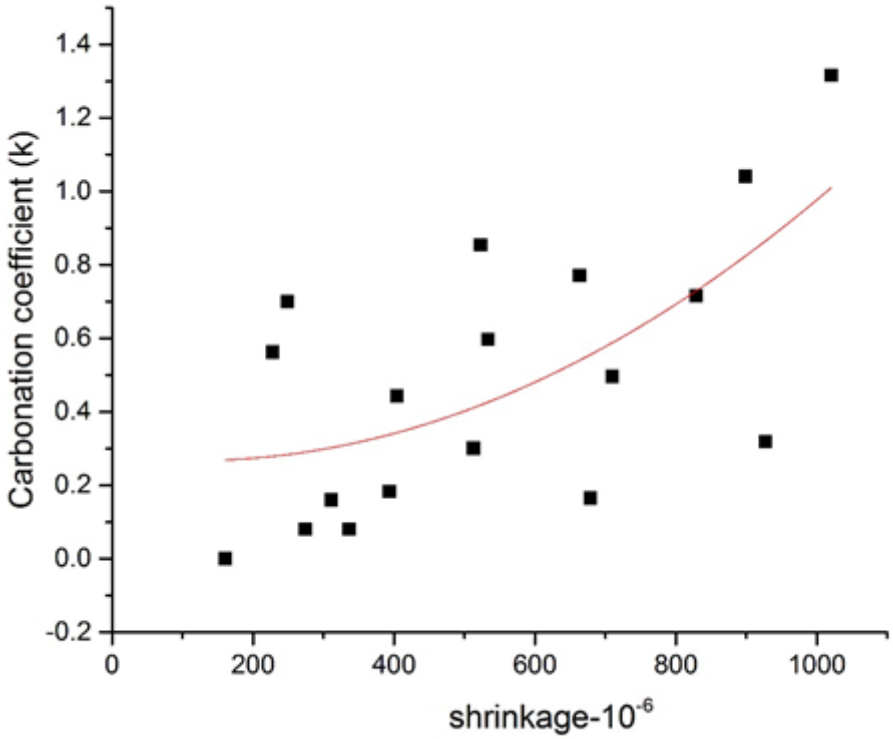

Figure 6-14 Carbonation coefficient vs shrinkage at 90 days

There exists an underlying microstructural effect to concrete that may explain the relationship between shrinkage and carbonation resistance. High shrinkage implies greater porosity, which in turn leads to a high carbonation coefficient.

6.6 **Summary**

In this chapter, the relationship between durability (carbonation resistance) and the concrete performance (strength & permeation properties) affecting the carbonation progress have been presented and discussed.

There is a strong positive relationship between concrete strength and carbonation resistance, showing an exponential correlation with a correlation coefficient of ~0.7 obtained. Further, it was shown that both strength and permeability were influenced by common variables: w/b ratio and slag replacement. Both these variables (w/b & slag incorporation) have a role to change the pore structure, where reduced w/b ratio led to increased strength because this w/b reduction reduced porosity, as observed on gas permeability and coarse porosity as found by SEM images analysis.

Meanwhile, there was a good exponential correlation between carbonation resistance and permeation properties (gas permeability & water sorptivity). Reducing carbon dioxide diffusion greatly limits carbonation, and this is strongly influenced by pore microstructure and connectivity. Again, this good correlation between the carbonation coefficient and permeation properties largely rely on the effect of common variables: w/b ratio and slag incorporation. In addition, the binder content had a significant role to change the carbonation depth, where the increasing the binder content led to increasing the carbonation resistance as a result of the quantity of carbonatable matter which is inversely proportional to carbonation. On the other hand, the relationship between the diffusion and the carbonation resistance is proportional. That means any increasing the permeability leads to increase the carbonation.

Chapter 7 Embodied Carbon dioxide (eCO_2) of concrete mixes

7.1 Introduction

While much of this study has focused on performance criteria, with increasing environmental concerns, consideration of the environmental performance of concrete is also important. In this chapter, embodied carbon dioxide (eCO_2) is discussed, to examine whether the factors producing a suitable low carbon mix design can also satisfy physical properties and carbonation resistance.

The aim of this project was to look for a strong, low carbon, durable concrete. The mixes are thus assessed on their potential to reduce carbon footprint, increase carbonation resistance and develop strength.

7.2 Embodied carbon dioxide vs compressive strength

Portland cement is the greatest contributor to the carbon footprint of concrete (Abu Saleh, 2014). Meanwhile, while the cement content itself does not affect the compressive strength directly, the w/b ratio is the greatest influencing factor on strength. Thus, reducing the w/b ratio without increasing the cement content is the best means of reducing eCO_2. However, this should not be done at the expense of carbonation resistance.

The best means of achieving this is by using an effective low-carbon binder. A good example of this is GGBS, where slag incorporation positively influences strength and reduces permeability. Therefore, the aim should be to reduce the w/b ratio without increasing the cement content and the best means of achieving this is by replacing the cement with an effective low-carbon binder. A good example of this is GGBS. Where the slag incorporation has a positive effect on compressive strength development as the results of high reactivity and low pore structure.

Analysing eCO_2 of each mix with its corresponding 28 days compressive strength indicates that there is an optimum strength which includes mix 5 and 16, at which the eCO_2 is minimized. Still, there is need to consider the durability (carbonation resistance) and low eCO_2 to achieve durable low-carbon concrete. As can be seen from Figure 7.1, a plot of eCO2 against strength shows three distinct

regions. Three clusters were identified subjectively, based on satisfying the specific requirements of minimizing the eCO_2 and improving the strength. The green cluster which included mixes 5 and 16 shown minimum eCO_2 with the high strength value compared with other 16 concrete mixes.

The green zone shows concretes with high compressive strength and lower eCO_2. The orange region represents concrete with a low carbon footprint, yet low compressive strength. The final, red, group comprises of concretes with a high eCO_2. Mixes 5 and 16, comprising the green group, have achieved low Portland cement contents by replacing 30% with fine and coarse slag. This led to a reduction in the eCO_2 to below 300 kg CO_2/m^3. Some of the concretes in the orange group had similarly low carbon footprints, but lower strength because of either a high w/b ratio or use of PFA, which helped to reduce the carbon dioxide emission but didn't satisfy the physical properties (strength)

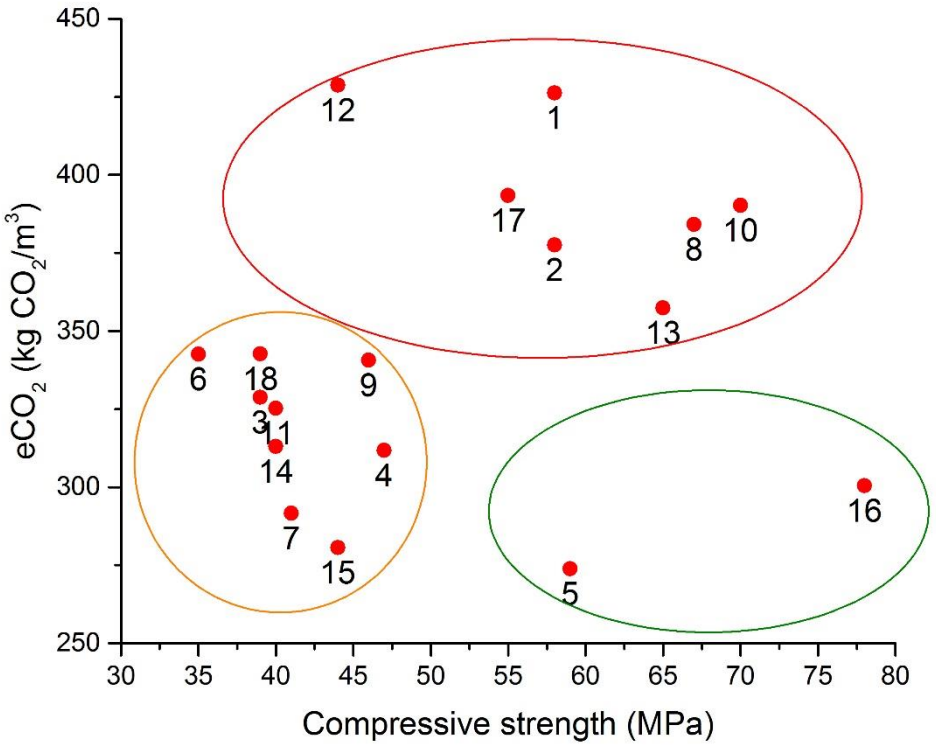

Figure 7-1 eCO_2 vs. compressive strength of concrete at age of 28 day

As can be seen from Figure 7.1, there are three areas classified on the carbon dioxide emission and the value of strength at 28 days. Plotting the embodied carbon against compressive strength revealed three distinct regions (Figure 7.1). The green zone shows concretes with high compressive strength and lower

eCO_2. The orange region represents concrete with a low carbon footprint, yet low compressive strength. The final, red, group comprises of concretes with a high eCO_2. Mixes 5 and 16, comprising the green group, have achieved low Portland cement contents by replacing 30% with fine and coarse slag. This led to a reduction in the eCO_2 to below 300 kg CO_2/m^3. Some of the concretes in the orange group had similarly low carbon footprints, but lower strength because of either a high w/b ratio or use of PFA, which helped to reduce the carbon dioxide emission but didn't satisfy the physical properties (strength).

However, it needs to be remembered that this study aimed to identify the factors which led to durable, low-carbon concrete. As such, the mixes identified above should not be judged on the basis of their strength and workability (as concrete mixes would normally be defined), but rather they indicate those factors which may be adopted in concrete mix design so as to achieve a low carbon footprint and good resistance to carbonation.

The normal way to design the concrete mixes is defining the performance of concrete, namely workability and strength. However, these were considered in this study as outputs, or dependent variables. Therefore, rather, the recommendations from this project should be used merely to inform concrete mix designs so as to reduce carbon footprint while preserving durability. The concrete design in this study it's not limited by slump and strength as would be typical when designing concrete mixes. This was a deliberate approach in adopting the Taguchi design method, selecting the mix design variables as independent variables and defining slump and strength as dependent variables.

As stated earlier, the independent variables were set at levels typical for general purpose concrete but with some of these combinations not being realistic in terms of strength and workability delivered, but maintaining the orthogonal array required by the Taguchi method. A possible limitation of the approach and use of the Taguchi method is that it is not possible to define mixes based on their characteristic strengths or workability. Thus, some of the mixes may seem unrealistic, but are a constraint of the use of an orthogonal array.

7.3 **Embodied carbon dioxide vs carbonation resistance**

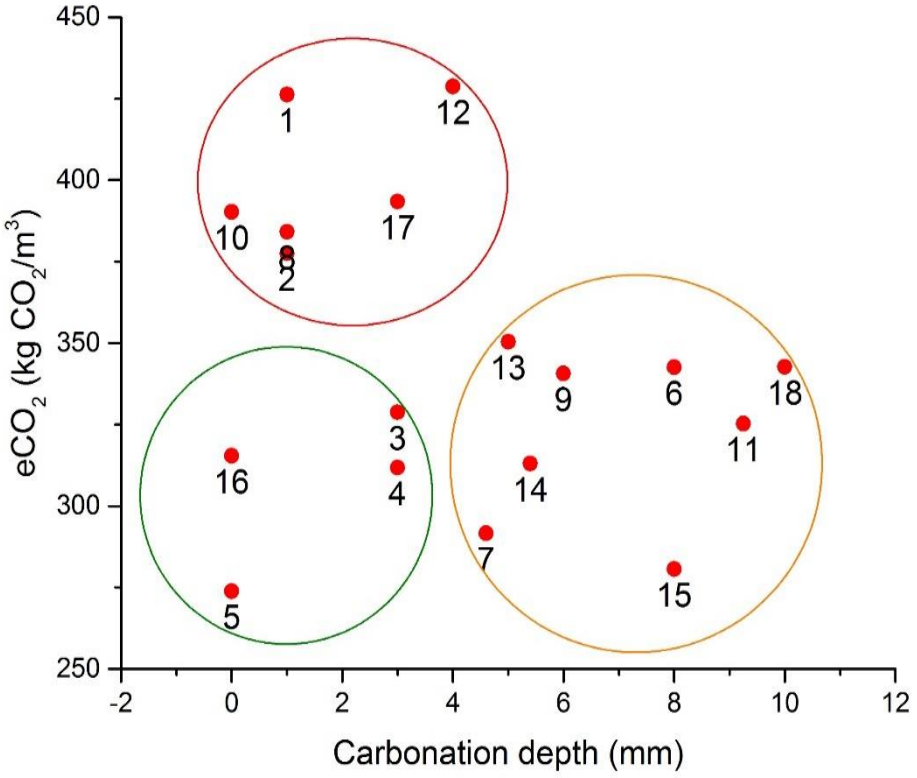

Figure 7-2 eCO_2 vs. carbonation depth of concrete at age of 28 day

The relationship between carbonation resistance and eCO_2 could also be similarly represented by three regions on a plot of eCO_2 versus carbonation depth (Figure 7.2). The red circle contains mixes showing good carbonation resistance, but at the expense of carbon footprint. The orange circle contains mixes which have a low carbon footprint, but don't necessarily offer carbonation resistance. Finally, the green circle contains concretes with good carbonation resistance and a low eCO_2, satisfying the requirement for concrete durability and environmental sustainability. Concrete with a very high Portland cement content, such as mixes 1, 2, 8, 10, 12, and 17, achieve good carbonation resistance due to their high binder content, but also have a high carbon footprint because of their low level of replacement.

(Purnell and Black, 2012) studied the theoretical relationship between eCO2 and strength and found that replacing 100% CEM I by 40% PFA led to a reduction in eCO2 of about 35%. Also, eCO2 could be reduced by using concrete of lower

workability, which can significantly reduce the CEM I content. Elsewhere, (Zaman, 2014) found that concrete mix proportion containing 15% Portland cement, 70% GGBS and 15% rice husk ash met the performance requirements, durability, and environmental sustainability compared to the Portland cement concrete.

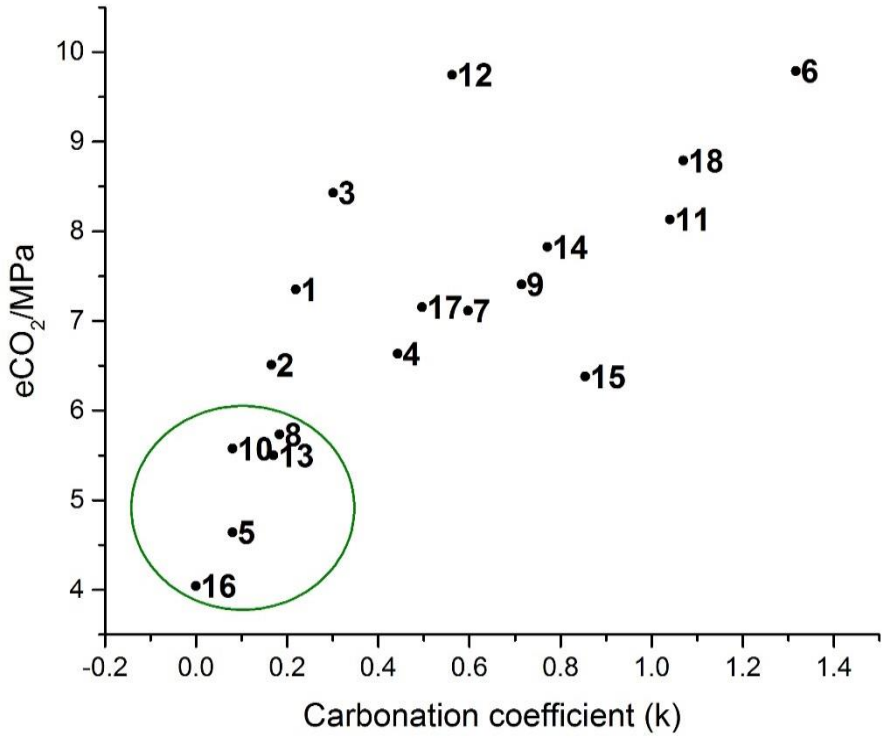

Figure 7-3 eCO_2/MPa versus carbonation coefficient

Figure 7.3 gives an insight into how to achieve durable low-carbon concrete. The mixes within the green circle in the plot, including mixes 5, 8, 10, 13, and 16, offer lower eCO_2 per unit strength while satisfying the high carbonation resistance. Mixes 5, 8, and 16 contain slag with 15% and 30% and low w/b, in which case slag and w/b have a major contributions to reduce the embodied carbon dioxide and increase the carbonation resistance. Meanwhile, concrete mixes 8 and 13 have a low w/b ratio and low binder content which in turn had the big contribution in achieving the durability and sustainability requirements. The common factors which in turn led to achieving durable low carbon concrete are binder content, w/b ratio, and slag replacement as shown in Table 7.1.

Table 7-1 Mix proportions for durable low carbon concretes

Mix No.	Binder content (Kg/m³)	W/b	SCM-Type	SCM (%)
5	350	0.45	FS	30
8	400	0.45	GGBS	0
10	450	0.35	FS	15
13	350	0.35	FS	0
16	400	0.35	GGBS	30

Table 7.1 shows the concrete mixes that have a significant effect to reduce the carbon footprint while offering carbonation resistance. However, it is notable that some of these mixes did not include an SCM, despite this being seen as an important factor in delivering durable, low-carbon concrete. This is because, in these instance, performance was delivered by other means. It is also noted from the significant effect of using low binder content of 350 kg/m^3 with low w/b ratio 0.35, required performance can be achieved. For example, reducing the w/b ratio and binder content, as is clear in mixes 8 and 13, where the binder content was reduced to a minimum value as was the water content. Again, it must be stressed that Table 7.1. Should not be used for definitive concrete mix designs.

7.4 **Summary**

In this chapter, the relationship between durability (carbonation resistance) and the concrete performance (strength & permeation properties) affecting the carbonation progress have been presented and discussed.

There is a strong positive relationship between concrete strength and carbonation resistance, showing an exponential correlation with a correlation coefficient of ~0.7 obtained. Further, it was shown that both strength and permeability were influenced by common variables: w/b ratio and slag replacement. Both these variables (w/b & slag incorporation) have a role to change the pore structure, where reduced w/b ratio led to increased strength because this w/b reduction reduced porosity, as observed on gas permeability and coarse porosity as found by SEM images analysis.

Meanwhile, there was a good exponential correlation between carbonation resistance and permeation properties (gas permeability & water sorptivity). Reducing carbon dioxide diffusion greatly limits carbonation, and this is strongly influenced by pore microstructure and connectivity. Again, this good correlation between the carbonation coefficient and permeation properties largely rely on the effect of common variables: w/b ratio and slag incorporation. In addition, the binder content had a significant role to change the carbonation depth, where the increasing the binder content led to increasing the carbonation resistance as a result of the quantity of carbonatable matter which is inversely proportional to carbonation. On the other hand, the relationship between the diffusion and the carbonation resistance is proportional. That means any increasing the permeability leads to increase the carbonation.

Chapter 8 Conclusion and further work

8.1 Conclusions

The aim of this research work was to develop durable, strong environmentally sustainable concretes. The new concretes would need to conform to the mechanical, durability and permeation properties of concretes which currently used and accepted by the construction industry.

In order to achieve the above aims a series of concrete samples were cast and assessed in terms of mechanical performance and durability. Equivalent paste samples were then investigated to relate their microstructures to performance.

A new approach is established using the Taguchi method for determination of the optimum compositions of materials proportions and the effect of mix design variables on the properties of low carbon concrete and its carbonation resistance. Mix designs consist of many components. This means it is critical to use a systematic approach for identifying the significance or insignificance for each factor. Due to this reason Taguchi method with L18 orthogonal array is used in this study to investigate levelling of the effective parameters and best possible mix proportions of low carbon concrete properties. This study has shown that it possible to design concrete that satisfies the criteria of strength and satisfy the durability properties (carbonation resistance). Eighteen different concrete mixes were chosen. The variables were selected in this programme according to the those theoretical influences that have the greatest effect on a concrete mix (Purnell and Black, 2012) such as cement content, different types of supplementary cementitious materials (Fly ash, GGBS and fine slag), maximum aggregate size and the workability by changing w/b ratio, also, using superplasticizer. These variables, with a full set of mixes encompassing all levels of each variable would give over 400 mixes. It is not feasible to test such a number of samples. Thus, it was reduced by using the Taguchi method to 18 mixes.

A comprehensive review of the fundamentals of the cement science and concrete technology was undertaken to have a clear understanding of the chemical and physical compositions, hydration mechanisms, hydration products and durability properties of Portland cements, GGBS, and fly ash. To understand the effect of the variables changing in the concrete mixture, for short, medium and long term

performance have been reviewed. These reviews were found to be extremely useful to relate the findings of concrete properties to microstructures which analytical techniques used namely STA, SEM and CCI to analyse the hydration products and microstructure of cement pastes.

In order to achieve the above aims as mentioned, the total works were divided into five phases or objectives as described in the Introduction chapter. In the following sections concluding remarks on these phases have been made as the work progressed to meet its final objectives:

1- Replacement of Portland cement with minerals such as fine slag provides suitable paste volume with low water content. It was shown that concrete with blended cement (clinker and slag) as low as between 15% to 30% were able to meet the requirements of concrete performance which included high strength, low embodied carbon dioxide and high resistance to carbonation. It has been seen that mix design variables such as slag incorporation, w/b, and binder content were the most significant contributors in terms of mechanical properties. In addition, using the SCMs, especially GGBS, is a common strategy to design concrete with appropriate durability and permeation properties such as low gas permeability and water absorption. In addition, use of finer particles, such as fine slag (in this case with a fineness of 7904 m^2/kg, also offers improved performance, especially if the compressive strength gain is affected due to lower content of Portland cement.

2- Compressive strengths at 28 days for concrete containing slag were slightly higher than CEM I and PFA blends, especially fine slag as the result of higher reactivity of slag and high fineness of slag particles. But the difference between the SCM types increased clearly at 90 days. This due to the pozzolanic reaction which characterized slowly and takes a long time to complete the hydration. Also, the role of high fineness which refined the pores which led to reducing the porosity, explaining that the compressive strength development relies on the hydration progress and the microstructure. On the other hand, low water/binder ratio concrete (0.35) showed higher strength than higher w/b ratio (0.55). This was attributed to increase dilution when increasing the water content which in turn increased the porosity. Meanwhile, the SP dosage increasing

contributed to increasing the strength value because of the positive effect basing on reducing the water content and in turn reduce the pore structure. PFA had a negative effect on compressive strength owing to its low reactivity and slow reaction kinetics, which in turn led to increase the porosity. Water sorption and gas permeability results showed slag concretes were impermeable compared with CEM I and PFA mixes, at both 28 and 90 days. This was due to the development of strong microstructure of paste due to the additional hydration products contributed by the pozzolanic reactions. Meanwhile, the w/b ratio contributed to reducing the permeability and sorptivity when decreasing the water content. This was due to reducing the bonding agent as the result of dispersion the hydration products and create more spaces inside the concrete. In addition, maximum aggregate size had a negative effect on permeation properties for concrete due to the increasing of ITZ which considers a weak point and easy to penetrate.

3- The carbonation resistance of fine slag mixes was greater than that of coarse slag and PFA blends. This was due to binding more CO_2 which means a low reaction to produce calcite as the results of the greater reactivity than coarse slag or PFA which have led to much dense microstructure. Also, Higher CaO content could lead to less CH consumption, and so a greater buffering capacity. As for coarse slag gave similar carbonation resistance as CEM I despite the low CaO content for coarse slag compared with CEM I, but the fineness of coarse slag gave the potential to refine the pores structure and led to reducing the carbon dioxide diffusion. As for w/b ratio, the increasing water content has a negative effect on carbonation resistance, whereas this increasing promote the porosity paste structure which eases the carbon dioxide diffusion. Increasing the binder content had a positive effect on carbonation resistance as the result of the high presence carbonateable matter amount which enhance the carbon dioxide binding capacity of cementitious materials and slowed the penetration of the carbonation front.

4- The microstructural investigation demonstrated the composition of blended cement and its relationship to performance. Two aspects were

considered to be important: (i) chemical kinetics and (ii the porosity of blended cement. Whereas twofold factors have relied on SCM type, SCM level, and w/b ratio. Pastes with high w/b ratio (0.55) showed high porosity, which has the potential to increase the carbon dioxide diffusion. However, the increasing water content had a different impact on hydration, where the hydration kinetics increased when w/b ratio increased and the CH consumption decrease. As for the blended system, slag especially (fine slag) offered the most carbonation resistance, despite reducing the CH content, but the high reactivity and refinement of porosity had the great potential to reduce the CO_2 diffusion.

5- Meanwhile, these durable low-carbon concretes were achieved with reduced Portland cement contents by incorporating fine or coarse slag at 15% and 30% replacement level, a reduced w/b ratio of 0.35 and reduced water content by using 1.0 wt% SP. Where the positive role of slag incorporation can be attributed to refining the microstructure and high reactivity compared with PFA or neat cement. Meanwhile, the SP improved concrete performance and reduced the carbon footprint as the result of deflocculation of the water which in turn allows more water to hydrate the cementitious materials. Also, reduced w/b ratio improved the concrete performance, behaviour attributed to significantly reduced porosity. As the result of permeation properties, the carbonation resistance controlled by the diffusion resistance of concrete.

8.2 **Further work**

This study has focused on the effect of mix design variables on carbonation resistance. A series of concrete samples were designed and tested their resistance to carbonation, then investigated their microstructures to relate concrete performance to paste composition. The results showed that w/b ratio and using SCM especially fine slag had a great impact on carbonation resistance as the large influence of these factors on pore structure refining. It was also found that carbonation resistance increase with incorporated fine slag with a blend, despite decreased the CH content. Therefore, it would be interesting to take this study further by investigating the C-S-H content and the decomposition which results in deep insight on the effect of chemical characteristics on carbonation.

Accelerated carbonation was adopted in this study for determining the carbonation depth for different ages 28, 56, 90 and a80 days. To relate the carbonation depth and composition, the chemical characteristics of the composition were investigated by using SEM-EDX and STA at ages 28 and 90 days, which represented the long term. Hence it may be necessary to reduce the age by considering the shorter drying samples from 1 to 3 days to check the effect of adding SCM on the microstructure of binder at the short and long term.

According to the large effect of pore structure on carbonation resistance, and the complicated role of using SCM on durability regarding pore structure. Based on that, SEM-BSE image analysis technique was used to investigate the pore structure for paste samples. Where the negative effect of preparing these samples was with the method of removing the pore water by drying method, which had a side effect on the microstructure. Therefore, using a less influence technique on the microstructure such as which considers a good way to complement this study.

References

ABU SALEH, M. 2014. *Development of Sustainable and Low Carbon Concretes for the Gulf Environment.* University of Bath.

AIMIN, X. 1997. Fly Ash in Concrete." dlm. Chandra, S."Waste Materials Used in Concrete Manufacturing." Westwood. NJ: Noyes Publications.

AKCAöZOĞLU, S. & ATIŞ, C. D. 2011. Effect of Granulated Blast Furnace Slag and fly ash addition on the strength properties of lightweight mortars containing waste PET aggregates. *Construction and Building Materials,* 25**,** 4052-4058.

AL-RAWI, K. 1987. Introduction to regression analysis. Mosul Univ. Press.

ALIGIZAKI, K. K. 2014. *Pore structure of cement-based materials: testing, interpretation and requirements*, CRC Press.

ALMUTAIRI, W. 2017. Optimization of Concrete Mixtures for Use in Structural Elements.

ALSADEY, S. Effects of super plasticizing and retarding admixtures on properties of concrete. International Conference on Innovations in Engineering and Technology, 2013. 25-26.

ALSADEY, S. 2015. Effect of superplasticizer on fresh and hardened properties of concrete. *Journal of Agricultural Science and Engineering,* 1**,** 70-74.

ANTONY, J., PERRY, D., WANG, C. & KUMAR, M. 2006. An application of Taguchi method of experimental design for new product design and development process. *Assembly Automation,* 26**,** 18-24.

AYUB, T., KHAN, S. U. & MEMON, F. A. 2014. Mechanical characteristics of hardened concrete with different mineral admixtures: a review. *The Scientific World Journal,* 2014.

BAERT, G., HOSTE, S., DE SCHUTTER, G. & DE BELIE, N. 2008. Reactivity of fly ash in cement paste studied by means of thermogravimetry and isothermal calorimetry. *Journal of Thermal Analysis and Calorimetry,* 94**,** 485-492.

BAI, J., SABIR, B., WILD, S. & KINUTHIA, J. 2000. Strength development in concrete incorporating PFA and metakaolin. *Magazine of concrete research,* 52**,** 153-162.

BAKHSHI, M., MAHOUTIAN, M. & SHEKARCHI, M. The gas permeability of concrete and its relationship with strength. Proceedings of the fib, 2nd international congress, 2006.

BARBHUIYA, S., GBAGBO, J., RUSSELL, M. & BASHEER, P. 2009. Properties of fly ash concrete modified with hydrated lime and silica fume. *Construction and Building Materials,* 23**,** 3233-3239.

BASHEER, L., BASHEER, P. & LONG, A. 2005. Influence of coarse aggregate on the permeation, durability and the microstructure characteristics of ordinary Portland cement concrete. *Construction and Building Materials,* 19**,** 682-690.

BASHEER, P., RUSSELL, D. & RANKIN, G. 1999. DESIGN OF CONCRETE TO RESIST CARBONATION.

BAYUAJI, R. & NURUDDIN, M. 2014. Influence of microwave incinerated rice husk ash on hydration of foamed concrete. *Advances in Civil Engineering,* 2014.

BCA 2009. Fact sheet 18 P2 - Embodied CO2 of UK cement, additions and cementitious materials.

BENTZ, D. P., FERRARIS, C. F. & SNYDER, K. A. 2013. Best practices guide for high-volume fly ash concretes: Assuring properties and performance.

BENTZ, D. P., GARBOCZI, E. J. & SNYDER, K. A. 1999. A Hard Core/Soft Shell Microstructural Model for Studying Percolation and Transport in Three-Dimensional Composite Media| NIST.

BENTZ, D. P. & STUTZMAN, P. E. 2006. Curing, hydration, and microstructure of cement paste. *ACI materials journal,* 103**,** 348.

BERNDT, M. 2015. Influence of concrete mix design on CO2 emissions for large wind turbine foundations. *Renewable Energy,* 83**,** 608-614.

BERODIER, E. & SCRIVENER, K. 2014. Understanding the Filler Effect on the Nucleation and Growth of C-S-H. *Journal of the American Ceramic Society,* 97**,** 3764-3773.

BERODIER, E. M. J. 2015. Impact of the supplementary cementitious materials on the kinetics and microstructural development of cement hydration. EPFL.

BIJEN, J. 1996. Benefits of slag and fly ash. *Construction and building materials,* 10**,** 309-314.

BIS October 2011. Estimating the Amount of CO2 Emissions that the Construction Industry can

Influence *Supporting material for the Low Carbon Construction IGT Report*.

BISAILLON, A., RIVEST, M. & MALHOTRA, V. 1994. Performance of high-volume fly ash concrete in large experimental monoliths. *Materials Journal,* 91**,** 178-187.

BOUGARA, A., LYNSDALE, C. & MILESTONE, N. 2010. Reactivity and performance of blastfurnace slags of differing origin. *Cement and Concrete Composites,* 32**,** 319-324.

BOUIKNI, A., SWAMY, R. & BALI, A. 2009. Durability properties of concrete containing 50% and 65% slag. *Construction and Building Materials,* 23**,** 2836-2845.

BRAND, R., PULLES, T., VAN GIJLSWIJK, R., FRIBOURG-BLANC, B. & COURBET, C. 2004. European pollutant emission register. Final report 2004.

BS EN 196-6:2010. BS EN 196-6:2010. British Standards Institute.

BS 882 1992 Specification for aggregates from natural sources for concrete. *British Standard*.

BS 1881-210 2013. Testing hardened concrete. Determination of the potential carbonation resistance of concrete. Accelerated carbonation method. *British Standards Institute*

BS EN 197-1 2011 Cement, Composition, Specifications and Conformity Criteria for Common Cements. London, England: British Standard Institution (BSI)

British European Standard.

BS EN 934-1 2008. BS EN 934-1:2008. British Standards Institute.

BS EN 1097-6 2013. Tests for mechanical and physical properties of aggregates. Determination of particle density and water absorption. *British European Standard*.

BS EN 12390-2 2009. Testing hardened concrete. Making and curing specimens for strength tests. *British European Standard*.

BS EN 12390-3 2002. BS EN 12390-3:2002. British Standards Institute.

BS ISO 1920-8 2009 Testing of concrete. Determination of the shrinkage of concrete for samples prepared in the field or in the laboratory. *British European Standard*.

BUENFELD, N. & OKUNDI, E. 1998. Effect of cement content on transport in concrete. *Magazine of Concrete Research,* 50.

CABRERA, J. G. & LYNSDALE, C. J. 1988. New gas permeameter for measuring the permeability of mortar and concrete. *Magazine of Concrete Research,* 40**,** 177-182.

CAVAZZUTI, M. 2012. *Optimization methods: from theory to design scientific and technological aspects in mechanics*, Springer Science & Business Media.

CHEN, B., LIU, J. & LI, P. Experimental Study on Pervious Concrete. 9th International Conference on Concrete PavementsInternational Society for Concrete PavementsFederal Highway AdministrationAmerican Concrete Pavement Association, 2008.

CONCRETE SOCIETY WORKING, P. 1988. *Permeability testing of site concrete : a review of methods and experience : report of a Concrete Society Working Party,* London, Concrete Society.

COOK, R. A. & HOVER, K. C. 1999. Mercury porosimetry of hardened cement pastes. *Cement and Concrete research,* 29**,** 933-943.

CORDON, W. A. & GILLESPIE, H. A. Variables in concrete aggregates and Portland cement paste which influence the strength of concrete. Journal Proceedings, 1963. 1029-1052.

DAMTOFT, J., LUKASIK, J., HERFORT, D., SORRENTINO, D. & GARTNER, E. 2008. Sustainable development and climate change initiatives. *Cement and concrete research,* 38**,** 115-127.

DARWIN, D., DOLAN, C. W. & NILSON, A. H. 2016. *Design of concrete structures*, McGraw-Hill Education.

DE LA RILEM, R. 1988. CPC-18 Measurement of hardened concrete carbonation depth. *Mater Struct,* 21**,** 453-455.

DE WEERDT, K., HAHA, M. B., LE SAOUT, G., KJELLSEN, K. O., JUSTNES, H. & LOTHENBACH, B. 2011. Hydration mechanisms of ternary Portland

cements containing limestone powder and fly ash. *Cement and Concrete Research,* 41**,** 279-291.

DE WOLF, C., YANG, F., COX, D., CHARLSON, A., HATTAN, A. S. & OCHSENDORF, J. Material quantities and embodied carbon dioxide in structures. Proceedings of the Institution of Civil Engineers-Engineering Sustainability, 2016. Thomas Telford Ltd, 150-161.

DEBOUCHA, W., LEKLOU, N. & KHELIDJ, A. Hydration degree development of blast furnace slag blended cement pastes using thermogravimetric Analysis (TGA). MATEC Web of Conferences, 2018. EDP Sciences, 04001.

DESCHNER, F., WINNEFELD, F., LOTHENBACH, B., SEUFERT, S., SCHWESIG, P., DITTRICH, S., GOETZ-NEUNHOEFFER, F. & NEUBAUER, J. 2012. Hydration of Portland cement with high replacement by siliceous fly ash. *Cement and Concrete Research,* 42**,** 1389-1400.

DHIR, R., LIMBACHIYA, M., MCCARTHY, M. & CHAIPANICH, A. 2007. Evaluation of Portland limestone cements for use in concrete construction. *Materials and Structures,* 40**,** 459.

DHIR, R. K., MCCARTHY, M. J., TITTLE, P. A. & ZHOU, S. 2006. Role of cement content in specifications for concrete durability: aggregate type influences. *Proceedings of the Institution of Civil Engineers-Structures and Buildings,* 159**,** 229-242.

DINKU, A. & REINHARDT, H. 1997. Gas permeability coefficient of cover concrete as a performance control. *Materials and Structures,* 30**,** 387.

DIVSHOLI, B. S., LIM, T. Y. D. & TENG, S. 2014. Durability properties and microstructure of ground granulated blast furnace slag cement concrete. *International Journal of Concrete Structures and Materials,* 8**,** 157-164.

DIXIT, M. K., FERNáNDEZ-SOLíS, J. L., LAVY, S. & CULP, C. H. 2012. Need for an embodied energy measurement protocol for buildings: A review paper. *Renewable and Sustainable Energy Reviews,* 16**,** 3730-3743.

DRAPER, N. R. & SMITH, H. 1998. *Applied regression analysis,* New York;Chichester;, Wiley.

DYER, T. 2014. *Concrete durability,* Boca Raton, Taylor & Francis.

ELAHI, A., BASHEER, P., NANUKUTTAN, S. & KHAN, Q. 2010. Mechanical and durability properties of high performance concretes containing supplementary cementitious materials. *Construction and Building Materials,* 24**,** 292-299.

ELCHALAKANI, M., ALY, T. & ABU-AISHEH, E. 2014. Sustainable concrete with high volume GGBFS to build Masdar City in the UAE. *Case Studies in Construction Materials,* 1**,** 10-24.

ESCALANTE-GARCIA, J. & SHARP, J. 1998. Effect of temperature on the hydration of the main clinker phases in Portland cements: Part I, neat cements. *Cement and concrete research,* 28**,** 1245-1257.

ESCALANTE, J., GOMEZ, L., JOHAL, K., MENDOZA, G., MANCHA, H. & MENDEZ, J. 2001. Reactivity of blast-furnace slag in Portland cement

blends hydrated under different conditions. *Cement and Concrete Research,* 31**,** 1403-1409.

FELDMAN, R. 1984. Pore structure damage in blended cements caused by mercury intrusion. *Journal of the American Ceramic Society,* 67**,** 30-33.

FLOWER, D. J. & SANJAYAN, J. G. 2007a. Green house gas emissions due to concrete manufacture. *The international Journal of life cycle assessment,* 12**,** 282.

FLOWER, D. J. M. & SANJAYAN, J. G. 2007b. Green house gas emissions due to concrete manufacture. *The International Journal of Life Cycle Assessment,* 12**,** 282.

FRAAY, A., BIJEN, J. & DE HAAN, Y. 1989. The reaction of fly ash in concrete a critical examination. *Cement and concrete research,* 19**,** 235-246.

GAMBHIR, M. L. & JAMWAL, N. 2014. *Building and Construction Materials: Testing and Quality Control, 1e (Lab Manual)*, Tata McGraw-Hill Education.

GAO, J., QIAN, C., LIU, H., WANG, B. & LI, L. 2005. ITZ microstructure of concrete containing GGBS. *Cement and concrete research,* 35**,** 1299-1304.

GAO, J., YU, Z., SONG, L., WANG, T. & WEI, S. 2013. Durability of concrete exposed to sulfate attack under flexural loading and drying–wetting cycles. *Construction and Building Materials,* 39**,** 33-38.

GARCíA-TAENGUA, E., SONEBI, M., HOSSAIN, K., LACHEMI, M. & KHATIB, J. 2015. Effects of the addition of nanosilica on the rheology, hydration and development of the compressive strength of cement mortars. *Composites Part B: Engineering,* 81**,** 120-129.

GARTNER, E. 2004. Industrially interesting approaches to “low-CO 2” cements. *Cement and Concrete research,* 34**,** 1489-1498.

GESOĞLU, M., GUNEYISI, E. & ÖZBAY, E. 2009. Properties of self-compacting concretes made with binary, ternary, and quaternary cementitious blends of fly ash, blast furnace slag, and silica fume. *Construction and Building Materials,* 23**,** 1847-1854.

GLINICKI, M., JóŹWIAK-NIEDŹWIEDZKA, D., GIBAS, K. & DĄBROWSKI, M. 2016. Influence of blended cements with calcareous fly ash on chloride ion migration and carbonation resistance of concrete for durable structures. *Materials,* 9**,** 18.

GRUYAERT, E., ROBEYST, N. & DE BELIE, N. 2010. Study of the hydration of Portland cement blended with blast-furnace slag by calorimetry and thermogravimetry. *Journal of thermal analysis and calorimetry,* 102**,** 941-951.

GUNEYISI, E., GESOĞLU, M. & ÖZBAY, E. 2010. Strength and shrinkage properties of self-compacting concretes incorporating multi-system blended mineral admixtures. *Construction and Building Materials,* 24**,** 1878-1887.

GUTTERIDGE, W. A. & DALZIEL, J. A. 1990. Filler cement: the effect of the secondary component on the hydration of Portland cement: part I. A fine non-hydraulic filler. *Cement and Concrete Research,* 20**,** 778-782.

HABERT, G. & ROUSSEL, N. 2009. Study of two concrete mix-design strategies to reach carbon mitigation objectives. *Cement and Concrete Composites,* 31**,** 397-402.

HACKER, J. N., DE SAULLES, T. P., MINSON, A. J. & HOLMES, M. J. 2008. Embodied and operational carbon dioxide emissions from housing: a case study on the effects of thermal mass and climate change. *Energy and Buildings,* 40**,** 375-384.

HADJSADOK, A., KENAI, S., COURARD, L., MICHEL, F. & KHATIB, J. 2012. Durability of mortar and concretes containing slag with low hydraulic activity. *Cement and Concrete Composites,* 34**,** 671-677.

HAMMOND, G. P. & JONES, C. I. 2008. Embodied energy and carbon in construction materials. *Proceedings of the Institution of Civil Engineers-Energy,* 161**,** 87-98.

HANSEN, T. C. 1986. Physical structure of hardened cement paste. A classical approach. *Materials and Structures,* 19**,** 423-436.

HARRISON, G. P., KARAMANLIS, S. & OCHOA, L. F. 2010. Life cycle assessment of the transmission network in Great Britain. *Energy policy,* 38**,** 3622-3631.

HELENE, P. R. D. L. & CASTRO-BORGES, P. 2009. A novel method to predict concrete carbonation. *Concreto y cemento. Investigación y desarrollo,* 1**,** 25-35.

HENDRIKS, C. A., WORRELL, E., DE JAGER, D., BLOK, K. & RIEMER, P. Emission reduction of greenhouse gases from the cement industry. Proceedings of the fourth international conference on greenhouse gas control technologies, 1998. 939-944.

HERTERICH, J. 2017. *Microstructure and phase assemblage of low-clinker cements during early stages of carbonation.* University of Leeds.

HEWLETT, P. 2003. *Lea's chemistry of cement and concrete*, Elsevier.

HILL, J. & SHARP, J. 2002. The mineralogy and microstructure of three composite cements with high replacement levels. *Cement and Concrete Composites,* 24**,** 191-199.

HıNıSLıOĞLU, S. & BAYRAK, O. Ü. 2004. Optimization of early flexural strength of pavement concrete with silica fume and fly ash by the Taguchi method. *Civil Engineering and Environmental Systems,* 21**,** 79-90.

HINISLIOGLU, S., BAYRAK, O. Ü., YILDIRIM, Y. & TAN, Ö. USE OF TAGUCHI OPTIMIZATION TECHNIQUE IN PAVEMENT CONCRETE MIX DESIGN. 9th International Symposium on Concrete Roads, 2003.

HO, D. & LEWIS, R. 1987. Carbonation of concrete and its prediction. *Cement and Concrete Research,* 17**,** 489-504.

HOENIG, V. & SCHNEIDER, M. CO2 reduction in the cement industry. VDZ Congress, 2002.

HONG, T., JI, C. & PARK, H. 2012. Integrated model for assessing the cost and CO2 emission (IMACC) for sustainable structural design in ready-mix concrete. *Journal of environmental management,* 103**,** 1-8.

HOOTON, R. D. 1986. Permeability and pore structure of cement pastes containing fly ash, slag, and silica fume. *Blended cements.* ASTM International.

HOUST, Y. F. & WITTMANN, F. H. 1994. Influence of porosity and water content on the diffusivity of CO2 and O2 through hydrated cement paste. *Cement and Concrete Research,* 24**,** 1165-1176.

I.-C. Yeh, “Computer-aided design for optimum concrete mixtures,” Cement and Concrete Composites, vol. 29, no. 3, pp. 193–202, 2007.

IDOWU, O. I. 2017. *Effect of improper curing on concrete properties that may affect concrete durability.* University of Leeds.

IGARASHI, S.-I., KAWAMURA, M. & WATANABE, A. 2004. Analysis of cement pastes and mortars by a combination of backscatter-based SEM image analysis and calculations based on the Powers model. *Cement and Concrete Composites,* 26**,** 977-985.

JAYA, R., BAKAR, B., JOHARI, M. & IBRAHIM, M. 2011. Strength and permeability properties of concrete containing rice husk ash with different grinding time. *Open Engineering,* 1**,** 103-112.

K. H. Yang, S. H. Tae, and D. U. Choi, “Mixture proportioning approach for low-CO_2 concrete using supplementary cementitious materials,” ACI Materials Journal, vol. 113, no. 4, pp. 533–542, 2016.

A. Khan, J. Do, and D. Kim, “Cost effective optimal mix proportioning of high strength self compacting concrete using response surface methodology,” Computers and Concrete, vol. 17, no. 5, pp. 629–638, 2016.

KANG, Y. 2010. Surface Scaling Mechanism and Prediction for Concrete.

KATZ, A., BENTUR, A. & WASSERMAN, R. 2015. EFFECT OF CEMENT CONTENT ON CONCRETE DURABILITY.

KHALE, D. & CHAUDHARY, R. 2007. Mechanism of geopolymerization and factors influencing its development: a review. *Journal of materials science,* 42**,** 729-746.

KHATIB, J. 2008. Performance of self-compacting concrete containing fly ash. *Construction and Building Materials,* 22**,** 1963-1971.

KHUNTHONGKEAW, J., TANGTERMSIRIKUL, S. & LEELAWAT, T. 2006. A study on carbonation depth prediction for fly ash concrete. *Construction and Building Materials,* 20**,** 744-753.

KIM, T., TAE, S. & ROH, S. 2013. Assessment of the CO2 emission and cost reduction performance of a low-carbon-emission concrete mix design using an optimal mix design system. *Renewable and Sustainable Energy Reviews,* 25**,** 729-741.

Kim, T. H., Lee, S. H., Chae, C. U., Jang, H. J., & Lee, K. H. (2017). Development of the CO2 emission evaluation tool for the life cycle assessment of concrete. Sustainability, 9, 2116–2130

Kim, T. H., Tae, S. H., Suk, S. J., Ford, G., & Yang, K. H. (2016). An optimization system for concrete life cycle cost and related CO2 emissions. Sustainability, 8, 361–380.

KLEMCZAK, B. & BATOG, M. 2016. Heat of hydration of low-clinker cements. *Journal of Thermal Analysis and Calorimetry,* 123**,** 1351-1360.

KOCABA, V., GALLUCCI, E. & SCRIVENER, K. L. 2012. Methods for determination of degree of reaction of slag in blended cement pastes. *Cement and Concrete Research,* 42**,** 511-525.

KOLANI, B., BUFFO-LACARRIERE, L., SELLIER, A., ESCADEILLAS, G., BOUTILLON, L. & LINGER, L. 2012. Hydration of slag-blended cements. *Cement and concrete composites,* 34**,** 1009-1018.

KONG, F. K. & EVANS, R. H. 1987. *Reinforced and prestressed concrete,* London, Chapman & Hall.

KOSIOR-KAZBERUK, M. & LELUSZ, M. 2007. Strength development of concrete with fly ash addition. *Journal of Civil Engineering and Management,* 13**,** 115-122.

KOSMATKA, S. H., KERKHOFF, B. & PANARESE, W. C. 2011. *Design and control of concrete mixtures*, Portland Cement Assoc.

KRAUSMANN, F., GINGRICH, S., EISENMENGER, N., ERB, K.-H., HABERL, H. & FISCHER-KOWALSKI, M. 2009. Growth in global materials use, GDP and population during the 20th century. *Ecological Economics,* 68**,** 2696-2705.

KROPP, J., HILSDORF, H. K. & RILEM. TECHNICAL COMMITTEE TC 116-PCD, P. O. C. A. A. C. O. I. D. 1995. *Performance criteria for concrete durability: state of the art report prepared by RILEM Technical Committee TC 116-PCD, Performance of concrete as a criterion of its durability,* London, E & FN Spon.

LAGERBLAD, B. 2005a. Carbon dioxide uptake during concrete life cycle–state of the art. *Swedish Cement and Concrete Research Institute CBI, Stockholm*.

LAGERBLAD, B. 2005b. *Carbon dioxide uptake during concrete life cycle: State of the art*, Swedish Cement and Concrete Research Institute Stockholm.

LAM, L., WONG, Y. & POON, C. 2000. Degree of hydration and gel/space ratio of high-volume fly ash/cement systems. *Cement and Concrete Research,* 30**,** 747-756.

LEE, S. H., KIM, H. J., SAKAI, E. & DAIMON, M. 2003. Effect of particle size distribution of fly ash–cement system on the fluidity of cement pastes. *Cement and Concrete Research,* 33**,** 763-768.

LEEMANN, A., NYGAARD, P., KAUFMANN, J. & LOSER, R. 2015. Relation between carbonation resistance, mix design and exposure of mortar and concrete. *Cement and Concrete Composites,* 62**,** 33-43.

LEVY, S. M. 2011. *Construction calculations manual*, Elsevier.

LI, C., SUN, H. & LI, L. 2010. A review: The comparison between alkali-activated slag (Si+ Ca) and metakaolin (Si+ Al) cements. *Cement and Concrete Research,* 40**,** 1341-1349.

LI, J. & YAO, Y. 2001. A study on creep and shrinkage of high performance concrete. *Cement and Concrete Research,* 31**,** 1203-1206.

LIM, S. & WEE, T. 2000. Autogenous shrinkage of ground-granulated blast-furnace slag concrete. *Materials Journal,* 97**,** 587-593.

LIMBACHIYA, M., BOSTANCI, S. C. & KEW, H. 2014. Suitability of BS EN 197-1 CEM II and CEM V cement for production of low carbon concrete. *Construction and Building Materials,* 71**,** 397-405.

LIU, Z., DE SCHUTTER, G., DENG, D. & YU, Z. 2010. Micro-analysis of the role of interfacial transition zone in “salt weathering” on concrete. *Construction and Building Materials,* 24**,** 2052-2059.

LIU, Z. W., ZHAO, K., HU, C. & TANG, Y. F. 2016. Effect of Water-Cement Ratio on Pore Structure and Strength of Foam Concrete. *ADVANCES IN MATERIALS SCIENCE AND ENGINEERING,* 2016**,** 1-9.

LONG, G., GAO, Y. & XIE, Y. 2015. Designing more sustainable and greener self-compacting concrete. *Construction and Building Materials,* 84**,** 301-306.

LOTHENBACH, B., SCRIVENER, K. & HOOTON, R. 2011. Supplementary cementitious materials. *Cement and concrete research,* 41**,** 1244-1256.

LUKE, K. 2002. Pulverized fuel ash as a cement extender. *Structure and performance of cements***,** 353.

MA, B., WANG, X. G., LI, X. & YANG, L. 2007. Influence of superplasticizers on strength and shrinkage cracking of cement mortar under drying conditions. *Journal of Wuhan University of Technology-Mater. Sci. Ed.,* 22**,** 358-361.

MAILVAGANAM, N. P. & RIXOM, M. 2002. *Chemical admixtures for concrete*, CRC Press.

MARCEAU, M., NISBET, M. A. & VAN GEEM, M. G. 2007. *Life cycle inventory of portland cement concrete*, Portland Cement Association.

MBADIKE, E. 2011. Effect of superplasticizer on the Compressive strength of concrete. *International Journal of Natural and Applied Sciences,* 7.

MEHTA, P. K. 1989. Pozzolanic and cementitious by-products in concrete--another look. *Special Publication,* 114**,** 1-44.

MEHTA, P. K. 2001. Reducing the environmental impact of concrete. *Concrete international,* 23**,** 61-66.

MEHTA, P. K. & MONTEIRO, P. 1993. *Concrete: structure, properties and materials,* Englewood Cliffs;London;, Prentice-Hall.

MINDESS, S., Y., J. F. & AND DARWIN, D. 2003. Concrete. 2nd Ed. *Prentice-Hall Inc., Englewood Cliffs, New Jersey.*

MISRA, A., RAMTEKE, R. & BAIRWA, M. L. 2007. Study on strength and sorptivity characteristics of fly ash concrete. *ARPN Journal of Engineering and Applied Sciences,* 2**,** 54-59.

MONTEIRO, P. & HELENE, P. 1994. Designing concrete mixtures for desired mechanical properties and durability. *Special Publication,* 144**,** 519-544.

MONTGOMERY, D. C. 2013. *Design and analysis of experiments,* Chichester;Hoboken, N.J;, John Wiley & Sons.

MORANDEAU, A., THIERY, M. & DANGLA, P. 2014. Investigation of the carbonation mechanism of CH and C-S-H in terms of kinetics, microstructure changes and moisture properties. *Cement and Concrete Research,* 56**,** 153-170.

MORANVILLE-REGOURD, M. 2003. 11 - Cements Made From Blastfurnace Slag A2 - Hewlett, Peter C. *Lea's Chemistry of Cement and Concrete (Fourth Edition).* Oxford: Butterworth-Heinemann.

M. A. Mosaberpanah and O. Eren, "CO_2-full factorial optimization of an ultra-high performance concrete mix design," European Journal of Environmental and Civil Engineering, vol. 22, no. 4, pp. 450–463, 2018.

NEUBAUER, C. M., BERGSTROM, T. B., SUJATA, K., XI, Y., GARBOCZI, E. J. & JENNINGS, H. M. 1997. Drying shrinkage of cement paste as measured in an environmental scanning electron microscope and comparison with microstructural models. *Journal of Materials Science,* 32**,** 6415-6427.

NEVILLE, A. M. 2011. *Properties of concrete,* Harlow, Longman Scientific & Technical.

NGALA, V. T. & PAGE, C. L. 1997. EFFECTS OF CARBONATION ON PORE STRUCTURE AND DIFFUSIONAL PROPERTIES OF HYDRATED CEMENT PASTES. *Cement and Concrete Research,* 27**,** 995-1007.

NIAN, C., YANG, W. & TARNG, Y. 1999. Optimization of turning operations with multiple performance characteristics. *Journal of Materials Processing Technology,* 95**,** 90-96.

OBLA, K. H., HILL, R. L., THOMAS, M. D., SHASHIPRAKASH, S. G. & PEREBATOVA, O. 2003. Properties of concrete containing ultra-fine fly ash. *ACI materials journal,* 100**,** 426-433.

OGIRIGBO, O. R. & BLACK, L. 2016. Influence of slag composition and temperature on the hydration and microstructure of slag blended cements. *Construction and Building Materials,* 126**,** 496-507.

OHGA, H. & NAGATAKII, S. 1989. Prediction of carbonation depth of concrete with fly ash. *Special Publication,* 114**,** 275-294.

Oliveira, L. S., Pacca, S. A., & John, V. M. (2016). Variability in the life cycle of concrete block CO2 emissions and cumulative energy demand in the Brazilian Market. Construction and Building Materials, 114, 588–594.

ONER, A. & AKYUZ, S. 2007. An experimental study on optimum usage of GGBS for the compressive strength of concrete. *Cement and Concrete Composites,* 29**,** 505-514.

ORTEGA, J., ESTEBAN, M., SáNCHEZ, I. & CLIMENT, M. 2017. Performance of sustainable fly ash and slag cement mortars exposed to simulated and real in situ Mediterranean conditions along 90 warm season days. *Materials,* 10**,** 1254.

OZBAY, E., OZTAS, A., BAYKASOGLU, A. & OZBEBEK, H. 2009. Investigating mix proportions of high strength self compacting concrete by using Taguchi method. *Construction and building materials,* 23**,** 694-702.

PACHECO-TORGAL, F., JALALI, S., LABRINCHA, J. & JOHN, V. 2013a. *Eco-efficient concrete*, Elsevier.

PACHECO-TORGAL, F., JALALI, S., LABRINCHA, J. & JOHN, V. M. 2013b. *Eco-efficient concrete*, Elsevier.

PAL, S., MUKHERJEE, A. & PATHAK, S. 2003. Investigation of hydraulic activity of ground granulated blast furnace slag in concrete. *Cement and Concrete Research,* 33**,** 1481-1486.

PAPADAKIS, V. & TSIMAS, S. 2002. Supplementary cementing materials in concrete: Part I: efficiency and design. *Cement and Concrete Research,* 32**,** 1525-1532.

Park, W. J., Noguchi, T., & Lee, H. S. (2013). Genetic algorithm in mix proportion design of recycled aggregate concrete. Computers and Concrete, 11, 183–199.

Passuello, A., Rodríguez, E. D., Hirt, E., Longhi, M., Bernal, S. A., Provis, J. L., et al. (2017). Evaluation of the potential improvement in the environmental footprint of geopolymers using waste-derived activators. Journal of Cleaner Production, 166, 680–689.

PAYA-ZAFORTEZA, I., YEPES, V., HOSPITALER, A. & GONZALEZ-VIDOSA, F. 2009. CO2-optimization of reinforced concrete frames by simulated annealing. *Engineering Structures,* 31**,** 1501-1508.

PETTY, M. D. Calculating and using confidence intervals for model validation. Proceedings of the Fall 2012 Simulation Interoperability Workshop, 2012. 10-14.

PHADKE, M. S. 1995. *Quality engineering using robust design*, Prentice Hall PTR.

PROCHON, P. & PIOTROWSKI, T. 2016. Bound water content measurement in cement pastes by stoichiometric and gravimetric analyses. *Journal of Building Chemistry,* 1**,** 18-25.

PRUSINSKI, J. R., MARCEAU, M. L. & VANGEEM, M. G. Life cycle inventory of slag cement concrete. Eighth CANMET/ACI International Conference on Fly Ash, Silica Fume, Slag and Natural Pozzolans in Concrete, 2004. American Concrete Institute Farmington Hills, 1-26.

PUNDIR, R., CHARY, G. & DASTIDAR, M. 2018. Application of Taguchi method for optimizing the process parameters for the removal of copper and nickel by growing Aspergillus sp. *Water resources and industry,* 20**,** 83-92.

PURNELL, P. 2013. The carbon footprint of reinforced concrete. *Advances in cement research,* 25**,** 362-368.

PURNELL, P. & BLACK, L. 2012. Embodied carbon dioxide in concrete: Variation with common mix design parameters. *Cement and Concrete Research,* 42**,** 874-877.

RIBEIRO, M. C. S., TAVARES, C. M. L., FIGUEIREDO, M., FERREIRA, A. J. M. & FERNANDES, A. A. 2003. Bending characteristics of resin concretes. *Materials Research,* 6**,** 247-254.

RICHARDSON, I. G., BROUGH, A. R., GROVES, G. W. & DOBSON, C. M. 1994. The characterization of hardened alkali-activated blast-furnace slag pastes and the nature of the calcium silicate hydrate (C-S-H) phase. *Cement and Concrete Research,* 24**,** 813-829.

RICHARDSON, M. G. 2014. *Fundamentals of durable reinforced concrete*, CRC Press.

Robati, M., Carthy, T. J. M., & Kokogiannakis, G. (2016). Incorporating environmental evaluation and thermal properties of concrete mix designs. Construction and Building Materials, 128, 422–435.

ROSS, P. J. & ROSS, P. J. 1988. *Taguchi techniques for quality engineering: loss function, orthogonal experiments, parameter and tolerance design*, McGraw-Hill New York.

SABIR, B. B., WILD, S. & O'FARRELL, M. 1998. A water sorptivity test for martar and concrete. *Materials and Structures,* 31**,** 568.

SALIHU, A. Y. 2011. Importance of concrete mix design quality control measure. *Journal of Engineering and Applied Sciences, Cenresin Publications*.

SALVOLDI, B., BEUSHAUSEN, H. & ALEXANDER, M. 2015. Oxygen permeability of concrete and its relation to carbonation. *Construction and Building Materials,* 85**,** 30-37.

SARI, M., PRAT, E. & LABASTIRE, J.-F. 1999. High strength self-compacting concrete original solutions associating organic and inorganic admixtures. *Cement and Concrete Research,* 29**,** 813-818.

ŠAVIJA, B. & LUKOVIĆ, M. 2016. Carbonation of cement paste: understanding, challenges, and opportunities. *Construction and Building Materials,* 117**,** 285-301.

SCHMITT, T. R. & DARWIN, D. 1999. Effect of material properties on cracking in bridge decks. *Journal of Bridge Engineering,* 4**,** 8-13.

SCHUBERT, P. 1987. CARBONATION BEHAVIOR OF MORTARS AND CONCRETES MADE WITH FLY ASH. CONCRETE DURABILITY. KATHERINE AND BRYANT MATHER INTERNATIONAL CONFERENCE, HELD AT ATLANTA, GEORGIA, USA, 27 APRIL-MAY 1987. *Publication of: American Concrete Institute*.

SCHULZE, J. 1999. Influence of water-cement ratio and cement content on the properties of polymer-modified mortars. *Cement and concrete research,* 29**,** 909-915.

SCRIVENER, K., SNELLINGS, R. & LOTHENBACH, B. 2018. *A practical guide to microstructural analysis of cementitious materials*, Crc Press.

SHARIQ, M., PRASAD, J. & MASOOD, A. 2010. Effect of GGBFS on time dependent compressive strength of concrete. *Construction and Building Materials,* 24**,** 1469-1478.

SHARMA, R. & KHAN, R. A. 2016. Effect of different supplementary cementitious materials on mechanical and durability properties of concrete. *Journal of Materials and Engineering Structures «JMES»,* 3**,** 129-147.

SHETTY, M. 2005. Concrete technology. *S. chand & company LTD***,** 420-453.

SHI, H.-S., XU, B.-W. & ZHOU, X.-C. 2009. Influence of mineral admixtures on compressive strength, gas permeability and carbonation of high performance concrete. *Construction and Building Materials,* 23**,** 1980-1985.

SHI, Z., LOTHENBACH, B., GEIKER, M. R., KAUFMANN, J., LEEMANN, A., FERREIRO, S. & SKIBSTED, J. 2016. Experimental studies and thermodynamic modeling of the carbonation of Portland cement, metakaolin and limestone mortars. *Cement and Concrete Research,* 88**,** 60-72.

SIDDIQUE, R. 2011. Properties of self-compacting concrete containing class F fly ash. *Materials & Design,* 32**,** 1501-1507.

SIDDIQUE, R. & BENNACER, R. 2012. Use of iron and steel industry by-product (GGBS) in cement paste and mortar. *Resources, Conservation and recycling,* 69**,** 29-34.

SIVAKUMAR, G. & RAVIBASKAR, R. 2009. Investigation on the hydration properties of the rice husk ash cement using FTIR and SEM. *Applied Physics Research,* 1**,** 71.

STARK, J., MöSER, B. & BELLMANN, F. 2007. Nucleation and growth of CSH phases on mineral admixtures. *Advances in Construction Materials 2007.* Springer.

SULAPHA, P., WONG, S., WEE, T. & SWADDIWUDHIPONG, S. 2003. Carbonation of concrete containing mineral admixtures. *Journal of materials in civil engineering,* 15**,** 134-143.

J. G. Tapali, S. Demis, and V. G. Papadakis, “Sustainable concrete mix design for a target strength and service life,” Computers and Concrete, vol. 12, no. 6, pp. 755–774, 2013.

TASDEMIR, C. 2003. Combined effects of mineral admixtures and curing conditions on the sorptivity coefficient of concrete. *Cement and Concrete Research,* 33**,** 1637-1642.

TAYLOR, H. F. 1997. *Cement chemistry*, Thomas Telford.

TAYLOR, P. C., KOSMATKA, S. H. & VOIGT, G. F. 2006. Integrated materials and construction practices for concrete pavement: A state-of-the-practice manual.

TAYLOR, R., RICHARDSON, I. & BRYDSON, R. 2007. Nature of C–S–H in 20 year old neat ordinary Portland cement and 10% Portland cement–90% ground granulated blast furnace slag pastes. *Advances in Applied Ceramics,* 106**,** 294-301.

TAYLOR, R., RICHARDSON, I. & BRYDSON, R. 2010. Composition and microstructure of 20-year-old ordinary Portland cement–ground granulated blast-furnace slag blends containing 0 to 100% slag. *Cement and Concrete Research,* 40**,** 971-983.

Teh, S. H., Wiedmann, T., Castel, A., & de Burgh, J. (2017). Hybrid life cycle assessment of greenhouse gas emissions from cement, concrete and geopolymer concrete in Australia. Journal of Cleaner Production, 152, 312–320.

TEYCHENNE, D. C., FRANKLIN, R. E., ERNTROY, H. C. & MARSH, B. 1975. *Design of normal concrete mixes*, HM Stationery Office.

THOMAS, M. 2013. *Supplementary cementing materials in concrete*, CRC press.

THOMAS, M. & MATTHEWS, J. 2004. Performance of pfa concrete in a marine environment—10-year results. *Cement and Concrete Composites,* 26**,** 5-20.

TRILL, K. & KAWAMURA, M. 1992. Pore structure and chloride permeability of concretes containing fly ash, blast furnace slag and silica fume. *Special Publication,* 132**,** 135-150.

TURKMEN, İ. M., GUL, R., ÇEL K, C. & DEM RBOĞA, R. 2003. Determination by the Taguchi method of optimum conditions for mechanical properties of high strength concrete with admixtures of silica fume and blast furnace slag. *Civil Engineering and Environmental Systems,* 20**,** 105-118.

TURNER, L. K. & COLLINS, F. G. 2013. Carbon dioxide equivalent (CO2-e) emissions: A comparison between geopolymer and OPC cement concrete. *Construction and Building Materials,* 43**,** 125-130.

UNAL, R. & DEAN, E. B. 1990. Taguchi approach to design optimization for quality and cost: an overview.

UYSAL, M. & SUMER, M. 2011. Performance of self-compacting concrete containing different mineral admixtures. *Construction and Building materials,* 25**,** 4112-4120.

VALCUENDE, M. & PARRA, C. 2010. Natural carbonation of self-compacting concretes. *Construction and Building Materials,* 24**,** 848-853.

VUKOTIC, L., FENNER, R. & SYMONS, K. Assessing embodied energy of building structural elements. Proceedings of the Institution of Civil Engineers-Engineering Sustainability, 2010. Thomas Telford Ltd, 147-158.

WASSERMANN, R., KATZ, A. & BENTUR, A. 2009. Minimum cement content requirements: a must or a myth? *Materials and Structures,* 42**,** 973-982.

WAWRZEŃCZYK, J., JUSZCZAK, T. & MOLENDOWSKA, A. 2016. Effect of Binder Composition on the Structure of Cement Paste and on Physical Properties and Freeze-Thaw Resistance of Concrete. *Procedia Engineering,* 161**,** 73-78.

WEE, T., SURYAVANSHI, A. & LOGENDRAN, D. 1999. Pore structure controlling the carbonation of a hardened cement matrix blended with mineral admixture. *Advances in cement research,* 11**,** 81-95.

WHITTAKER, M., ZAJAC, M., HAHA, M. B., BULLERJAHN, F. & BLACK, L. 2014. The role of the alumina content of slag, plus the presence of additional sulfate on the hydration and microstructure of Portland cement-slag blends. *Cement and Concrete Research,* 66**,** 91-101.

WHITTAKER, M. J. 2014. *The impact of slag composition on the microstructure of composite slag cements exposed to sulfate attack.* University of Leeds.

WIEDMANN, T. & MINX, J. 2008. A definition of 'carbon footprint'. *Ecological economics research trends,* 1**,** 1-11.

WORRELL, E., PRICE, L., MARTIN, N., HENDRIKS, C. & MEIDA, L. O. 2001. Carbon dioxide emissions from the global cement industry 1. *Annual review of energy and the environment,* 26**,** 303-329.

YANG, H., LIU, R., ZHENG, Z., LIU, H., GAO, Y. & LIU, Y. 2018. Experimental Study on Permeability of Concrete. *IOP Conference Series: Earth and Environmental Science,* 108**,** 22067.

YANG, K.-H., JUNG, Y.-B., CHO, M.-S. & TAE, S.-H. 2015. Effect of supplementary cementitious materials on reduction of CO_2 emissions from concrete. *Journal of Cleaner Production,* 103**,** 774-783.

YANG, W. P. & TARNG, Y. 1998. Design optimization of cutting parameters for turning operations based on the Taguchi method. *Journal of materials processing technology,* 84**,** 122-129.

YU, Z. & YE, G. 2013. The pore structure of cement paste blended with fly ash. *Construction and Building Materials,* 45**,** 30-35.

YU, Z. Q., MA, J., YE, G., VAN BREUGEL, K. & SHEN, X. D. 2017. Effect of fly ash on the pore structure of cement paste under a curing period of 3 years. *CONSTRUCTION AND BUILDING MATERIALS,* 144**,** 493-501.

Yepes, V., Martí, J. V., & García-Segura, T. (2015). Cost and CO2 emission optimization of precast–prestressed concrete U-beam road bridges by a hybrid glowworm swarm algorithm. Automation in Construction, 49, 123–134.

ZAMAN, A. S. M. A. U. 2014. *Development of Sustainable and Low Carbon Concretes for the Gulf Environment.* Ph.D Thesis, University of Bath.

ZHANG, J., HAN, Y. D. & GAO, Y. 2013a. Effects of water-binder ratio and coarse aggregate content on interior humidity, autogenous shrinkage, and drying shrinkage of concrete. *Journal of Materials in Civil Engineering,* 26**,** 184-189.

ZHANG, J. & SCHERER, G. W. 2011. Comparison of methods for arresting hydration of cement. *Cement and Concrete Research,* 41**,** 1024-1036.

ZHANG, M. H. 1995. Microstructure, crack propagation, and mechanical properties of cement pastes containing high volumes of fly ashes. *Cement and Concrete Research,* 25**,** 1165-1178.

ZHANG, W., ZAKARIA, M. & HAMA, Y. 2013b. Influence of aggregate materials characteristics on the drying shrinkage properties of mortar and concrete. *Construction and Building Materials,* 49**,** 500-510.

Zhang, Y. R., Zhang, J. Z., Luo, W., Wang, J. D., Shi, J. L., Zhuang, H. X., et al. (2019). Effect of compressive strength and chloride diffusion on life cycle CO2 assessment of concrete containing supplementary cementitious materials. Journal of Cleaner Production, 218, 450–458.

ZHOU, X. M., SLATER, J. R., WAVELL, S. E. & OLADIRAN, O. 2012. Effects of PFA and GGBS on early-ages engineering properties of Portland cement systems. *Journal of Advanced Concrete Technology,* 10**,** 74-85.

ZHU, H., LI, Q. B. & HU, Y. 2017. Self-Developed Testing System for Determining the Temperature Behavior of Concrete. *MATERIALS,* 10**,** 419.

Appendices

Regression Analysis: Carbonation depth versus ... , SCMs%, SCMs type

Method

Categorical predictor coding (1, 0)

Analysis of Variance

Source	DF	Adj SS	Adj MS	F-Value	P-Value
Regression	7	77.804	11.115	5.21	0.010
Aggregate size	1	4.909	4.909	2.30	0.160
Binder content	1	10.547	10.547	4.94	0.050
w/b	1	26.701	26.701	12.51	0.005
SP%	1	2.297	2.297	1.08	0.324
SCMs%	1	1.960	1.960	0.92	0.360
SCMs type	2	31.390	15.695	7.36	0.011
Error	10	21.336	2.134		
Total	17	99.140			

Model Summary

S	R-sq	R-sq(adj)	R-sq(pred)
1.46070	78.48%	63.41%	26.77%

Coefficients

Term	Coef	SE Coef	T-Value	P-Value	VIF
Constant	0.56	4.12	0.13	0.895	
Aggregate size	0.1044	0.0689	1.52	0.160	1.00
Binder content	-0.01875	0.00843	-2.22	0.050	1.00
w/b	14.92	4.22	3.54	0.005	1.00
SP%	-1.09	1.05	-1.04	0.324	1.00
SCMs%	0.0269	0.0281	0.96	0.360	1.00
SCMs type					
GGBS	0.750	0.843	0.89	0.395	1.33
PFA	3.100	0.843	3.68	0.004	1.33

Regression Equation

SCMs type			
FS	Carbonation depth	=	0.56 + 0.1044 Aggregate size - 0.01875 Binder content + 14.92 w/b - 1.09 SP% + 0.0269 SCMs%
GGBS	Carbonation depth	=	1.31 + 0.1044 Aggregate size - 0.01875 Binder content + 14.92 w/b - 1.09 SP% + 0.0269 SCMs%
PFA	Carbonation depth	=	3.66 + 0.1044 Aggregate size - 0.01875 Binder content + 14.92 w/b - 1.09 SP% + 0.0269 SCMs%

Regression Analysis: Carbonation depth versus ... , SCMs%, SCMs type

Method

Categorical predictor coding (1, 0)

Analysis of Variance

Source	DF	Adj SS	Adj MS	F-Value	P-Value
Regression	7	201.903	28.843	3.87	0.027
Aggregate size	1	16.627	16.627	2.23	0.166
Binder content	1	29.141	29.141	3.91	0.076
w/b	1	63.941	63.941	8.57	0.015
SP%	1	23.520	23.520	3.15	0.106
SCMs%	1	7.053	7.053	0.95	0.354
SCMs type	2	61.621	30.811	4.13	0.049
Error	10	74.593	7.459		
Total	17	276.496			

Model Summary

S	R-sq	R-sq(adj)	R-sq(pred)
2.73117	73.02%	54.14%	4.78%

Coefficients

Term	Coef	SE Coef	T-Value	P-Value	VIF
Constant	6.40	7.70	0.83	0.426	
Aggregate size	0.192	0.129	1.49	0.166	1.00
Binder content	-0.0312	0.0158	-1.98	0.076	1.00
w/b	23.08	7.88	2.93	0.015	1.00
SP%	-3.50	1.97	-1.78	0.106	1.00
SCMs%	-0.0511	0.0526	-0.97	0.354	1.00
SCMs type					
GGBS	-0.42	1.58	-0.26	0.797	1.33
PFA	3.70	1.58	2.35	0.041	1.33

Regression Equation

SCMs type			
FS	Carbonation depth	=	6.40 + 0.192 Aggregate size - 0.0312 Binder content + 23.08 w/b - 3.50 SP% - 0.0511 SCMs%
GGBS	Carbonation depth	=	5.98 + 0.192 Aggregate size - 0.0312 Binder content + 23.08 w/b - 3.50 SP% - 0.0511 SCMs%
PFA	Carbonation depth	=	10.10 + 0.192 Aggregate size - 0.0312 Binder content + 23.08 w/b - 3.50 SP% - 0.0511 SCMs%

Regression Analysis: Permeability versus Aggregate size, ... SCMs type

Method

Categorical predictor coding (1, 0)

Analysis of Variance

Source	DF	Adj SS	Adj MS	F-Value	P-Value
Regression	7	3875.55	553.65	9.21	0.001
Aggregate size	1	452.60	452.60	7.53	0.021
Binder content	1	25.40	25.40	0.42	0.530
w/b	1	2195.11	2195.11	36.50	0.000
SP%	1	6.16	6.16	0.10	0.755
SCMs%	1	75.00	75.00	1.25	0.290
SCMs type	2	1121.27	560.64	9.32	0.005
Error	10	601.44	60.14		
Total	17	4476.99			

Model Summary

S	R-sq	R-sq(adj)	R-sq(pred)
7.75524	86.57%	77.16%	56.77%

Coefficients

Term	Coef	SE Coef	T-Value	P-Value	VIF
Constant	-48.0	21.9	-2.19	0.053	
Aggregate size	1.003	0.366	2.74	0.021	1.00
Binder content	-0.0291	0.0448	-0.65	0.530	1.00
w/b	135.3	22.4	6.04	0.000	1.00
SP%	-1.79	5.60	-0.32	0.755	1.00
SCMs%	-0.167	0.149	-1.12	0.290	1.00
SCMs type					
GGBS	6.41	4.48	1.43	0.183	1.33
PFA	19.00	4.48	4.24	0.002	1.33

Regression Equation

SCMs type			
FS	Permeability	=	-48.0 + 1.003 Aggregate size - 0.0291 Binder content + 135.3 w/b - 1.79 SP% - 0.167 SCMs%
GGBS	Permeability	=	-41.6 + 1.003 Aggregate size - 0.0291 Binder content + 135.3 w/b - 1.79 SP% - 0.167 SCMs%
PFA	Permeability	=	-29.0 + 1.003 Aggregate size - 0.0291 Binder content + 135.3 w/b - 1.79 SP% - 0.167 SCMs%

Regression Analysis: Permeability versus Aggregate size, ... SCMs type

Method

Categorical predictor coding (1, 0)

Analysis of Variance

Source	DF	Adj SS	Adj MS	F-Value	P-Value
Regression	7	2093.81	299.12	6.24	0.005
Aggregate size	1	284.09	284.09	5.93	0.035
Binder content	1	0.19	0.19	0.00	0.951
w/b	1	1256.65	1256.65	26.22	0.000
SP%	1	2.61	2.61	0.05	0.820
SCMs%	1	2.13	2.13	0.04	0.837
SCMs type	2	548.13	274.07	5.72	0.022
Error	10	479.20	47.92		
Total	17	2573.01			

Model Summary

S	R-sq	R-sq(adj)	R-sq(pred)
6.92245	81.38%	68.34%	45.31%

Coefficients

Term	Coef	SE Coef	T-Value	P-Value	VIF
Constant	-48.9	19.5	-2.50	0.031	
Aggregate size	0.795	0.326	2.43	0.035	1.00
Binder content	-0.0025	0.0400	-0.06	0.951	1.00
w/b	102.3	20.0	5.12	0.000	1.00
SP%	-1.17	5.00	-0.23	0.820	1.00
SCMs%	0.028	0.133	0.21	0.837	1.00
SCMs type					
GGBS	5.82	4.00	1.45	0.176	1.33
PFA	13.48	4.00	3.37	0.007	1.33

Regression Equation

SCMs type			
FS	Permeability	=	-48.9 + 0.795 Aggregate size - 0.0025 Binder content + 102.3 w/b - 1.17 SP% + 0.028 SCMs%
GGBS	Permeability	=	-43.1 + 0.795 Aggregate size - 0.0025 Binder content + 102.3 w/b - 1.17 SP% + 0.028 SCMs%
PFA	Permeability	=	-35.4 + 0.795 Aggregate size - 0.0025 Binder content + 102.3 w/b - 1.17 SP% + 0.028 SCMs%

Regression Analysis: Sorptivity versus Aggregate size, ... %, SCMs type

Method

Categorical predictor coding (1, 0)

Analysis of Variance

Source	DF	Adj SS	Adj MS	F-Value	P-Value
Regression	7	278.822	39.832	11.78	0.000
Aggregate size	1	18.809	18.809	5.56	0.040
Binder content	1	7.680	7.680	2.27	0.163
w/b	1	136.013	136.013	40.22	0.000
SP%	1	5.333	5.333	1.58	0.238
SCMs%	1	1.613	1.613	0.48	0.505
SCMs type	2	109.373	54.687	16.17	0.001
Error	10	33.818	3.382		
Total	17	312.640			

Model Summary

S	R-sq	R-sq(adj)	R-sq(pred)
1.83896	89.18%	81.61%	62.93%

Coefficients

Term	Coef	SE Coef	T-Value	P-Value	VIF
Constant	-5.12	5.19	-0.99	0.347	
Aggregate size	0.2044	0.0867	2.36	0.040	1.00
Binder content	-0.0160	0.0106	-1.51	0.163	1.00
w/b	33.67	5.31	6.34	0.000	1.00
SP%	-1.67	1.33	-1.26	0.238	1.00
SCMs%	-0.0244	0.0354	-0.69	0.505	1.00
SCMs type					
GGBS	1.57	1.06	1.48	0.171	1.33
PFA	5.83	1.06	5.49	0.000	1.33

Regression Equation

SCMs type			
FS	Sorptivity	=	-5.12 + 0.2044 Aggregate size - 0.0160 Binder content + 33.67 w/b - 1.67 SP% - 0.0244 SCMs%
GGBS	Sorptivity	=	-3.55 + 0.2044 Aggregate size - 0.0160 Binder content + 33.67 w/b - 1.67 SP% - 0.0244 SCMs%
PFA	Sorptivity	=	0.72 + 0.2044 Aggregate size - 0.0160 Binder content + 33.67 w/b - 1.67 SP% - 0.0244 SCMs%

Regression Analysis: Sorptivity versus Aggregate size, ... %, SCMs type

Method

Categorical predictor coding (1, 0)

Analysis of Variance

Source	DF	Adj SS	Adj MS	F-Value	P-Value
Regression	7	198.488	28.355	5.04	0.011
Aggregate size	1	14.045	14.045	2.50	0.145
Binder content	1	2.167	2.167	0.39	0.549
w/b	1	107.401	107.401	19.08	0.001
SP%	1	2.083	2.083	0.37	0.556
SCMs%	1	1.267	1.267	0.23	0.645
SCMs type	2	71.523	35.762	6.35	0.017
Error	10	56.277	5.628		
Total	17	254.765			

Model Summary

S	R-sq	R-sq(adj)	R-sq(pred)
2.37229	77.91%	62.45%	24.92%

Coefficients

Term	Coef	SE Coef	T-Value	P-Value	VIF
Constant	-8.10	6.69	-1.21	0.254	
Aggregate size	0.177	0.112	1.58	0.145	1.00
Binder content	-0.0085	0.0137	-0.62	0.549	1.00
w/b	29.92	6.85	4.37	0.001	1.00
SP%	-1.04	1.71	-0.61	0.556	1.00
SCMs%	-0.0217	0.0457	-0.47	0.645	1.00
SCMs type					
GGBS	1.82	1.37	1.33	0.214	1.33
PFA	4.83	1.37	3.53	0.005	1.33

Regression Equation

SCMs type			
FS	Sorptivity	=	-8.10 + 0.177 Aggregate size - 0.0085 Binder content + 29.92 w/b - 1.04 SP% - 0.0217 SCMs%
GGBS	Sorptivity	=	-6.28 + 0.177 Aggregate size - 0.0085 Binder content + 29.92 w/b - 1.04 SP% - 0.0217 SCMs%
PFA	Sorptivity	=	-3.26 + 0.177 Aggregate size - 0.0085 Binder content + 29.92 w/b - 1.04 SP% - 0.0217 SCMs%